Feasibility of Mesenchymal Stem Cells as Modulators of Inflammation and as a Cellular Model to Study Cartilage Damage in Osteoarthritis

A thesis submitted to the National University of Ireland as fulfillment of the requirement for the degree of

Doctor of Philosophy

By

Swarna Raman

Regenerative Medicine Institute (REMEDI),

College of Medicine, Nursing and Health Sciences,

National University of Ireland, Galway.

Thesis Supervisor: Prof. Mary Murphy

November 2019

Table of Contents

Abstract

Osteoarthritis (OA) is the most common degenerative condition affecting whole joints and causing pain and cartilage degeneration, particularly in the elderly population. Inflammation of the synovium is now recognised as an important clinical feature initiating and promoting disease progression. Activated macrophages and T lymphocytes infiltrating the OA synovial lining mediate inflammatory responses such as production of pro-inflammatory cytokines, which can induce destructive processes in the cartilage. In addition to this danger signals like alarmins, released as an immune response, further lead to production of soluble mediators that could accelerate cartilage matrix degradation resulting in altered chondrocyte behaviour and hypertrophy. Mesenchymal stem cells (MSCs) have been considered as an attractive option for OA cell therapy. However, inflammation induced catabolic factors are also known to negatively impact cartilage engineering strategies, perhaps inhibiting the use of therapeutic cells for the treatment of OA. The work presented in this thesis sought to investigate the use of engineered MSCs as cellular mediators of anti-inflammation via viral interleukin-10 (vIL10) expression and also the potential of an *in vitro* model using MSCs to study inflammation-driven cartilage damage in OA. The tetracycline system (Tet) was used to modify mouse mesenchymal stem cells (mMSCs) to over-express vIL10 via adenoviral transduction. Doxycycline acted as a pharmacological switch to control the Tet system and successfully demonstrated efficient and tightly controlled vIL10 production by mMSCs. Engineered vIL10 MSCs proved to be immunosuppressive on activated macrophages and splenocytes *in vitro* via juxtacrine and paracrine signalling. These finding suggest that the Tet system of inducible vIL10 expression by MSCs may serve as a feasible strategy to enhance MSC-mediated immune regulation that can be translated towards attenuation of inflammation in OA.

Furthermore, a three-dimensional *in vitro* cartilage model to study the effects of inflammation-triggered chondrocyte alterations in OA was developed. Activation of the pathogen recognising receptor NLRP3 inflammasome pathway in the presence of the S100A8/A9 danger ligand signal, in alginate encapsulated articular chondrocyte progenitors (ACPs) and human MSCs (hMSCs) demonstrated anti-chondrogenic effects.

This novel model interrogating this ligand receptor interaction could offer a new direction to control/prohibit the release of catabolic factors associated with early inflammatory responses, thereby improving MSC and/or chondroprogenitor-based cartilage engineering strategies. Overall, this thesis showcased the viability of MSCs as potential modulators of inflammation and a possible model to generate novel cartilage regeneration strategies.

Acknowledgements

I would first of all like to convey my deepest gratitude to my supervisor, **Prof. Mary Murphy**, who made this PhD possible with her constant motivation, guidance and endless patience. Her optimistic method of tackling any situation and her visionary approach towards the welfare of a student's career cannot be appreciated or acknowledged with just words. I am truly proud and honoured to call her 'my beacon of light' in my scientific path and a great inspiration for women who aspire a career in science. I would also like to sincerely thank **Prof. Frank Barry**, for all his support and scientific advice he provided throughout my PhD.

Prof. Thomas Ritter, Dr. Aideen Ryan and Dr. Roisin Dwyer , thank you for offering such great support as my GRC advisors.

My heart-felt appreciation goes to **Dr. Linda Howard** for all her encouragement and goodwill. Special thanks goes to **Ms. Georgina Shaw** and **Ms. Martina Harte** for their phenomenal help and constant motivation in the lab.

There are not enough words to thank **Dr. Patrizio Mancuso** (*my scemo*) for being the coolest lab partner and a wonderful friend for life! Thank you for tolerating my tantrums and mood swings and constantly supporting me.

My heart-felt regards to Mr. Pietro Marchese, for being not just an amazing friend but also a little brother (whom I wish I had) and a well-wisher who always exudes an aura of positivity. Thank you for being my second family in Galway!

Ms. Claire Dooley, thank you for being *my home away from home*. Your presence and life-saving help in the last three years of my PhD life is invaluable. **Dr. Ana Ivanovska** and **Dr. Emily Ann Growney**, thank you for being such amazing friends and research partners whose immense support and help was priceless and something I will always be grateful for.

I want to thank all members of the Orthobiology group and REMEDI, who have helped and supported me down through the years. I have been so fortunate to have worked with such a great group of people.

I would like to sincerely thank the University, for awarding the **Hardiman Scholarship** which was instrumental in providing this great opportunity to pursue a PhD.

Finally, I thank the Almighty for giving me my Amma and Appa. I am truly blessed to have such wonderful parents who have always been my pillars of strength, my role models of resilience and willpower and the reason behind all my success in life. I am eternally grateful to my dearest parents for their abysmal love and for raising me to be a strong and independent person.

Dedications

Dedicated in loving memory of my grandfather, the great Philosopher Prof. R. *Balasubramanian who always inspired and motivated me to follow my dreams.*

Declaration

I declare that this thesis is all my own work and I have not obtained a degree in NUIG, or elsewhere, on the basis of this work

Abbreviations

ACI- Autologous chondrocyte implantation

ACP- Articular cartilage progenitors

Ad/AD- Adenoviral vector

ADAMTS- A disintegrin and metalloproteinase with thrombospondin motifs

APC- Antigen presenting cell

AIA- Antigen-induced arthritis

ASC- Apoptosis-associated speck-like protein containing a CARD

ATP- Adenosine triphosphate

BMP- Bone morphogenic protein

BMs- Bone-marrow macrophages

CCL- Chemokine ligand

CCM- Complete chondrogenic medium

CD- Cluster of differentiation

CM- Conditioned medium

CMV- Cytomegalovirus promoter

CIOA- Collagenase-induced osteoarthritis

CTV- Cell trace violet

CXCL- Chemokine (C-X-C motif) ligand

DAMP- Damage-associated molecular pattern

DC- Dendritic cell

dH_2O- Deionised water

dl- Deciliter

DMEM- Dulbecco's modified essential medium

DMMB- Dimethyl methylene blue

DMSO- Dimethyl sulfoxide

DNA- Deoxyribonucleic acid

DOX- Doxycycline

ECM- Extracellular matrix

EDTA- Ethylenediamine tetra acetic acid

ELISA- Enzyme-linked immunosorbent assay

FACS- Fluorescent activated cell sorting

FBS- Fetal bovine serum

FCM- Flow cytometry

FGF- Fibroblastic growth factor

FMO- Fluorescence minus one

g- Gram

GAG- Glycosaminoglycans

GFP- Green fluorescent protein

h- Hour

HG- High glucose

HRP- Horseradish peroxidase

IA- Intra-articular

ICM- Incomplete chondrogenic medium

IDO- Indoleamine 2, 3-dioxygenase

IFN-γ- Interferon-gamma

IGF- Insulin-like growth factor

IL- Interleukin

IL-10- Interleukin 10

IMS- Industrial methylated spirits

ISCT- International Society for Cell Therapy

LPS- Lipopolysaccharide

M- Molar

M-CSF- Macrophage colony-stimulating factor

MCP- Monocyte chemoattractant protein

MEM- Minimum essential medium

MFI- Mean fluorescent intensity

min- Minute

ml- Millilitre

mM- Millimolar

MMP- Matrix metalloproteinase

MSCs- Mesenchymal stem cells

mMSCs- mouse/ murine mesenchymal stem cells

MOI- Multiplicities of infection

ng- Nanogram

NLRP3- Nucleotide-binding domain and leucine-rich repeat containing protein 3

NO- Nitric oxide

OA- Osteoarthritis

P- Passage

PA- Palmitic acid

P/S- Penicillin/Streptomycin

PBS- Phosphate buffered saline

Pfu- plaque-forming units

Pg- Picogram

PGE2- Prostaglandin-E2

PRG4- Proteoglycan 4

PRR- Pathogen recognition receptor

qRT-PCR- Quantitative real time polymerase chain reaction

RANTES- Regulated on Activation, Normal T Cell Expressed and Secreted

RLI- Relative luminescent intensity

RT- Room temperature

ROS- Reactive oxygen species

s- Second

S100A8- S100 calcium-binding protein A8

S100A9- S100 calcium-binding protein A9

Sca-1- Stromal cell antigen-1

SD- Standard deviation

SEM- Standard error of the mean

sGAG- sulfated gylcosaminoglycans

SOX-9- (Sex-Determining Region Y)-Box 9

TA- Transactivator

T reg- Regulatory T

TCR- T cell receptor

TE- Tris-EDTA

Tet- Tetracycline

TGF-β- Transformation growth factor-beta

TLR- Toll-like receptor

TNF- Tumor necrosis factor

TIMP- Tissue inhibitor of metalloproteinases

TJR- Total joint replacement

TRE- Tet responsive element

VEGF- Vascular endothelial growth factor

vIL10- viral interleukin 10

w- week

xg- times gravity

α-MEM- Minimal essential medium- α

μg- microgram

List of Figures

List of Tables

Chapter 1

Introduction

Parts of this chapter has been adapted with permission from Frontiers in Bioengineering and Biotechnology: Raman S, FitzGerald U, Murphy JM. Interplay of Inflammatory Mediators with Epigenetics and Cartilage Modifications in Osteoarthritis. *Front Bioeng Biotechnol.* 2018; 6:22.

1.1 Osteoarthritis

Osteoarthritis (OA) is the most common, progressive and debilitating musculoskeletal disease. OA is typically characterized by loss of articular cartilage and thickening of the synovial lining, with simultaneous formation of osteophytes and subchondral sclerosis, ultimately causing severe pain and stiffness of affected joints. Although OA can affect any synovial joint, joints affected mainly include hips, knees, hands, metatarsophalangeal joints and apophyseal joints of the lower cervical and lumbar spine (Musumeci et al., 2015, Abhishek and Doherty, 2013, Harrell et al., 2019). OA can be broadly categorized into two forms namely primary and secondary, with aging and genetic predisposition considered as the main causes of primary OA (Arden and Cooper, 2005). Secondary forms arise from sports injuries, fractures, repetitive joint use, metabolic diseases like diabetes and abnormal mechanical loading due to obesity and estrogen deficiency (Felson et al., 1988, Carman et al., 1994, Cicuttini et al., 1996, Berenbaum, 2011, Felson et al., 2000). Apart from these reasons, the avascular nature, poor replicative potential and inability to produce sufficient functional matrix by chondrocytes in damaged cartilage adds to OA progression (Burke et al., 2016). The disease has a detrimental effect on quality of life and is the leading cause of disability in elderly populations with co-morbidities such as depression and sleep disorders adding to its' impact (Barry and Murphy, 2013, Kong et al., 2017, Gore et al., 2011).

According to World Health Organization (WHO) reports, 10-15% of all adults over the age of 60 have some degree of OA, with a higher prevalence among women. It is also estimated that these numbers will increase to 20% and by 2050 around 130 million people worldwide will suffer from OA, of whom >40 million people will be severely disabled as a consequences of the disease (Wittenauer et al., 2013). Unfortunately, without proper therapeutic strategies or effective treatment options, the socio-economic burden of OA per annum is also quite concerning. In terms of treatment costs, for knee OA alone around 185.5 billion US dollars is incurred per year. Furthermore, with an associated reduction in employment, short-term disability and work absenteeism, OA is indeed a huge liability on the global economy (Michaud et al., 2006).

The use of non-steroidal anti-inflammatory drugs (NSAIDS) and opioids for OA attenuation offer only temporary pain relief and these treatments do not prevent disease progression (Zhang et al., 2016). Non-operative methods with pre-clinical evidence of chondroprotection include viscosupplementation with hyaluronic acid (HA), platelet rich plasma, pulsed electromagnetic fields and the use of chondroitin, glucosamine or other nutraceutical agents (Zaslav et al., 2012, Bannuru et al., 2009). These options however come with multiple shortcomings like the need for repetitive use, and variations in efficacy and failure to reverse cartilage damage leaving total joint arthroplasty/replacement (TJR) as the only possible option. Although TJR has been successful in improving mobility and pain, the procedure comes with major pitfalls like the risk of infection and thrombosis after this invasive trauma, and is very expensive (Grayson and Decker, 2012).

In the last two decades, the FDA have approved a cell therapy treatment called autologous chondrocyte implantation (ACI) and this therapy has dramatically improved in terms of its patient success rate from 76 to 86% (Burke et al., 2016). However, efficacy of ACI is localized to the damaged cartilage site with de-differentiation of chondrocytes an issue (Viste et al., 2012, Mobasheri et al., 2014, Nazempour and Van Wie, 2016). Hence there is a pressing need for improved cell-based therapeutic strategy with long-term reparative and regenerative potential.

1.2 Immunopathogenesis of OA

OA was originally classified as a non-inflammatory form of arthritis, mainly affecting the articular cartilage. This was based on the observation that the leukocyte count in OA synovial fluid is lower than the average threshold of 2000 cells/mm^3 to define it as an 'inflammatory' disorder; numbers are lower than what is seen in septic arthritis, reactive arthritis and rheumatoid arthritis (RA) (Dougados, 1996, Sokolove and Lepus, 2013). Although cartilage is avascular and aneural with low chondrocyte replicative potential, in a disease environment these cells quickly respond to physical injury and halt the production of anabolic factors. Under the influence of soluble mediators like cytokines and prostaglandins from the synovial lining, chondrocytes release higher levels of catabolic enzymes such as matrix metalloproteinases (MMPs), leading to further cartilage damage (Jasin, 1988, Berenbaum, 2013).

In fact, continuous crosstalk between chondrocytes and the synovium creates an inflammatory stimulus, wherein either degraded cartilage products accumulate in the synovial lining and aggravate synovial inflammation or pro-inflammatory mediators and resident immune cells of the synovium begin to alter the normal function of chondrocytes resulting in cartilage damage. Inflammation is therefore an important driving factor in OA pathogenesis with involvement of an innate and adaptive immune response typically seen in cartilage, synovium and plasma in OA patients (Haseeb and Haqqi, 2013) (Figure 1.1).

1.2.1 Synovium in OA

The synovium, and in particular the cell and molecular components of the synovial membrane, play a vital role in modulating the function of chondrocytes in cartilage. Lubricin and HA are two critical molecules produced by cells of the synovial lining that offer optimal protection to diarthrodial joints by reducing friction, providing lubrication and inhibiting deposition of catabolic proteins at the articular surface. Under normal physiological conditions, the synovial lining is a thin layer, devoid of inflammatory cells. The synovial membrane controls molecular trafficking in the joint space by acting like a semi-permeable sieve, that retains high molecular weight lubricating molecules like lubricin and HA within the joint in order to maintain viscosity and composition of the synovial fluid but allows smaller molecules like cytokines and growth factors diffuse through the synovium. However, in an OA setting, inflammation causes synovial hyperplasia and alters the permeability of the membrane. On a molecular level, this leads to influx of macrophages, T cells and MMPs (MMP-1, 3, 9 and 13) leading to degradation of the articular matrix, increased neovascularisation and secretion of pro-inflammatory cytokines (Bondeson et al., 2010, Sellam and Berenbaum, 2010). Hence the synovial membrane loses its cartilage protective role and the synovial fluid eventually becomes a hub of catabolic mediators such as tumor necrosis factor-α (TNF-α) and interleukins (IL) like interleukin-1 beta (IL-1β), interleukin-6 (IL-6), interleukin-8 (IL-8), interleukin-15 (IL-15), interleukin-17 (IL-17) and interleukin-21 (IL-21)(Scanzello and Goldring, 2012, Bondeson et al., 2006, Bresnihan et al., 2013).

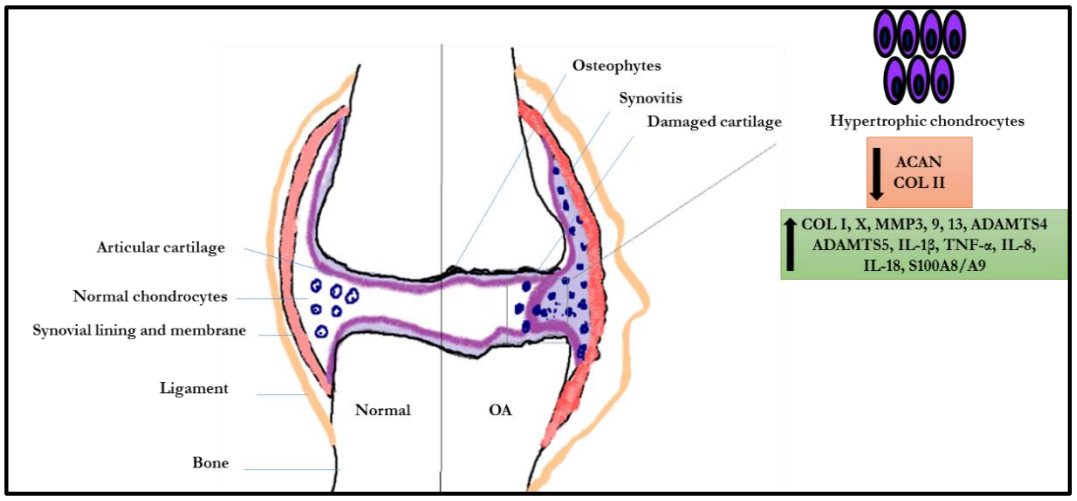

Figure 1.1: Immunopathogenesis of OA development. A constant pathological loop of synovitis and cartilage degradation creates an inflammatory environment, altering the chondrocyte phenotype and pushing the cells into a hypertrophic state. Chondrocytes undergo terminal differentiation or de-differentiation with elevated expression of catabolic cytokines (IL-1β, TNF-a, IL-8, IL-18), aggrecanases (ADAMTS4, ADAMTS5), alarmins (S100A8/A9), metalloproteinases (MMP1, 3, 9, 13), collagens (type I, X) and depletion of ACAN and COL II. Abbreviations: ACAN-aggrecan; COL II-type II collagen; COL I-type I collagen; MMPs 1, 3, 9, 13- matrix metalloproteinases-1, 3, 9, 13; ADAMTS 4,5- a disintegrin and metalloproteinase with thrombospondin motifs 4,5; TNF-a-tumor necrosis factor-a; IL-1β-interleukin-1β; IL-8-interleukin-8; IL-18-interleukin-18; S100A8/A9- S100 family of calcium binding proteins A8/A9. (Raman et al., 2018)

According to the American College of Rheumatology, the current criteria for OA classification necessitates the presence of radiographic osteophyte formation or bony enlargement (Sokolove and Lepus, 2013). However using a combination of imaging modalities and direct arthroscopic visualization techniques, inflammation of the synovium/synovitis has now been documented as an important clinical feature of OA that precedes the development of any significant radiographic modifications and/or notable occurrence of cartilage degeneration (Altman et al., 1986, Ayral et al., 2005). Synovitis, has also been associated with meniscal injury leading to OA and is associated with pain and dysfunction (Berenbaum, 2013). It is also known to directly influence many clinical symptoms including knee effusion, redness, heat and swelling (Sellam and Berenbaum, 2010, Ayral et al., 1999). Numerous studies utilizing magnetic resonance imaging (MRI) have shown a clear association between the presence of synovitis from early stages of OA and through progression of the disease (Felson et al., 2003, Roemer et al., 2011, Krasnokutsky et al., 2011). Microarray and gene pattern analysis of synovial tissues from patients without radiographic evidence of OA undergoing arthroscopic meniscectomy showed that 43% of patients had synovial inflammation that correlated with traumatic meniscal injury and pain. Synovial biopsy specimens that showed high inflammation scores recorded a strong chemokine signature, involving significant levels of chemokine ligand-5 (CCL5), chemokine ligand-7 (CCL7), chemokine ligand-19 (CCL19) and IL-8 (Scanzello et al., 2011).

The impact of synovitis throughout disease progression was demonstrated by Benito *et al.* who compared key immunohistological features of inflammation during early and late OA. Immunohistochemical staining of synovial tissue samples with gross synovial hypertrophy showed high expression of markers of inflammatory cell infiltration (CD4+ and CD68+ cells), angiogenesis with increased levels of vascular endothelial growth factor (VEGF) and blood vessel formation (as shown by factor VIII expression). Intercellular adhesion molecule-1 and pro-inflammatory cytokines (TNF-α, IL1β) were also seen in both early and late OA with significantly higher expression in early OA (Benito et al., 2005). Analysis of proteins in the synovial fluid collected from patients with knee OA showed the presence of 108 different proteins that included plasma proteins, serine protease inhibitors, proteins pertaining to cartilage turnover and proteins involved in

inflammation and immunity (Sohn et al., 2012). In addition to this, these authors also demonstrated higher levels of pro-inflammatory cytokines like TNF-α, IL-6 and VEGF in OA synovial fluid compared to healthy individuals. Analysis of stimulated macrophages derived from toll-like repcetor-4 (TLR-4) deficient and wild type mice, proved that plasma proteins and inflammatory cytokines present in synovial fluid indeed function as damage-associated molecular patterns (DAMPs) signalling through TLRs to mediate an early response to injury and damage to the joint (Sohn et al., 2012, Midwood et al., 2009, Scanzello et al., 2008).

Although synovitis is a known histological feature reported in the vicinity of degrading cartilage at early stage OA (Ayral et al., 2005), one cannot exclude the individual roles of chondrocytes and cartilage during early and late OA. Macroscopic and histopathological analysis of human knee OA showed that products of cartilage breakdown are present in the microfissures of articular cartilage and synovial fluid long before any signs of degeneration are evident (Mow et al., 1974, Sokolove and Lepus, 2013, Pauli et al., 2011). It may be that events associated with early cartilage degradation could be a trigger for synovitis in OA.

1.2.2 Cartilage and chondrocytes in OA

Articular cartilage is a highly specialized connective tissue that ensures normal function and optimal load-bearing capacity (Sophia Fox et al., 2009, Buckwalter, 1991, Buckwalter, 1990). It coordinates with the synovial membrane and synovial fluid to bring about frictionless movement. The components of articular cartilage are the extra-cellular matrix (ECM) with sparsely distributed specialized cells, the chondrocytes and collagen fibres (mainly type II and IX), proteoglycans, water and a small volume of non-collagenous proteins and glycoproteins such as fibronectin (Sophia Fox et al., 2009, Wooley et al., 2005). With respect to the collagen network, the complex triple helical structure of collagen type II α-polypeptide chains, along with associated collagenous and non-collagenous matrix proteins, provides vital sheer and tensile properties to stabilize the matrix (Goldring, 2000). The cartilage matrix of a healthy individual typically contains collagen type II and the subchondral bone tissue is where collagen type I is mainly localised (Martel-Pelletier et al., 2008, Poole et al., 2002, Pearle et al., 2005).

Aggrecan is the most abundant proteoglycan in cartilage, followed by decorin, biglycan and fibromodulin. The interaction of aggrecan with hyaluronan through link protein to form proteoglycan aggregates, is optimal for resisting compressive loads (Sophia Fox et al., 2009, Kiani et al., 2002). Other associated matrix components, playing a vital role in cartilage structure and function in association with the collagen network include small leucine-rich proteoglycans: decorin, biglycan, fibromodulin, and lumican (HeinegÅRd et al., 2006, Mow et al., 2012, Halper and Kjaer, 2014). Cartilage matrix disruption in OA is usually associated with altered chondrocyte behaviour and clustering, which in turn changes the composition of matrix components (Goldring and Otero, 2011, Goldring, 2000). As lesions progress, changes in structural configuration and function of chondrocytes cause local loss of proteoglycan, cleavage of type II collagen at the cartilage surface and downregulation of aggrecan (ACAN) gene expression, further resulting in an influx of water content and loss of tensile strength in the cartilage ECM matrix (Goldring, 2000, Nam et al., 2011, Maldonado and Nam, 2013)(Figure 1.1).

Stable, articular chondrocytes are indispensable for the development, maintenance and repair of the cartilaginous ECM. They are highly-specialised cells with adult articular cartilage being an avascular tissue in nature (den Hollander et al., 2015, Goldring et al., 2011). Under normal conditions, permanent hyaline cartilage found in articulating joints, does not undergo terminal differentiation (van der Kraan and van den Berg, 2012b). However, based on *in vitro* and *in vivo* evidence, re-programming of articular chondrocytes towards a hypertrophic, degradative phenotype frequently occurs as OA develops (van der Kraan and van den Berg, 2012b, van der Kraan and van den Berg, 2007). The process of chondrocyte hypertrophy can be divided into four stages namely initiation, progression, and late and end stages. In the joint of a healthy adult, chondrocyte hypertrophy is inhibited by transformation growth factor-β (TGF-β) via Smad2 and 3 signalling molecules (Van der Kraan and Van den Berg, 2012a, Schuh et al., 2010).

Some studies have shown that synovitis influences changes to the cartilage ECM increasing local matrix stiffness. Chondrocytes in OA cartilage, sense the matrix stiffness and respond by acting in a hypertrophy-like manner. They begin to express hypertrophic markers such as collagen type X and MMP13, with signs of matrix calcification similar to terminally differentiated chondrocytes in the growth plate of long bones (a process known

as endochondral ossification) (Van der Kraan and Van den Berg, 2012a, Schuh et al., 2010). The maintenance of optimal cartilage matrix stiffness via the TGF-β signalling pathway controls chondrocyte function promoting expression of critical genes like ACAN, type II collagen (COL2A1) and sex determining region Y-Box 9 (SOX9). Any change in matrix stiffness, can lead to chondrocyte dedifferentiation with an abnormal fibrochondrocytic phenotype and/or production of a non-functional ECM in arthritic joints (Yang et al., 2006, Allen et al., 2012, Marlovits et al., 2004, Lin et al., 2008). *In vitro* studies have also demonstrated the mechanosensitive nature of chondrocytes, wherein culturing chondrocytes on stiff tissue culture plastics causes the cells to eventually dedifferentiate (Das et al., 2008, Maldonado and Nam, 2013). Several studies conducted both *in vitro* and *in vivo* have proved the involvement of pro-inflammatory cytokines and metalloproteinases in matrix disruption (Sellam and Berenbaum, 2010). These factors mainly target chondrocytes, causing aberrant expression of catabolic and anabolic genes. Of the matrix-degrading enzymes produced by hypertrophic chondrocytes, MMP-13 is critical in its ability to cleave type II collagen with cleavage products shown to produce OA-like effects in the mouse knee joint (Neuhold et al., 2001, Goldring et al., 2011). Hence, understanding and identifying key molecules and associated pathways that promote inflammation and OA progression can aid in generating disease-preventing/modifying strategies.

1.2.3 Pro-inflammatory cells associated with OA

Although OA is not an inflammatory disease with an active adaptive immune response like RA, cellular infiltrates harboured within the inflamed synovium, clearly indicate the central role of the innate immune system in OA. Macrophages account for the major cell type present during synovitis in OA, followed by neutrophils and dendritic cells/antigen-presenting cells (DCs/APCs). These cells mediate the host-immune response by eliciting a pro-inflammatory and anti-microbial activity, induced by innate receptors called pattern-recognition receptors (PRRs). PRRs are known to recognise pathogen motifs of invading pathogens including but not limited to bacteria, fungi and viruses (Hajishengallis and Lambris, 2011, Haseeb and Haqqi, 2013). Toll-like receptors (TLRs), the NLRP3 (Nacht, leucine-rich and pyrin domain containing protein 3) inflammasome and advanced glycated end product receptors (RAGE) are key PRRs present on macrophages, chondrocytes and

synovial fibroblasts (SFs). These cells can be found in the synovium and cartilage matrix of OA patients and are responsible for triggering signalling cascades like mitogen-activated protein kinases (MAPK) and nuclear factor-kappa B (NF-ϰB) pathways leading to inflammation (Kawai and Akira, 2010, Rosenberg et al., 2017, Radstake et al., 2004).

Synovial macrophages (SMs) residing in the synovial lining, play a crucial role in inflammation and OA progression. Apart from antigen presentation and phagocytosis, SMs are responsible for the production of critical soluble mediators (cytokines and chemokines) like IL-β, TNF-α, IL-6 and oncostatin M (OSM) that cause cartilage breakdown (Beekhuizen et al., 2013, IWANAGA et al., 2000). This action of cytokine and chemokine production occurs when PRRs like TLR-2 and TLR-4 (Radstake et al., 2004) sense tissue damage in the form of damage associated molecular patterns (DAMPs) such as fibronectin (Okamura et al., 2001, Su et al., 2005), hyaluronan (Termeer et al., 2002, Jiang et al., 2005), biglycan (Schaefer et al., 2005) and tenascin-c (Midwood et al., 2009) present in OA cartilage matrix (Sokolove and Lepus, 2013, Sellam and Berenbaum, 2010). Bondeson et al. showed that SMs act as a driving force in influencing the production of IL-1, TNF-α, MMP3, MMP9, MMP13 and aggrecanases like ADAMTS4 (a disintegrin and metalloprotease with thrombospondin motifs 4) and ADAMTS5 in the OA synovium (Bondeson et al., 2010, Bondeson et al., 2006). Studies have shown how macrophage activation, especially by SMs, has a default role in MMP-mediated matrix damage in experimental models of OA cartilage. In one study, synovial MMP-3 production led to the formation of MMP-neoepitopes, causing cartilage degeneration and another study displayed how pro-MMP-9 production by SMs resulted in activation of mature MMP-9 via the MMP-3/MMP-13 signalling pathway (Dreier et al., 2004, Blom et al., 2007).

Selective depletion of SMs by injecting clodronate-laden liposomes *in vivo* impeded the formation of TGF-β induced osteophytes, thereby depicting the role of SMs in osteophyte formation (Van Lent et al., 2004). Similar to the inflammatory actions of SMs, SFs also contribute towards synovitis, either by enabling the adhesion of infiltrating immune cells or by activation of inflammatory soluble mediators. In a study conducted by Inoue et al., stimulation of SFs with IL-1β resulted in the production of macrophage colony stimulating factor (M-CSF), VEGF, IL-6 and IL-8 (Inoue et al., 2001). Secondly, SFs demonstrated their capacity to facilitate adhesion of mononuclear cells to specific sites of

inflammation by increasing the expression of vascular cell adhesion molecule-1 (VCAM-1), in response to chemokines commonly detected in synovial fluid of patients with OA such as: C-C motif) ligand 2 (CCL2) and CCN family member 4 (Liu et al., 2013a, Lin et al., 2012).

Natural killer cells (NKs) and dendritic cells are two other important cell types found to be present in the synovial tissue. Evidence of activated DCs has been reported in the synovium of a rabbit OA model at early stages of the disease (Huss et al., 2010, Xiaoqiang et al., 2012, Pettit et al., 2001). Other than the role of SFs in recruiting these cells to sites of inflammation, the exact mechanism of NKs and DCs in OA progression is not fully understood. Complement activation plays a part in the immunopathogenesis of OA and represents the involvement of an innate immune response via clearance of pathogens. Elevated gene expression of complement factors in the cartilage and synovium of OA patients and animals models have been recorded (Cantatore et al., 1988, Moskowitz and Kresina, 1986, Wang et al., 2011). Over-expression of the C5a (C5aR/CD88) receptor during RA and OA by human articular chondrocytes suggested the activation of complement factors leading to cartilage degradation (Onuma et al., 2002). Proteomic analysis of synovial fluid samples, collected from the knee joint of OA patients, revealed a differential expression of complement proteins, further confirming the involvement of complement system in OA (Ritter et al., 2013).

Adaptive immune responses via activation of T cell subsets and B cells are not readily functioning in the early phases of OA. A number of possible explanations for their subsequent activation in OA are: 1. recruitment of these cells by the cytokine milieu produced during synovitis (Chevalier et al., 2013); 2. interaction of mononuclear cell infiltrates in the synovium (APCs and SMs) with the adaptive immune system during inflammation and signal T and/or 3. B cells taking an active role in producing antibodies against autoantigens similar to but less abundant than in RA (Sakkas et al., 1998, Jasin, 1985). Active T cell populations found in the synovium are mainly $CD4^+$, with equal or lesser percentages of $CD8^+$ T cells and also B cells.

Evidence of localised chronic T cell induction in OA synovitis is seen via expression of CD3ζ on $CD4^+$ T cells (Ishii et al., 2002, Sakkas et al., 2004). Sakkas et al found that among the T Helper cells found in most OA patients, Th1 cells were detected five times

more than Th2. This data concurs with data to suggest that Th1 presents a pro-inflammatory and Th2 an anti-inflammatory profile during OA (Sellam and Berenbaum, 2010). Also, Th1 cytokines secreted in high levels included IL-2 and interferon-gamma (IFN-γ). These authors also proposed that IL-12 released by SMs in OA patients could be responsible for this Th1-like cytokine pattern, since IL-12 has been reported as a stimulator of Th1 during inflammation (Sakkas et al., 1998, Sakkas and Platsoucas, 2007). Two separate studies, revealed the role of OA chondrocytes in activating an autologous T cell response *in vitro*. Co-culture of chondrocytes derived from OA patients with autologous T cells, showed high production of Regulated on Activation, Normal T Cell Expressed and Secreted (RANTES - an inflammatory chemokine) in addition to release of MMP-1, MMP-3 and MMP-13 (Sakata et al., 2003, Nakamura et al., 2006). In a murine model of surgically induced OA by anterior cruciate ligament transection (ACLT), activated $CD4^+$ T cells in the synovium accelerated the production of macrophage inflammatory protein- 1γ (MIP-1γ) and NF-κB and also elevated the expression of MMP-9, leading to cartilage damage and osteoclast formation (Shen et al., 2011). Unlike T cells, the presence and percentage of B cells in the OA synovial membrane is quite low. Yet those present exhibit an activated state as a result of secreted CXC-chemokine ligand (CXCl) 13, serving as a chemoattractant for these B cells (Shi et al., 2001, Jasin, 1985, Smith et al., 1992). B cells infiltrating the synovium tend to have detrimental effects in OA in the form of cytotoxicity and generation of autoantibodies against cartilage ECM components like type II collagen (Takagi and Jasin, 1992, De Rooster et al., 2000, Niebauer et al., 1988, Cooke et al., 1980, Jasin, 1985).

1.2.4 Soluble mediators and pathways promoting inflammation in OA

One of the main degradative events occurring in OA is the production of soluble catabolic mediators by activated macrophages, OA chondrocytes and SFs in the inflamed joint (Sellam and Berenbaum, 2010, Scanzello and Goldring, 2012). These pro-inflammatory mediators mainly include cytokines, chemokines, MMPs and aggrecanases and secretion of these mediators via transcriptional activation of their respective genes is mediated by PRRs and their corresponding signalling pathways such as: TLR, NF-κB, MAPK, WNT/β-catenin (wingless int-1) and RAGE (Haseeb and Haqqi, 2013, Goldring and Otero, 2011, Rosenberg et al., 2017, Sun et al., 2016, Sassi et al., 2014a). The aim of this

section is to discuss the role of key mediators associated with cartilage matrix breakdown and aggravation of inflammation in OA. Among the cytokines causing altered chondrocyte behaviour and inducing production of proteolytic enzymes leading to disruption of cartilage homeostasis, the most studied cytokines include IL-1β, TNFα, IL-6, IL-15, IL-17, and IL-18 (Sellam and Berenbaum, 2010). Table 1.1 provides an overview of the critical inflammatory mediators and their targeted downstream effects in OA.

Table 1.1 Inflammatory mediators and their targeted downstream effects in OA

Mediator	Protein category	Effects in OA	Pathways/receptor	References
IL-1β	Cytokine	Synovitis, chondrocyte hypertrophy	TLR, NF-κB	(Dingle et al., 1979, Dingle, 1981, Stannus et al., 2010, Henrotin et al., 1996)
TNF-α	Cytokine	Synovitis, chondrocyte alteration	TLR, NF-κB, MAPK	(Saklatvala, 1986, Stannus et al., 2010, Henrotin et al., 1996)
IL-6	Cytokine	Synovitis, chondrocyte alteration	TLR, NF-κB, STAT1/3	(Kaneko et al., 2000, Yang et al., 2017, Guerne et al., 1990, Kishimoto, 2006)
IL-8	Cytokine	Synovitis, chondrocyte hypertrophy	TLR, NF-κB	(Kaneko et al., 2000, Chauffier et al., 2012, Lotz et al., 1992, Merz et al., 2003)
IL-18	Cytokine	Synovitis, chondrocyte hypertrophy	TLR, NF-κB	(Olee et al., 1999, Mao et al., 2018)
CCL5	Chemokine	Synovitis, chondrocyte alteration	NF-κB	(Borzì et al., 1999, Alaaeddine et al., 2001)

Table 1.1: Continued

Mediator	Protein category	Effects in OA	Pathways/receptor	References
ADAMTS4	Proteinase	Synovitis, chondrocyte alteration	NF-κB	(Bondeson et al., 2006, Bondeson et al., 2010, Amos et al., 2006)
ADAMTS5	Proteinase	Synovitis	NF-κB	(Bondeson et al., 2006, Bondeson et al., 2010)
MMP3	Proteinase	Synovitis, Cartilage breakdown, chondrocyte hypertrophy	TLR, NF-κB, MAPK, WNT,	(Sakata et al., 2003, Nakamura et al., 2006, Dreier et al., 2004)
MMP9	Proteinase	Synovitis, Cartilage breakdown, chondrocyte hypertrophy	TLR, NF-κB, MAPK, WNT,	(Sakata et al., 2003, Nakamura et al., 2006, Dreier et al., 2004)
MMP13	Proteinase	Synovitis, Cartilage breakdown, chondrocyte hypertrophy	TLR, NF-κB, MAPK, WNT,	(Dreier et al., 2004, Blom et al., 2007, van der Kraan and van den Berg, 2012b, Goldring et al., 2011)

Table 1.1: Continued

Mediator	Protein category	Effects in OA	Pathways/receptor	References
S100A8	Alarmin	Synovitis, chondrocyte cell death	TLR, NF-ϰB, RAGE	(van Lent et al., 2012, Zreiqat et al., 2010, Schelbergen et al., 2012)
S100A9	Alarmin	Synovitis, chondrocyte cell death	TLR, NF-ϰB, RAGE	(van Lent et al., 2012, Zreiqat et al., 2010, Björk et al., 2009)
ATP	Alarmin	Synovial and chondrocyte cell death	TLR, ROS, P2X7R	(Zhao et al., 2018, Ryan et al., 1992, Berenbaum et al., 2003)
NLRP3	Inflammasome	Synovitis, Cartilage calcification, chondrocyte alteration	TLR, ROS, P2X7R	(Zhao et al., 2018, Pazár et al., 2011, Cullen et al., 2015, McAllister et al., 2018, Clavijo-Cornejo et al., 2016)
MSU/BCPs	Alarmin	Synovitis, Cartilage breakdown	TLR, ROS	(Denoble et al., 2011, Midwood et al., 2009)

Since the discovery of IL-1β protein (catabolin) in a porcine synovial tissue sample and described as responsible for induction of cartilage destruction, the catabolic role of IL-β in controlling OA chondrocytes has been extensively studied (Dingle, 1981, Dingle et al., 1979, Saklatvala et al., 1984). In OA cartilage, altered chondrocytes form complex clonal clusters and cells in these clusters express molecules of the IL-1 family. These include pro-IL-1, IL-1β-converting enzyme (caspase-1), and type 1 IL-1 receptor (IL-1RI). Synthesised pro-IL-1 is converted into its bioactive form following upregulation of the NLRP3 inflammasome through 1) a priming signal from a TLR agonist like lipopolysaccharide (LPS) and 2) activation cues from 'danger'-associated signal like adenosine triphosphate (ATP) (Goldring and Otero, 2011, Dinarello, 1998, Latz, 2010).

Mature IL-1β functions in an autocrine manner, inducing its own secretion, while simultaneously impacting synthesis of other pro-inflammatory cytokines such as TNFα, IL-6, IL-8 (or the CXCL8 chemokine) and the chemokine CCL5/RANTES by chondrocytes in the joint. (Pulsatelli et al., 1999, Aigner et al., 2005, Alaaeddine et al., 2001, Lotz et al., 1992, Guerne et al., 1990). The ability of IL-1β to induce catabolic effects was displayed in a study where intra-articular administration of IL-1β caused severe loss of proteoglycan in the superficial cartilage layer in an OA-rat model (Chandrasekhar et al., 1992). In addition to IL-1β, IL-1R1 over-expression by chondrocytes found near the OA lesions in cartilage enhanced the effects of IL-1β, an effect also observed in human OA SFs (Sadouk et al., 1995, Shlopov et al., 2000). Gene therapeutic strategies using the IL-1 receptor antagonist (IL-1Ra) have shown partial prevention of cartilage damage in *in vivo* models; although effective the concentration must be at least 100 times higher than IL-1β (Santangelo et al., 2012, Pelletier et al., 1997, Caron et al., 1996, Fernandes et al., 1999, Zhang et al., 2004).

IL-18 is another pro-inflammatory cytokine belonging to the IL-1 family and produced by SMs, SFs and chondrocytes in the OA joint. Like IL-1β, the mature form of IL-18 requires caspase-1 activation and NLRP3 complex formation. In OA, elevated levels of caspase-1 in the synovium and articular cartilage further promote the production of IL18 and IL-1β (Udagawa et al., 1997, Möller et al., 2003, Saha et al., 1999). Upregulation of IL18Rα receptor on the surface of chondrocytes causes excessive production of MMP1, MMP3 and MMP13.

This upregulation also causes depletion of proteoglycan, aggrecan, and type II collagen, inducing altered chondrocyte behaviour and apoptosis (John et al., 2007a, Dai et al., 2005, Joosten et al., 2004). Similar to IL-1β, TNF-α is a critical pro-inflammatory cytokine that binds to receptors on the surface of chondrocytes and is typically found in high levels in serum and synovium of patients with knee OA (Schlaak et al., 1996, Stannus et al., 2010). It also exerts a catabolic response by activating chondrocyte-mediated protease production (Kapoor et al., 2011). TNF-α and IL-β alone or together, cause abnormal activation of NF-κB and MAPK pathways in OA chondrocytes. Since NF-κB signalling is a regulator of inflammatory processes in these cells, the inflammatory cytokines can drive the cells to over-express MMPs, nitrous oxide synthase 2 (NOS2), cyclooxygenase-2 (COX2) and IL-1 and supress the expression of ACAN and COL2A1, required for maintenance of the terminally differentiated, stable chondrocyte phenotype (Goldring and Otero, 2011, Goldring, 2012).

The pro-inflammatory role of NF-κB in OA development has previously been shown both *in vitro* and *in vivo* (Bondeson et al., 2007, Amos et al., 2006). Over-expression of the inhibitory subunit kappa-B-alpha inhibited NFκB (IκB) post adenoviral transfer in SFs of OA patients, suppressed the secretion of TNF-α, IL-6, IL-8, monocyte-chemoattractant protein-1 (MCP-1/CCL-2), MMP1, 3, 9, 13 and oncostatin M. In another study, IL-1β stimulated expression of ADAMTS-4 but not ADAMTS-5 was impeded by IκB over-expression (Amos et al., 2006). In a surgically induced rat model of OA, adenoviral delivery of an siRNA specific for NF-κB-p65 resulted in complete inhibition of NF-κB. This approach not only prevented p65 expression but also significantly decreased the stimulation of TNF-α and IL-1β in synovial fluid, lowering clinical signs of synovitis and cartilage degeneration (Chen et al., 2008, Haseeb and Haqqi, 2013).

As described earlier, OA chondrocytes also display hypertrophy, expressing high levels of MMP13. In this context, activation of the MAPK pathway occurs via ERK (Extracellular Signal-Regulated Kinase), JNK (c-Jun N-terminal kinase) and the p38 kinase signalling cascade further leading to induction of COL10A1 and MMP13 gene expression in OA chondrocytes (Nishitani et al., 2010, Goldring, 2012). Similarly, the WNT signalling pathway is critical in determining chondrocyte cell fate and homeostasis, and previous genetic data indicated that aberrant WNT signalling can induce early chondrocyte

hypertrophy/de-differentiation, a sign of OA development (Yuasa et al., 2008, Luyten et al., 2009, Loughlin et al., 2004). For instance, WNT5a and 5b induced *in vitro* chondrogenesis in mesenchymal stem/stromal cells (MSCs) by activating cartilage nodule development and controlling the expression of cell cycle regulators like cyclinD1 and p130 (Ladher et al., 2000, Yang et al., 2003). In two independent studies, IL-1 treatment of rabbit and human chondrocytes resulted in significant upregulation of WNT5a and β-catenin, causing inhibition of type II collagen production and increased type I collagen and MMP13 expression ultimately leading to cartilage destruction (Ryu and Chun, 2006, Sassi et al., 2014b).

IL-6 is one among the three main cytokines to be produced during synovial inflammation apart from IL-1β and TNF-α (Chevalier et al., 2013). Activation of mature IL-6 occurs following IL-6 receptor complex formation and stimulation of the STAT1/STAT3 (Signal transducer and activator of transcription 1/3) pathway (Zhong et al., 1994). Although there is strong evidence of catabolic IL-6 activity in the synovial fluid and cartilage of OA patients, this cytokine also acts in a pleotropic and regulatory manner (Kishimoto, 2006, Goldring, 2000). Both IL-6 and IL-8 do not have the capacity to activate cartilage degradation alone or directly, rather they are produced by human SFs and chondrocytes in response to IL-1β (Guerne et al., 1989), TNF-α (Guerne et al., 1990), prostaglandin E_2 (PGE_2) (Inoue et al., 2002, Tetlow and Woolley, 2006), IL-17, IL-18 (Wojdasiewicz et al., 2014) or stromal cell-derived factor 1/C-X-C motive chemokine 12 (SDF-1/CXCL12) (Chen et al., 2011). IL-6 is one of the principal molecules responsible for the recruitment, proliferation and differentiation of T- and B-cells to sites of synovial inflammation (Kishimoto, 2006, Gabay, 2006).

Leukemia inhibitory factor (LIF) is an important member of the IL-6 cytokine family. It is a catabolic cytokine that triggers cartilage proteoglycan resorption, nitric oxide (NO) production and synthesis of MMPs during OA pathogenesis (Henrotin et al., 1996, Goldring, 2000). In contrast to its pro-inflammatory action, de Hooge et al. demonstrated the regulatory/protective role of IL6 in OA development where mice deficient in IL-6 showed enhanced cartilage loss in a spontaneous aging model of OA (de Hooge et al., 2005).

Elevated levels of IL-15 and IL-17 in the synovial fluid in early stages of knee OA has been documented and these two cytokines are involved in inducing the differentiation and proliferation of T ($CD4^+$ and $CD8^+$) cells, NK cells and mast cells (Suurmond et al., 2015, Waldmann and Tagaya, 1999, Korn et al., 2009). In addition to this Scanzello et al. showed that these cytokines also stimulate MMP1, MMP3 and IL-6 in the synovial fluid of OA patients (Scanzello et al., 2009).

Like cytokines, previous reports have shown the presence of a chemokine profile in the synovial fluid and their over-expression by human chondrocytes in OA (Endres et al., 2010). Chemokines are smaller secreted molecules involved in chemotaxis of immune cells (Haseeb and Haqqi, 2013). Some of the critical chemokines reported in OA are: macrophage inflammatory protein-1alpha/chemokine (C-C motif) ligand 3 (MIP-1α/CCL-3), macrophage inflammatory protein-1beta/ chemokine (C-C motif) ligand 4 (MIP-1β/CCL-4), MCP-1/CCL-2, RANTES/CCL-5, IL-8/CXCL-8 and chemokine (C-X-C motif) ligand 1 (CXCL1) (Borzì et al., 1999). CXCL-1 in combination with different cytokines produced varying deleterious effects on chondrocytes. In one study, human chondrocytes underwent cell death, displaying signs of necrosis and apoptosis in the presence of CXCL12 and CXCL1 (Wei et al., 2010, Borzi et al., 2002). Another study by Merz et al. showed that CXCL1 in combination with CXCL8 induced calcification and hypertrophic differentiation in chondrocytes (Merz et al., 2003). In addition to inflammation, IL8/CXCL8 expression is triggered by mechanical stimuli and metabolic stress (Chauffier et al., 2012).

1.2.5 Alarmins and their 'DAMPening' effects in OA

Among the cascade of catabolic events, synovial inflammation, subchondral bone modifications, angiogenesis and cartilage ECM breakdown are important clinical processes thought to occur either in the early stages or throughout OA progression (Weinans et al., 2012, Ayral et al., 2005, Sellam and Berenbaum, 2010). As a consequence, tissue damage, mechanical and cellular stress is induced and this causes the activation of endogenous danger/warning signals called alarmins (Oppenheim and Yang, 2005). These alarmins are a class of DAMPs that get released by activated, apoptotic or even altered cells like OA synoviocytes, modified chondrocytes or necrotic bone cells (Nefla et al.,

2016). They trigger innate immune responses and predominantly contribute towards chronic inflammation by acting as ligands that recognise and bind to PRRs such as TLRs: TL2 and TLR4 and RAGE (Bianchi, 2007, Sokolove and Lepus, 2013, Rosenberg et al., 2017). Activated PRRs stimulate downstream signalling pathways and produce pro-inflammatory mediators like cytokines, chemokines aggrecanases, proteolytic enzymes and MMPs, as previously discussed.

Alarmins are therefore key molecules in the context of OA initiation and inflammation based on two of their fundamental properties: 1) under normal physiological conditions, alarmins regulate cell proliferation, DNA transcription, differentiation and calcium homeostasis and 2) they have the capacity to bind and crosslink multiple receptors or PRRs on the same cell, activating synergistic yet distinct signalling pathways (Chan et al., 2012, Foell et al., 2007, Nefla et al., 2016). Hence one can hypothesise that increased understanding and targeting of alarmins in OA therapy can potentially attenuate the disease. Among the alarmins implicated in OA, high-mobility group box 1 protein (HMGB-1) and the S100 family of proteins are the two intracellular alarmins recognised by RAGE and TLRs in the OA joint (Sokolove and Lepus, 2013, van Lent et al., 2012, Liu-Bryan and Terkeltaub, 2010). The S100 family of proteins are one of the most extensively studied alarmins in both inflammatory arthritis and OA. The catabolic effects of these molecules in OA include synovial inflammation, angiogenesis, cartilage degradation, hypertrophic differentiation of chondrocytes, production of inflammatory cytokines and osteophyte development.

Some of the well-documented S100s in the serum and synovial fluid of OA patients are: S100A4, A8, A9, A10, A11, A12 and S100B (Nefla et al., 2016). However, the focus of this section is to review the data reporting the role of S100A8/A9 in inflammation and cartilage breakdown in OA. S100A8 and S100A9 are calcium binding proteins that regulate the pathways controlling the cytoskeleton, movement, migration, and adhesion in a calcium-dependent manner (Sunahori et al., 2006, Zreiqat et al., 2010). Evidence of S100A8 and A9 roles in pain generation, activation in SMs and high levels of secreted S100A8/A9 heterodimer complex leading to synovitis have been reported in *in vivo* models of antigen induced arthritis (AIA) and OA(Zreiqat et al., 2010, van Lent et al., 2003, Nabbe et al., 2003). The S100A8/A9 complex binds to surface PRRs like RAGE

and TLR4 and enables higher volumes of leukocyte recruitment to the inflammatory environment (Sunahori et al., 2006). When stimulated with IL-1, human chondrocytes express S100A8 and A9 in addition to S100B, which causes activation of ERK and NF-ϰB pathways, leading to MMP13 expression; hence chondrocyte hypertrophy and cartilage degradation occurs (Zreiqat et al., 2010, Loeser et al., 2005, Donato, 2013).

Extensive studies conducted by van Lent et al. showed the role of S100A8 and A9 in human and collagenase-induced murine OA. The group demonstrated that mice deficient in S100A9 displayed a significant reduction in disease severity (van Lent et al., 2012). Similarly, Schelbergen and colleagues showed that stimulation of human OA chondrocytes with S100A8 and A9 resulted in a TLR4-driven downregulation of aggrecan and type II collagen and upregulation of IL-6 and MMPs 1, 3, 9 and 13, evidence for S100-mediated cartilage catabolism (Schelbergen et al., 2012). S100A8 and A9 or the S100A8/A9 heterodimer complex are indeed potential biomarkers to predict and analyse alarmin-driven OA cartilage damage *in vitro* and *in vivo*, based on the evidence that elevated and prolonged retention of S100A8 and S100A9 levels in OA patients, was indicative of a higher risk of developing severe OA (van Lent et al., 2012, Vogl et al., 2018, Björk et al., 2009).

1.2.6 Role of inflammasomes in OA

Among the family of PRRs activated during infection and inflammation, the NOD-like receptor (nucleotide binding domain and leucine-rich repeat containing receptor; NLR) contributes to the formation of large cytosolic multiprotein complexes called inflammasomes (Palm et al., 2014, Schroder and Tschopp, 2010). NLRP3 is well-studied as a factor involved in inflammasomes and their assembly in response to LPS and contributes to caspase-1 activation and subsequent release of mature IL-1β and IL-18 (Cullen et al., 2015). NLRP3 assembly followed by caspase-1 activation is also induced by high levels of extracellular ATP via the P2X7 receptor and potassium (K^+) efflux (Franchi et al., 2007). In the context of inflammation and OA development, ATP is one of the critical DAMPs that interacts with the PRR:LPS complex (TLR4 activator) and causes release of reactive oxygen species (ROS) from chondrocytes and synovial cells undergoing cell stress.

Studies have previously shown NLRP3-mediated, LPS/ATP-induced pyroptosis in OA fibroblast-like synoviocytes and calcification of cartilage in knee OA (Zhao et al., 2018, Shi et al., 2018, Ryan et al., 1992). Another class of DAMPs seen in the vast majority of knee and hip OA patients requiring arthroplasty are crystals such as: basic calcium phosphate (BCP) (Gordon et al., 1984), calcium pyrophosphate dihydrate (Midwood et al., 2009) and monosodium urate (MSU) or uric acid (Denoble et al., 2011). The presence of BCP crystals enhanced the secretion of IL-1β by macrophages and monocytes via NLRP3 activation (Pazár et al., 2011). Hydroxyapatite is the main type of BCP crystal found in OA joints. Data from both *in vitro* and *in vivo* studies have shown that hydroxyapatite crystals activate NLRP3 and this process is dependent on K+ efflux, phagocytosis and ROS production. This data indicates that the pathogenic effects of hydroxyapatite in OA is mediated by NLRP3, followed by cartilage degeneration and synovitis via production of IL-1β, IL-18, and MMPs (Jin et al., 2011) High levels of uric acid and a 5.4-fold increase in NLRP3 protein expression in the synovial membrane of patients with knee OA correlated with the consequential generation of ROS and secretion of IL-1β and IL-18.

These reports depict the role of NLRP3 in aiding the release and interaction of two critical cytokines, IL-1β and IL-18, known to contribute towards chondrocyte death and cartilage catabolism in OA (Olee et al., 1999, Clavijo-Cornejo et al., 2016, Denoble et al., 2011, McAllister et al., 2018). In conclusion, NLRP3 activation in OA and related inflammation provides a reason to utilise this DAMP member as a diagnostic marker for the development of therapeutic strategies to halt OA progression by targeting its role in activating IL-1β.

1.3 Anti-inflammatory cytokines in OA: Interleukin-10 as a potential target

During the process of OA development, synovial inflammation and cartilage degradation are the two main intertwined processes in joints as described earlier. As a consequence, activated synovial cells produce high levels of pro-inflammatory cytokines, collagenases and other hydrolytic enzymes, creating a deleterious feedback loop involving cartilage breakdown and synovitis. Synovial cells and chondrocytes attempt to counteract this inflammatory response by releasing anti-inflammatory cytokines like: interleukin-4 (IL-4),

interleukin-13 (IL-13), interleukin-10 (IL-10) and IL-1Ra, based on their presence in the synovial fluid of patients with OA (Sellam and Berenbaum, 2010, Goldring, 2000, Martel-Pelletier et al., 1999). These anti-inflammatory cytokines reduce or inhibit the production of PGE_2, IL-1β, TNF-α and MMPs and additionally induce the secretion of tissue inhibitor of metalloproteinase (TIMP) (Pelletier et al., 2001).

IL-10 in particular, is a well-established immunoregulatory cytokine with pleotropic properties. It is the most widely studied cytokine known to predominantly have an anti-inflammatory effect in the context of inflammation and immunomodulation in arthritis (both RA and OA) (Iannone et al., 2001, Asadullah et al., 2003). Mossman and colleagues originally identified a cytokine synthesis inhibitory factor (CSIF) produced by mouse Th2 cells with a capacity to inhibit the activation of IFN-γ by Th1 cells. This factor was later described as IL-10 which plays a key role in regulating the proliferation and differentiation of B cells, NK cells, mast cells, granulocytes, cytotoxic and helper T cells, dendritic cells, endothelial cells and keratinocytes (Fiorentino et al., 1989, Moore et al., 2001, Rousset et al., 1992).

Apart from Th2 cells, macrophages and monocytes also produce IL-10 and this production aids in inhibiting their release of IL-1, TNF, IL-6 and IL-8 and the antigen-presenting capacity of monocytes during inflammation (de Waal Malefyt et al., 1991b, de Waal Malefyt et al., 1991a). Structural analysis of IL-10 by X-ray crystallography revealed that the murine form is a 35kDa heterodimer and human IL-10 is a 37kDa with similar CSIF activity. Activation occurs when the cytokine binds to the interleukin-10 receptor (IL-10R) complexes via JAK1 and STAT3 pathways. Recombinant human IL-10 and viral IL-10 are smaller polypeptides of 17-18kDa (de Waal Malefyt et al., 1991a, Moore et al., 1990, Moore et al., 2001, Asadullah et al., 2003). During synovial inflammation and cartilage degradation, TNF-α is one of the main pro-inflammatory cytokines released (Saklatvala, 1986). However, studies have shown the capacity of IL-10 to reduce or inhibit TNF-α secretion in OA. In one study, the addition of IL-10 to synovial fibroblast cells from patients with OA resulted in a reduction of TNF-α and PGE_2 release (up to 90% compared to controls) (Alaaeddine et al., 1999). In another recent study, stimulation of human synovial fibroblasts with TNF-α increased protein synthesis of several catabolic MMPs and IL-10, indicative of a defensive/regulatory role of IL-10 during inflammation

in OA (Mrosewski et al., 2014). Similar to production of catabolic factors by synovial cells in response to PRRs like TLRs, infiltrating macrophages, APCs and DCs also express high levels of IL-10; an event by which IL-10 demonstrates immunoregulation (Saraiva and O'garra, 2010).

Another important role of IL-10 is chondroprotection. Both IL-10 and IL-10R are expressed by human chondrocytes and this production aids in stimulating the synthesis of type II collagen and aggrecan, inhibiting MMP production and prevention of chondrocyte apoptosis. Secondly, IL-10 administration also enhanced synthesis of proteoglycan in both healthy and OA cartilage *in vitro* (Iannone et al., 2001, John et al., 2007b, EEKB and Siquan žEf, 2001). A number of studies have also demonstrated the anti-apoptotic property of IL-10. Human articular cartilage explants subjected to axial unconfined compression injury showed significant nuclear blebbing, cell death and elevated expression of MMP-3, MMP-13, ADAMTS-4 and NOS2. However, following IL-10 administration all these catabolic events were dramatically reduced, indicative of IL-10 mediated chondroprotection (Behrendt et al., 2016).

In another recent study, with the same compression injury model, administration of IL-10 following injury to bovine articular cartilage resulted in significantly lower expression of *COL1A1* and COL10A1 and elevated expression of *SOX9*, *ACAN* and *COL2A1*. In addition to this, culture of cellularized collagen ACI grafts with human IL-10 showed improved cartilage matrix formation and chondrogenic differentiation, suggestive of the ability of IL-10 in preventing cartilage damage and promoting chondrogenesis simultaneously (Behrendt et al., 2018). Recent *in vitro* and *in vivo* studies have also suggested an immunoregulatory and anti-apoptotic mechanism of IL-10 via dampening the assembly of the NLRP3 inflammasome and inhibition of caspase-8 and IL-1β activation in models of epileptic seizure and AIA (Gurung et al., 2015, Sun et al., 2019, Greenhill et al., 2014). Evidence from the above studies support the use of IL-10 as a potential drug candidate for OA attenuation.

1.4 Cell therapy for OA: MSC mediated immunomodulation in OA

To date ACI is the only FDA approved cell-based therapy for OA patients. Despite demonstrating therapeutic success in terms of patient improvement, ACI is associated with a number challenges such as efficacy limited to localised cartilage defects, low

proliferative capacity and undesired dedifferentiation of chondrocytes and lack of long-term follow-up (Harrell et al., 2019). MSCs are multipotent adult cells that are fibroblastic in nature, based on their origin from the stromal compartment of bone marrow first reported by Friedenstein and colleagues (Friedenstein et al., 1970, Friedenstein et al., 1966, Owen and Friedenstein, 1988). Although marrow has been the primary source of MSCs to date, these cells have also been successfully isolated from umbilical cord blood (Weiss and Troyer, 2006), skeletal muscle (Crisan et al., 2008), adipose tissue (Bunnell et al., 2008) and Wharton's jelly (Troyer and Weiss, 2008). As progenitor cells of multiple origins, MSCs also display multi-lineage differentiation *in vitro* into tissues that form mesodermal lineage such as cartilage, fat, bone and muscle (Barry and Murphy, 2013).

MSCs have been in the limelight of orthopaedic research as an attractive option for OA cell therapy, due to a number of reasons. These include the capacity to expand with sustained proliferation, differentiation into chondrocytes in spite of undergoing multiple passages *in vitro* and minimal immunological rejection following engraftment are some of the basic beneficial characteristics of these cells (Harrell et al., 2019).

In addition to this, the property of paracrine signalling via secretion of bioactive active molecules enables MSCs to achieve therapeutic efficacy demonstrated by immunomodulation, angiogenesis, anti-apoptosis, chemo-attraction, wound-healing and aid in proliferation and differentiation of neighbouring stem and progenitor cells (Duijvestein et al., 2011, Liu et al., 2018b, Lee et al., 2013). MSCs modulate inflammation in the joint by sensing the inflammatory molecules in the microenvironment and alter their phenotype accordingly (English, 2013, Bernardo and Fibbe, 2013, Németh et al., 2009). For instance, they adopt an anti-inflammatory phenotype in response to high levels of TNF-α and IFN-γ through TLR3 signalling. As a result, MSCs secrete large quantities of indolamine 2, 3 dioxygenase (IDO), NO, TGF-β, PGE_2, hepatocyte growth factor (HGF), and hemoxygenase (HO) leading to suppression of T cell proliferation (Tomchuck et al., 2008). In a non-inflammatory environment, MSCs polarise to a pro-inflammatory phenotype under the influence of low levels of LPS-induced TLR4 signalling. Under this phenotype, MSCs secrete chemokines like RANTES, C-X-C Motif Chemokine Ligand 9 (CXCL9), C-X-C Motif Chemokine Ligand 10 (CXCL10), MIP-1α and MIP-1β (Ren et al., 2008). These chemokines in turn engage in recruitment of lymphocytes to sites of inflammation by binding to receptors on T cells and ultimately

leading to MSC-mediated T cell regulation. This pre-organised switch between pro- and anti-inflammatory phenotypes is one mechanism whereby MSCs promote host defence and joint repair and prevent excessive tissue damage (Waterman et al., 2010, Bernardo and Fibbe, 2013, Li et al., 2012). MSCs also regulate activated immune cells in the joint by inducing production of anti-inflammatory cytokines, IL-10 in particular. Infiltrating macrophages in the synovium produce high amounts of IL-1 and TNF and by adapting an anti-inflammatory phenotype, MSCs convert these macrophages to IL-10 producing immunosuppressive cells. Similarly, MSC-secreted PGE_2 binds to specific receptors on these macrophages and stimulates the production of IL-10, thereby suppressing inflammation of the joint (Németh et al., 2009). MSCs therefore act as sensors/switchers of inflammation and modulate the joint environment by suppressing activated immune cells either by juxtacrine or paracrine signalling.

1.5 MSCs as mediators of anti-inflammation: an MSC: IL-10 story

Another positive aspect associated with MSCs is their ability to escape immune rejection and traffic to sites of injury. This enables them to act as carriers of immunosuppressive agents/cytokines or undergo genetic engineering in order to express therapeutic proteins (Jorgensen et al., 2003). Viral transduction of MSCs has been carried out successfully with an efficiency of up to 85% using retroviral vectors (Harrington et al., 2002). A number of *in vivo* studies have demonstrated the efficacy of IL-10 produced by transduced MSCs-expressing the cytokine (Manning et al., 2010, Nakajima et al., 2017, Apparailly et al., 2002). In 2008, Choi et al., successfully performed the first systemic administration of MSCs over-expressing retroviral-transduced IL-10 to mice with symptoms of rheumatoid arthritis in a collagen-induced arthritic mouse model. Treatment with MSCs or the vehicle alone did not show much inhibition of arthritis. However, the group treated with IL-10-expressing engineered MSCs demonstrated disease inhibition, suppression of an autoimmune response to type II collagen and regulated cytokine production (Choi et al., 2008). In a recent study using a murine model of collagenase-induced OA (CIOA), treatment with human MSCs over-expressing viral interleukin-10 (vIL10) resulted in reduction in populations of activated CD4+ and CD8+ T cells (Farrell et al., 2016). Interestingly, a previous study on anti-inflammatory gene delivery demonstrated uniform therapeutic efficacy of human, viral and mutant IL-10 in a rabbit model of AIA (Keravala

et al., 2006). Therefore, engineering MSCs to express or deliver vIL10 could potentially regulate their secretome profile towards immunomodulation in OA.

1.6 Tissue engineering strategies using 3D encapsulation of MSCs

Marrow-derived human MSCs have been extensively studied as a potential cell therapy for cartilage regeneration and tissue repair. Several pre-clinical and clinical studies have tested the efficacy of autologous, allogenic and xenogeneic MSCs via intra-articular injections for cartilage repair (Orozco et al., 2013, Kasemkijwattana et al., 2011, Emadedin et al., 2012, Murphy et al., 2003, Kim et al., 2014, Pigott et al., 2013, Saulnier et al., 2015, Hatsushika et al., 2013, Barry, 2019). Their capacity to undergo multi-lineage differentiation including chondrogenesis and self-renewing potential (Ma et al., 2012) make them a potential cell source for generating neo-cartilage. In addition, MSCs also allow simultaneous analysis of temporal changes in chondrogenic genes involved in ECM alterations leading to altered chondrocyte behaviour during OA (Ma et al., 2012, Debnath et al., 2015, Xu et al., 2008). The field of tissue engineering offers hope to repair damaged tissues using functional replacement constructs made of biocompatible scaffolds seeded with cells of interest i.e., MSCs (Diduch et al., 2000, Yamagata et al., 2018). The process of encapsulation of MSCs also enables the potential to isolate and study MSC-mediated paracrine signalling, changes in gene expression patterns and cell-matrix interactions during chondrocyte differentiation and hypertrophy in OA (Ibarra et al., 2000, McKinney et al., 2019, Xu et al., 2008).

Numerous types of scaffolds have been used in cartilage tissue engineering to investigate MSC differentiation and natural hydrogels are among the most commonly studied (Yamagata et al., 2018, Awad et al., 2004). Among the types of natural hydrogels, sodium alginate derived from marine algae has been a preferred choice of scaffold to culture MSCs and chondrocytes (Debnath et al., 2015, van Susante et al., 1995, Rowley et al., 1999, Barry et al., 2001). Previous studies have shown that alginate facilitated a softer mechanical environment which enabled maintenance of a rounder chondrocyte morphology, optimal chondrocytic phenotype and enhanced stronger gene and protein expression of SOX9, aggrecan and type II collagen (Ma et al., 2012, Xu et al., 2008, Hwang et al., 2007). Xue et al. successfully demonstrated the capacity of human MSCs cultured on softer gels to

differentiate into a chondrocytic phenotype, irrespective of initial seeding density. This is not possible with chondrocytes due to their tendency to dedifferentiate and adopt a fibroblastic phenotype *in vitro* (Cucchiarini et al., 2015, Chubinskaya et al., 2001). Chelluri and co-workers showed that 3D encapsulation of human adipose derived stem cells in alginate resulted in uniform cell distribution and enhanced chondrogenic marker expression when compared to 2D pellet cultures with lower growth potential (Debnath et al., 2015). There is also *in vivo* evidence of cartilage matrix formation by MSCs encapsulated in alginate (Pleumeekers et al., 2014, de Vries–van Melle et al., 2013). Apart from enabling cartilage regeneration, alginate acts like a semi-permeable membrane for MSCs to secrete trophic factors into the surrounding environment and modulate inflammation as demonstrated by *in vitro* models of LPS-induced neuro-inflammation (Stucky et al., 2015, Stucky et al., 2017).

1.7 Feasibility of MSCs for long-term cartilage repair/reconstruction

In the context of inflammation-triggered cartilage damage in OA, one study conducted by Fahy et al. has demonstrated the anti-chondrogenic effect of OA synovial conditioned medium (SCM) in MSC-alginate beads. These authors further identified that M1 (classically activated) polarised macrophages in the SCM were responsible for hindering the chondrogenic differentiation of MSCs (Fahy et al., 2014). Despite their therapeutic potential via paracrine signalling, bone-marrow derived MSCs tend to form fibrocartilage and demonstrate chondrocyte hypertrophy, seen with production of collagen type X and MMP-13 *in vitro* (Barry et al., 2001, Johnstone et al., 1998, Xu et al., 2008). This tendency towards terminal differentiation may be favourable for tissue engineering strategies related to bone formation mimicking the route of endochondral ossification. (Farrell et al., 2011, Farrell et al., 2008). However, this is not ideal for cartilage regeneration due to the risk of implanted MSCs forming terminally differentiated cartilage showing signs of mineralisation and possible bone formation (Pelttari et al., 2006, Scotti et al., 2010). Articular cartilage progenitors (ACPs) are cell populations residing in the upper zone of adult articular cartilage with evidence that these cells generate stable articular chondrocytes of native tissue through appositional growth (Williams et al., 2010, Dowthwaite et al., 2004, Kozhemyakina et al., 2015, Hayes et al., 2001). ACPs are fundamentally undifferentiated precursors of cartilage, developmentally primed to

become chondrocytes with minimal tendency towards terminal hypertrophic differentiation. Previous studies have demonstrated potential reparative effects of these cells in OA cartilage in response to injury (Jayasuriya and Chen, 2015, Khan et al., 2009a, Williams et al., 2010, Seol et al., 2012, Gerter et al., 2012, Koelling et al., 2009, Nelson et al., 2014, McCarthy et al., 2012) . The use of 3D chondrogenic models comparing MSCs and ACPs to identify primary inflammatory cues/mediators is a novel experimental strategy. This strategy may also enable identification of catabolic factors and possibly pinpoint the mechanisms responsible for aberrant chondrogenic gene expression leading to initiation of cartilage matrix disruption and chondrocyte apoptosis in early stages of OA pathogenesis.

1.8 Hypotheses and aims

OA is a multi-factorial disease of the whole joint with inflammation acting as a driving force in OA pathogenesis. Synovial inflammation and cartilage degradation are two main events contributing to a constant pathological loop and mediated by a number of inflammatory factors and activated immune cells. MSCs are progenitors of the mesenchymal lineage, capable of multi-lineage differentiation including chondrocytes and display immunomodulation via secretion of trophic factors with previous pre-clinical studies demonstrating the regenerative potential of these cells in OA joints via activation of endogenous progenitors. Given the fact that MSCs tend to form fibrocartilage and attain a hypertrophic phenotype during *in vitro* chondrogenesis, there is no data to indicate that these cells cannot successfully differentiate into a stable articular cartilage phenotype. Also, inflammation induced catabolic factors from activated synovium have been shown to negatively impact the use of chondrogenically differentiating MSCs as a therapy for this disease. On the other hand, chondroprogenitors form stable cartilage with the capacity to do this in the appropriate environment.

Therefore two main goals of this thesis were:

1. **To develop an inducible anti-inflammatory cell-based therapy and evaluate the efficacy of controlled vIL10 expression by MSCs towards attenuation of immune responses in OA and**
2. **To establish *in vitro* models of terminal and stable cartilage for investigation of inflammation-driven cartilage damage in OA.**

The aims and hypothesis of each chapter are as follows:

Chapter 2: Development of a stable and efficient method of vIL10 over-expression by adenoviral transduction of murine MSCs (mMSCs)

Hypothesis: Bone marrow derived mMSCs regulate and enhance the expression of vIL10 using the Tetracycline system under the influence of doxycycline**.**

Specific aim: The main aim of this chapter was to develop a stable method of efficient adenoviral transduction in MSCs. To achieve this, three biological preparations of bone marrow derived mMSCs were isolated, expanded and characterized. Secondly, two different types of adenoviral vectors contained in a CMV promoter; a direct vIL10 expressing adenoviral construct and a drug-controlled vIL10 expressing construct was compared and tested on mMSCs. Finally, the optimal dose and time point to achieve high levels of inducible vIL10 overexpression by MSCs was identified in order to generate engineered MSCs with a capacity to display positive immunomodulation.

Chapter 3: Assessment of immunomodulatory effects of vIL10 over-expressing MSCs on activated macrophages and T cells *in vitro*.

Hypothesis: Tetracycline induced vIL10 MSCs modulate inflammatory processes *in vitro* in a juxtacrine and paracrine manner.

Specific aims: The aim of the work performed was to test the anti-inflammatory ability of engineered vIL10 MSCs on activated immune cells. For this, bone-marrow derived murine macrophages (BMs) and T cells from mouse spleen were stimulated *in vitro* and treated with different mMSC preparations from Chapter 2 and assessed using secretome and/or direct co-culture assays. Immunomodulatory effects of vIL10 MSC treatment on

macrophage polarisation, gene expression of macrophage-secreted pro and anti-inflammatory factors and T cell activation and proliferation were analysed.

Chapter 4: Establishment of a novel in vitro model investigating the impact of acute and chronic inflammatory effectors on cartilage development.

Hypotheses: Inflammasome activation acts as an acute inflammatory insult to induce altered behaviour of stable or terminal chondrocytes and chronic inflammatory input of S100A8/A9 alarmins in conjunction with inflammasome activation promotes an OA-like hypertrophic phenotype.

Specific aims: To develop an *in vitro* cartilage model to study the effects of acute and chronic mediators of inflammation leading to cartilage damage, using ACPs (articular-like cartilage) and MSCs (hypertrophic cartilage). To achieve this, chondrogenic differentiation of bone-marrow derived human ACPs and MSCs was carried out by encapsulating these cells in sodium alginate for 28 days. To examine the impact of inflammatory mediators on cartilage development, ACP and MSC beads were treated with the S100A8/A9 alarmin complex and/or activators of the NLRP3 inflammasome (LPS and palmitic acid). Effects of the dual inflammatory stimuli on cartilage development was assessed using caspase-1 activity, GAG quantitation, histological analysis and gene expression patterns of inflammatory and chondrogenic markers after 28 days of differentiation.

Chapter 2

Development of a stable and efficient method of vIL10 over-expression by adenoviral transduction of mMSCs.

2.1 Introduction

OA is still considered a 'wear and tear' disease of the joint, causing degradation of the articular cartilage (Rezend and Campos, 2013, Kong et al., 2017). Over the last decade, a disease, initially perceived as cartilage driven, is now known to be far more complex. This is due to the role of synovial inflammation or synovitis and release of inflammatory mediators by underlying bone, cartilage itself and synovium, making it an inflammation-mediated condition of the whole joint (Rezend and Campos, 2013, Kapoor et al., 2011, Loeser et al., 2012, Goldring and Otero, 2011). Synovitis, has become an important clinical feature of OA with an increase in joint volume and evidence of higher levels of inflammatory cytokines in serum and synovial fluid in OA patients (Sohn et al., 2012, Pearle et al., 2007). The impact of synovitis extends from early to end stage OA. Other than manifesting as clinical signs like joint swelling, synovitis also displays its detrimental effects at a cellular and molecular level, acting as a trigger of OA progression.

Mechanical load and ECM tissue breakdown can also initiate synovial inflammation. Synovial hypertrophy occurs as a result of products of ECM breakdown accumulating in the synovial cavity, with cells within the synovium acting to phagocytose these products. As a consequence, synovial cells start to release several hydrolytic enzymes such as collagenases that with the input of pro-inflammatory cytokines create a never-ending loop of cartilage degradation and synovitis (Sellam and Berenbaum, 2010). Despite the counteractive efforts of the immune system to halt this inflammatory cascade by producing anti-inflammatory cytokines, the quantities and duration of release is not enough to reverse the loop. Hence there is an urgent need to find a long-term and sustainable anti-inflammatory biological factor or drug for delivery to attenuate the osteoarthritic environment.

IL-10, originally identified in 1989 (Fiorentino et al., 1989) is a well-studied multi-functional cytokine, known for its ability to inhibit activation of macrophages, monocytes and T cells. IL-10 was chosen as the target protein in this chapter, based on its capacity to inhibit cytokine production by NK cells and T cells via indirect inhibition of macrophage/monocyte function, the latter being principal innate cells known to infiltrate and reside in the synovial fluid in OA (Moore et al., 2001, Sellam and Berenbaum, 2010,

Sohn et al., 2012). The field of cellular therapy for OA, has advanced significantly in the last 20 years from ACI being the sole FDA approved cellular therapy to use of stem cell-based approaches taking the spotlight in recent years (Burke et al., 2016). MSCs possess a wide range of advantages for choosing them as a therapeutic vehicle for gene delivery, including and not limited to their self-renewal capacity, differentiation into chondrocytes (neo-cartilage formation), ease of engraftment and migration to injured mesenchymal tissues (Jorgensen et al., 2003, Manning et al., 2010). MSCs have been efficacious for gene therapy with a transduction rate of up to 85% using retroviral vectors and as a vehicle to express therapeutic cytokines such as secreted human erythropoietin, which was detected *in vivo* for 90 days after subcutaneous cell implantation (Harrington et al., 2002, Bartholomew et al., 2001, Jorgensen et al., 2003).

The viral counterpart of IL-10, vIL10 encoded by the EBV gene (BCRF1), is 80% homologous to murine IL-10 and the mature protein sequences of human IL-10 and vIL10 are 84% identical. One critical reason to select vIL10 over human IL-10 for gene therapy, is the absence of immunostimulatory properties in the viral form of IL-10 (Hsu et al., 1990, Go et al., 1990, MacNeil et al., 1990, Moore et al., 1990, Vieira et al., 1991). A number of pre-clinical studies have demonstrated the therapeutic efficacy of delivering vIL10 using adeno/retroviral vectors in models of endotoxemia (Drazan et al., 1996), atherosclerosis (Han et al., 2010), wound healing (Peranteau et al., 2008), cardiac allograft survival (Qin et al., 1995) and particularly rheumatoid arthritis (Ma et al., 1998, Lechman et al., 1999, Vermeij et al., 2015, Broeren et al., 2016). One disadvantage of direct delivery of vIL10 *in vivo* is its short half-life, with the requirement for repetitive administrations to see a therapeutic effect (Ma et al., 1998). On the other hand, using engineered MSCs to express the target cytokines *in vivo* offers an advantage over direct vIL10 delivery due to the combined immunosuppressive property of MSCs and vIL10 (Manning et al., 2010). Choi and co-workers successfully demonstrated attenuation of collagen-induced arthritis following delivery of MSCs overexpressing vIL10 in mice (Choi et al., 2008).

Two critical aspects to be carefully considered while choosing viral vectors for efficient gene therapy are tightly controlled gene activation and a high level of regulated gene expression (Perez et al., 2002). The tetracycline (Tet) mediated gene regulatory system (Gossen and Bujard, 1992) fulfils both criteria and operates either in the presence (Tet-On system) or absence (Tet-Off system) of a pharmacological switch, doxycycline (DOX) to control target gene expression (Schonig et al., 2010, Sato et al., 2013). Apparailly et al. were first to demonstrate successful tetracycline-inducible gene transfer of vIL10 in two consecutive studies in a murine model of experimental arthritis (Apparailly et al., 2002, Perez et al., 2002). A recent study published in 2014 showed the efficacy of the Tet-On system in MSCs expressing the IL-1 receptor antagonist (IL-1Ra) to treat cartilage injuries in OA, where engineered cartilage constructs expressing IL-1Ra displayed inhibition of IL-1-mediated upregulation of MMPs and enhanced GAG production.(Glass et al., 2014).

The current chapter examines the hypothesis that bone marrow derived mMSCs can demonstrate regulated and enhanced expression of vIL10 using the Tet-On system under the influence of doxycycline. The main aim of this chapter was to develop a stable method of efficient adenoviral transduction in mMSCs. To achieve this, three biological preparation of bone marrow derived mMSCs were isolated, expanded and characterized. Secondly, two different types of adenoviral vectors contained in a CMV promoter; a direct vIL10 expressing adenoviral construct and a drug-controlled vIL10 expressing construct were compared and tested on mMSCs to assess the efficiency of direct vs-controlled release of vIL10. Finally, the optimal dose and time point to achieve high levels of inducible vIL10 overexpression by MSCs was identified in order to generate engineered MSCs with a capacity to display positive immunomodulation.

2.2 Materials and methods

2.2.1 Isolation of bone marrow derived mMSCs

Three biological preparations of mMSCs, were generated from the bone marrow of C57BL/6J female mice. For each preparation, 4 mice at approximately 6 weeks (w), were euthanized and the femur and tibia were dissected and placed in a 50ml tube with phosphate buffered saline (PBS, Sigma) containing 1% P/S (100U/ml penicillin and 100 µg/ml streptomycin, Sigma). Using a sharp forceps and scissors, the bones were cleaned to remove muscles and snipped at both ends to enable expulsion of the marrow into a Petri dish containing MSC medium (Appendix 2; Table 1). A 26G needle fitted on a 2ml syringe filled with mMSC medium was used to plunge out the marrow and repeated until the bones appeared white. The marrow was passed through a 40µm cell strainer (Corning®) attached to a 50ml tube and the strainer was washed twice with 10ml MSC medium. The bones were crushed and placed in a sterile Eppendorf (Sarstedt) and digested with 0.4% collagenase I (Sigma, diluted at a 1:1 ratio in MSC medium) by incubating at 37°C for 20min. The collagenase mixture was pooled with the marrow and spun at 400g for 5min. Medium was changed and cell counting performed. The cell suspension (10µl) was mixed with 10µl of 4% acetic acid (Sigma) diluted in 40µl PBS (1:5 dilution) in an Eppendorf and further diluted at a ratio of 1:1 with Trypan Blue (Sigma). Cell counting was performed using a haemocytometer. Based on the mononuclear cell count, approximately 35-40 million cells were seeded per T175cm^2 flask and incubated at 37°C with 5% O_2 (hypoxia). Medium was changed on day 5 and the culture passaged at day 9 to 10 depending on growth of the colonies formed by the MSCs in the marrow sample.

2.2.2 Culture expansion and generation of mMSCs

Cells were passaged at 70 to 80% confluency. The medium was removed from each flask and cells were washed with 15ml of PBS. Adherent cells were detached from the culture surface with 4ml of 0.25% 1X Trypsin-1mM Ethylene diamine tetra-acetic acid (Trypsin-EDTA; Gibco) per flask and incubated at 37°C for 4min. During incubation the process of cell detachment was enhanced by tapping the sides of the flask a few times. Trypsin

was then neutralized with an equal volume of mMSC medium. Cells were counted as previously described and spun down. After spinning at 400g for 5min, the supernatant was discarded and the pellet suspended in a volume sufficient to seed $5x10^5$ cells per flask. Once seeding was completed, the flasks were labelled with the passage (P) number, date, strain and initials, and incubated in hypoxic conditions at 37ºC. Based on the yield obtained from the pooled population at P1, a minimum of $2x10^6$ cells were cryopreserved for future use. Briefly, the required cell number was spun at 400g for 5min at room temperature (RT) and the cell pellet resuspended in 1ml of freezing medium comprising 10% dimethyl sulphoxide (DMSO, Sigma) and fetal bovine serum (FBS, Sigma). The suspension was transferred to a cryovial tube (Thermo Scientific) labelled with the strain, passage number, cell number and date. The vial was placed in a Mr. Frosty (ThermoFisher Scientific) at -80ºC overnight and later transferred to the liquid nitrogen storage container.

2.2.3 Assessment of cumulative population doubling

The growth rate of C57BL/6 mouse MSCs was assessed by calculating the cumulative population doubling (CPD) over time. Following each passage, population doublings were determined based on the number of cells plated (input) and harvested (yield) versus duration of culture time in days. The analysis was performed starting from the end of P2 to P12. To maintain the same conditions with respect to yield, medium changes were done at a set interval of 3 to 4 days and cells were harvested at 80% confluence.

2.2.4 Characterisation of mMSCs

C57BL/6 MSCs were characterized by assessing their ability to differentiate into the three classical mesenchymal lineages i.e., bone, fat and cartilage. For this, differentiation assays namely osteogenesis, adipogenesis and chondrogenesis were performed using cells at P6.

2.2.4.1 Osteogenic differentiation of mMSCs

Cells were trypsinised, neutralized and counted, and seeded at a density of $10x10^3$ cells/well in a 24-well plate (Thermo Scientific) with 1ml mMSC medium/well. A total of 4 sets of control and 4 sets of test wells were set up and incubated at 37ºC, 5% CO_2 until a confluent monolayer was formed. Osteogenic medium (1ml) (Appendix 2; Table 2) was added to the test wells and control wells received 1ml mMSC medium after removal of spent medium. The media were changed every 2 days, ensuring the addition of the correct medium to each well. The cells were harvested between days 10 and 12, based on the appearance of dark mineralized deposits in test wells. Three sets of control and test wells were processed for calcium quantitation and the last set was used for Alizarin Red S staining.

2.2.4.2 Alizarin Red S staining

Alizarin Red S (2%, Sigma) was prepared using deionised water (dH_2O) and the pH adjusted to 4.1-4.3. Control and test wells were washed twice with 1ml PBS and the cells were fixed with ice cold 95% Methanol (Sigma) for 10min, followed by rinsing with dH_2O. Alizarin Red S (1ml, 2% solution) was added and plates incubated at RT for 5min. The stain was then removed and cells washed with dH_2O, leaving some water in the wells for microscopy. The plates were later air-dried and stored at 4ºC in the dark.

2.2.4.3 Quantitation of calcium using StanBio Calcium assay

Media was removed from control and test wells. After washing twice with PBS, cells were scraped from each well after exposure to 0.2ml of 0.5M hydrochloric acid (HCl) and collected in labelled Eppendorf tubes. This step was repeated once and remaining cells were scraped and pooled into the respective tubes. The solution was placed in the shaker overnight at 4ºC and calcium levels measured using the StanBio Calcium Liquicolour kit. Briefly, the calcium standard provided was diluted to generate a range of concentration from 0.05 to 1µg/ml prepared in 0.5M HCl (Appendix 2; Table 3). 10µl of sample or standard was plated in triplicates in a 96-well plate and 200µl of working solution (1:1 working solution of CPC Liquicolor binding reagent and working dye) was added to each well and the plate was incubated at RT for 15min in the dark . The absorbance was read

at 550-650nm using the Victor™ X3 Multimode plate reader (Perkin Elmer). A trendline was derived from the standard curve and the concentration of calcium in each sample was represented as a bar graph.

2.2.4.4 Adipogenic differentiation of mMSCs

Cells were trypsinised, neutralized and counted prior to seeding in a 24-well plate (Thermo Scientific) at a density of $2x10^4$ cells/well. Three control and 3 adipogenic test wells were set up using mMSC medium and incubated at 37ºC, 5% CO_2 till the monolayer formed was confluent. Once confluent, 1ml/well adipogenic induction medium (Appendix 2; Table 4) was added to the test wells and left for 3 days. The control wells received the same volume of mMSC medium. After 3 days, the medium in test wells was changed to 1ml/well of maintenance medium (Appendix 2; Table 5) and left for 1 day. The medium in control wells were replaced with mMSC medium Three cycles of changing from induction to maintenance media were performed and during the final maintenance step, cells were left in the maintenance medium for 5 days. The cells were then processed for Oil Red O staining.

2.2.4.5 Oil Red O staining

A working solution of Oil Red O (Sigma) was prepared by mixing 6 parts of Oil Red O stock solution with 4 parts of dH_2O. This was left to stand for 10min followed by filtration using a Whatman no.1 filter (Fisher Scientific). Medium was removed from all wells and cells rinsed twice with PBS. The cells were then fixed using 1ml of 10% neutral buffered formalin (Sigma) for 10min to 1h at RT. Formalin was discarded and the plate was rinsed with dH_2O. Oil Red O working solution (1ml) was added and left for 5min. The stain was discarded and excess stain cleared by adding 1ml/well of 60% isopropanol (Sigma). The plate was then rinsed under tap water and stained with 0.5ml/well of hematoxylin (Sigma) working solution made up as 1:5 parts of dH_2O. The stain was left for 1min and wells washed with warm tap water until clear; some water was left in the well for photography.

2.2.4.6 Chondrogenic differentiation of mMSCs

Cells were trypsinised, neutralized, counted and seeded at a density of $5x10^5$ cells/pellet culture. A total of 12 cultures with control (6) and test (6) were set up for harvesting on day 21. The required number of cells for all pellet cultures were placed in a tube and centrifuged at 400g for 5min. The cells were resuspended in incomplete chondrogenic medium (ICM) (Appendix 2; Table 6) and cell suspensions were aliquoted into microfuge tubes (Sarstedt) with $5x10^5$ cells/tube. The tubes were spun at 100g for 5min using the Eppendorf 5417C Centrifuge and control cells resuspended in ICM. Test samples were resuspended in 0.5ml complete chondrogenic medium (CCM). CCM was prepared fresh each time by adding 0.5µl of 10ng/ml TGF-β3 (Peprotech) and 2µl of 100ng/ml BMP-2 (Peprotech) per 1ml of ICM. All tubes were spun at 100g for 5min and caps of all tubes (ICM and CCM) were loosened and placed in the incubator at 37ºC in hypoxic conditions. Medium was changed thrice a week without disrupting the pellet using 0.5ml ICM or CCM. After 21 days, the pellets were washed twice with PBS. Pellets of 3 cultures were then allowed to air-dry and stored at minus 80ºC until required for measurement of glycosaminoglycan (GAG) and DNA. The remaining 3 cultures were processed for histology and Safranin O staining.

2.2.4.7 Histological analysis

Pellets were washed, collected and fixed with 1ml of 10% formalin for 1h. After fixation the pellets were prepared for histological processing through the Leica tissue processor and run overnight in the following steps: 70% IMS 1h, 90% IMS 1h, 100% IMS 1h (replaced and repeated three times (x3)), Xylene (Sigma) 1h (x3) and melted paraffin wax 1h (x3). Samples were then embedded in paraffin wax using the wax embedding station (Leica) and the wax block placed on a cooling block (Leica) to harden the wax. 5µm sections of each pellet were cut using a microtome (Leica) and placed on Superfrost plus slides (Thermo Scientific). The slides were heated at 60ºC in a slide oven (Leica) for 1.5-2h prior to use. Representative slides for each pellet were chosen for the staining procedure.

2.2.4.8 Safranin O staining

Selected ICM and CCM slides were stained as follows: 100% xylene for 5min, 100% xylene for 5min, 100% IMS for 2min, 100% IMS for 2min, 95% IMS for 1min, 70% IMS for 1min, dH_2O 1min, 0.02% Fast Green FCF (w/v) (Sigma) for 4min, 1% acetic acid (Sigma) for 3s, 0.1% Safranin-O (Sigma) for 6min, 95% IMS for 1min, 100% IMS for 2min, 100% IMS for 2min, 100% xylene for 2min, 100% xylene for 2min. The slides were mounted with the distyrene plasticizer xylene (DPX; Sigma), cover slipped and left to air dry in the fume hood.

2.2.4.9 Quantitation of GAG

Prior to starting the assay, the chondrogenic pellets were digested overnight at 60ºC in 200µl solution of papain (Sigma) at a final concentration of 0.1mg/ml. Papain solution was prepared in a dilution buffer (Appendix 2; Table 7). 1,9 Dimethyl methylene blue (DMMB; Sigma) stock solution (Appendix 2; Table 8) was prepared and pH was adjusted to 1.5. The samples were vortexed to ensure pellet disruption. Chondroitin-6-sulfate (C-6-S; Sigma) at a concentration of 400µg/ml was diluted 1:5 in dilution buffer to give a working stock (80µg/ml) and was used to make dilutions for the standard curve (Appendix 2; Table 9). The appropriate standards or samples (25µl) were added to a 96-well plate. All standards and samples to be assayed were set up in triplicate. Dilution buffer (75µl) and 200µl of DMMB stock solution was added to each well and incubated at RT for 5min. The plate was read at 595nm using Victor™ X3 Multimode plate reader.

2.2.4.10 Measurement of DNA using PicoGreen assay

The assay was performed using the Quant-iT PicoGreen dsDNA assay kit (Molecular Probes). A 1X Tris-EDTA (TE) solution was prepared from the 20x stock provided in the Quant-iT Kit (1.2ml for each sample and 6ml for standards). A dilute PicoGreen solution, 200-fold dilution of dimethyl sulfoxide (DMSO) stock in 1xTE was then prepared. DNA stock (100µg/ml) at a working concentration of 2µg/ml (20µl stock+980µl 1XTE) was used to prepare the standard curve (Appendix 2; Table 10). The samples were diluted 1:20 (20µl sample + 380µl 1xTE). Relevant standards or samples in triplicate (100µl) were added to the wells of a 96-well black plate (Thermo Scientific).

100µl of PicoGreen solution was added to each well and incubated at RT for 2-3min, protected from light. The plate was read on a fluorescent plate reader using a Pico DNA protocol (excitation at 485nm, read at 538nm) and the final results were expressed as the amount of GAG/pellet as a ratio of the amount of DNA/pellet (µg/µg).

2.2.5 Assessment of surface marker expression by flow cytometry

MSCs were tested for expression of typical cell surface markers by flow cytometry (FCM) at P4 to ensure they conformed to a mesenchymal lineage devoid of myeloid/hematopoietic cell populations. The experimental groups (in triplicates) consisted of unstained control cells and cells to be stained with MSC markers: cluster of differentiation/cell (CD) 90.2 (Thy-1), stem cell antigen-1(Sca-1), CD105 (endoglin) and CD140a (the alpha chain of the platelet derived growth factor receptor (PDGF receptor) (Dominici et al., 2006). Hematopoietic markers CD34 (Mucosialin), CD45 (Ly-5) and CD11b (αM integrin) were used to ensure purity of the cell population and corresponding isotypes were used to differentiate non-specific background signal. Cells in culture were trypsinised and counted as described previously. The cells were resuspended in fluorescent activated cell sorting (FACS) buffer (Appendix 2; Table 13) with $1x10^5$ cells/100µl of buffer in a 96-well V bottom plate (Sarstedt) and spun at 400g for 3min. This process was repeated twice followed by staining each well with the antibodies and isotype controls as above (list of antibodies and isotype controls in Appendix 2; Table 11&12) for 30 min at 4°C. Stained cells were centrifuged at 400g for 3min and resuspended in fresh buffer. The process was repeated twice to remove any excess/unbound stain. The samples were transferred to a 5ml tube suitable for FCM in a final volume of 200µl buffer and analysis performed using the BD FACS Canto II instrument.

2.2.6 Expansion and titration of adenoviral vectors

The adenoviral vectors used to modify mMSCs were purified stocks provided by Dr. Martina Anton, Technische Universität München and Prof. Thomas Ritter at REMEDI, NUI Galway. Four different first-generation adenoviral vectors with a cytomegalovirus (CMV) promoter, namely, (i) Adenoviral empty vector (AD NULL), (ii) Adenoviral

Epstein Barr viral Interleukin-10 (ADCMVIL10) and (iii) the bicistronic Tet inducible system vector with an adenoviral reversible tetracycline (tet)-controlled transactivator element (AdCMVrtTA) and (iv) Adenoviral Tet responsive element for vIL10 expression (AdTREtvIL10) were used in the study. Vectors (iii) and (iv) were expanded and titrated separately but used as a single vector in further experiments as ADTET, either supplemented with (ADTET +DOX) or without (ADTET –DOX) doxycycline. The method of Tet induction in these vectors will be explained in Section 2.2.8. The human embryonic kidney cell line HEK 293 (provided by Ms. Martine Harte, REMEDI, NUI Galway) transformed with sheared fragments of Adenovirus type 5 DNA was used for viral infection and propagation of vectors (Graham et al., 1977). Cesium chloride density centrifugation was used to purify viral stocks and the final lysate was reconstituted in 10% glycerol (Sigma) for storage at -80°C. The vectors were titrated based on plaque formation. For the plaque assay, dilutions of frozen lysates of each vector, ranging from 10^{-8} to 10^{-10} (3 dilutions) were prepared in 2% medium (Appendix 2; Table 14). Prior to starting the assay, HEK-293 cells were seeded in 6mm dishes at a density of $5x10^5$ cells/dish. At 80% confluency, the cells were rinsed with PBS and 1ml of 2% medium was added along with 1ml of relevant diluted adenoviral lysate. A negative control dish with cells alone in 2% medium was included in the assay. The cultures were incubated at 37°C for 90min, rocking every 15min. This was followed by removing the adenovirus and 5 ml of 1.25% low melting point agarose (Sigma) in 10% medium (Appendix 2; Table 15) was overlaid on cells in each dish. After 48h incubation, the overlay was repeated with 3ml of 1.25% agarose. Plaque formation was seen in 7-10 days after adenoviral infection and the viral titre for all vectors was calculated as follows: *number of plaques x dilution = plaque forming units (PFU)/ml.*

2.2.7 Adenoviral transduction of mMSCs using lanthanum chloride ($LaCl_3$)

Adenoviral transduction of mMSCs was performed using cells at P5-P7 utilizing the lanthanide-based method (Palmer et al., 2008). Briefly, on day 0 cells were trypsinised, neutralized, counted and seeded in 6-well plates ($1x10^5$ cells/well), set up in triplicates in 2ml mMSC medium and incubated overnight at 37ºC 5% CO_2. On day 1, $LaCl_3$ (Sigma) was weighed and dissolved in dH_2O to make a 0.4M stock. The stock solution was filtered and from this the final working solution of 0.04mM $LaCl_3$ was prepared in sterile

conditions using α-MEM (Gibco). To determine the optimal viral dose, various multiplicities of infection (MOI) ranging from 0 (untransduced) to 100, 250, 500 and 1000 were tested for ADCMVIL10.

The amount of viral stock to be added for the desired MOI was calculated using the formula: *viral MOI x cell number/ viral titre (pfu/ml)*. For each MOI a 15ml centrifuge tube was taken and serum-free α-MEM was added based on the number of wells. The calculated volume of virus stock in medium was added to the corresponding tubes and 0.04mM $LaCl_3$ was added at a 1:1 ratio and mixed well. The virus/$LaCl_3$ mix was allowed to stand at RT for 30min. Cell culture medium was then removed from mMSCs that were seeded on day 0 (overnight) and replaced with 2ml virus/$LaCl_3$ mix. The cells were incubated for 3h at 37ºC. Following incubation for 3h, the virus/$LaCl_3$ mix was removed and the cells were washed twice with mMSCs medium and replaced with fresh mMSC medium. Once the optimum MOI was obtained, the experiment was repeated with the final MOI alongside other vectors. Efficacy of vIL10 release was measured by viral ELISA, using media collected at 24, 48 and 72h post transduction and stored at -80ºC and viability was assessed at 72h by FCM.

2.2.8 Transduction of mMSCs using the Tet inducible system

Cells at P7 were used for transduction with the Tetracycline (Tet) virus system. AdCMVrtTA and AdTREtvIL-10 were used for the experiment. Briefly, on day 0 cells were trypsinied, neutralized, counted and seeded ($1x10^5$ cells/well) in 6-well plates. Three groups namely untransduced, ADTET +DOX (AdCMVrtTA+AdTREtvIL-10 with doxycycline) and ADTET –DOX (AdCMVrtTA+AdTREtvIL-10 without doxycycline) were tested. All groups were set up in triplicate, with viral doses ranging from MOI 0 (untransduced) to 5, 10, 15, 20, 25 and 50. The cells were seeded using complete mMSC medium and incubated at 37ºC at 5% CO_2. On day 1, cells were transduced with the viruses using the $LaCl_3$ protocol. After 3h incubation with the $LaCl_3$/virus mix, the mix was removed and cells washed twice with complete mMSC medium. The Tet system utilizes DOX as the pharmacological switch for activation and expression of vIL10. A stock solution of 50mg/ml was prepared by dissolving 250mg DOX (Sigma) in 5ml of dH_2O. This solution was sterile filtered, aliquoted and stored at 4ºC. From this stock solution a final working solution of 3µg/ml DOX was prepared in mMSC medium in

such a way that each well received 2ml of this agent. After the final rinse with medium, the group designated as ADTET +DOX, was supplemented with this agent mixed in medium. The other group received complete mMSC medium alone. A fresh working solution DOX was prepared daily and added to the ADTET +DOX group. Transduced medium was collected at 24, 48 and 72h post transduction for quantitation of vIL-10 production by viral ELISA and viability was assessed at 72h by FCM. The experiment was repeated with the final MOI alongside other vectors for final validation of the system.

2.2.9 Assessment of viability and CPD of transduced mMSCs

Cells transduced with all viral groups including an untransduced group were processed for assessment of viability using flow cytometry after 72h of transduction. Briefly, media from the wells were removed and washed with 2ml PBS/well. This was followed by trypsinisation using 300µl of trypsin-EDTA/well for 4min. Cells were then neutralized with 2ml of complete mMSC medium/well and the cells trypsinized and transferred to labelled 15ml centrifuge tubes. Prior to processing for flow cytometry, the cells in each group were counted and CPD was calculated as described in Section 2.2.3 using the initial seeding density on day 0 and yield on day 3. The cells were then spun at 400g for 5min at RT. The pellet was resuspended in 2ml of FACS buffer and spun twice at 400g for 5min. After the second spin, the pellet was resuspended in 200µl FACS buffer and transferred to labelled flow tubes. A working solution of Sytox Red dead cell stain (Life technologies; final dilution - 1:14000 as optimized based on manufacturer's protocol) was prepared. The untransduced cells prior to staining with Sytox were used to gate mMSCs as single cells and live vs dead cells. Sytox fluorescence was detected at 640/658nm when bound to DNA. The gating parameters were set as follows; forward scatter (FSC) = 0, side scatter (SSC) = 340 and APC (red filter for detection of viability) = 560. After completing the gating strategy, 200µl of the dye was added to all samples set in triplicates and analysed. The gating strategy was represented as dot plots and/or histograms and viability and CPD were represented as a bar graph.

2.2.10 Quantitation of vIL-10 production by transduced mMSCs using viral ELISA.

Media collected after 24, 48 and 72h transduction from mMSCs treated with ADNULL, ADCMVIL10, ADTET +DOX, ADTET -DOX and untransduced groups were subjected to ELISA for measurement of vIL10 levels. Briefly, the surface of each well of a 96-well plate was coated with 100µl of purified rat anti-human and viral IL-10 capture antibody (BD Biosciences) at a final working concentration of 0.5µg/ml in PBS and kept overnight at RT. The wells were rinsed with 1X wash buffer (10X wash buffer diluted in dH_2O: R & D systems) thrice and blocked by adding 300µl of reagent diluent (1% bovine serum albumin (BSA; Fisher Scientific) in PBS) to all wells and incubated for a minimum of 1h at RT. The plate was then rinsed thrice with 1X wash buffer. Prior to addition of samples, a working solution of 2ng/ml of vIL-10 standard was prepared by performing a 1:5000 dilution of recombinant EBVIL-10 stock (R & D systems) in reagent diluent. Using this working solution, standards were prepared as serial dilutions to make up the standard curve. Standard 1 was prepared at a final concentration of 1ng/ml. For this 700µl of 2ng/ml working solution was added to 700µl of reagent diluent in an Eppendorf tube and vortexed. From standard 1, 700µl was added to a second tube with 700µl of reagent diluent making standard 2. In this way up to 7 standards were prepared by serial dilution. The last vial was regarded as the BLANK containing only reagent diluent. The standards were set up in triplicates and the samples from each MOI and time period of transduction were set up as experimental triplicates and technical duplicates. Standard or samples (100µl) were added to relevant wells and incubated for 2 h at RT. After incubation, the samples were discarded and the washed thrice with 1X wash buffer. A final working concentration of 0.5µg/ml of Biotin labelled detection antibody (BD Biosciences) prepared in reagent diluent, was added to all wells and incubated for 2 h at RT. This was followed by a washing step and addition of 100µl of Streptavidin-HRP (R & D systems) to all wells for 20min RT. The wash step was repeated followed by addition of 100µl of Substrate solution A and B (R & D systems) in a 1:1 ratio to all wells for 20min at RT. The reaction was ceased by addition of 50µl 2N Sulfuric acid (H_2SO_4) solution to all wells and the absorbance was read at 450-550 nm. Results were plotted as a bar graph with vIL10 release in pg or ng/ml on the Y axis against time point of medium collection post transduction on the X axis.

2.2.11 Statistical analysis.

Statistical analysis was performed using GraphPad Prism software, version 6. Data were analysed utilizing either Unpaired t-test with Welch's correction or two-way ANOVA followed by Bonferroni's multiple comparisons test. Error bars represent the mean ± standard error of the mean (SEM). For all analyses, differences were considered statistically significant at $p<0.05$ and significance was assessed in three biological donors (sample number, $n=3$) assayed using technical triplicates.

2.3 Results

2.3.1 mMSCs showed an accelerating trend in growth rate and displayed a homogenous population of fibroblast-like cells over time.

Bone marrow derived cells from C57BL/6 mice were culture expanded at 37°C in hypoxia (5% O_2) and maintained until P12. The growth rate was assessed from P2 to P12 and CPD calculated while maintaining the seeding density at $5x10^5$ cells/T175 cm2 flask. Media changes were performed every 2 days and at the same time daily throughout the expansion. The input of cells before initiating a new passage and the yield of cells from the previous passage was noted. Calculation of CPD showed a clear trend of acceleration in growth starting from P3 on day 14 up to P12 on day 56 (Figure 2.1A). All three biological preparations of mMSCs displayed and maintained a steady doubling time during this time. There was a dramatic change in morphology and size, with cells growing in multiple colonies of small heterogeneous clusters (Figure 2.1B) around day 10 to adherent, convex, round and stretched-out shapes with high contamination of hematopoietic cells populations at P2 (Figure 2.1C). This was followed by an increase in cell size by P4 with more uniform spindle-shaped MSC-like cells and abundant doublets (Figure 2.1 D). The cells acquired a homogenous fibroblastic mesenchymal morphology around P6 (Figure 2.1 E) till P12.

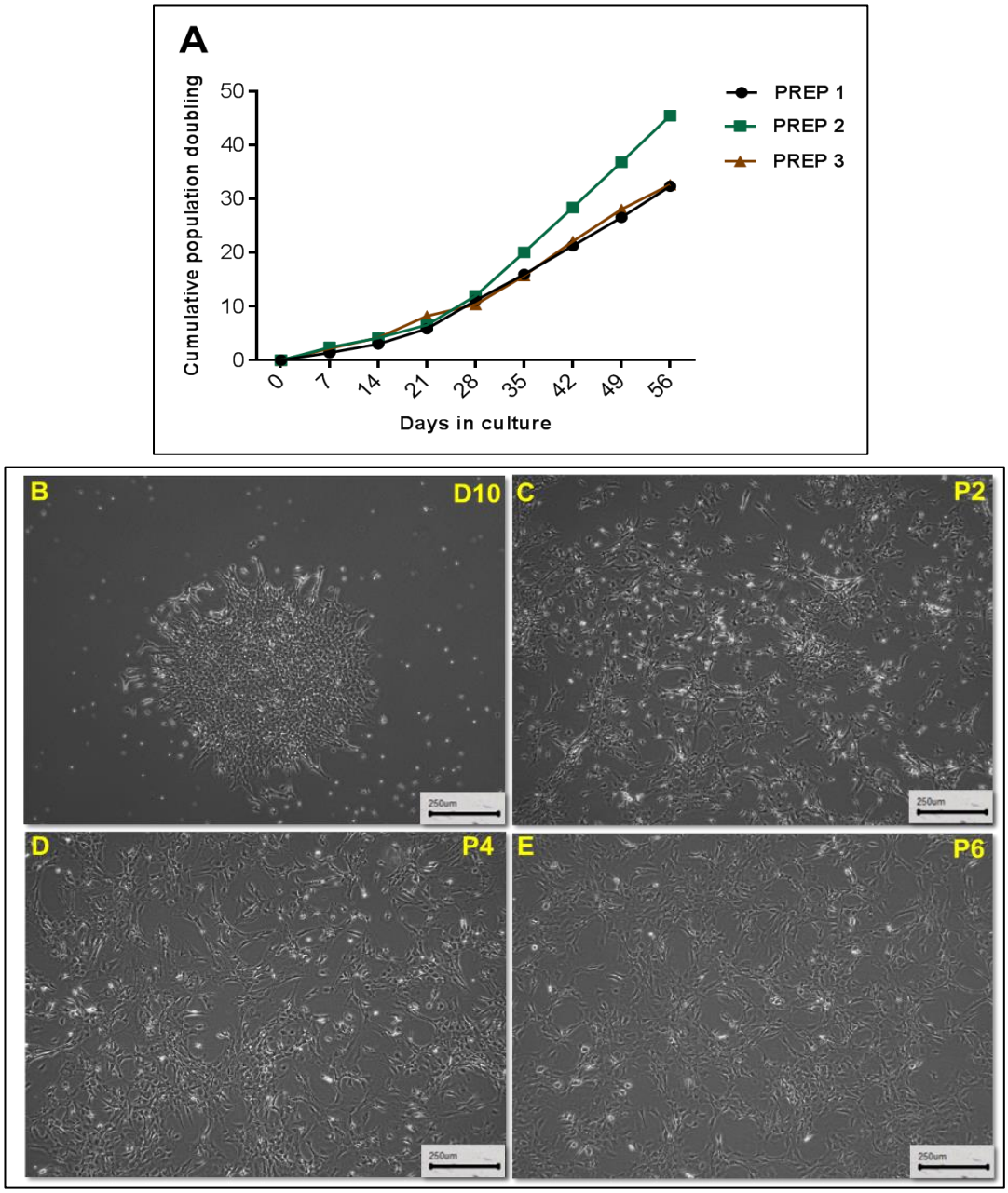

Figure 2.1 Growth and morphology of mMSCs. A) XY scatter graph showing CPD values of C57BL/6 mMSCs, calculated based on yield after every passage and number of days in culture. Bright-field images of cells on B) day 10, C) P2, D) P4, and E) P6 depicting morphological changes in monolayer culture over time. Scale bars, 250μm; Prep 1 to 3 – individual biological preparations (n=3).

2.3.2 Tri-lineage differentiation

mMSCs showed the ability to differentiate into osteogenic, adipogenic and chondrogenic lineages when induced with the appropriate differentiation medium.

2.3.2.1 Osteogenic differentiation of mMSCs

mMSCs ($10x10^3$ cells/well) demonstrated osteogenesis when induced with the osteogenic medium and maintained for 12 days, as evidenced by Alizarin Red S staining. Cells in test wells showed a clear presence of calcium deposits (Figure 2.2B) and control cells that were cultured in mMSC medium did not show any change in morphology or the presence of calcium deposition (Figure 2.2A). Osteogenesis was further confirmed with quantitation of calcium using the Stanbio Calcium assay (Figure 2.2.C). Cells from osteogenic wells showed a significant amount of calcium in comparison to controls ($p=0.0028$).

2.3.2.2 Adipogenic differentiation of mMSCs

MSCs were tested for their adipogenic differentiation by maintaining them in an adipogenic induction medium followed by a week in maintenance medium. The cells in test wells (Figure 2.3B) started to form fat right after the completion of first cycle of induction, followed by maturation and further lipid deposition over the next two cycles. Oil red O staining for detection of fat production showed adipogenesis in test but not control wells (Figure 2.3A). Semi-quantification (Figure 2.3C) of lipid deposition by comparing the absorbance values between control and test showed a significantly higher quantities in test samples ($p=0.0006$).

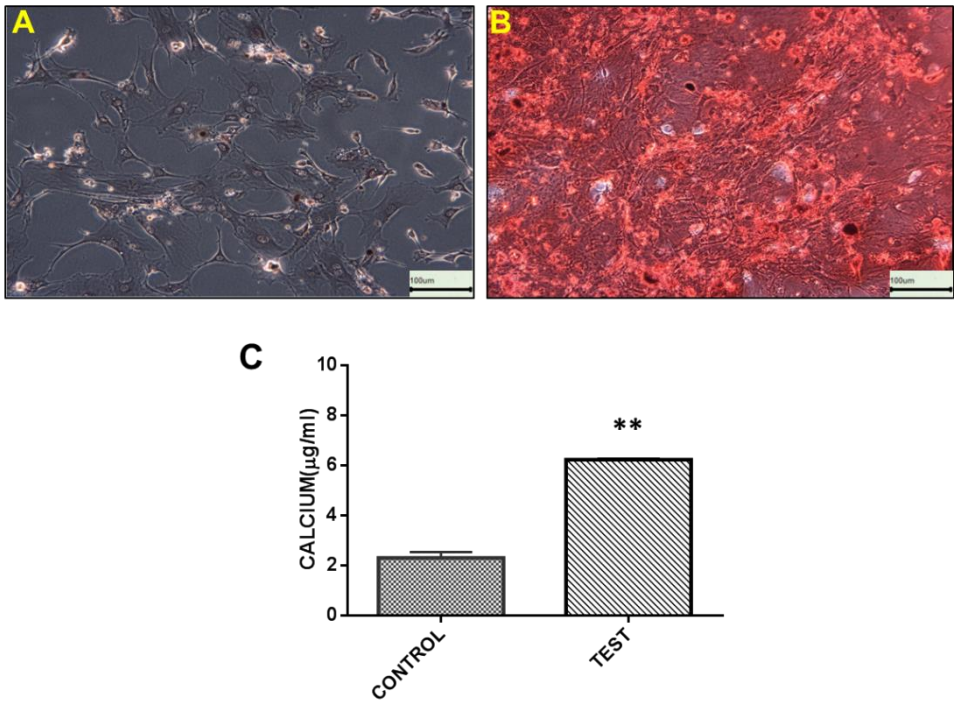

*Figure 2.2 Osteogenic differentiation of mMSCs. A) Control cells cultured in mMSC medium did not show any calcium deposition. B) Osteogenically induced test cells showed calcium deposition with strong Alizarin Red S staining. C) Quantitation of calcium deposition was significantly higher in test cells compared to control mMSCs. Values are expressed as the Mean±SEM (**n**=3, technical triplicates). Statistical significance was determined by Unpaired t test with Welch's correction. **p<0.005. Scale bars, 100µm.*

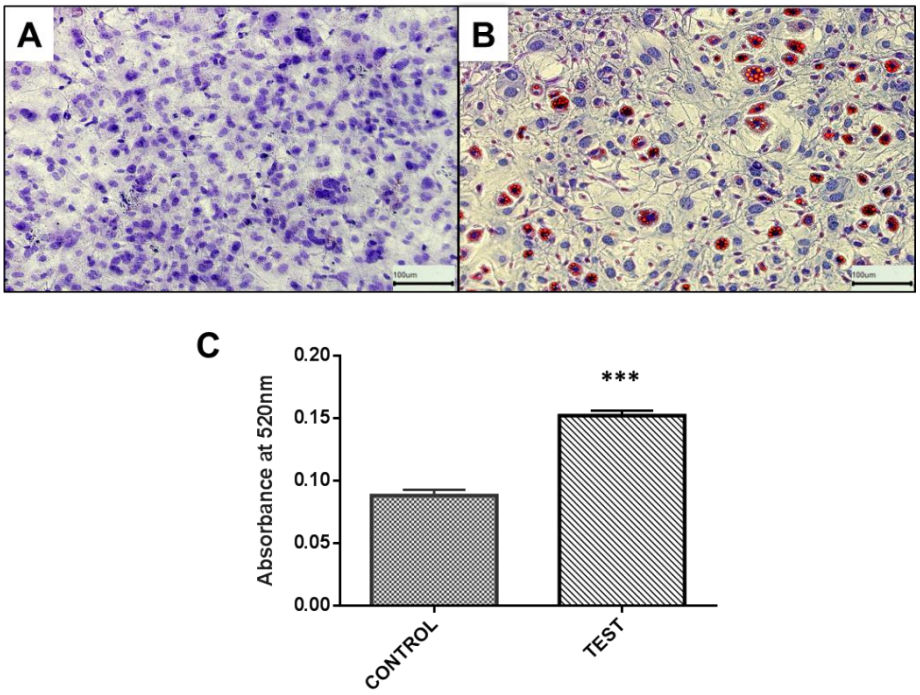

*Figure 2.3 Adipogenic differentiation of mMSCs. A) Control cells cultured in mMSC medium did not show lipid deposition. B) Test cells induced with adipogenic medium showed fat deposition with strong Oil Red O staining. C) Quantitation of fat deposition was significantly higher in test cells compared to control mMSCs. Values are expressed as the Mean±SEM (n=3, technical triplicates). Statistical significance was determined by Unpaired t test with Welch's correction. ***p<0.001. Scale bars, 100µm.*

2.3.2.3 Chondrogenic differentiation of mMSCs

Mouse MSCs cultured in complete chondrogenic medium from all three preparations proved to have the potential to differentiate to chondrocytes. In comparison to test CCM pellets, ICM control samples failed to condense into a pellet. Mature chondrocytes with cartilage formation were seen with Safranin O staining in pellets exposed to CCM (Figure 2.4A). Total GAG production measured post 21 days in culture using the DMMB assay revealed that the test samples produced 9.6μg GAG/pellet in comparison to ICM where no GAG was detected (Figure 2.4B). Similarly, DNA content (Figure 2.4C) of CCM pellets was significantly higher than in ICM pellets as seen using PicoGreen determination. GAG production normalised against the DNA content (Figure 2.4D), clearly showed a significant difference between ICM and CCM samples for all three biological preparations of mMSCs.

2.3.3 Surface marker characterisation of mMSCs

Bone marrow derived MSCs were tested for compliance to one of the criteria proposed by the International Society for Cellular Therapy (ISCT) of being positive for surface markers of the MSC phenotype (Dominici et al., 2006). Cells of all three mouse preparations were processed for FCM (Figure 2.4) and an initial gating strategy was performed to select singlets that were mMSCs (Figure 2.5A). All 3 mMSC preparations demonstrated positive expression for CD90.2 (95.7 $\%^{+}$), CD105 (98.6 $\%^{+}$), and mesenchymal progenitor markers Sca-1 (73.5 $\%^{+}$) and CD140a (PDGFRα; 90.1 $\%^{+}$) in comparison to their isotype controls (Figure 2.5B – top panel; 2.5C). These cells showed no expression of the hematopoietic marker CD45, macrophage marker CD11b and endothelial marker CD34 (Figure 2.5B; bottom panel), thereby conforming to criteria for a mesenchymal line of stromal cells.

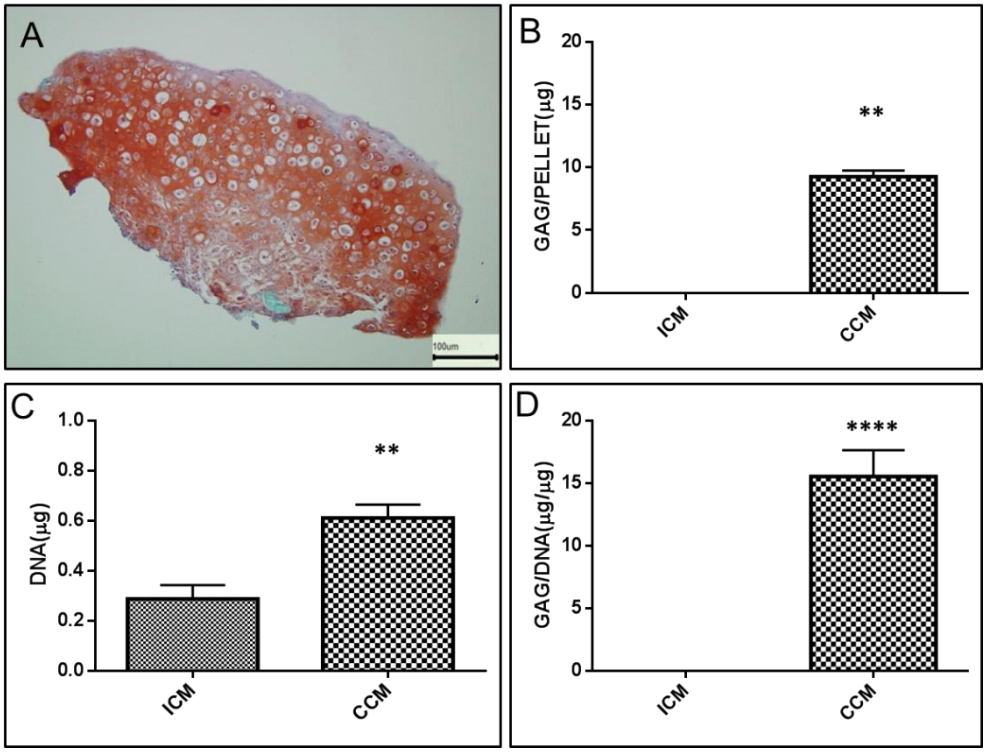

*Figure 2.4 Chondrogenic differentiation of mMSCs. A) Qualitative analysis of mMSCs induced into chondrogenesis showed formation of mature cartilage in CCM pellets with Saffranin O (red) and Fast Green (green) staining after 21 days of culture. No pellet formation seen in ICM samples B) Quantification of glycosaminoglycans (GAG) content showed significant levels in CCM samples. C) DNA content was significantly higher in CCM and D) GAG/DNA ratio was also significant in CCM compared to ICM cultures Values are expressed as the Mean±SEM (**n**=3, technical triplicates). Statistical significance was determined by Unpaired t test with Welch's correction. **p<0.01****p<0.0001. Scale bars, 100µm.*

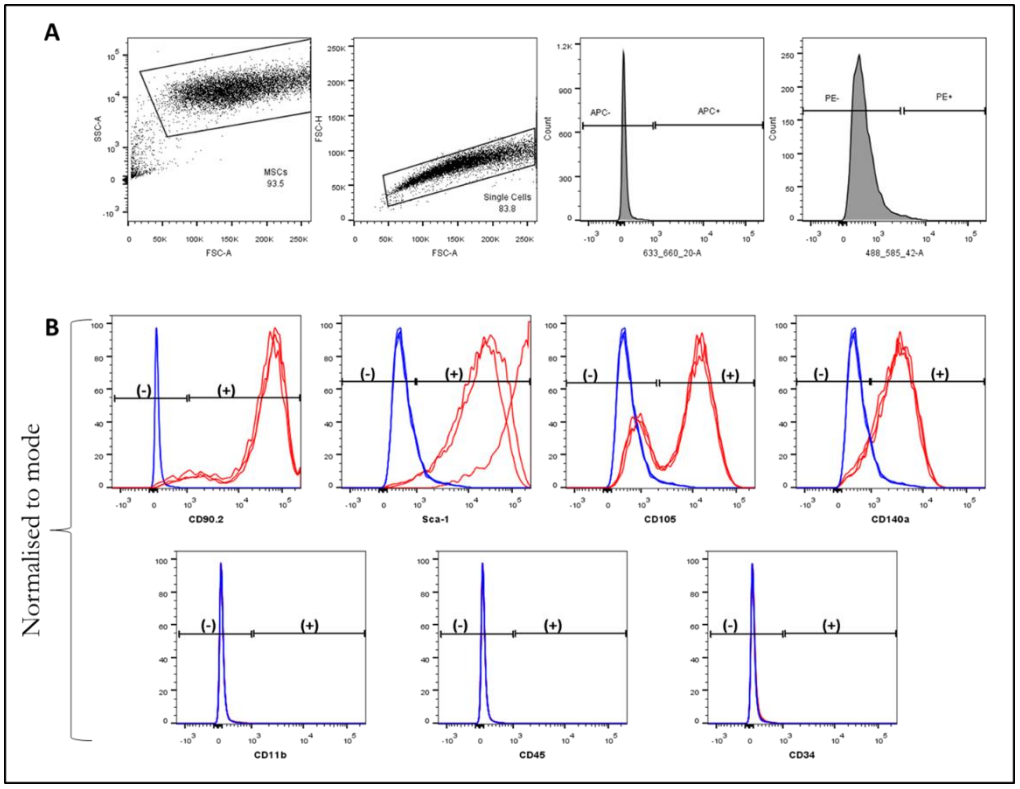

C

MARKER	FLUORESCENCE EXPRESSION (%) N=3.
CD90.2	95.7
Sca-1	98.6
CD105	73.5
CD140a	90.1
CD11b	3.9
CD45	0.25
CD34	0.98

Figure 2.5 Surface marker characterisation of mMSCs. A) Cells were analysed by FCM, and gated to include singlets and MSCs, B-top panel) histograms of positive markers vs isotypes, (B-bottom panel) negative markers vs isotype controls and C) mean fluorescence expression of all markers. Mean ± SEM, (n=3; technical triplicates).

2.3.4 Titration of expanded adenoviral vectors

Adenoviral vectors ADNULL, ADCMVIL10, AdCMVrtTA and AdTREtvIL10 were expanded by transfection of HEK 293 cells using crude viral lysates (CVL). Infection of 293 cells was confirmed by a cytopathic appearance 24h post transfection (Figure 2.6A). Viral stocks prepared from these cells for each vector, were purified by ultracentrifugation and separation of infectious viral particles, that were then extracted and frozen down as the final lysate to be titrated (Figure 2.6B). A plaque assay was performed and viral titres defined for the adenoviral stocks were: $1x10^{11}$ PFU/ml for ADNULL, $2x10^{10}$ PFU/ml for ADCMVIL10, $1.2x10^{9}$ PFU/ml for AdCMVrtTA and $3x10^{8}$ PFU/ml for AdTREtvIL10.

2.3.5 Viral transduction of mMSCs with ADCMVIL10

Adenoviral transduction of mMSCs with the ADCMVIL10 vector using the $LaCl_3$ method at a titre of $2x10^{10}$ PFU/ml was performed using $1x10^{5}$ mMSCs (P5) that were transduced with MOIs 0, 100, 250, 500 and 1000. vIL10 release was measured after 24, 48 and 72h by ELISA. Transduction had no effect on morphology by microscopic analysis or cell viability (tested by FCM). Cells maintained their size and fibroblastic morphology (Figure 2.7A) and viability (Figure 2.7C) above 90-95% for MOIs 100, 250 and 500, at 72h post transduction. Viability was less than 80% using MOI 1000. Measurement of vIL10 levels by ELISA (Figure 2.7B), showed consistently increasing levels of vIL10 using MOI 500. At lower MOIs of 100 and 250, there was no IL10 production after 24h and 48h, and at MOI of 1000, IL10 secretion was not statistically significant at 24h. In addition, the release of vIL10 was five-fold lesser than MOI 500 across all time points. Although, the release was statistically significant for doses 250, 500 and 1000 at 72h, the use of an MOI of 500 for 72h was found to be the optimal condition that resulted in a stable and significant increase in vIL10 over-expression by all 3 preparations of mMSCs.

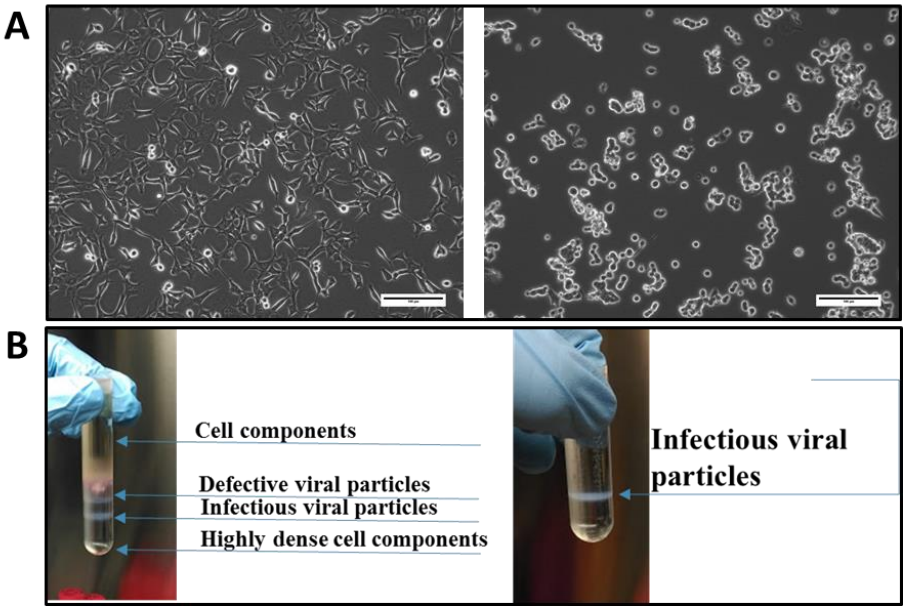

Figure 2.6 Expansion and titration of vectors. Bright field images of HEK 293 cells before A- left panel) and after A- right panel) viral infection. B) Purified viral lysates were obtained by ultracentrifugation as depicted. The right panel illustrates the purity obtained after ultracentrifugation Scale bars, 100µm.

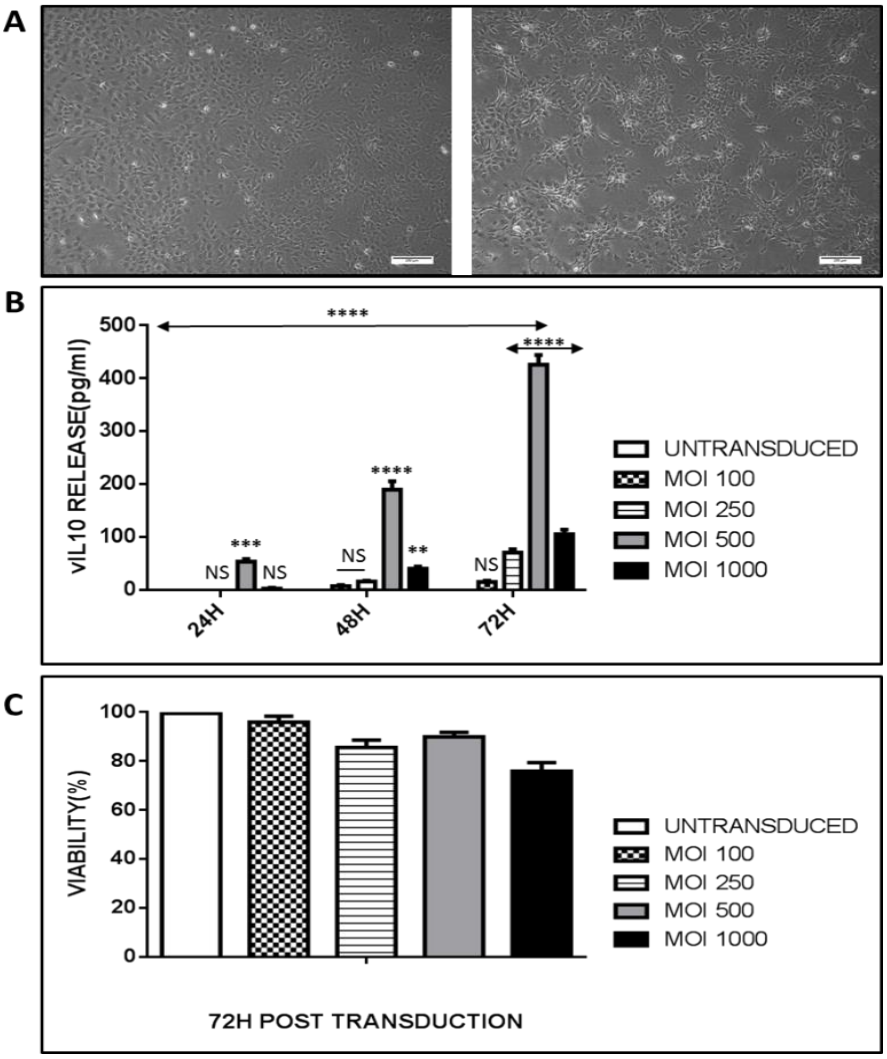

*Figure 2.7 Transduction efficiency of ADCMVIL10 using LaCl3. A) Bright field images of mMSCs before (left panel) and 72h (right panel) post transduction at an MOI 1000. B) Measurement of vIL10 levels by viral ELISA at 24, 48 & 72h post transduction. C) Assessment of viability at 72h post transduction by FCM. Values are expressed as the Mean±SEM (n=3, technical triplicates) Statistical significance was determined by two-way ANOVA with Bonferroni's multiple comparisons test. *p<0.05, **p<0.005 ***p<0.001, ****p<0.0001. MOI- multiplicities of infection. NS- Not Statistically Significant. Scale bars, 250µm*

2.3.6 Inducible and controlled vIL10 expression by mMSCs using the Tet system

With data showing successful expression of vIL10 by mMSCs transduced with ADCMVIL10, control of vIL10 expression was assessed to develop a therapeutic vector suitable for timed release of vIL10. mMSCs ($1x10^5$, P7) were transduced with the ADTET bi-cistronic vector, consisting of equal quantities of AdCMVrtTA ($1.2x10^9$ PFU/ml) and AdTREtvIL10 ($3x10^8$ PFU/ml) using the $LaCl_3$ method. Controlled release of vIL10 by the ADTET vector was assessed by measuring levels produced by transduced mMSCs after treatment with ADTET +DOX or ADTET –DOX at MOIs 0, 5, 10, 15, 20, 25 and 50. Quantification of vIL10 release by ADTET +DOX cells proved the system to be efficient at MOIs of 10 to 50 across all time points (Figure 2.8A). Although vIL10 production was seen at MOI 5, values were not significant. Secondly, addition of DOX acted as a pharmacological switch based on the absence of IL10 secretion by all groups of transduced cells not treated with the drug. Statistical analyses comparing vIL10 release between MOIs showed consistent, yet stable production at MOIs 10, 15, 20, 25 and 50 with strong significance ($P<0.0001$). However, examination of viability (Figure 2.8B) with Sytox dye by FCM for these doses showed increased cell death at MOI 50 (74%). Hence, the optimal dose to be tested for final validation was MOI 25 with cells and medium collected at 72h for maximum vIL10 expression.

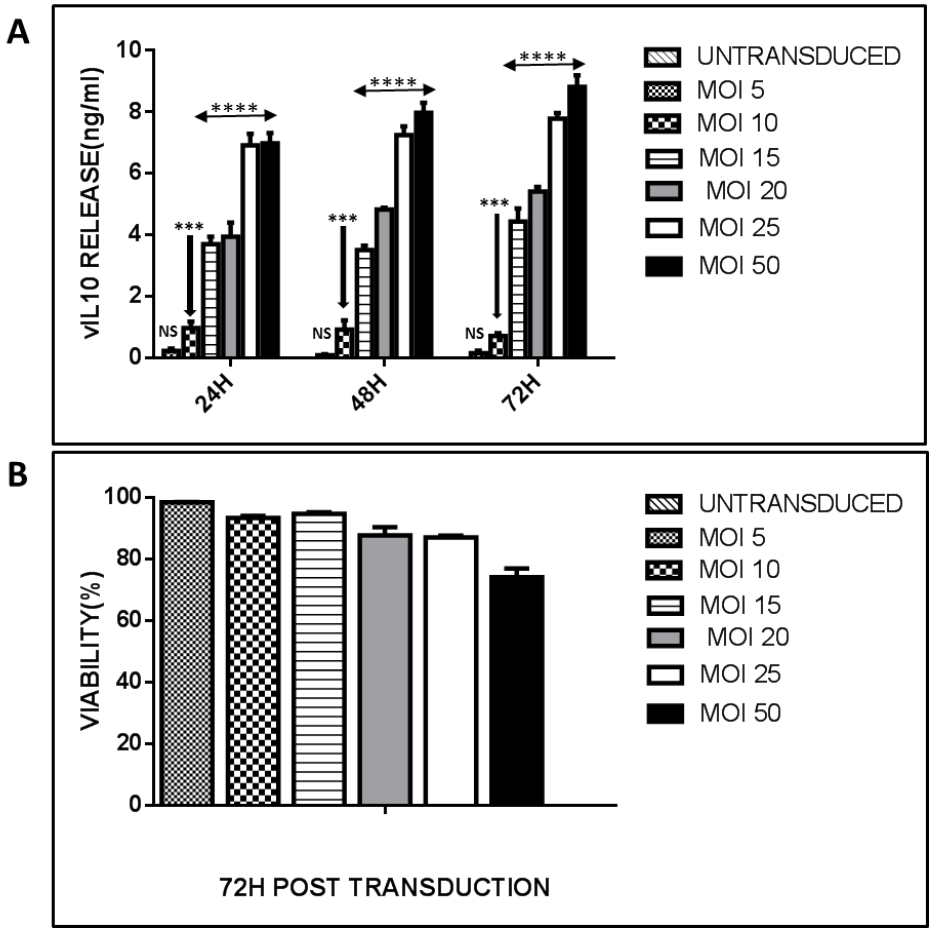

*Figure 2.8 Inducible release of vIL10 using doxycycline as a control-switch. A) Measurement of vIL10 levels released by mMSCs transduced with the adenoviral Tet-ON vector treated with DOX at 24, 48 & 72h post-transduction. Transduced cells showed no release of vIL10 by ELISA in the absence of DOX (data not shown). B) Assessment of mMSC viability measured by FCM at 72h post transduction with the ADTET system. Values expressed as the mean ± SEM,(n=3, technical triplicates) was analysed by two-way ANOVA with Bonferroni's multiple comparisons test, *p<0.05; **p<0.01, ***p<0.005, ****p<0.0001 MOI - multiplicities of infection; NS - Not statistically significant.*

2.3.7 Controlled production of vIL10

The capacity of the Tet system to control vIL10 expression in response to a pharmacological switch was compared to ADCMVIL10 and the empty vector, ADNULL. mMSCs were subjected to a final round of transduction with all vectors. Briefly, $1x10^5$ cells/well were transduced with either ADNULL, ADCMVIL10 at MOI 500 or ADTET +DOX at MOI 25 for 24, 48 and 72h. An untransduced and ADTET –DOX group was also included to investigate optimal functioning of adenoviruses and to rule out leakiness in the Tet system, respectively. Firstly, assessment of viability by FCM staining for Sytox (Figure 2.9, Panel A) and growth rate (CPD, Figure 2.9C) calculated at 72h showed that none of the vector groups had a detrimental effect on MSCs. Percentage cell viability among the three MSC preparations was maintained above 75-80% (Figure 2.9B). Measurement of vIL-10 release at all time points by viral ELISA (Figure 2.9D) displayed stable vIL10 production by the ADCMVIL10 and ADTET +DOX group. Transduction using the Tet system demonstrated a cumulative, two-fold higher vIL10 production by ADTET +DOX (MOI 25) compared to ADCMIL10 (MOI 500), but also demonstrated tightly controlled IL10 expression, not seen in the absence of DOX (ADTET –DOX). Statistical inter-comparison of all groups and 3 MSC preparations exhibited overall significance with $p<0.0001$.

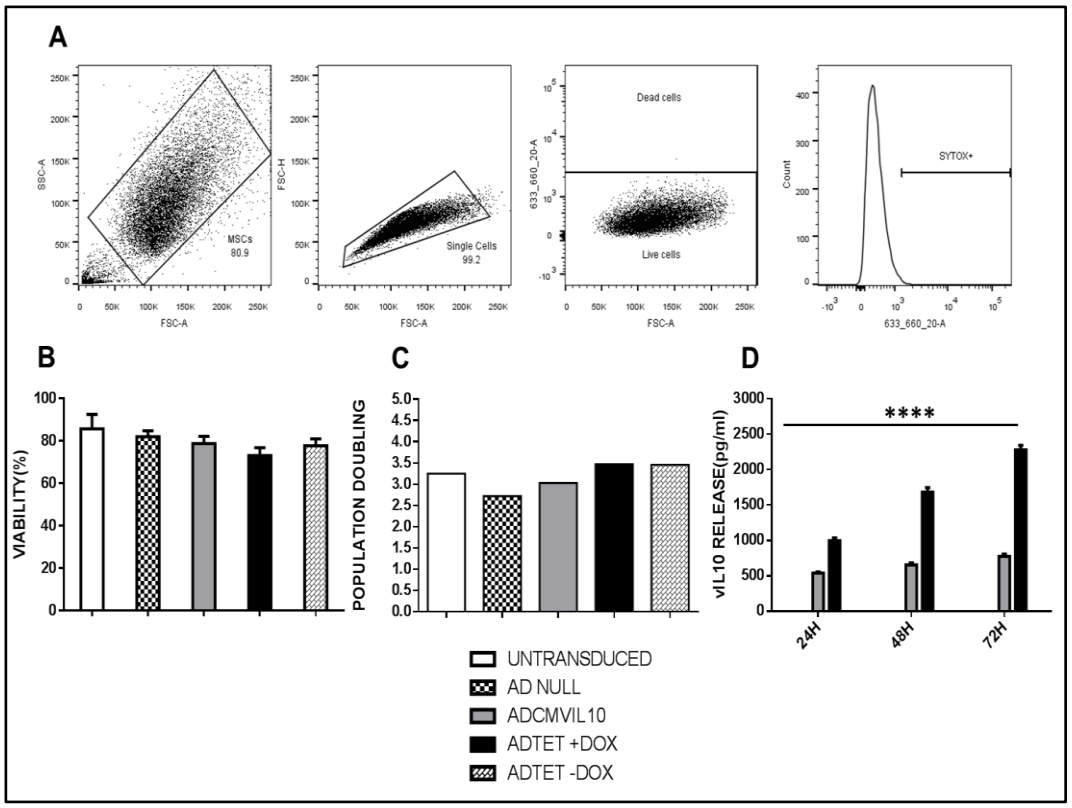

*Figure 2.9 Comparison of vector transduction efficiency. A) Gating strategy showing dot plots, segregation of live and dead MSCs by FCM and gating for Sytox Red^{+} cells. B) Assessment of viability by FCM and C) CPD at 72h post transduction was shown to be unaffected by adenoviral transduction. D) Measurement of vIL10 levels by viral ELISA 24, 48 & 72h post transduction for untransduced, ADNULL, ADCMVIL10, ADTET +DOX and ADTET -DOX showed significant vIL10 production only by ADCMVIL10 and ADTET +DOX MSCs. Values expressed as mean ± SEM, (n=3, technical triplicates) and analysed by two-way ANOVA using Bonferroni's multiple comparisons test, **** p<0.0001.*

2.4 Discussion

Originally discovered by Friedenstein, as resident cells in rat bone marrow acting as precursors to osteocytes, with fibroblastic morphology, colony forming capacity and adhering to tissue culture surfaces (Friedenstein et al., 1966, Barry, 2019), MSCs later gained the reputation of being multipotent, self-renewing cells having a regulatory effect on skeletal tissue homeostasis and repair as described by Caplan (Caplan, 1991, Houlihan et al., 2012). The first objective of this work was to isolate, expand and characterize bone marrow mMSCs suitable for further genetic engineering. Culture expansion of all three biological preparations from C57BL/6J mice, cultured at 5% O_2 (hypoxia) yielded a population of cells with fibroblastic morphology by P6, displaying enhanced proliferation and accelerated CPD. The impact of oxygen concentrations on MSC plasticity, proliferation and differentiation *in vitro* has been studied for a considerable time and culture of bone marrow MSCs at 21% O_2 (normoxia) leads to reduced growth potential and senescence following a number of passages (Hu et al., 2018b). This can be attributed to the fact that the physiological oxygen pressure in the marrow environment typically ranges between 1-7% (Hung et al., 2007). All three marrow preparations proved to originate from a mesenchymal lineage via demonstration of tri-lineage differentiation, with significant quantities of calcium (osteo), lipid (adipo) and GAG (chondro) elaborated by the cells under the appropriate conditions, in comparison to control samples.

The minimal criteria to define human MSCs, also applicable to other species with small differences in surface markers, as proposed by ISCT are: (1) adherence to plastic; (2) positive expression (>95%) of CD105, CD73 and CD90 and negative expression (< $2\%^{+}$) of CD45, CD34, CD14 or CD11b, CD79a or CD19 and MHC class II; and (3) ability to differentiate into adipocytes, osteoblasts, and chondrocytes under standard *in vitro* differentiating conditions (Dominici et al., 2006, Harrell et al., 2019). Based on these criteria, bone marrow MSCs have been successfully isolated and characterized previously from different species including human (Pittenger et al., 1999, Ghoniem et al., 2015, Zaim et al., 2012), dog (Muir et al., 2016), goat (Li et al., 2017a), rat (Chen et al., 2004, Ridzuan et al., 2016) and rabbit (Wang et al., 2016). Deriving a pure line of MSCs from mouse marrow is more complex due to a more diverse cell population in marrow consisting of higher percentage of hematopoietic cells (Phinney et al., 1999). Strict adherence to ISCT

recommended surface maker characterization for mouse MSCs is difficult because of strain related differences, especially seen with Sca-1 and CD34 expression (Peister et al., 2004, Chen et al., 2016). Hence, surface marker characterization of marrow derived MSCs by FCM showed positive expression for CD90 (regulates differentiation of MSCs), Sca-1 (involved in MSC migration, (Xishan et al., 2014)), CD105 (also called SH2, recognising a member of TGF-β family, endoglin which is involved in differentiation, migration and proliferation of MSCs (Barry et al., 1999, Lv et al., 2012)) and CD140a (murine MSC development and maturation (Rostovskaya and Anastassiadis, 2012)). Sca-1 has been considered a critical marker for murine MSC characterisation based on previous studies. Bone marrow MSCs isolated from C57BL/6 mouse were positive for Sca-1 and these cells displayed higher proliferative capacity compared to Sca-1 negative cells (Peister et al., 2004, Baustian et al., 2015). Selective isolation of MSCs based on expression of Sca-1 and PDGFR-α yielded a purer population of cells without hematopoietic contamination, negligible cellular senescence and robust differentiation into bone, fat and cartilage (Houlihan et al., 2012, Morikawa et al., 2009). While MSCs were negative for hematopoietic markers CD34 and CD45, a small percentage of cells were unexpectedly positive for the macrophage/monocyte marker CD11b. Although this is indicative of hematopoietic cell contamination early passage number (P6) and hypoxic culture conditions may have contributed to this unexpected expression. Previous studies have also shown that murine MSCs derived from C57BL/6, cultured at 5% oxygen stained positive for CD11b until P8 and this expression was absent at later cell passage number (Meirelles Lda and Nardi, 2003, Hu et al., 2018a). Mouse MSC preparations generated for this study did demonstrate capacity towards tri-lineage differentiation. However, qualitative and quantitative analysis of lipid formation was relatively lower and this could be an effect of culturing under hypoxic conditions (Hu et al., 2018b). While higher adipogenic differentiation of MSCs is a strong indicator of the cells' multipotent ability, MSCs are also known to exhibit tendency towards adipogenesis in normoxia, with accumulation of adipose tissue and reduced bone formation as result of aging or stress induced senescence in the marrow (Rosen and Bouxsein, 2006, Jin et al., 2010).

IL-10 is a well-established pleotropic cytokine with immunoregulatory properties and previous in vivo studies of direct delivery or systemic administration of recombinant IL-

10 protein or adenovirus-mediated transfer of IL-10 has demonstrated ability to suppress the development of arthritis (Joosten et al., 1997, Katsikis et al., 1994, Kuroda et al., 2006). However, this observed efficacy was seen only when treatment was administered prior to the onset of arthritis and not after disease induction. While clinical trials have shown that a dose of up to 25μg/kg of human IL-10 is safe and well-tolerated, a fraction of patients showed moderate flu-like symptoms at doses up to 100μg/kg. In addition, RA patients present a pathophysiological correlation between IL-10 and elevated autoantibody production and B cell activation (Moore et al., 2001, Narula, 2000). In another trial, systemic administration of recombinant IL-10 did show clinical improvement but also had toxic effects in RA patients (Tilg et al., 2002). Similar to this, doses beyond 8μg/kg resulted in induction of anaemia and headaches in patients with Crohn's disease. Also, direct IL-10 delivery, has the disadvantage of a short half-life of just 2 hours, MSC-mediated gene therapy offers long-term inducible protein expression for sustainable effects (Milligan et al., 2005, Li et al., 1994). While clinical data supporting the use of IL-10 has been disappointing with respect to RA, there are no clinical studies targeting OA via IL-10 therapy.

The main aim of this chapter was to therefore develop a stable method of efficient adenoviral transduction in MSCs. Adenoviral transduction of MSCs to deliver therapeutic factors/cytokines using adenoviral vectors offers major advantages such as ease of manufacturing and the ability to transduce even quiescent cells without integrating into the host genome (Kovesdi et al., 1997, Ehrhardt et al., 2003). The ability of MSCs to effectively transfer/deliver exogenous genes, while simultaneously migrating into affected organs carrying the target genes, along with low immunogenicity and innate immunosuppressive properties, make the cells an attractive option for cellular and/or gene therapy (Manning et al., 2010).

Gene therapy based pre-clinical trials have demonstrated effective delivery of vIL10 using genetically engineered MSCs and anti-inflammatory factor expression to enable attenuation of RA (Vermeij et al., 2015, Choi et al., 2008). Although MSCs are quite receptive to adenoviral transduction, additional co-incubation with a chemical agent such as $LaCl_3$ enhances transgene expression compared to incubation with adenoviral construct alone (Palmer et al., 2008). This was also found for the data reported here where

transduction of mMSCs with ADCMVIL10 using lanthanide-based transduction yielded efficient and continuous vIL10 release by mMSCs with significant levels ($P<0.0001$) maintained at MOI 500 to 72h post transduction and no alteration in cell viability. Unlike retroviral constructs that integrate with the host genome, adenoviral vectors lack this ability making them more suitable for further use in clinical studies. However, this aspect can be associated with a negative outcome, as efficient transgene expression gradually lowers following lineage-specific differentiation (Hung et al., 2004, Schlimgen et al., 2016). To overcome this, the current chapter proposed and tested the hypothesis that bone marrow-derived mMSCs can demonstrate regulated and enhanced expression of vIL10 using the Tet-On system under the influence of doxycycline. In support of this, tetracycline-inducible, controlled vIL10 gene transfer has been previously demonstrated effective in a murine model of experimental arthritis (Apparailly et al., 2002, Perez et al., 2002). Transduction of mMSCs with ADTET vector in the presence of doxycycline displayed enhanced yet stable increase in vIL10 release at all time points with results statistically significant ($p<0.0001$) at 72h at an optimal dose of MOI 25 adenoviral vector.

Two critical objectives of the work were: (1) to compare the efficiency of vIL10 production between ADCMVIL10 and ADTET system constructs, in order to analyse the impact of using a pharmacological switch in controlling transgene expression and (2) to determine the optimal time point and dose of viral vector that can give rise to vIL10 MSCs with positive immunomodulatory capacities. To achieve this, mMSCs were transduced with ADNULL (empty vector), ADCMVIL10, and ADTET with (ADTET +DOX) or without (ADTET -DOX) doxycycline. The hypothesis was effectively proved based on the following results: (1) the Tet-On system, executed using ADTET +DOX enabled inducible and regulated vIL10 expression that was approx., two times higher ($p<0.0001$) at a dose (MOI 25) nearly 20 times lower than the dose required for ADCMVIL10 (MOI 500) even at 72h post transduction; (2) the use of the adenoviral vector did not alter the proliferation or the viability of vIL10 positive mMSCs and, (3) doxycycline acts as a pharmacological switch, providing tightly controlled vIL10 expression by ADTET +DOX and not by ADTET -DOX mMSCs. While overexpression of IL-10 by murine MSCs using a retroviral vector previously yielded a release of 22ng/ml which was ten times more than the release observed with Tet-ON

MSCs in this chapter, over-dose of IL-10 comes with reversal of immunoregulatory (i.e. immune-stimulation as previously reported) effects, which would not be desirable when looking at utilising the Tet-ON system for clinical translation (Choi et al., 2008, Asadullah et al., 2003). The findings of this chapter therefore support the use of this novel bi-cistronic Tet-On vector system to generate vIL10 MSCs and further investigate the immunomodulatory capacity of these engineered MSCs on activated immune cells *in vitro*, towards the ultimate aim of prevention/attenuation of inflammation in OA.

Chapter 3

Assessment of immunomodulatory effects of vIL10 over-expressing mMSCs on activated macrophages and T cells *in vitro.*

3.1 Introduction

Although OA is regarded as a degenerative disease of articular cartilage it affects the whole joint with a growing body of evidence suggesting that inflammatory processes may be the main contributing factor to disease progression (Sokolove and Lepus, 2013, Scanzello and Goldring, 2012). Synovial inflammation in particular is believed to trigger several clinical signs and symptoms and it plays a major role in the progression of OA (Kraus et al., 2016). Resident and infiltrating cells in the OA synovium include macrophages, fibroblasts and a quantifiable number of B and T cells. Activation of joint cells, including synovial fibroblasts (SFs) and chondrocytes occur in response to endogenous stimuli (e.g., TLRs) from their microenvironment after injury or infection. This event results in innate immune activation and production of inflammatory cytokines, aggrecanases, degradative proteases and MMPs further leading to cartilage destruction (Mosser and Edwards, 2008, Utomo et al., 2016, Sokolove and Lepus, 2013).

There is substantial evidence that synovial macrophages are the most crucial cell types responsible for initiating the recruitment and activation of other immune cells and controlling inflammation (Mantovani et al., 2013). *In vivo* studies in CIA models have shown reduction in chondrocyte death and proteoglycan degradation following depletion of phagocytic synoviocytes and also indicated that macrophages/monocytes were the predominant innate cells involved in induction of cartilage damage (Van Lent et al., 1998, Van Lent et al., 1997). Depletion of synovial macrophages also resulted in substantial reduction of osteophyte formation in a murine model of experimental OA (Blom et al., 2004). Macrophages display a high degree of plasticity and are capable of altering their phenotype depending on the type of PRR or external cue they interact with (Murray et al., 2014, Mantovani et al., 2013). Macrophage phenotypes can be categorised as classically activated (M1) induced by IFN-γ, TNF-α, or LPS and alternatively activated (M2) macrophages, which can be further split into wound healing (stimulated by IL-4) and regulatory (activated by IL-10) subsets. In general M1 macrophages trigger local inflammation via cell surface expression of the major histocompatibility complex- class II (MHC-II) and CD86, needed for activation of T cells and high production of cytokines TNF-α, IL-1, IL-6 and IL-12 (Mosser, 2003).

This cytokine production by M1 subsets leads to chondrocyte alterations and subsequent down regulation of aggrecan and collagen type II, and the simultaneous up regulation of COX-2 and MMP-9 expression (Fahy et al., 2014). On the other hand, M2 macrophage subsets adopt an anti-inflammatory profile and secrete high levels of TGF-β and IL-10, and express the mannose receptor (CD206) on their cell surface (Mosser, 2003, Mantovani et al., 2013, Bernardo and Fibbe, 2013). $CD4^+$ effector and $CD8^+$ cytotoxic T lymphocytes are the most abundant adaptive immune cells found in the OA synovium (Ishii et al., 2002) and their reactivity towards chondrocyte membranes is caused by exposure to antigens possibly arising from products of cartilage degradation (Alsalameh et al., 1990). Based on previous reports, activation of $CD4^+$ T cells occurs in conjunction with secretion of IFN-γ, IL-2, MIP-1γ and osteoclastogenesis in OA patients with chronic joint lesions. This T cell reactivity in the OA synovial membrane is mediated by IL-12 produced as a consequence of macrophage polarisation, suggestive of the role of T cells in chronic inflammation and disease progression (Shen et al., 2011, Sakkas and Platsoucas, 2007).

MSCs are adult multi-potent fibroblast-like cells that were originally regarded as a favourable source for cell therapy to effect cartilage regeneration due to their self-renewal and chondrogenic differential potential (Yoo et al., 1998, Barry and Murphy, 2013, Mancuso et al., 2019). However, numerous studies have identified MSCs as cells with immune regulatory properties based on their ability to sense an inflammatory environment and adopt differential phenotypes following active interaction with cellular members of the innate immune system (Bernardo and Fibbe, 2013). MSCs display both pro- and anti-inflammatory effects via secretion of trophic factors that can further orchestrate either regulation or suppression of activated immune cells (Prockop and Oh, 2012, Murphy et al., 2003, Le Blanc and Mougiakakos, 2012, Keating, 2012, Mancuso et al., 2019). In the context of synovial inflammation in OA, MSCs have mediated macrophage polarisation from the M1 to M2 phenotype, and also suppressed $CD4^+$ Th1 reactivity and enhanced generation of anti-inflammatory $CD4^+$ Tregs in human OA synovium (Németh et al., 2009, Van Buul et al., 2012, Yang et al., 2009). Many other *in vitro* studies have demonstrated a strong correlation between the ability of MSCs to favour the generation of $CD4^+CD25^+FoxP3^+$ Tregs (Burr et al., 2013, Maccario et al., 2005) to

their polarising effect on M2 macrophages (Eggenhofer and Hoogduijn, 2012), i.e., MSC mediated T cell regulation is monocyte-dependent and happens via juxtacrine and paracrine signalling (François et al., 2012, English et al., 2009, Cutler et al., 2010, Melief et al., 2013b). IL-10 is an important anti-inflammatory factor involved in MSC-mediated immunomodulation of macrophages and T cells (Melief et al., 2013a). Chondrocytes express IL-10 and IL-10R (Iannone et al., 2001) and this 34kDa heterodimeric cytokine is also produced by activated macrophages, B and T cells (Fiorentino et al., 1989, Evans et al., 2007, Zdanov et al., 1997). When exposed to an inflammatory environment, endogenous and/or exogenously injected MSCs engrafted in the joint, produce TSG-6, IDO and PGE_2 which enables inhibition of TLR2/NFκ-B signalling resulting in macrophage polarisation. PGE_2 in particular binds to EP2 and EP4 receptors on macrophages and alters their phenotype to IL-10 producing M2 subsets. Similarly, TGF-β and PGE_2 produced from the MSCs influence the production of chemokine (C-C motif) ligand 18 (CCL-18) by M2 macrophages and together all three factors favour the generation of Tregs (Németh et al., 2009, Prockop and Oh, 2012, Melief et al., 2013b, Melief et al., 2013a). Early studies on IL-10 mediated immunomodulation on macrophages have shown that reduced expression of NO, CD86, IL-12 and MHC-II by activated macrophages/monocytes led to regulation of APCs followed by inhibition of T-cell presentation and proliferation (Moore et al., 2001, de Waal Malefyt et al., 1991b).

Viral and human IL-10 exhibit structural similarities and share 84% amino acid sequence homology (Vieira et al., 1991). Although both forms of IL-10 display similar immunosuppressive potential, vIL10 is much favoured for therapy as it lacks stimulatory functions (Go et al., 1990). Anti-inflammatory gene delivery strategies using adenoviral vectors or over-expression of vIL10 by transduced MSCs have been successfully carried out in *in vivo* models of experimental arthritis (Apparailly et al., 2002, Lechman et al., 1999, Vermeij et al., 2015, Ma et al., 1998, Choi et al., 2008). Van de Loo and co-workers showed that lentiviral mediated inducible expression of vIL10 resulted in reduced production of TNF-α, IL-1β and IL-6 in a 3D micro mass model of human synovial membrane (Broeren et al., 2016). Furthermore in a study conducted by Farrell et al. vIL10-overexpressing human MSCs induced long-term reduction in activated CD4 and CD8 T cell populations

in draining lymph nodes of mice with collagenase-induced osteoarthritis (CIOA) (Farrell et al., 2016).

Here the hypothesis that tetracycline induced vIL10 MSCs modulate inflammatory processes in vitro in a juxtacrine and paracrine manner is interrogated. The main aim of this work was to test the anti-inflammatory ability of engineered vIL10 MSCs on activated immune cells. For this, bone-marrow derived murine macrophages (BMs) and T lymphocytes from mouse spleen were stimulated *in vitro* and treated with different groups of MSCs and assessed using secreted factors and/or effects on direct co-culture assays. Immunomodulatory effects of vIL10 MSC treatment on macrophage polarisation, gene expression of macrophage-secreted pro and anti-inflammatory factors and T cell activation and proliferation was particularly analysed.

3.2 Materials and methods

3.2.1 Preparation of mMSCs and collection of conditioned medium (CM)

To test the immunomodulatory capacity of C57BL/6J mMSCs (untransduced and vIL10 MSCs derived in chapter 2) on activated macrophages and T cells *in vitro,* the mMSC-CM and cells were collected as described below. The cells ($2x10^5$) were seeded in triplicate in 6-well plates and cultured overnight (day 0) using 2ml of mMSC medium/well at 37ºC 5% CO_2. Adenoviral transduction was performed on day 1 as described in section 2.2.7. The experimental groups were as follows: 1. untransduced MSCs, 2. ADNULL (MOI 500), 3. ADCMVIL10 (MOI 500), 4. ADTET +DOX (MOI 25) and 5. ADTET –DOX (MOI 25). Transduction of ADTET +DOX and –DOX was carried out as described in sections 2.2.7 and 2.2.8. The medium from all these groups was collected on day 4/72h (as optimised in Chapter 2, Figure 2.9) and centrifuged at 400g for 5min. The supernatants were filter sterilised using a 0.45µm syringe filter (Sarstedt) and stored at -80°C until further use. The cells from each experimental group were trypsinised and collected as previously described (see Section 2.2.9). The MSCs were used in direct co-culture experiments with activated BMs and/or T cells and the CMs from MSCs were used in macrophage secretome assays.

3.2.2 Collection of L929-CM

The murine fibroblast cell line NCTC clone 929 (also called L929) was received from Dr. Aideen Ryan and Dr.Kevin Lynch, REMEDI. These cells were used as the source of M-CSF to grow BMs. L929s were seeded at a concentration of $1x10^6$ cells per T175 culture flask using L929 medium (Appendix 2; Table 16). The cells were supplemented with fresh medium every two days and the CM containing M-CSF was collected when cells reached 90% confluence (around day 4). The collected CM was centrifuged at 400g for 5min and filter sterilised using a 0.45µm syringe filter, aliquoted in smaller volumes and stored at -20°C until further use.

3.2.3 *In vitro* isolation and differentiation of macrophages

Bone marrow progenitor cells were cultured in the presence of M-CSF derived from L929-CM to obtain differentiated macrophages. Briefly, femurs and tibias were obtained from 6-8 w old C57BL/6 mice, the muscles were removed and cleaned bones were placed in a sterile petri-dish. The ends of the bones (epiphyses) were snipped and bone marrow was flushed out of each of the shafts with RPMI-1640 (Sigma) using a 2 ml syringe locked onto a 25Gx 5/8" needle. The cells were filtered through a 40μm cell strainer and centrifuged at 500g for 5min. To lyse the red blood cell population, the pellet was re-suspended in 1 ml of Red Blood Cell Lysing Buffer Hybri-Max™ (Sigma) and incubated for 3 min on ice, protected from light. RPMI-1640 (10 ml) was used to neutralise the lysis buffer and centrifuged again. This step was repeated twice and at the end of the third spin, the pellet was re-suspended in BM medium (Appendix 2; Table 17) and cells were counted using a haemocytometer. After obtaining the count, the cells were divided among 6-well plates at $3x10^5$ cells/well with 3ml of BM medium, containing 15% of L929-CM (M-CSF) for differentiation. The medium was changed once at day 2 and at the end of 6 days, cells were collected by gentle scarping using a 25cm cell scraper (Sarstedt) and counted. Macrophage differentiation was confirmed by FCM (as described for MSCs in section 2.2.5) using the antibodies F4/80, CD45.2 and CD11b and their corresponding isotype controls (Appendix 2; Table 11&12).

3.2.4 Macrophage secretome assay

Differentiated BMs between 6 and 10 days were collected by gentle scraping and spun at 500g for 5min. A cell count was performed and the BMs were primed with 20ng/ml IFN-γ (Peprotech) and seeded in 24-well plates at $2x10^5$ cells/well in triplicate, on day 0. The following day (day 1), cells were stimulated with 10ng/ml LPS (Sigma; optimisation shown in Appendix 1; S1) and treated with 50% mMSC-CM from all 5 experimental groups (described in Section 3.2.1). A negative control group of BMs without exposure to IFN-γ and LPS ('unstimulated') and a positive control group with only IFN-γ+LPS ('stimulated') and no mMSC-CM was included. Seven experimental groups were included in all assays as follows: 1. Resting (negative control), 2. Stimulated (positive control), 3. Untransduced, 4. ADNULL, 5. ADCMVIL10, 6. ADTET +DOX and 7. ADTET –

DOX. After 6h (See Appendix 1; S1 for optimisation), medium was collected for ELISA and levels of mouse TNF-α (also used for optimisation of LPS dose and time-points), IL-1β, IL-6 and IL-10 were measured. The levels of these cytokines were also measured in all the mMSC-CM groups.

3.2.5 Cytokine quantification by ELISA

The mouse DuoSet ELISA kits (R&D Systems) for TNF-α, IL-1β/IL-1F2, IL-6 and IL-10 were used to quantify the release of the cytokines from activated/treated BMs and mMSC-CMs. As per manufacturer's instructions, 96-well flat-bottom plates were coated with 100µl of rat anti-mouse TNF- α/IL-1β/IL-1F2/IL-6/IL-10 capture antibody (See Appendix 2; Table 18 for concentrations used) diluted in PBS, and incubated overnight at RT. The wells were rinsed thrice with 1X wash buffer (10X wash buffer diluted in dH_2O: R&D Systems) and blocked with 300µl of reagent diluent (1% bovine serum albumin (BSA; Fisher Scientific) in PBS) and incubated for a minimum of 1h at RT. Following the blocking step, the plates were washed three times and 100µl of appropriate recombinant standard or sample was added as experimental triplicates and technical duplicates and incubated for 2h at RT. After sample incubation, the plates were washed three times before the addition of 100µl of biotinylated goat anti-mouse TNF-α/IL-1β/IL-1F2/IL-6/IL-10 detection antibody (concentrations in Appendix 2; Table 18) diluted in reagent diluent and incubated for 2h at RT. The plates were rinsed three times and streptavidin-HRP (R&D Systems) was diluted to a ratio of 1:40 in reagent diluent and added to all the plates at final volume of 100µl. After 20min incubation at RT, the plates were rinsed again three times, followed by addition of 100µl TMB/E substrate solution (Merck Millipore). After an incubation of another 20min, the reaction was stopped with 50µl of stop solution (2N H_2SO_4) added to each well, and optical density was determined using a Victor X3 plate reader set to 540/450 nm. The reagent diluent was added in technical triplicates served as the blank. The absorbance values at 540 nm were divided by the 450 nm readings and the blank value was then subtracted from all readings. A linear curve was generated using the known standard concentrations and the sample measurements were interpolated using the linear equation obtained. The results were plotted as a bar graph with appropriate cytokine values in pg/ml or ng/ml on the Y axis against respective LPS/CM treatment on X axis.

3.2.6 Measurement of nitric oxide production by Griess assay

NO production by activated/CM treated BMs was tested using culture supernatants, collected as described in section 3.2.4, by standard Greiss assay protocol. Briefly, 100µl of standard or supernatant was added in triplicate to wells of a 96-well flat-bottom plate. Sodium nitrite ($NaNO_2$ at 100µM), prepared in RPMI-1640 with an assay range from 100µM (highest standard point) to 3.125µM, was used as the standard for the assay. This was followed by addition of 100µl Greiss reagent (solution A: solution B at 1:1 ratio; Appendix 2; Table 19) to all the wells. The plate was then incubated in dark for 10min at RT and absorbance was measured at 540nm using the Victor X3 plate reader.

3.2.7 Gene expression analyses of macrophages

To test the immunomodulatory potential of vIL10 MSCs on the gene expression profile of activated BMs, macrophages were processed in the same manner as explained in section 3.2.4, but stimulated with LPS for 24h and treated with appropriate MSC-CMs (test groups as in Section 3.2.4). After 24h, the cells were collected by gentle scraping and centrifuged at 400g for 5min. The cell pellets were suspended in 350µl RLT buffer (Qiagen) containing β-mercaptoethanol (10µl for every 1ml of buffer; Sigma) and stored at -80°C until RNA extraction. For identification of pro-inflammatory cytokines mediating inflammatory responses in BMs, the RT^2 Profiler PCR array (PAMM-011ZA; 96-well format; Qiagen) was initially used to profile the expression of 84 relevant mouse inflammatory cytokine and receptor genes (for the plate layout, please see Appendix 2; Table 22.). Based on the analysis of the array, 8 genes were selected (see Appendix 1; S2 for details) for validation and assessment using the macrophage secretome assay and cell collection was repeated for further analysis.

3.2.7.1 RNA isolation

Total RNA was isolated from frozen BM cell pellets using the RNeasy Mini kit (Qiagen). Briefly, cell pellets were thawed for 20min at RT followed by centrifugation of the lysates at 13,000g for 3min. The supernatants were carefully collected and an equal volume of 70% ethanol (350µl) was added prior to mixing by gentle pipetting. The lysates (up to 700µl) were transferred to RNeasy Mini spin columns placed in 2ml collection tubes for

centrifugation at 8000g for 15s. The flow-through was discarded and 350µl of Buffer RW1 (Qiagen) added to the columns and spun again. On-column DNase digestion was performed using the RNase-Free DNase Set (Qiagen). For this 10µl of DNase I stock solution (provided in RNase-Free DNase Set) was mixed with 70µl of Buffer RDD (Qiagen). This mixture was added directly to the RNeasy spin column membranes with BM lysates and incubated at RT for 15min. After incubation, 350µl of Buffer RW1 was added on top of the DNase solution in the columns and spun again. The flow-through was discarded and 500µl of Buffer RPE (Qiagen) was added to the columns and spun. This step was repeated again and spun for 2min the second time. The spin columns were placed in new collection tubes and spun at full speed for 1min to dry the membrane. The collection tubes were replaced again with 1.5ml tubes (supplied in kit). 50µl of RNase-free water (Qiagen) was added to the spin columns and spun at maximum speed for 1min and RNA was eluted. The nucleic acid content was determined spectrophotometrically using a NanoDrop ND1000 spectrophotometer at 260 and 280 nm.

3.2.7.2 First strand cDNA synthesis

cDNA synthesis was performed using the QuantiNova™ Reverse Transcription Kit (Qiagen). For this, cDNA was synthesised as a two-step process. The first step involved genomic DNA (gDNA) elimination where the maximum volume for every reaction/sample was 15µl. For this 400ng of RNA stock was added to RNase-free water to a final volume of 12µl, followed by the addition of 1µl of Internal Control RNA and 2µl of gDNA Removal Mix (both supplied in the kit) to 0.2ml tubes. The samples were heated to 45°C for 2min, and placed immediately on ice. To facilitate reverse transcription (step 2), the following components were added to each reaction to a final volume of 20µl: 1µl of Reverse Transcription Enzyme and 4µl of Reverse Transcription Mix (both supplied in the kit) to each template RNA (15µl samples in ice). After this, first strand cDNA synthesis was performed on the Veriti Gradient Thermal cycler, by incubating the samples at 25°C for 3min (annealing step), 45°C for 10min (reverse-transcription step) and 85°C for 5min (inactivation of reaction). The newly synthesised cDNA were stored at -20°C until required.

3.2.7.3 Quantitative Real-Time polymerase chain reaction (qRT-PCR)

For the initial identification of inflammatory mediators, qRT-PCR was carried out using the RT^2 Profiler PCR array. Each array consisted of a 96-well plate pre-coated with primers for 84 key genes, five housekeeping genes (HKG), three positive PCR controls, three reverse transcription controls (RTC) and one well to account for mouse genomic DNA contamination (MGDC). Prior to starting the experiment, the cDNA samples were thawed on ice and diluted with RNase-free water to make up the final volume to 102µl. Each 96-well block was assigned for a sample and the PCR reaction mix was prepared in the following manner: 650µl of RT^2 SYBR Green Mastermix, 102µl of cDNA reaction sample and 548µl of RNase-free water (all supplied in the kit). Components were mixed gently by pipetting and transferred onto the RT^2 supplied loading reservoir. To each well, 10µl of prepared PCR reaction mix was loaded and the block was sealed tightly with Optical adhesive film. The block was placed in the Roche® LightCycler® 480 (96-well block). The amplification conditions were as follows: 95°C for 10min, 45 cycles of 95°C for 10s and 60°C for 1min. Gene expression levels were normalised to Glyceraldehyde-3-phosphate dehydrogenase (GAPDH) and threshold cycle (C_T) was calculated using the real-time cycler software (Roche). After this, the obtained C_T values for all 7 test groups of BMs (described in section 3.2.4) were exported to an excel spreadsheet linked with the online SABiosciences PCR Array Data analysis template (Qiagen software). The data was reported in the software as fold change/regulation using delta-delta C_T method, in which delta C_T was calculated between gene of interest (GOI) and an average of reference genes (HKG), followed by delta-delta C_T calculations (delta C_T (Test Group)-delta C_T (Control Group)). Fold change in expression was calculated using the 2^ (-delta C_T) formula (Schmittgen and Livak, 2008).

Based on the analysis of the array, a total of 8 genes were selected for final validation. qRT-PCR for single gene analysis was carried out using the QuantiNOVA™ SYBR® Green PCR Kit and pre-designed mouse SYBR green primers (see primer sequences listed in Appendix 2; Table 23) were obtained from the KiCqStart® SYBR® Green Primers for Gene expression analysis (Sigma-Merck). The reaction was run on the StepOne Real-Time PCR Systems (Thermo Fisher Scientific). In brief, a master mix was prepared using the PCR kit to yield a volume of 19µl per reaction as follows: 10µl SYBR Green PCR

master Mix was mixed with 2µl of ROX reference dye. The forward and reverse primer pairs for each gene were re-constituted in 1X Tris-EDTA (TE) buffer (Sigma) and added at a final concentration of 0.7µM; the volume of RNase-free water was varied accordingly. To each well of a MicroAmp™ Optical 96-Well Reaction Plate (Applied Biosystems), 1µl of each cDNA sample (10ng) was added in triplicate, followed by 19µl of PCR master mix bringing the total reaction volume in each well to 20µl (as per the instructions). Wells designated for RTCs were replaced with TE buffer instead of cDNA. The plate was sealed with MicroAmp™ Optical adhesive film (Applied Biosystems) and the amplification conditions were as follows: 95°C for 2min, 40 cycles of 95°C for 5s and 60°C for 10s. A melt-curve analysis was automatically performed by the software. Gene expression levels were normalised to *Gapdh* and threshold cycle (CT) was calculated using the real-time cycler software (Thermo Fisher Scientific). The fold change for each gene was calculated as described above.

3.2.8 Macrophage co-culture assay

Differentiated BMs between 6 and 10 days were collected by gentle scraping and counted. Cells were seeded at a concentration of $5x10^4$/well in 96-well U-bottom plates supplemented with 100µl BM medium. The cells in all wells except the resting group, were primed with 20ng/ml IFN-γ and incubated overnight (day 0). On day 1, all wells were rinsed twice with 200µl PBS and stimulated with 10ng/ml LPS aliquoted in 100ul of BM medium and incubated for 6h. The control, resting group was unstimulated. After incubation, all wells were rinsed twice with 200µl PBS. The appropriate mMSCs (collected in Section 3.2.1) were seeded over the BMs at an optimal final ratio of 1:5 (Appendix 1; S3.) in 100µl of MSC medium. After 3 days (72h; time-point optimised in Appendix 1; S3), BMs were collected and stained for flow cytometric analysis using antibodies for F4/80, MHC-II and CD206 (see Appendix 2; Table 21). Prior to analysis, 0.5µl of SYTOX viability dye was added to each well.

3.2.9 Isolation of murine splenocytes

Spleens were dissected from 8-10 w old C57BL/6 mice, and placed in PBS on ice. The spleen was then placed in a 40um cell strainer and mashed gently using a 10ml syringe to obtain a single cell suspension. The suspension was centrifuged at 800g for 5min and the pellet was resuspended in 1 ml of Red Blood Cell Lysing Buffer Hybri-Max™ to eliminate red blood cells. The suspension was incubated on ice for 5min after which the lysis buffer was neutralised by adding 10 ml of PBS and the cells were spun again. The pellet was resuspended in PBS and a cell count was performed using a haemocytometer.

3.2.10 Splenocyte:MSC co-culture assay

A cell count was obtained and splenocytes were segregated as 'labelled' or 'activated'. Labelled splenocytes were re-suspended at $10x10^6$ cells/ml and Cell Trace Violet dye (CTV, Invitrogen, Thermo Fisher Scientific) was used to label the cells to trace multiple generations. CTV was initially aliquoted in DMSO (5mM CTV stock) and was added at the concentration of 1µl/ml/$10x10^6$ cells and incubated for 20 min at RT in the dark. The dye was neutralised by adding 5 times the volume of T cell medium (Appendix 2; Table 20) for 5 min. The cells were then centrifuged at 800g for 5min. Cells to be activated were re-suspended at the concentration of $1x10^6$ cells/ml and 0.1µl/ml each of the anti-CD3e and anti-CD28 (eBiosciences) soluble antibodies were added and incubated for 30min in the dark at RT. mMSCs ($1x10^5$) were seeded in 100µl of T cell medium in a 96-well U-bottom plate (see Section 3.2.4 for details) with T cells at a final ratio of 1:10 as optimised previously (Appendix 1; S4), in 100µl of MSC medium. After 3 days (time-point optimised in Appendix 1; S4), T cells were collected and stained using the antibodies CD4, CD8 and CD25 for flow cytometry (Appendix 2; Table 21). Prior to analysis, 0.5µl of SYTOX viability dye was added to each well.

3.2.11 Statistical analysis

Statistical analysis was performed using GraphPad Prism software, version 6. Data were analysed utilising one-way ANOVA followed by Bonferroni's or Sidak's multiple comparisons test. Error bars represent the mean±SEM. For all analyses, differences were considered statistically significant at $p<0.05$ and significance was assessed in three

biological donors (sample number, n=3) assayed using technical triplicates. Where biological replicates were not available (n=1), mean±SEM of technical triplicates is shown without statistical analysis.

3.3 Results

3.3.1 Marrow derived murine progenitor cells differentiated into macrophages

Bone-marrow progenitor cells from C57BL/6J mice were isolated and differentiated *in vitro* by culturing in the presence of M-CSF derived from L929-CM as described in Section 3.2.3. The cells were replenished with fresh BM medium every two days and after 6 days of culture expansion the cells proliferated and differentiated from a heterogeneous population of round cells (Figure 3.1A: D0 & B: D2) into a homogenous population of mature elongated BMs (Figure 3.1C: D4 & 3.1D: D6). To further confirm and validate macrophage differentiation, the presence of surface markers was evaluated by flow cytometry. The cells were positive for the specific macrophage/monocyte markers F4/80 (>99%), CD11b (>96%) and leukocyte marker CD45.2 (99%) as shown in Figure 3.2.

3.3.2 Paracrine effects of vIL10 MSCs on activated BMs

BMs at day 6 were stimulated into classically activated macrophages using IFN-γ priming and addition of LPS and subsequently treated with vIL10 MSC-CM (as described in Section 3.2.4). First the activation of BMs was optimised by testing at different time points followed by selection of the optimal dose of LPS. All samples were primed with 20ng/ml of IFN-γ overnight (Meng and Lowell, 1997) prior to activation with LPS. TNF-α release was chosen as an outcome measure and the optimal time point for stimulation was found to be 6h after addition of 2ng/ml of LPS to the culture (Appendix 1; S1A). BMs were then stimulated for 6h with different concentrations of LPS ranging from 0, 1, 2, 4, 6, 8, 10 and 20ng/ml. Peak release of TNF-α was observed at a concentration of 10ng/ml of LPS beyond which saturation was observed (Appendix 1; S1B). Therefore 10ng/ml of LPS was chosen as the best dose for BM activation. To study the paracrine effects of vIL10 MSCs on activated BMs, BMs were primed and stimulated using optimal conditions as above and treated with different groups of CM from untransduced /ADNULL, ADCMVIL10, ADTET +DOX or ADTET –DOX-transduced MSCs. Supernatants collected from BMs after 6h and MSC-CMs were analysed for TNF-α, IL-1β, IL-6 and IL-10 release by ELISA. There was significant reduction of TNF-α production by BMs treated with the ADTET+DOX CM compared to the stimulated group. No differences

were observed with other treated groups and none of the MSCs produced TNF-α (Figure 3.3A). The pro-inflammatory cytokine IL-1β was not detectable in either BM supernatants or MSC-CMs (Figure 3.3B). The trend for IL-6 production was similar in BMs and MSC-CMs and the levels were higher compared to the stimulated group in BMs with no differences among the CM treated groups (Figure 3.3C). MSCs did not produce any murine IL-10 but MSC-CM treated BMs demonstrated increased production compared to the stimulated group. Furthermore, BMs treated with ADCMVIL10 and ADTET +DOX CMs displayed significantly higher release of IL-10 compared to all other groups (Figure 3.3D).

3.3.3 Nitric oxide production by activated BMs

NO production by classically activated BMs was measured in the supernatant collected from these cells using Griess assay (Section 3.2.6). In comparison to stimulated BMs, the production of NO was lower in all MSC-CM treated BMs with significant reduction seen in the group treated with CM from the ADCMVIL10 ($p= 0.0018$), ADTET +DOX ($p<0.0001$) and ADTET –DOX ($p= 0.0003$) MSCs. Among the significant groups ADTET +DOX CM treated BMs showed maximum reduction of NO as shown in Figure 3.4.

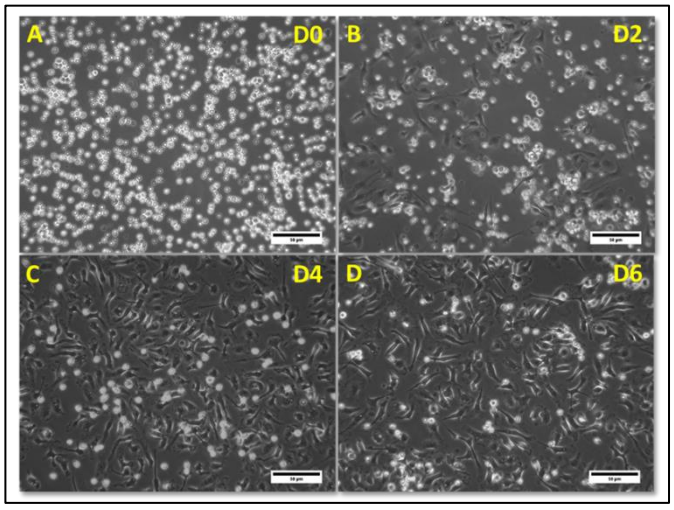

Figure 3.1 Morphology of differentiated BMs. A) Marrow-derived progenitor cells were cultured in the presence of M-CSF for 6 days starting at day 0 (D0). B) Medium was replaced every two days and cells demonstrated an elongated phenotype from day 2 (D2), C) with increased levels of these cells at day 4 (D4). D) A homogenous macrophage phenotype was achieved by day 6 (D6). Scale bars, 50μm.

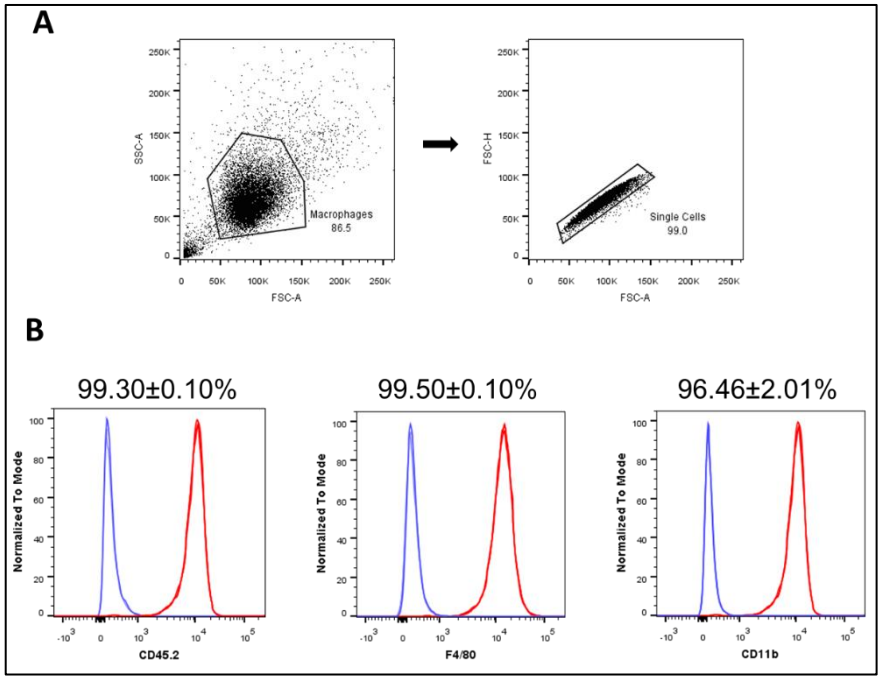

Figure 3.2 Validation of BM differentiation. A) Gating strategy used to include macrophages and single cells by flow cytometry. B) Histograms showing positive staining of differentiated cells for CD45.2, F4/80 and CD11b (red peaks) and negative for isotype controls (blue peaks). Data is represented as the Mean ± SEM (n=3, technical triplicates).

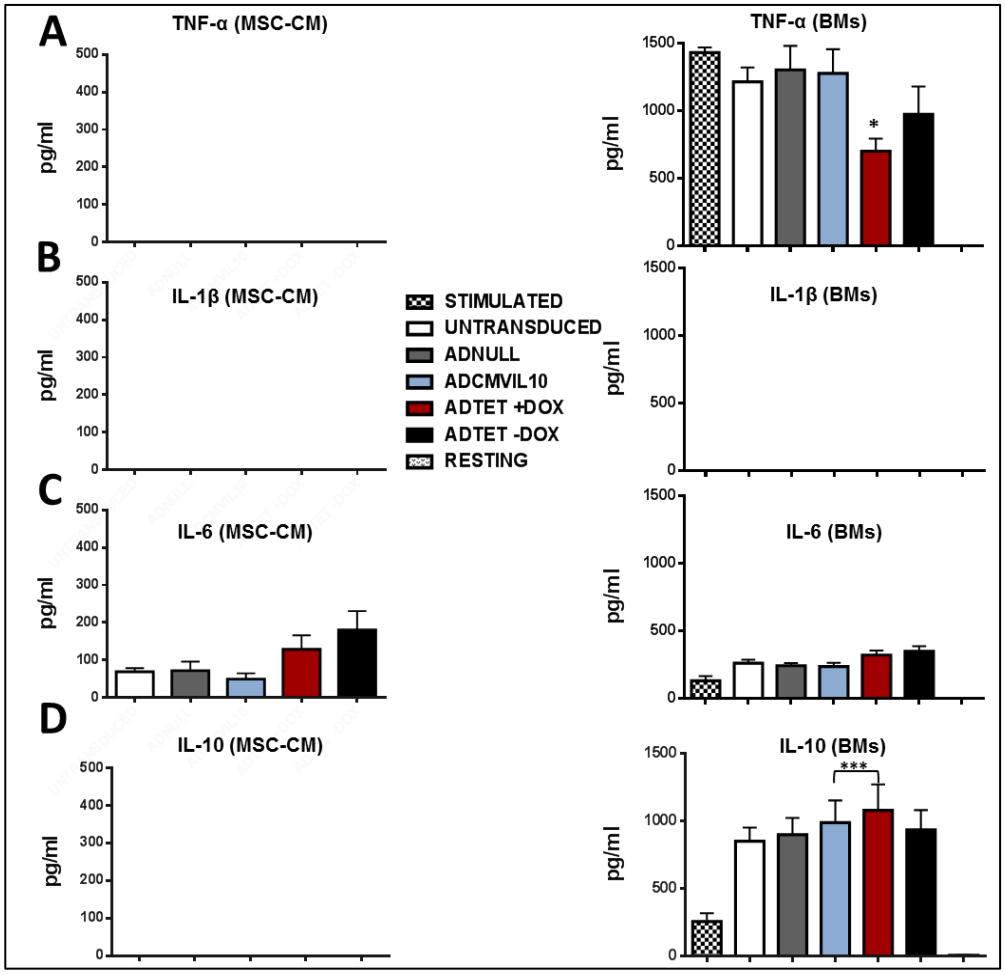

*Figure 3.3 Paracrine effects of vIL10 MSCs on activated BMs. BMs were primed with IFN-γ (20ng/ml) and activated with LPS (10ng/ml) for 6h. Cells were incubated with or without conditioned medium (CM) from untransduced, ADNULL, ADCMVIL10, ADTET +DOX or ADTET –DOX mMSCs. Levels of murine A) TNF-a, B) IL-1β, C) IL-6 and D) IL-10 were measured by ELISA in both MSC-CMs (left panels) and supernatants collected from resting, stimulated and treated BMs (right panels). BMs treated with CM from ADTET +DOX MSCs showed significantly reduced levels of TNF-a and increased IL-10. A significant increase in IL-10 levels was also observed in ADCMIL10 CM treated BMs. Values are expressed as the Mean±SEM (n=3, technical triplicates). Statistical significance was determined by one-way ANOVA with Bonferroni's multiple comparisons test. *p<0.05, ***p<0.001.*

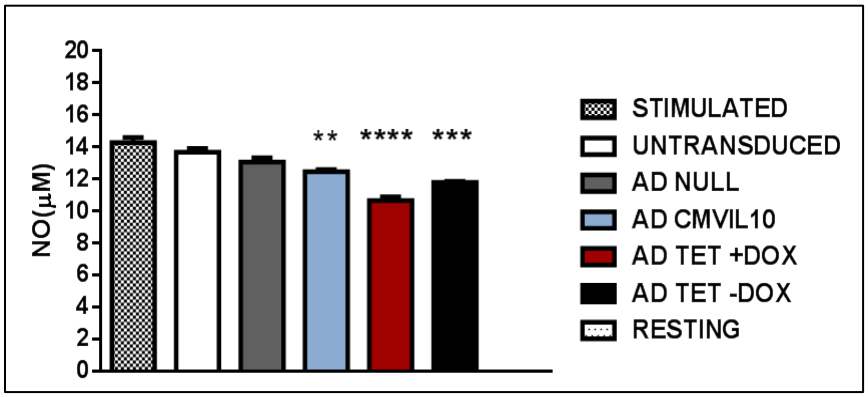

*Figure 3.4 Suppression of nitric oxide production by vIL10 MSCs. LPS activated and MSC-CM treated BMs were tested for release of nitric oxide (NO) by a Griess after 6h incubation. BMs treated with CM from ADCMVIL10, ADTET +DOX and ADTET –DOX MSCs demonstrated significantly lower levels of NO production compared to stimulated BMs. Values are expressed as the Mean±SEM (n=3, technical triplicates). Statistical significance was determined by one-way ANOVA with Bonferroni's multiple comparisons test. **p<0.005, ***p<0.001, ****p<0.0001.*

3.3.4 MSC-mediated regulation of macrophage gene expression

To test the immunomodulatory potential of vIL10 MSCs on the pro-inflammatory gene expression profile of activated BMs, macrophages were stimulated with IFN-γ and LPS for 24h and treated with MSC-CMs. From a panel of 84 critical mouse inflammatory cytokine and receptor genes the expression of Chemokine (C-C motif) ligand 4 (*Ccl4*), *Ccl6*, *Ccl9*, Chemokine (C-X-C motif) ligand 5 (*Cxcl5*), Interleukin 33 (*Il33*) and Platelet factor 4/ Chemokine (C-X-C motif) ligand 4 (*Pf4*/*Cxcl4*) were the highest downregulated genes in BM treated CM from ADTET+DOX MSCs in comparison to the stimulated BMs based on a heat map analysis (Appendix 1; S2: A&B) and fold regulation data (Appendix 1: S2) (SA Biosciences PCR Array Data analysis-Qiagen). The experiment was repeated in three biological donors to validate the array results. Mouse Interleukin 10 (*Il10*) and Arginase-1 (*Arg1*) genes were also included in this assessment to test the efficacy of vIL10 MSCs in modulating macrophage polarisation to an anti-inflammatory phenotype. Treatment of activated BMs with CM from ADTET +DOX MSCs significantly deceased *Ccl4* ($p= 0.003$), *Ccl9* ($p= 0.0004$) and *Cxcl5* ($p= 0.0015$) gene expression compared to stimulated BMs (mean fold change= 8.7). Expression of *Pf4* was significantly reduced in BMs treated with untransduced ($p=0.01$), ADCMVIL10 ($p=0.03$) and ADTET +DOX ($p=0.01$) MSC-CMs. Although there was reduced expression of *Ccl6* and *Il33* in ADCMVIL10 and ADTET +DOX treated BMs, the results were not statistically significant. On the other hand, ADTET +DOX CM significantly increased mouse *Il10* gene expression in treated BMs. The expression of *Arg1* was significantly over-expressed in BMs treated with ADCMVIL10 ($p<0.0001$) and ADTET +DOX ($p=0.0003$) MSC-CMs indicative of anti-inflammatory M2 phenotype-like macrophage polarisation (Figure 3.5).

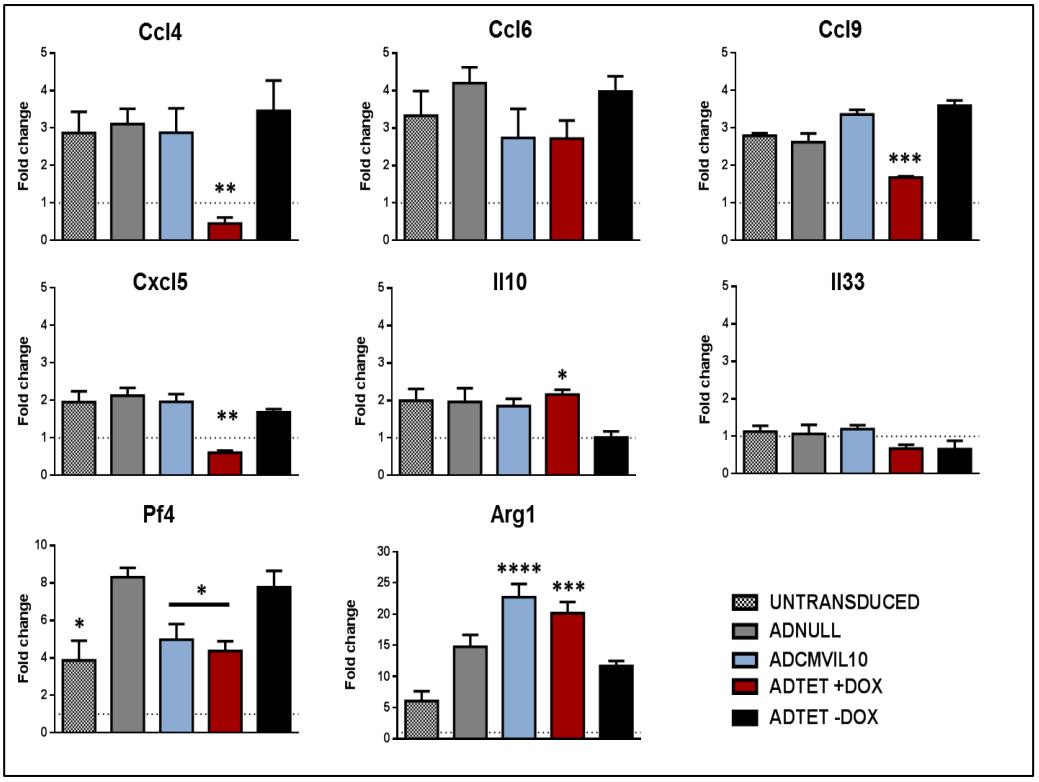

*Figure 3.5 Regulation of macrophage gene expression by MSCs. BMs were activated with LPS and/or treated with MSC-CMs for 24h followed by analysis of gene expression. Significantly decreased expression (fold change) was observed for Ccl4, Cxcl5, Ccl9 and Pf4 compared to stimulated BMs (relevant expression normalised to Gapdh indicated by the dashed line). There was no significance seen in altered Ccl6 and Il33 gene expression. vIL10 MSC treatment altered macrophage polarisation to a M2-like phenotype as shown by increased expression of Il10 and Arg1. Values are expressed as the Mean±SEM (n=3, technical triplicates). Statistical significance was determined by one-way ANOVA with Sidak's multiple comparisons test. *p<0.05, **p<0.005, ***p<0.001, ****p<0.0001.*

3.3.5 Polarisation of activated macrophages towards a regulatory phenotype by vIL10 MSCs

Differentiated BMs at day 6 were primed with IFN-γ (overnight) and stimulated with LPS for 6h. Activated BMs were treated with untransduced or transduced MSCs in direct co-cultures. The optimal ratio of BMs to MSCs and the time-point for efficient co-culture in terms of macrophage polarisation from M1 to M2 phenotype was identified by flow cytometry (Appendix 1; S3A) as 3 days of culture (72h) at a ratio of 1:5. The expression of the M1 marker MHC-II was consistently reduced (minimal inter-replicate variation) in all groups of MSC treated BMs compared to stimulated BMs at 72h at a ratio of 1:5 (Appendix 1; S3B). Similarly, the expression of the M2 marker, CD206 was two times higher in BMs co-cultured with ADTET +DOX MSCs at 72h at a ratio of 1:5 in comparison to stimulated BMs (Appendix 1; S3C). The overall expression pattern of MHC-II and CD206 was more consistent at 72h compared to 48h in all MSC-treated groups.

This experiment was repeated with three biological replicates, at the optimised ratio of 1:5, with MSCs and BMs co-cultured for 72h. Classically activated, F4/80+ BMs polarised to a M1 phenotype as seen by increased Mean Fluorescence intensity (MFI) of MHC-II (Figure 3.6A). There was significantly lower expression of MHC-II by BMs treated with ADCMVIL10 MSCs ($p=0.0071$) which was reduced further with ADTET +DOX ($p<0.001$) MSCs compared to stimulated BMs. A clear shift in polarisation from a M1 to a M2 phenotype was shown by increased CD206 expression in activated and vIL10-treated BMs (Figure 3.6B). Expression of CD206 was significantly higher in BMs treated with ADCMVIL10 MSCs ($p<0.05$) and ADTET +DOX ($p= 0.0052$) MSCs compared to stimulated BMs.

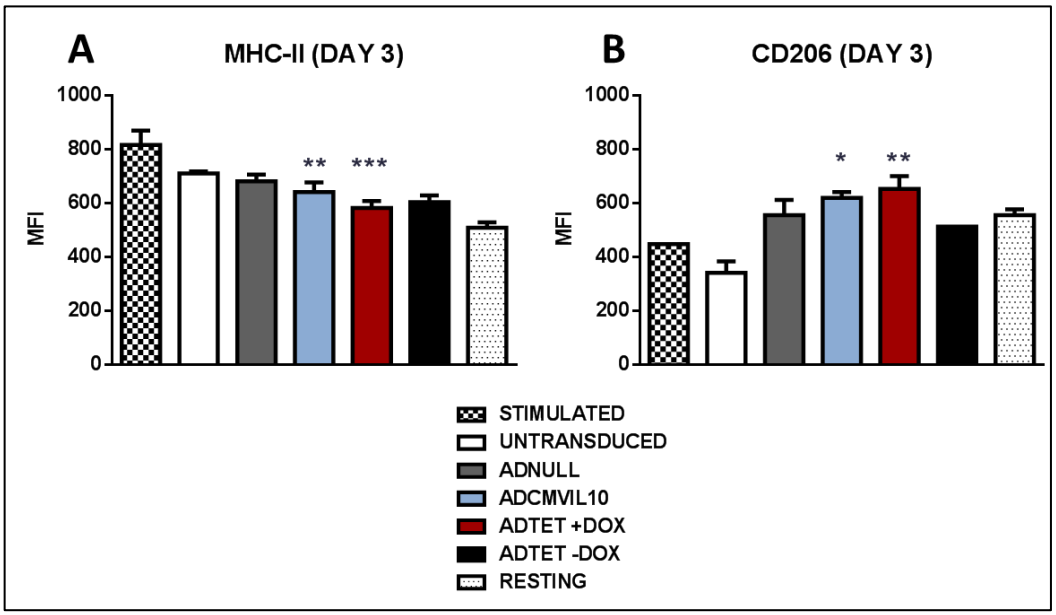

*Figure 3.6 Macrophage polarisation by vIL10 MSCs. Differentiated BMs were activated with IFN-γ and LPS and/or co-cultured with MSCs at a ratio of 1:5 for 72h followed by analysis of changes in expression of MHC-II (M1 marker) and CD206 (M2 marker). A) Significant decreases in mean fluorescence intensity (MFI) of MHC-II and B) increases in CD206 were observed in BMs cultured with ADCMVIL10 and ADTET +DOX MSCs compared to stimulated BMs. No significant differences were observed in BMs cultured with untransduced, ADNULL or ADTET –DOX MSCs. Values are expressed as the Mean±SEM (n=3). Statistical significance was determined by a one-way ANOVA with Sidak's multiple comparisons test. *p<0.05, **p<0.005, ***p<0.001.*

3.3.6 Suppression of T cell proliferation by vIL10 MSCs

To test the immunomodulatory capacity of vIL10 MSCs on T cell proliferation, splenocytes isolated from C57BL/6J murine spleen were labelled with CTV and activated with anti-CD3e and anti-CD28 antibodies. In order to evaluate the duration and quantity of MSCs needed to obtain a significant effect, different ratios of MSC:activated T cell co-cultures were tested for 3 and 5 days followed by staining for CD4 and CD8 antibodies to measure cell proliferation by flow cytometry (Appendix 1; S4A). Suppression of $CD4^+$ cell proliferation was higher on day 3 at a ratio of 1:10 compared to 1:25 and day 5 (Appendix 1; S4B). $CD8^+$ lymphocyte proliferation was suppressed at day 3 and 5 at a ratio of 1:10 and not 1:25 (Appendix 1; S4C). The descending trend (untransduced to ADTET +DOX MSCs) in $CD4^+$ and $CD8^+$ T cell inhibition by MSCs was more consistent on day 3 at 1:10 ratio than 1:25 cell ratio and day 5 proliferation.

To validate the effect of vIL10 MSCs on splenocyte proliferation at the optimised ratio of 1:10, the experiment was repeated with three biological replicates. Cells at day 3 co-culture were stained for CD4, CD8 and the early activation marker CD25 for analysis by flow cytometry. Proliferation of $CD4^+$ lymphocytes was significantly suppressed by untransduced ($p<0.0001$), ADCMVIL10 ($p<0.0001$) and ADTET +DOX MSCs ($p<0.0001$) with maximum inhibition seen with the Tet-ON MSCs (~40% suppression; Figure 3.7A). There was also significant suppression of activated $CD4^+$ T cell populations in all of the MSC treated groups with a mean value overall of 49% in comparison to stimulated cells. However, there were no differences seen between the MSC groups (Figure 3.7C). Additionally, neither suppression of activated $CD8^+$ T cells nor change in $CD8^+$ T cell proliferation was seen following treatment with MSCs (Figure 3.7B & D).

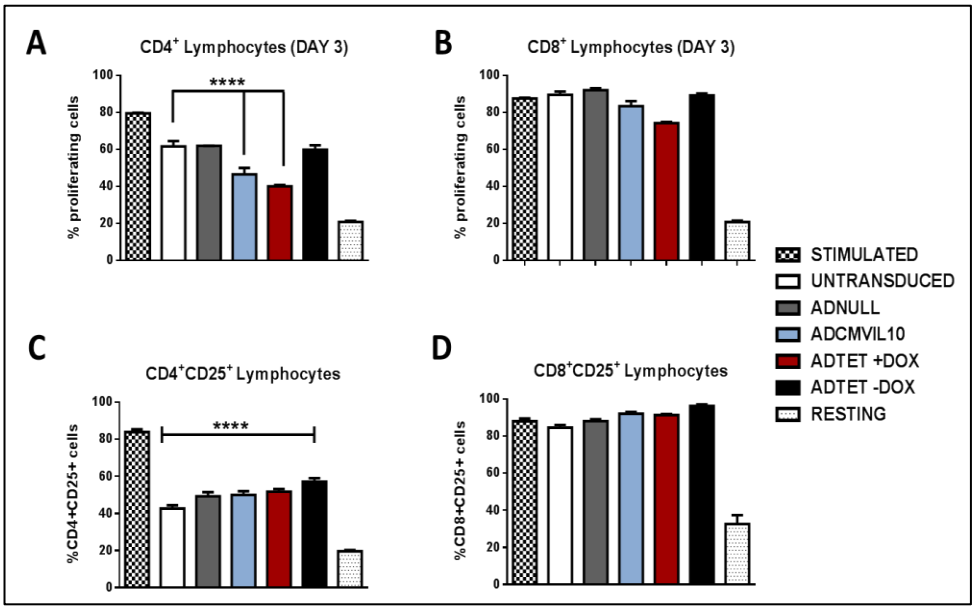

*Figure 3.7 Suppression of T cell proliferation by vIL10 MSCs. Splenocytes isolated from C57BL/6 murine spleens were labelled with CTV and activated with anti-CD3e and anti-CD28 antibodies. Stimulated cells were co-cultured with MSCs at an optimised ratio of 1:10 for 72h and stained for CD4, CD8 and CD25. A) Significant decreases in proliferation of $CD4^+$ lymphocytes were observed in cells treated with untransduced, ADCMVIL10 and ADTET +DOX MSCs at day 3. B) $CD8^+$ lymphocytes were suppressed following treatment with ADCMVIL10 and ADTET +DOX MSCs compared to stimulated cells but not significantly. C) CD25 was used as an activation marker and the proliferation of $CD4^+CD25^+$ T cells was significantly suppressed by all groups of MSCs. D) Suppression of activated $CD8^+CD25^+$ lymphocytes following MSC treatment was not observed. Values are expressed as the Mean±SEM (n=3, technical triplicates). Statistical significance was determined by one-way ANOVA with Sidak's multiple comparisons test. ****$p<0.0001$.*

3.4 Discussion

Inflammation of the synovium is considered a key contributing factor towards OA progression based on studies that detected synovitis using ultrasonography and MRI, even in patients with early OA (Benito et al., 2005, Coari, 2000, Loeuille et al., 2005). Among the several pathological roles of synovitis in OA, infiltration of inflammatory cells and their production of catabolic soluble mediators in the synovial lining expedites and perpetuates the processes of cartilage degradation (van Lent and van den Berg, 2013, Sellam and Berenbaum, 2010). Of the immune cells infiltrating the OA synovial lining, activated macrophages, T and B cells are the most predominant cell types with high levels of $CD4^+$ T lymphocytes and $CD68^+$ macrophages found in synovial tissue of patients with early OA (Benito et al., 2005, Nakamura et al., 1999). Bone-marrow derived MSCs are adult stromal cells with multi-lineage differentiation capacities. They exert potent immunomodulatory effects via section of trophic factors and tissue regenerative ability by homing to damaged tissues (Caplan and Dennis, 2006b, Maggini et al., 2010).

In addition, the immunosuppressive capacity of MSCs is enhanced based on the inflammatory stimulus/environment. For example, two independent studies demonstrated that MSCs adopt an immunosuppressive phenotype in the presence of IFN-γ, TNF-α and IL-1α/β produced by activated macrophages and in turn secrete high levels of soluble factors including NO, TGF-β, IDO and PGE_2 leading to suppression of T cell proliferation and macrophage polarisation (Crop et al., 2010, Maggini et al., 2010). Liu et al. showed that transduced human MSCs over-expressing human tumour necrosis factor receptor II (hsTNFR) aided in reduction of joint inflammation in a murine immune competent CIA model, compared to untransduced human MSCs (Liu et al., 2013b). Similarly, Choi et al. demonstrated reduced disease severity in a RA model as a result of treatment with IL-10 over-expressing murine MSCs (Choi et al., 2008). Hence MSCs can portray enhanced therapeutic potential via overexpression of immunomodulatory factors. So far, only one study conducted by Farrell et al. showed that vIL10 over-expressing human MSCs induced long-term reduction of activated $CD4^+$ and $CD8^+$ T cell populations in the draining lymph nodes of mice with collagenase-induced OA. However, the question remains as to whether the immunomodulatory efficacy of MSCs improve when inducible vIL10 expression occurs in a controlled manner. Data shown here

highlight the enhanced immune-regulatory activity of Tet-ON controlled vIL10 MSCs on activated murine macrophages and T cells *in vitro* via paracrine and juxtacrine signalling.

Synovial macrophages account for the majority of innate immune activation and cytokine production in OA (Bondeson et al., 2006, Bondeson et al., 2010). Among the activated population of macrophages, classically activated macrophages (M1) are generated in response to a combination of dual signalling from IFN-γ and TNF (autocrine cytokine) with the latter stimulus induced by a TLR ligand such as LPS (Mosser and Zhang, 2008, Mosser and Edwards, 2008). In the context of synovitis and OA these activated M1 macrophages display enhanced microbicidal ability and secrete high levels of pro-inflammatory cytokines and mediators, typically TNF-α, IL-1β and IL-6 (Yamamoto et al., 2003, Mackaness, 1977, Mosser, 2003).

Here, BMs, derived from C57BL6/J mice, stimulated with IFN-γ and LPS polarised into M1 macrophages as seen by production of TNF-α and IL-6. Treatment of activated BMs with CMs collected from ADTET +DOX MSCs resulted in significantly reduced production of TNF-α and increased secretion of IL-10 in BMs treated with ADCMVIL10 and ADTET +DOX CMs. Furthermore, these MSCs produced murine recombinant IL-6 but not TNF-α, IL-1β or IL-10. Although IL-6 is considered a pro-inflammatory cytokine found in high levels in the synovial fluid of OA and RA patients (Pearle et al., 2007, Kaneko et al., 2000, Sohn et al., 2012), a number of studies have pointed out the ambivalent nature of this cytokine and its protective role towards proteoglycan synthesis in murine models of experimental arthritis (Van de Loo et al., 1997, de Hooge et al., 2005).

In a study conducted by Asami et al. treatment of TLR7/8 ligand stimulated bone-marrow derived BL6 macrophages with MSC CM resulted in significantly lower expression of TNF-α and IL-6 and higher levels of IL-10 compared to untreated macrophages. This immunomodulatory activity of MSCs was attributed to secretion of PGE_2 (Asami et al., 2013). One possible explanation for the enhanced immunosuppressive activity of vIL10 expressing Tet ON MSCs is that the secreted trophic factors from MSCs interact with EP2 and EP4 receptors on macrophages which can boost IL-10 mediated immunomodulation by MSCs (Hayes et al., 2002, Németh et al., 2009). Secondly, an inflammatory environment created by LPS and IFN-γ results in the sensitisation of MSCs

to adopt an anti-inflammatory phenotype leading to polarisation of M1 macrophages to an IL-10 secreting regulatory phenotype via ERK signalling (Lucas et al., 2005, Waterman et al., 2010, Tomchuck et al., 2008). In comparison to the immunomodulatory effects of ADCMVIL10 MSC CM, BMs treated with Tet-ON controlled ADTET +DOX MSCs displayed enhanced suppression of TNF-α and increased production of IL-10. Eddie and co-workers have shown that $Il10^{-/-}$ macrophages derived from a murine model of colitis exhibited accumulation of dysregulated mitochondria. In addition, they further showed that macrophages from inflammatory bowel disease (IBD) patients carrying a null mutation in the IL-10R gene demonstrated aberrant activation of the NLRP3 inflammasome and IL-1β secretion. Mitochondria have been identified as an important signalling organelle contributing towards inflammasome activation and dysregulated mitochondria are associated with high levels of reactive oxygen species (ROS) production leading to NLRP3 activation and IL-1β secretion (Weinberg et al., 2015). Following treatment of IL-10-deficient murine and human macrophages with recombinant IL-10, an anti-inflammatory response was elicited and this led to reprogramming of macrophages with regulated mitochondrial function (Ip et al., 2017). This data illustrates the important role of IL-10 in macrophage regulation and that doxycycline mediated release of vIL10 enables sustained anti-inflammatory activity.

NO is a cytotoxic messenger molecule generated due to up-regulation of NO synthase produced by synovial macrophages that have been activated by TNF-α, IFN-γ and/or IL-1β (Hölscher et al., 1998, Abramson et al., 2001). Production of NO leads to cartilage degradation, alterations in mitochondrial activity and subsequent chondrocyte apoptosis (Cillero-Pastor et al., 2011) based on detection of high levels of NO in the synovium and cartilage of patients with RA and OA (Rediske et al., 1994, Vuolteenaho et al., 2007, Hilliquin et al., 1997). Here, LPS stimulated BMs produced high levels of NO. Upon treatment with CMs from ADCMVIL10, ADTET +DOX and ADTET –DOX MSCs, NO was significantly reduced with maximum inhibition seen after treatment with ADTET +DOX CM. This immune-suppressive activity of MSCs was also previously observed in a rat model of bleomycin-induced lung injury. Following intravenous transfer of bone-marrow derived MSCs, the levels of nitrate and nitrite production was significantly reduced in the disease group. (Lee et al., 2010). Typically in patients with

grade 2 and 3 knee OA, the levels of synovial nitrite/nitrate ranges between 50.26±23.63 μg/L (0.05μM/ml; (Karan et al., 2003)) which is not comparable to *in vitro* mouse macrophage values which is almost 280 times higher (~14μM/ml as seen with stimulated BMs in the present study, Figure 3.4). Also unlike murine macrophages, endotoxin stimulated human chondrocytes *in vitro* release NO at nanomolar concentrations and OA-affected cartilage express a 150kD isoform of NOS which is completely different in structure and regulatory properties of mouse macrophage derived iNOS (Abramson et al., 2001, Palmer et al., 1993, Blanco et al., 1995). Hence MSC-mediated reduction in NO levels in the present chapter is indicative of an immunomodulatory effect through paracrine signalling, but to derive a clinical relevance in terms of biological significance/efficacy, further studies in stimulated human macrophages/chondrocytes would enable further validation.

Gene expression analysis on stimulated BMs treated with CMs from MSCs revealed significant downregulation of the inflammatory chemokines *Ccl4, Ccl9, Cxcl5, Cxcl4/Pf4* and up-regulation of anti-inflammatory gene cytokine *Il10* and the M2 marker Arg1. MSC-mediated immunomodulation was highest in BMs treated with ADTET +DOX CM followed by ADCMVIL10 CM. Chemokines are factors secreted by a number of immune cells including macrophages and T cells and their role is to act as a chemoattractant and /or recruiters of macrophages to sites of inflammation. Chemokines CCL4, CCL6 and CCL9 belong to the family of macrophage inflammatory proteins (MIPs) and are involved in several stages of OA development. CCL4 is expressed by human chondrocytes and elevated levels have been observed in synovial fluid of OA patients (Borzì et al., 1999, Koch et al., 1995, Furman et al., 2015). It is also produced by hypertrophic chondrocytes as evidenced in a murine model of diabetic fracture (Alblowi et al., 2013). CCL9 (Shen et al., 2011) and CXCL4 (Affandi et al., 2018, Yeo et al., 2016) on the other hand are produced in high levels by activated $CD4^+$ T cells and lead to OA disease progression by increasing macrophage infiltration in the synovium. CXCL5 is a neutrophil chemoattractant and pro-angiogenic chemokine produced by M1 macrophages (Mantovani et al., 2004). In a murine model of IL-17 induced arthritis, blockade of CXCL5 inhibited joint vascularisation mediated by IL-17.

IL-33 is a newer addition to the IL-1 family of pro-inflammatory cytokines. Previous studies have reported the secretion of IL-33 in the serum and synovial fluid of RA and OA patients and synovial fibroblasts produced high amounts following *in vitro* stimulation with TNF-α (Talabot-Ayer et al., 2012, El-Aziz Farag et al., 2017, Palmer et al., 2009). Here, expression of murine *Il33* was downregulated in stimulated BMs treated with ADTET +DOX CM, however statistical significance was not observed. *Arg1* is typically produced by M2-wound healing macrophages and has a critical role in converting L-arginine into urea and ornithine required for collagen synthesis and cell proliferation (Arlauckas et al., 2018, Murray et al., 2014). It is one of the early genes expressed in the joint following inflammation and high levels may be indicative of infiltration of regulatory macrophages involved in immune-regulation and tissue repair (Rath et al., 2014, Campbell et al., 2013). Significant upregulation of *Arg1* expression was observed in stimulated BMs treated with ADCMVIL10 and ADTET +DOX MSC CMs suggesting possible polarisation of BMs into M2-like subsets typically induced by IL-4 *in vitro* with high levels of IL-10 secretion (Mosser and Edwards, 2008, Mosser, 2003). This was further confirmed with significant upregulation of *Il10* expression in ADTET +DOX CM treated BMs.

M1 macrophages typically represent a pro-inflammatory phenotype identified by expression of MHC-II, CD68, CD80 and CD86 (Daghestani et al., 2013, Fahy et al., 2014). On the other hand M2 macrophages produce high amounts of IL-10 and express CD163 and CD206 on their cell surface (Murray et al., 2014, Mosser, 2003, Utomo et al., 2016). Maggini et al. demonstrated that MSCs suppress and switch LPS activated macrophages into IL-10 producing regulatory cells *in vitro* (Maggini et al., 2010). M2 macrophages subsets can be either wound-healing (IL-4-induced) or regulatory (IL-10-induced) in function (Mosser and Edwards, 2008, Utomo et al., 2016). However, data generated by the current study clearly depicted that macrophage polarisation was mediated via IL-10 through vIL10 MSCs and that controlling the release of vIL10 using doxycycline further enhanced the immune-regulatory capacity of MSCs on macrophages. MSCs are also known to constitutively produce IL-6, which polarizes macrophages toward an anti-inflammatory IL-10-producing M2 subset by juxtacrine signalling (Eggenhofer and Hoogduijn, 2012). This mechanism was also observed here with analysis of the secretome

showing that MSC-CMs constitutively produced IL-6 and simultaneously demonstrated suppression of TNF-α in stimulated BMs.

The ability of vIL10 MSCs to polarise activated macrophages into an anti-inflammatory M2 phenotype was further confirmed here based on results from direct co-culture experiments. Flow cytometry analysis of activated BMs co-cultured with mMSCs for 3 days showed overall suppression of MHC-II in all MSC treated BMs in comparison to stimulated BMs alone. The extent of suppression was significantly higher in BMs cultured with ADCMVIL10 and ADTET +DOX MSCs. Apart from this, activated BMs were pushed towards an anti-inflammatory M2 phenotype as illustrated by increased CD206 expression with significantly higher levels observed in ADCMVIL10 and ADTET +DOX cultured BMs. With respect to the association of macrophage polarisation leading to OA progression or attenuation, Liu et al. alone showed that an imbalance in the ratio of M1/M2 macrophages directly impacts the severity of knee OA. They also demonstrated that expression of CD206 was significantly lower in the synovial fluid and peripheral blood samples of knee OA patients compared to healthy donors (Liu et al., 2018a). Despite previous reports demonstrating the presence of both M1 and M2 macrophage phenotypes and increase in M1/M2 ratio in OA synovial fluid, the exact quantity of specific markers leading to disease severity or polarisation status is unknown (De Lange-Brokaar et al., 2012, Blom et al., 2004, Favero et al., 2015, Daghestani et al., 2013, Fahy et al., 2014). Moreover, in a study conducted by Manferdini et al. high level of inter-patient variability was observed in the expression of M1 and M2 markers in the OA synovium (Manferdini et al., 2017). Therefore ADTET +DOX MSC mediated suppression of MHC-II and increased expression of CD206 does indicate a polarisation in macrophage phenotype from M1 to M2, but the actual level of change required to indicate polarisation is difficult to define and requires further exploration.

$CD4^+$ and $CD8^+$ T cells constitute the majority of the T cell population in the synovial aggregates of OA patients (Haynes et al., 2002). Recent studies have identified the role of $CD4^+$ T cells in osteoclastogenesis and induction of MIP-1γ (Shen et al., 2011), while activation of $CD8^+$ T cells has been directly correlated with TIMP-1 expression and cartilage degeneration (Hsieh et al., 2013). Although higher percentages of $CD4^+$ T lymphocytes were observed during the onset of OA in an anterior cruciate ligament

transection (ACLT) model, another study showed that the percentages of $CD3^+$, $CD4^+$ and $CD8^+$ cells were significantly higher in OA patients over the age of 75, suggestive of the role of T cell activation in chronic inflammation (Moradi et al., 2015, Pawłowska et al., 2009). In this study, vIL10 MSCs demonstrated suppression of splenocyte proliferation following 3 days of co-culture at a ratio of 1:10. Proliferation of $CD4^+$ lymphocytes was significantly suppressed by untransduced, ADCMVIL10 and ADTET +DOX MSCs with maximum inhibition seen with the Tet-ON MSCs (~40% suppression).

Significant suppression of activated $CD4^+$ T cells was seen in all of the MSC treated groups. This suppression of activated CD^+ T cells correlated with downregulation of *Ccl9* and *Cxcl4* gene expression in BMs treated with ADTET +DOX MSC CM. Previous reports suggest the stimulatory role of CCL9 and CXCL4 released by activated CD4+ T cells in response to infiltrating synovial macrophages in psoriatic arthritis, RA and OA (Affandi et al., 2018, Moradi et al., 2015, Yeo et al., 2016). Unlike suppression of $CD4^+$ lymphocytes, no suppression of activated $CD8^+$ T cells was seen following treatment with MSCs. This is quite the opposite effect observed in comparison to similar studies involving autologous lymphocytes that responded equally to co-cultures (Di Nicola et al., 2002). An explanation for this modified efficacy of MSCs towards $CD8^+$ lymphocytes could be the line of murine MSCs used (Schurgers et al., 2010). While $CD8^+$ T cells are found in the synovial membrane and aggregates of OA patients these cytotoxic T cells do not comprise of the major T cell infiltrate (Li et al., 2017b, Reidbord and Osial, 1987, Johnell et al., 1985). Also the only known pathological role of $CD8^+$ T cells is based on induction of TIMP-1 expression and associated OA severity (Hsieh et al., 2013). The only known previous study using vIL-10 expressing human MSCs by Farrell et al. showed significant reduction in the amount of activated $CD4^+$ and $CD8^+$ T cells in the popliteal and inguinal lymph nodes of collagenase induced OA mice. However the exact biological mechanism behind this MSC mediated T cell suppression is unknown (Farrell et al., 2016). More comprehensive *in vitro* and *in vivo* studies are therefore required to exactly understand the interaction between MSCs and cytotoxic T cells ($CD8^+$ T lymphocytes).

Overall the data generated here demonstrated that engineered murine vIL10 MSCs elicited an immune-suppressive response by switching activated macrophages into an anti-

inflammatory phenotype and regulated the activation and proliferation of $CD4^+$ T lymphocytes. Secondly, vIL10 MSCs displayed enhanced levels of immune modulation when operated under the control of the tetracycline system of induction. Finally, MSC-mediated anti-inflammation was achieved in activated macrophages and splenocytes using both direct co-cultures and conditioned medium treatments further validating the hypothesis that tetracycline induced vIL10 MSCs can modulate inflammatory processes *in vitro* via juxtacrine and paracrine signalling.

Chapter 4

Establishment of a novel *in vitro* model investigating the impact of acute and chronic inflammatory effectors on cartilage development.

4.1 Introduction

Cartilage degradation is a hallmark feature of OA, with catabolic products of altered chondrocytes involved in early changes to articular cartilage. Synoviocytes such as macrophages, fibroblasts and also chondrocytes at or adjacent to the sites of a cartilage lesion contribute to progression of the disease (Goldring, 2000, Maldonado and Nam, 2013, Sokolove and Lepus, 2013). Cytokines and chemokines play a central role in the immunopathogenesis of OA by constantly switching the inflammatory microenvironment and modulating the function of chondrocytes themselves as well as critical immune cells such as monocytes and T cells (Bernardo and Fibbe, 2013, Goldring and Otero, 2011, Goldring et al., 2011). In the very early stages of OA prior to complete dysregulation of cartilage homeostasis and destruction of articular cartilage, resident articular chondrocytes make attempts at repair by exhibiting a temporary clonal growth phase and synthesising increased quantities of cartilage matrix components like type II collagen and aggrecan, and catabolic cytokines and MMPs (IL-1β, TNF-α and MMP13 for example). However as OA progresses, chondrocytes undergo physiologic and metabolic alterations leading to cell clustering, fibrillation of the cartilage surface, decreased synthesis of type II collagen and aggrecan, and an imbalance of cytokines and proteinase/inhibitor content (Goldring et al., 2008, Goldring and Otero, 2011, Goldring et al., 2011).

The pro-inflammatory cytokine IL-1β has been well-studied both *in vitro* and *in vivo* in the context of cartilage degeneration and chondrocyte apoptosis in OA (Mueller and Tuan, 2011, Haseeb and Haqqi, 2013). Along with TNF-α, IL-1β is known to induce and accelerate the production of IL-6 and IL-8 by synoviocytes and chondrocytes (Fernandes et al., 2002, Stannus et al., 2010). In addition, OA chondrocytes exhibit elevated expression of *MMP13, ADAMTS4, ADAMTS5* and suppressed expression of *COL2A1* as a consequence of activation of intracellular signalling pathways like JNK, p38 MAPK, NF-κB and TLR-4 mediated by IL-1β and TNF-α (Goldring et al., 1994, Mengshol et al., 2000, Bobacz et al., 2007, Kim et al., 2006, Reginato et al., 1993). Unlike other pro-inflammatory cytokines, IL-1β release requires a two-step process. Initially, PAMPs/DAMPs interact to induce NF-κB signalling that causes production of IL-1β. Oligomerisation of the NLRP3 inflammasome also requires adaptor apoptosis associated speck-like protein containing a CARD (C-terminal caspase recruitment domain) (ASC) to

form a bridge with procaspase-1 in the inflammasome complex. Activation of caspase-1 then leads to NLRP3 inflammasome complex formation to further mediate cleavage of pro-IL-1β and release of its mature form (Shao et al., 2015, Man and Kanneganti, 2015, Latz et al., 2013). NLRP3 is therefore a crucial mediator of IL-1β production through its unique ability to detect 'danger signals' or DAMPs, the second activation step in IL-1β release. Some of the well-studied DAMPs acting as stimuli of NLRP3 activation require high concentrations of extracellular ATP, ROS generation, uric acid and BCP crystals (Pétrilli et al., 2007, Martinon et al., 2006, Mariathasan et al., 2006). NLRP3 has been suggested to contribute to OA pathogenesis by mediating IL-1β release which has been associated with cartilage degradation, synovial inflammation and chondrocyte apoptosis via pyroptosis (Scanzello and Goldring, 2012, McAllister et al., 2018, Jin et al., 2011).

Obesity is a well-known risk factor of OA and plays a predominant role in induction of metabolic stress and low-grade inflammation (Courties et al., 2015). High-fat diets containing saturated free fatty acids (FFA) contribute towards metabolic inflammation and cartilage degradation as a result of accumulation of FFA and extracellular lipids in synovial fluid (Alvarez-Garcia et al., 2014) and in chondrocytes (Lippiello et al., 1990). Palmitate or palmitic acid (PA), the most abundant type of saturated FFA in humans, is known to induce chondrocyte apoptosis and production of pro-inflammatory cytokines by synoviocytes and chondrocytes through TLR-4 signalling (Alvarez-Garcia et al., 2014). Accumulation of PA has been associated with the generation of acute lesions in OA joint cartilage (Lippiello et al., 1991, Bonner Jr et al., 1975). Previous studies have also demonstrated the capacity of PA to induce NLRP3 inflammasome formation, caspase-1 activation and production of IL-1β by macrophages and MSCs (Wang et al., 2017, Wen et al., 2011).

Similar to NLRP3, the S100 proteins are yet another class of alarmins/DAMPs with a central role in eliciting low-grade inflammatory responses by inducing positive feedback loops of inflammation, synovial cell reactivation and degradation of cartilage during OA (van Lent et al., 2012, Nefla et al., 2016). Alarmins released by activated synoviocytes and chondrocytes during tissue damage stimulate TLRs and RAGE leading to production of large amounts of cytokines, chemokines and MMPs that further cause aberrant breakdown of cartilage and amplify joint inflammation (Loeser et al., 2012, Seol et al.,

2012, Liu-Bryan and Terkeltaub, 2012). Among the S100 family proteins, S100A8, S100A9 and the S100A8/A9 heterodimer complex are the most extensively studied alarmins with high levels documented in the serum and synovial fluid of patients with OA (van Lent et al., 2012, Cremers et al., 2017, Sunahori et al., 2006). In addition to the pro-inflammatory and catabolic effects of S100A8 and A9 on stimulated macrophages and human OA synovial tissue through activation of TLR-4 and Wnt signalling, (Fassl et al., 2015, van den Bosch et al., 2016), direct *in vitro* stimulation of chondrocyte explants from OA donors with these 2 proteins resulted in the increased production of IL-6, IL-8, MCP-1, MMP-1, 3, 9 and 13 and down-regulation of aggrecan and type II collagen. It was also found that this catabolic effect of S100A8 and A9 on human chondrocytes was mainly associated with TLR-4 activation and was not RAGE dependent (Schelbergen et al., 2012).

Articular cartilage is a structurally unique tissue with a highly organised ECM that has a poor potential to repair following injury, due to low cell density and avascular characteristics (Buckwalter, 1990). Along with these drawbacks, patients with OA present with an inflammatory milieu that promotes disruption of the cartilage matrix and stimulates chondrocyte apoptosis, ultimately leading to irreversible breakdown of cartilage (Yamagata et al., 2018). Currently available cell-based cartilage tissue engineering/repair strategies using chondrocytes (ACI therapy for example) pose some limitations due to their tendency towards terminal differentiation and premature hypertrophy following transplantation (Jayasuriya and Chen, 2015).

MSCs have been regarded historically as a cell source for OA therapy, primarily due to their immunomodulatory, paracrine and chondrogenic differentiation capacities (Barry and Murphy, 2013, Barry, 2019). The ability of the cells to modulate the immune environment in the osteoarthritic joint through paracrine mechanisms is clear in pre-clinical and clinical models (Iijima et al., 2018, Augello et al., 2007, Bouffi et al., 2010, ter Huurne et al., 2012, Desando et al., 2013, Maumus et al., 2016) and data from Murphy et al. also indicated the potential of the cells to promote regeneration of the meniscus in OA joints through activation of endogenous progenitors (Murphy et al., 2003). However, there is no data to indicate that these cells can successfully differentiate into a stable articular cartilage phenotype. MSCs tend to form fibrocartilage and attain a hypertrophic

phenotype during *in vitro* chondrogenesis (Williams and Harnly, 2007, Johnstone et al., 1998, Johnstone et al., 2013, Jayasuriya et al., 2019). The cells therefore undergo terminal differentiation to form the template for endochondral bone formation and not stable articular cartilage (Farrell et al., 2008, Oliveira et al., 2008, Scotti et al., 2010)

Secondly, an active inflammatory environment created by pro-inflammatory cytokines like IL-1β, IL-17 and TNF-α have detrimental effects on cells committed to the chondrogenic lineage. Inflammatory cytokines cause down-regulation of *Sox9* gene by inhibiting Smad signalling and thereby tamper with chondrogenic differentiation of MSCs (Baugé et al., 2008, Kondo et al., 2013, Baugé et al., 2007, Sitcheran et al., 2003, De Crombrugghe et al., 2000).

ACPs on the other hand are undifferentiated precursors of cartilage, developmentally primed to become chondrocytes (Dowthwaite et al., 2004, Jayasuriya and Chen, 2015). Unlike MSCs, clonal populations of ACPs *in vitro* have previously demonstrated maintenance of chondrogenic potential over extended population doublings, while being resistant to terminal hypertrophic differentiation (McCarthy et al., 2012). This capacity was also correlated with their ability to preserve their telomerase activity and Sox9 expression through extensive monolayer culture (Khan et al., 2009a). In addition, a number of studies have shown their reparative effects in OA cartilage in response to injury (Gerter et al., 2012, Seol et al., 2012, Jayasuriya et al., 2019, Koelling et al., 2009, Nelson et al., 2014).

Although ACPs are primed for chondrogenic programming, another important aspect to consider in cartilage repair/engineering strategies is a favourable and balanced ECM microenvironment promoting stable chondrogenesis and/or stem cell homing and growth towards cartilage regeneration. Synthetic scaffolding materials have been extensively tested and used to encapsulate chondrocytes and MSCs for cartilage engineering and repair strategies (Yamagata et al., 2018, Chubinskaya et al., 2001, Diduch et al., 2000, Kavalkovich et al., 2002) as they offer flexibility and lower levels of cytotoxicity, while mimicking molecules/structures of natural cartilage tissue (Rowley et al., 1999). Hydrogels such as alginate have been used for cartilage tissue engineering and repair (Diduch et al., 2000, Fragonas et al., 2000). Alginate shares similar conformational

flexibility to glycosaminoglycans and can generate an optimal mechanical environment due to their structural versatility and gentle gelling conditions (Arlov and Skjåk-Bræk, 2017). The use of alginate as a matrix has also been shown to enhance chondrogenesis of MSCs (Xue et al., 2013, Kavalkovich et al., 2002) and with successful delivery of MSCs for treatment of OA (McKinney et al., 2019, Leijs et al., 2016, Reppel et al., 2015).

The current chapter therefore aims to investigate the following hypotheses:
1. That inflammasome activation acts as an acute inflammatory insult to induce altered behaviour of chondrocytes derived from ACPs (articular-like chondrocytes) or MSCs (hypertrophic chondrocytes) and
2. Chronic inflammatory input of S100A8/A9 alarmins in conjunction with inflammasome activation promotes an OA-like hypertrophic phenotype.

To test these hypotheses the specific aims of the chapter were the:

1. **Comparison of chondrogenic differentiation potential of alginate encapsulated human ACPs and bone-marrow derived MSCs *in vitro*.**

To achieve this aim, ACPs and MSCs were initially tested for their chondrogenic potential without encapsulation for 7, 14, 21 and 28 days to optimise the time points for encapsulation experiments with GAG quantitation and histological analysis as outputs. Thereafter a three-dimensional (3D) model of cartilage was created by encapsulating ACPs and MSCs in sodium alginate and maintaining the resulting alginate beads in chondrogenesis for 28 days in hypoxic conditions.

2. **Examining the impact of inflammasome activation in the encapsulated cells following chondrogenic differentiation.**

Here ACPs and MSCs were initially optimised for inflammasome activation and IL-1β release by stimulating the cells with a combination of LPS (TLR-4 signal inducer, Signal 1) and either ATP or PA (Signal 2) and tested for caspase-1 activation and gene expression of NLRP3 and IL-1β. After identification of optimal conditions, encapsulated ACPs and MSCs beads at day 27 of chondrogenic differentiation were stimulated with an acute inflammatory insult of LPS and PA for 24h. Experimental endpoints included caspase-1 activation assay, GAG quantitation, gene expression and histological analysis.

3. **Investigate the effects of dual inflammatory stimuli using continuous administration of S100A8/A9 alarmins in addition to inflammasome activators (LPS and PA) during chondrogenic differentiation of encapsulated cells.**

Encapsulated ACPs and MSC beads were stimulated by exposure to S100A8/A9 as a chronic/continuous inflammatory input with administration once every 48hrs during chondrogenic differentiation. In addition, stimulation with LPS and PA was performed for the last 24h of culture as described for aim 2 to study the effects of TLR-4 signal (PRR) and alarmin (DAMP) interactions. Experimental endpoints were the same as for Aim 2 and included assessment of caspase-1 activation, GAG quantitation, gene expression and histological analysis.

4.2 Materials and methods

4.2.1 Isolation and culture of human MSCs and ACPs

MSCs were isolated from heparinised bone marrow aspirates taken from the iliac crest of healthy volunteers with approval from the National University of Ireland Galway and University College Hospital ethics committees and after obtaining informed consent. The isolation and characterisation of MSCs was performed as previously described (Murphy et al., 2002). MSCs derived from two separate donors, were culture expanded and maintained in human MSC medium (Appendix 2; Table 23) supplemented with 5ng/ml fibroblast growth factor-2 (FGF-2, PeproTech). ACPs were received from Professor Brian Johnstone's lab at Oregon Health and Science University, USA and the cells were isolated from leftover tissues from fresh allograft femoral condyles of two individual donors (Williams et al., 2010, Anderson et al., 2016). The cells were expanded and maintained in ACP medium (Appendix 2; Table 24) supplemented with 1ng/ml transformation growth factor β1 (TGF-β1; PeproTech) and 5ng/ml FGF-2. Both MSCs and ACPs were plated at $1x10^6$ cells, cultured at 37°C and 5% CO_2 and used for subsequent chondrogenesis experiments at passage 3.

4.2.2 Validation of chondrogenic capacity of ACPs and MSCs

ACPs and MSCs were tested for their chondrogenic differentiation capacities prior to alginate encapsulation. Briefly, cells expanded from two separate donors were trypsinised and counted. A total of $1x10^5$ cells/pellet was transferred into sterile screw cap tubes and designated as ICM (control) or CCM (test). The samples were processed for chondrogenic differentiation as previously described in Section 2.2.4.6 with ICM samples cultured in 0.5ml of incomplete chondrogenic medium (Appendix 2; Table 6) alone and CCM samples induced with the same medium supplemented with 10ng/ml TGF-β1. Both cell types were maintained at 37°C with 2% O_2 and 5% CO_2 for 7, 14, 21 and 28 days. Medium was changed once in two days and at the end of every time point the pellets were washed twice with PBS and subjected to overnight papain digestion followed by measurement of GAG and DNA (previously described in Section 2.2.4.9 and 2.2.4.10, respectively). The remaining pellets were processed for histology followed by Safranin O (previously

described in Section 2.2.4.7 and 2.2.4.8, respectively) and Toluidine blue staining (Section 4.2.7.1).

4.2.3 Caspase-Glo® 1 Inflammasome assay to optimise inflammasome activation

To identify the optimal combination of inflammatory stimuli for activation of the NLRP3 inflammasome complex and IL-1β release in ACPs and MSCs, the Caspase-Glo® 1 Inflammasome assay kit (Promega) was utilised; caspase-1 is an essential component of the inflammasome and its activation is crucial towards formation of the NLRP3 complex and processing of IL-1β and IL-18 (Palm et al., 2014, Franchi et al., 2009). ACPs and MSCs ($1x10^5$ cells/well) were seeded in 24-well plates. After 24h, cells were segregated into 5 groups and treated (for 24h) in the following manner: 1: Control (no treatment);2: LPS (0.1μg/ml; Sigma) + 5mM ATP; 3: LPS+ 500μM PA (Sigma); 4: group 2+50μM Ac-YVAD-cmk (capase-1/inflammasome inhibitor; Sigma) and 5: group 3+ Ac-YVAD-cmk (Table 4.1). Preparation and chosen concentrations of LPS, ATP, PA and Ac-YVAD-cmk were based on manufacturer's instructions and published literature (Wen et al., 2011, Alvarez-Garcia et al., 2014, Jeong et al., 2016, Lu et al., 2012). Groups that received ATP and/or Ac-YVAD-cmk were treated with these two agents for 45 minutes prior to collection of supernatants (Table 4.1). This selection was based on their maximum reactivity period (Garcia-Calvo et al., 1998, Zha et al., 2016). Supernatants were collected from all groups for Caspase-Glo® 1 assay. Prior to the assay, reagents were equilibrated at room temperature and the Caspase-Glo® 1 reagent was prepared by mixing Caspase-Glo® 1 buffer with the Z-WEHD Substrate solution generating 40μM Z-WEHD-aminoluciferin and a final assay concentration of 20μM (K_m value for caspase-1). ACP/MSC medium (blank reaction) or collected supernatants from each experimental group (100μl) were added to triplicate wells of a 96-well flat bottom plate. The prepared Caspase-Glo® 1 reagent was added to all wells yielding a 1:1 ratio of Caspase-Glo® 1 reagent volume to sample volume. Contents were mixed at 300–500rpm for 30s using a plate shaker and samples incubated at room temperature for 1h followed by measurement of luminescence indicative of relative capsase-1 activity using a Victor X3 luminometer. Treated cells were collected by gentle scraping and centrifuged at 400g for 5min. The cell pellets were suspended in 350μl of Buffer RLT containing β-mercaptoethanol and processed for RNA extraction to test the gene expression of IL-1β and NLRP3. The same

protocol was adopted for subsequent measurement of caspase activity in conditioned medium collected from encapsulated cells (see Sections 4.2.5 and 4.2.6).

Table 4.1 Treatments used for optimisation of inflammasome activation

Group No.	Treatment groups	Treatments used	
		Signal 1* **(for 24h)**	**Signal 2***
1	Control	N/A	N/A
2	LPS+ATP	LPS	ATP for last 45min of LPS exposure
3	LPS+PA	LPS	PA for 24h
4	LPS+ATP+Ac-YVAD-cmk	LPS	ATP and Ac-YVAD-cmk for last 45min of LPS exposure
5	LPS+PA+Ac-YVAD-cmk	LPS	PA for 24h and Ac-YVAD-cmk for last 45min of LPS exposure

***Signal 1: Priming** step using LPS (TLR4 signal); ***Signal 2: activation** of NLRP3 and release of mature IL-1β using ATP (P2X7 channel)/PA- ROS signalling through FFA activation.*

4.2.4 Gene expression of IL-1β and NLRP3 following inflammasome activation

Total RNA was isolated from lysed ACP and MSC cell pellets (groups 1, 2 and 3; Table 4.1) using the RNeasy Mini kit as previously described in Section 3.2.7.1. Nucleic acid content was determined using a NanoDrop ND1000 spectrophotometer at 260 and 280 nm. cDNA synthesis was performed using the QuantiNova™ Reverse Transcription Kit as described in Section 3.2.7.2. Following this, qRT-PCR for single gene analysis of *IL1B* and *NLRP3* was carried out using the QuantiNOVA™ SYBR® Green PCR Kit. Human SYBR green primers (Appendix 2; Table 26 for details of primer sequences) were obtained from the KiCqStart® SYBR® Green Primers for Gene expression analysis (Sigma-Merck). The reaction was run as previously described in Section 3.2.7.3. Gene expression levels were normalised to human *GAPDH* (Appendix 2; Table 26) and threshold cycle (CT) was

calculated using the real-time cycler software (Thermo Fisher Scientific). Fold change was calculated using 2^ (delta C_T) formula (Schmittgen and Livak, 2008).

4.2.5 Encapsulation and chondrogenic differentiation of ACPs and MSCs

ACPs and MSCs were encapsulated in sodium alginate and induced towards chondrogenic differentiation for 28 days at 37°C with 2% O_2 and 5% CO_2. The alginate solution (1.2%) was prepared by dissolving UV sterilized alginic acid sodium salt (Sigma) in 0.15M sodium chloride (NaCl; Sigma)and stored at 4°C. Prior to use for cell encapsulation, the solution was thawed for 15min in a water bath at 37°C and passed through a 0.45μM filter syringe. ACPs and MSCs (passage 2) were trypsinised, counted and centrifuged at 400g for 5min. The cell pellet was then resuspended in 1.2% alginate solution at a density of $8x10^6$cells/ml. Alginate beads were formed by pipetting 100μl of alginate-cell suspension through a 1000μl sterile filter tip allowing droplets to fall into 102mM $CaCl_2$ from a distance of 15cm. The volume of 100μl yielded 3-4 beads per test sample, corresponding to ~$2x10^5$ cells/bead. After 10min, the beads were rinsed twice with 0.15M NaCl solution for 10min each time. The beads (4 beads per sample) designated as negative control (ICM), were cultured in 1ml incomplete chondrogenic medium (Appendix 2; Table 6) with or without inflammatory stimulants (Section 4.2.6) and CCM samples were induced with the same medium supplemented with 10ng/ml TGF-β1. The beads were cultured in a free-swelling method in 12-well plates (Sarstedt) and medium was changed every 48h.

4.2.6 Stimulation of encapsulated cells using inflammasome activators and/or S100A8/A9

ICM and CCM beads were further divided into three experimental groups within ICM and CCM, based on the stimulants/treatment used (Table 4.2). Group 1 (G1) ICM/CCM beads did not receive any stimulants. Group 2 (G2) beads were cultured without any stimulants for 27 days and then stimulated with a combination of 0.1μg/ml LPS and 500μM PA (LPS/PA) (optimised in Section 4.2.3) for the last 24h. Group 3 (G3) beads were continuously treated with 0.5μg/ml recombinant human S100A8/A9 heterodimer (carrier-free; BioLegend) for 28 days (added once every 48h), in addition to LPS+PA stimulation on day 27 for last 24h (see G2). On day 28, the beads were processed for

histological (Section 4.2.7) and gene expression (Section 4.2.8) analyses. Supernatants were also collected from all the samples and tested for Caspase-1 activity as previously described in Section 4.2.3.

Table 4.2 Treatments used for stimulation of encapsulated cells

Experimental group	Treatments used	Treated on/for
G1	No stimulants	N/A
G2	LPS+PA (acute inflammatory insult)	Day 27 for 24h
G3	LPS+PA (acute inflammatory insult) **+**	Day 27 for 24h **+**
	Recombinant S100A8/A9 (chronic inflammatory input)	Once every 48h during medium change for 28 days

4.2.7 Histological analysis of encapsulated cells

After 28 days, ACPs and MSCs beads (ICM and CCM) were washed with 1ml of 1x PBS (x2) and fixed with 0.5ml of formalin containing 10mM $CaCl_2$ overnight. After fixation the pellets were prepared for manual histological processing as follows: 70% ethanol 15min, 90% ethanol 15min, 100% ethanol 15min (x3) and 100% xylene 15min. All solutions were supplemented with 10mM $CaCl_2$ to maintain alginate cross-links. After the first xylene incubation, the beads were transferred into cassettes and samples were further processed as follows using a Leica tissue processor: 100% xylene 30min (x2) and melted paraffin wax 30min (x3). Samples were then embedded in paraffin wax using the wax embedding station (Leica) and the wax block was placed on a cooling block (Leica). Sections (5µm) were obtained using a microtome (Leica) and placed on Superfrost Plus slides (Thermo Scientific). Slides were heated at 60ºC in a slide oven (Leica) for 1.5-2hrs and representative slides for each sample stained with Toluidine blue.

4.2.7.1 Toluidine blue staining for chondrogenic pellets/alginate beads

A working solution of Toluidine blue was prepared by combining 6ml of 0.5% Toluidine blue stock solution (0.5g Toluidine blue powder from Sigma in 100ml dH_2O) to 44ml of phosphate buffer solution (Appendix 2; Table 25). The solution was heated to 60°C and maintained at 56-60°C. ICM and CCM slides were deparaffinised and stained as follows: 100% xylene 2 min, 100% xylene 2 min, 100% IMS 2 min, 95% IMS 2 min, 70% IMS 2 min, dH_2O 1 min, heated Toluidine blue working solution 5 min, tap water 30s, and air dried for 10min. Slides were immersed in 100% xylene for 30s and mounted with DPX, cover slipped and left to air dry in a fume hood.

4.2.7.2 Measurement of GAG and DNA content in encapsulated cells

ACPs and MSCs were harvested from the alginate beads after 28 days culture by incubation with 500µl of 0.1M sodium citrate solution containing 0.01M 3-(N-Morpholino)propanesulfonic acid (MOPS; Sigma) and 0.027M NaCl for 10min on a plate shaker. Samples were then centrifuged at 400g for 5min. GAG and DNA were measured after digestion of cell pellets in a papain solution (0.25mg/ml) at 60°C overnight. Digests were assayed for GAG using the DMMB assay and DNA content was determined using the Quant-iT PicoGreen® dsDNA assay kit as previously described in Sections 2.2.4.9 and 2.2.4.10, respectively. The total amount of GAG was normalized against the total amount of DNA.

4.2.8 Gene expression analyses of encapsulated ACPs and MSCs

After 28 days of chondrogenic differentiation, ICM and CMM beads of ACPs and MSCs were processed for gene expression analyses. First, 3 beads per experimental group of ICM/CCM samples were rinsed with 1ml 1X PBS twice and immersed in 500µl of 0.1M sodium citrate solution for 10min on a plate shaker to release the cells from alginate. After 10min, the samples were centrifuged at 400g for 5min. The supernatant was discarded and the pellets were rinsed with PBS once, followed by resuspension in 350µl of Buffer RLT containing β-mercaptoethanol and processed for RNA extraction. Total RNA was isolated using the RNeasy Mini kit as previously described in Section 3.2.7.1. Nucleic acid content was determined spectrophotometrically using a NanoDrop ND1000

spectrophotometer at 260 and 280 nm. cDNA synthesis was performed using the QuantiNova™ Reverse Transcription Kit as described in Section 3.2.7.2. Following this, qRT-PCR for single gene analysis of *IL1B, NLRP3, IL6, IL8, IL33, ACAN, COL2A1, COL1A1, COL9A1, COL10A1, ADAMTS4, ADAM5P, MMP13, SOX9 and PRG4* was carried out using the QuantiNOVA™ SYBR® Green PCR Kit and pre-designed human SYBR green primers (Appendix 2; Table 26 for primer information). The reaction was run as previously described in Section 3.2.7.3. Gene expression levels were normalised to human *GAPDH* (Appendix 2; Table 26) and threshold cycle (CT) was calculated using the real-time cycler software (Thermo Fisher Scientific). Fold change in expression was calculated using the 2^ (-delta C_T) formula (Schmittgen and Livak, 2008).

4.2.9 Statistical analysis

Statistical analysis was performed using GraphPad Prism software, version 6. Data were analysed utilising two-way ANOVA followed by Tukey's multiple comparisons test. Error bars represent the mean±SEM. For all analyses, differences were considered statistically significant at $p<0.05$ and significance was assessed in two biological donors (sample number, n=2) both assayed using technical triplicates. Where biological replicates were not available (n=1), mean±SEM of technical triplicates is shown without statistical analysis.

4.3 Results

4.3.1 ACPs and MSCs maintain their chondrogenic capacities over an extended period of time

Chondrogenic differentiation of ACPs and MSCs was carried out for 7, 14, 21 and 28 days (D) in the presence of TGF-β1 to assess their ability to differentiate into chondrocytes and maintain this status over an extended period. Quantification of sulphated GAG content in the CCM chondrogenic pellets showed MSCs (Figure 4.1B) to have a steady increase in GAG accumulation from D7 (2.94μg) to D28 (13.6μg), while ACPs (Figure 4.1A) displayed peak GAG levels on D14 (3.5μg) with lower GAG levels detected over time to D28 (2.1μg). DNA content assessed by the PicoGreen assay displayed relatively constant levels for MSC cultures (Figure 4.1B) (~1.5μg to D28). A decrease from an average of 1.2 (D7) to 0.7μg (D28) for ACPs was evident (Figure 4.1A). Assessment of the sulphated GAG:DNA content showed MSCs (Figure 4.1B) to have a higher content (9.4μg) compared to ACPs (2.8μg) at D28 (Figure 4.1A). Overall, the comparison of GAG:DNA levels between ICM and CCM pellets of both ACPs and MSCs found ICM samples to have substantially lesser GAG content than CCMs. Qualitative analysis of proteoglycan deposition by Safranin O (Figure 4.2) and Toluidine blue staining (Figure 4.3) also confirmed chondrogenic differentiation in both ACP and MSC CCM pellets compared to ICM pellets. MSC CCM pellets formed terminal cartilage by D28 with chondrocytes having a hypertrophic phenotype (Figure 4.2B & 4.3B). ACP CCM pellets on the other hand, differentiated into stable cartilage with uniform proteoglycan deposition and high metachromasia staining similar to MSCs, but devoid of hypertrophic chondrocyte morphology even at D28 (Figure 4.2A & 4.3A).

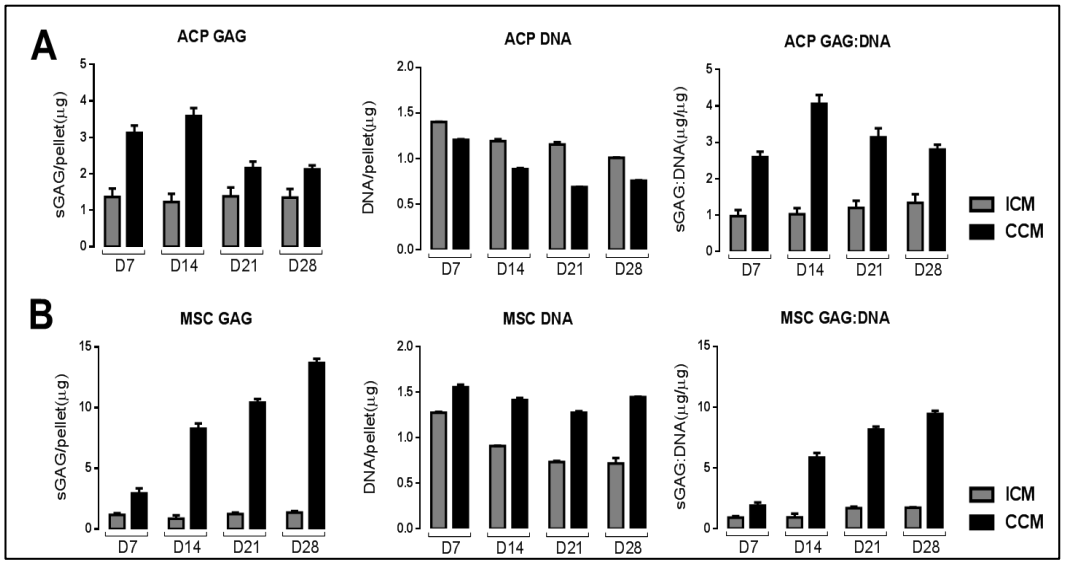

Figure 4.1 Chondrogenic differentiation capacities of ACPs and MSCs. ACPs and MSCs were induced towards chondrogenic differentiation with or without 10ng/ml TGF-β1 for 7, 14, 21 and 28 days (D) under hypoxic conditions followed by quantification of total sulphated glycosaminoglycan (sGAG) and DNA content per pellet. The sGAG to DNA ratio was calculated for cultures exposed to both ICM/CCM. A) Overall GAG production in ACP pellets was maintained around 3μg to D28. B) Total GAG content in MSC CCM pellets increased with time and was higher than in ACP pellets (~9μg by D28). Values are expressed as Mean±SEM (n=1, technical triplicates).

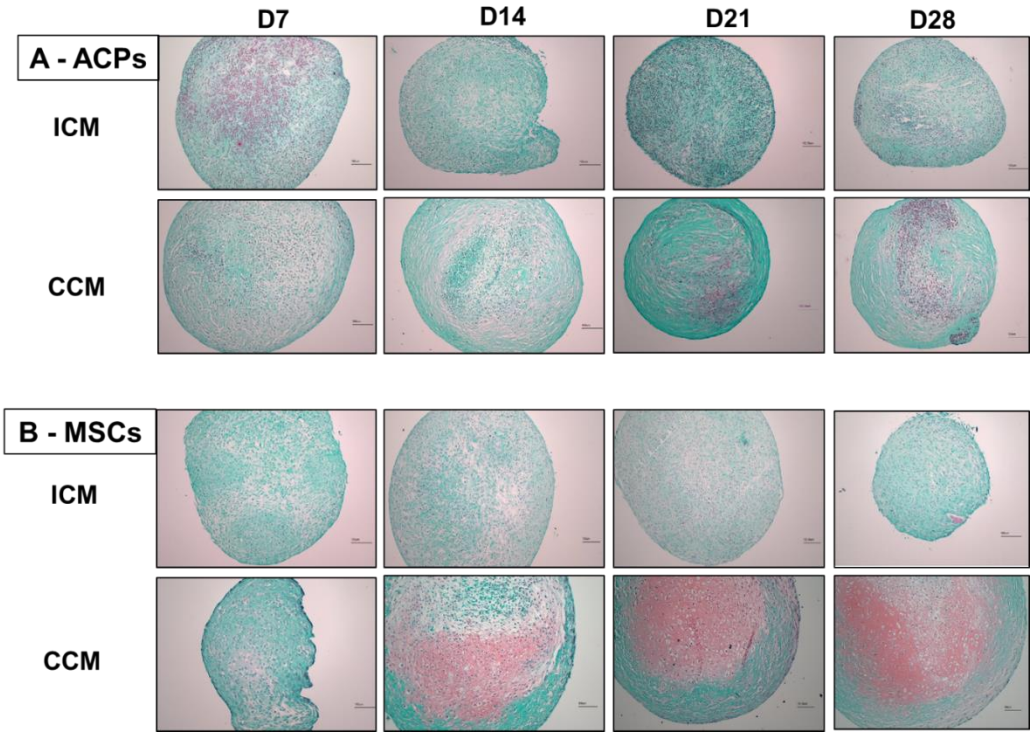

Figure 4.2 Qualitative analysis of proteoglycan synthesis by Safranin O staining. ACPs and MSCs were induced towards chondrogenic differentiation ± TGF-β1 for 7, 14, 21 and 28 days (D). Pellets fixed and embedded in paraffin were sectioned and stained with Safranin O and Fast green. A) ACP CCMs differentiated into cartilage with clear deposition of proteoglycan compared to ICMs. B) MSCs formed mature cartilage with chondrocytes displaying a hypertrophic phenotype and higher production of proteoglycan than ICM-treated and ACP CCM pellets. Scale bar, 100μm.

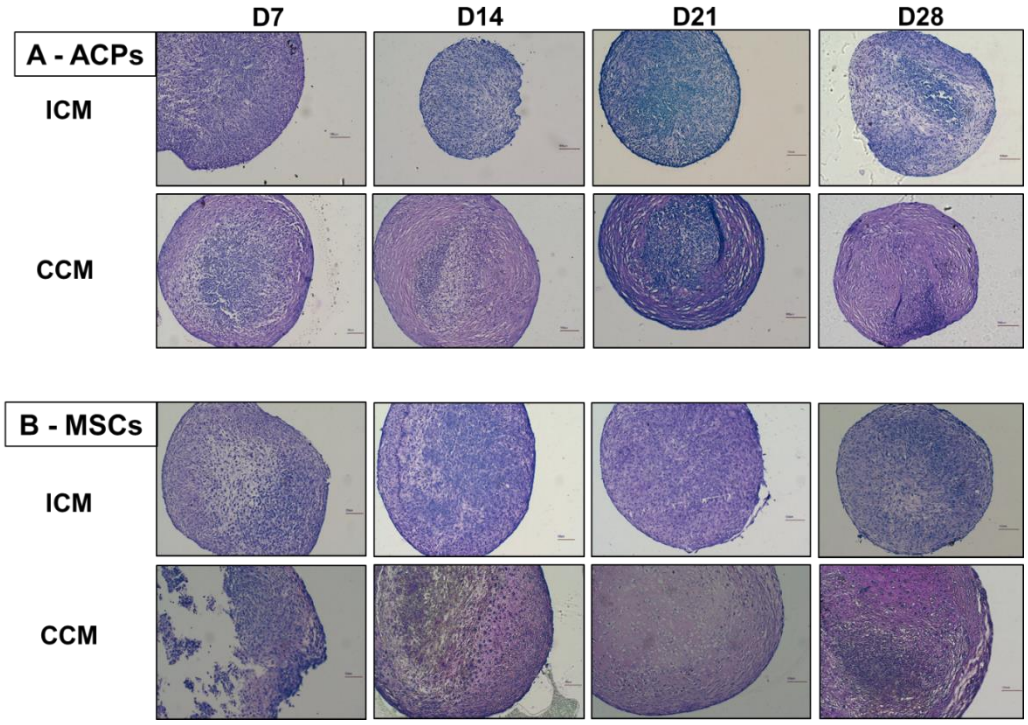

Figure 4.3 Qualitative analysis of total proteoglycan production by Toluidine blue staining. ACPs and MSCs were induced towards chondrogenic differentiation ± TGF-β1 for 7, 14, 21 and 28 days (D). Pellets fixed and embedded in paraffin were sectioned and stained with Toluidine blue for proteoglycan. A) ACPs treated with CCM differentiated into cartilage with more uniform deposition of proteoglycan compared to ICM treated pellets. B) MSCs formed mature cartilage with chondrocytes displaying a hypertrophic phenotype. Scale bar, 100μm.

4.3.2 Inflammatory response of MSCs but not ACPs to inflammasome activation

ACPs and MSCs were subjected to a combination of inflammatory stimuli involving either LPS and ATP or LPS and PA to identify the best combination to initiate NLRP3 inflammasome complex formation and IL-1β release following caspase-1 activation. Firstly, ACPs and MSCs demonstrated casapase-1 activity (Figure 4.4A) following stimulation with both ATP and PA (groups 2 and 3; Table 4.1) compared to control (group 1). Furthermore, this specific activation was confirmed by testing these two reagents in the presence of Ac-YVAD-cmk, a selective casapase-1 inhibitor that blocked the activation and release of Caspase-1 (groups 4 and 5; Table 4.1). Secondly, in comparison to ATP, stimulation with PA induced a significantly higher level of caspase-1 activation signal in both cell types ($p<0.05$ for ACPs and $p<0.0001$ for MSCs). MSCs treated with PA produced caspase-1 signal at levels three times higher than ACPs, indicating that MSCs were more responsive to the inflammatory environment created after exposure to LPS (TLR-4 signalling activation) and PA. Molecular analysis of ATP- and PA- treated ACPs and MSCs for expression of *IL1B* and *NLRP3* confirmed significant upregulation of both genes by MSCs as compared to that in ACPs (Figure 4.4B). Similar to the results obtained from the Caspase-1 signal, stimulation with PA yielded statistically higher expression of *IL1B ($p<0.005$)* and *NLRP3 ($p<0.0001$)* by MSCs compared to ATP. In particular, the capacity of PA in inducing caspase-1 mediated upregulation of *NLRP3* in MSCs was significantly higher and more consistent than ATP (ATP vs PA: $p<0.001$; Figure 4.4B).

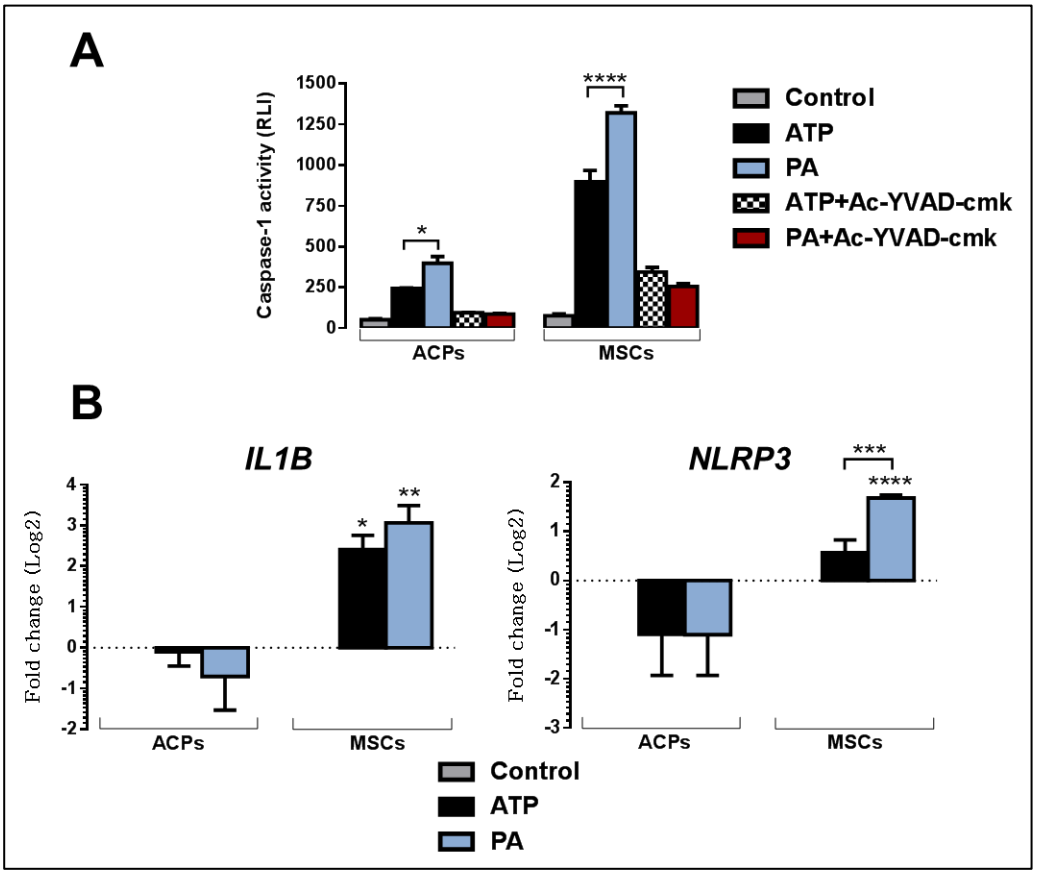

*Figure 4.4 Optimisation of inflammasome activation. ACPs and MSCs were stimulated with either adenosine triphosphate (ATP) or palmitic acid (PA) in the presence of lipopolysaccharide (LPS) to identify the optimal reagent to initiate NLRP3 inflammasome complex formation and IL-1β release, following caspase-1 activation. A) Caspase-1 activity was seen in both cell types with significantly higher signal induced by PA measured as relative luminescence intensity (RLI). B) Gene expression analysis of stimulated cells from (1) Control (untreated), (2) ATP and (3) PA treated groups showed significant upregulation of IL1B and NLRP3 with higher expression seen in PA stimulated MSCs. Values are expressed as Mean±SEM (n=2, technical triplicates; normalised to GAPDH) and data is presented as fold change on a logarithmic scale (Log 2). Statistical analysis was performed on 2^(⊥⊥Ct) values and significance determined by two-way ANOVA with Tukey's multiple comparisons test. *P<0.05, **P<0.005, ***P<0.001, ****P<0.0001. Individual asterisks (compared to control); asterisks on square bars (comparison between two treatment groups).*

4.3.3 Encapsulated MSCs exhibit elevated caspase-1 activation than ACPs

To identify the activation of the inflammasome pathway and assess chondrocyte viability, caspase-1 activity was measured in the medium collected from unstimulated/stimulated, ACP- and MSC-derived beads after 28 days (see Section 4.2.5 and 4.2.6). The supernatants analysed using the Caspase-Glo® 1 Inflammasome assay (Section 4.2.3) demonstrated activation of caspase-1 in ACPs and significantly higher activity in MSC CCM compared to ICM treated beads. While ACPs displayed a descending trend in caspase activity with every CCM group (G3<G2<G1), an escalated inflammatory effect was observed with MSC CCMs when compared with their corresponding ICMs [G3 ($p<0.0001$)>G2 ($p<0.0001$)>G1 ($p=0.0008$)]. Similarly, MSC CCM beads treated with LPS and PA alone (G2) demonstrated significantly higher levels of activated caspase-1 compared to G1 CCM ($p=0.0140$) and approximately double than that demonstrated by G2 treated ACP CCM beads. This effect was mirrored, and more pronounced in MSC CCMs continuously treated with S100A8/A9 (G3) when compared to G1 CCM ($p=0.0005$) and 2.5 times more than G2 ACP CCM. (Figure 4.5).

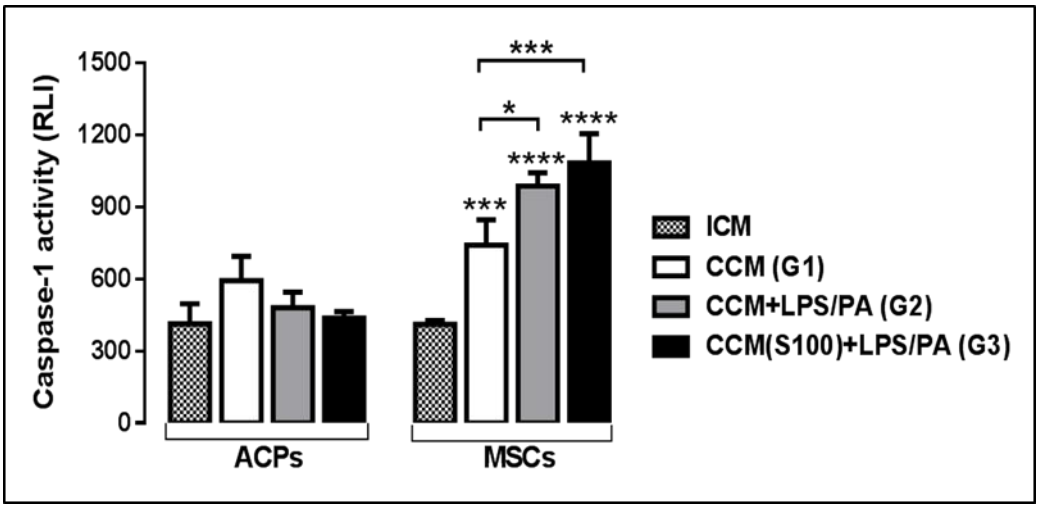

*Figure 4.5 Inflammatory insults and Caspase-1 activation. Encapsulated ACPs and MSCs induced towards chondrogenic differentiation with or without TGF-β1 for 28 days (D) were segregated into groups (G)1: unstimulated, G2: stimulated with LPS&PA for the last 24h or G3: simultaneously treated with recombinant S100A8/A9 alarmin complex every 48h till D28 and stimulated with LPS&PA for the last 24h. Caspase-1 activity was seen in both cell types with significantly higher signals induced in MSCs measured as relative luminescence intensity (RLI). Caspase-1 activity dropped with each treatment group in ACP CCM beads and significantly escalated in MSC CCM beads. Values are expressed as Mean±SEM (n=2, technical triplicates). Statistical significance was determined by two-way ANOVA with Tukey's multiple comparisons test. *P<0.05, **P<0.005, ***P<0.001, ****P<0.0001. Individual asterisks (compared to ICM); asterisks on square bars (comparison between two CCM groups).*

4.3.4 Inflammatory insults negatively impact chondrogenic differentiation of encapsulated MSCs but not ACPs

To test the impact of acute (LPS/PA) and chronic inflammatory stimuli (recombinant S100A8/A9 complex +LPS/PA) on chondrocyte fate and function during differentiation, alginate encapsulated ACP and MSC beads were induced and maintained in chondrogenesis for 28 days in both ICM and CCM . The beads were segregated into five groups (G1 (Control, unstimulated), G2 where the chondrogenic beads were stimulated with LPS and PA for 24h before harvest and G3 with beads treated with the S100A8/A9 alarmin complex every 48h and stimulated with LPS and PA for the final day of culture (Table 4.2). Both ACP and MSC beads treated with CCM produced increased total sGAG levels (Figure 4.6A) compared to ICM control beads. Statistical significance was observed in MSCs treated with CCM and in cells challenged with LPS and PA for the final 24 hours of differentiation. There was a gradual increase in the quantity of sGAG produced by CCM treated ACPs (Figure 4.6A) and significant elevation in DNA content for all treated groups with cells exposed to the combined inflammatory challenge showing significantly higher compared to the CCM and the pellets challenged by exposure to LPS/PA for 24 hours pre harvest (Figure 4.6B). No differences were observed in the ratio of sGAG to DNA (Figure 4.6C) in ACPs with an average sGAG of 2.1μg maintained across the CCM groups. MSCs on the other hand, displayed inverse results to ACPs where the sGAG and DNA content displayed a descending trend with every CCM group (G3<G2<G1) (Figure 4.6B). When compared to CCM-treated beads (total sGAG:76μg; ratio:12μg), those stimulated with an acute hit of LPS and PA produced significantly lesser GAG (49μg; $p<0.001$) and continuous treatment with S100A8/A9 complex in addition to the acute insult of PA was even more impactful with yet significantly lower GAG production. A similar descending trend was observed in the DNA content (Figure 4.6B). Quantitative analyses therefore depicted the negative impact of inflammasome activators and S100A8/A9 alarmins on MSC differentiation by inducing cell death (decrease in DNA content; Figure 4.6B) and possible inhibition of differentiation (lower total sGAG and ratio; Figure 4.6A&C) mimicking formation of the OA-like chondrocyte phenotype.

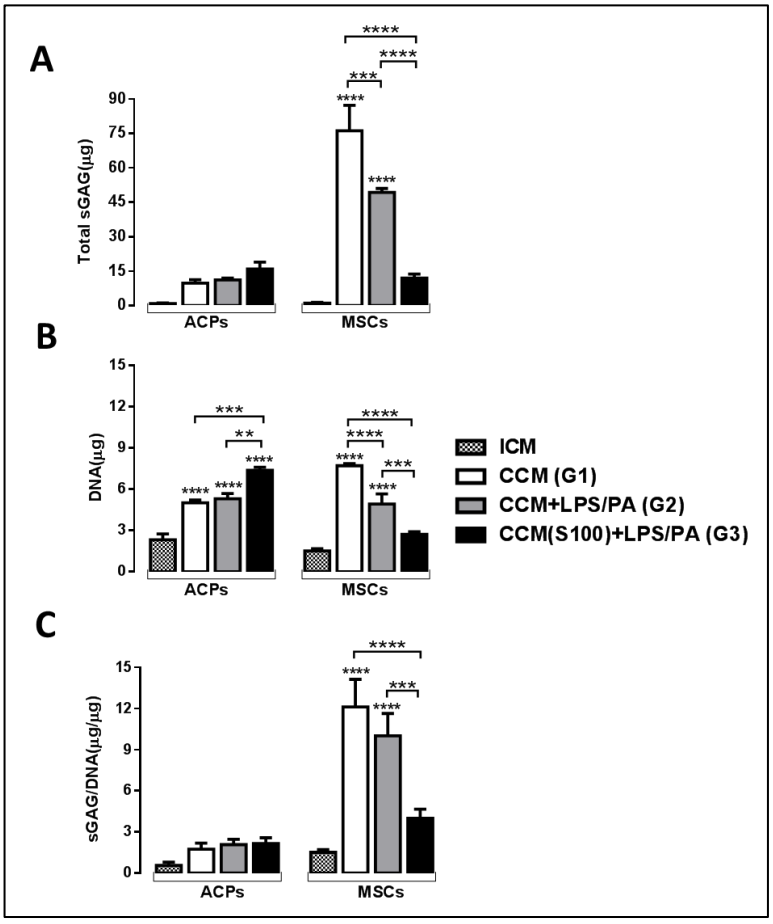

*Figure 4.6 Effects of inflammatory insults on proteoglycan (GAG) and DNA levels. Encapsulated ACPs and MSCs induced towards chondrogenic differentiation by exposure to TGF-β1 (CCM) for 28 days were segregated into groups (G)1: unstimulated; G2: stimulated with LPS&PA for 24h before harvest or G3: treated throughout with recombinant S100A8/A9 alarmin complex every 48h and stimulated with LPS&PA for the last 24h. A) Total sulphated glycosaminoglycan production was significantly higher in MSCs than ACPs . sGAG levels were significantly lower in each MSC treatment group but not ACPs. B) DNA content increased for ACPs compared to ICM treated beads and was significantly lower in treated MSC beads. C) The sGAG to DNA ratio was unaffected by inflammatory insults in ACPs but was significantly lower in MSCs treated with CCM and both inflammatory signals. Constructs treated with ICM were included as chondrogenic assay controls. Values are expressed as Mean±SEM (n=2, technical triplicates). Statistical significance was determined by a two-way ANOVA with Tukey's multiple comparisons test. *P<0.05, **P<0.005, ***P<0.001, ****P<0.0001. Individual asterisks (compared to ICM); asterisks on square bars (comparison between two CCM groups).*

4.3.5 Effect of inflammatory insults on GAG production corresponds with hypertrophic differentiation of chondrocytes

Qualitative analysis for total proteoglycans by toluidine blue staining was performed on unstimulated/stimulated ACP and MSC beads that had been formalin fixed, paraffin embedded and sectioned (Section 4.2.7) after 28 days of chondrogenic differentiation (Section 4.2.5 and 4.2.6). Both ACP and MSC CCM beads had undergone more substantial chondrogenic differentiation compared to ICM cultures (Figure 4.7A&E), as seen by increased metachromasia and proteoglycan accumulation. Unstimulated ACP CCM beads (G1; Figure 4.7B) differentiated into stable cartilage while MSC CCM (G1; Figure 4.7F) developed into mature cartilage with chondrocytes exhibiting a hypertrophic phenotype. Proteoglycan distribution was uniformly seen in these control CCM beads. ACP and MSC CCM beads stimulated with LPS and PA for 24h displayed irregular proteoglycan distribution with larger cell sizes and visible chondrocyte death (low cell number compared to the control cultures/G1; Figure 4.7C&G). While ACP beads had decreased areas of cartilage and empty lacunae at the periphery of the bead, MSC CCM beads showed loss of structural integrity and appearance of chondrocyte death. This observation of cell death concurred with increased caspase-1 activity in treated MSCs (Figure 4.5). Analysis of MSCs continually treated with the S100A8/A9 alarmin complex (G3) showed cell death and depleted matrix at the periphery of the bead in comparison to unstimulated and LPS/PA treated beads (Figure 4.7H). The cartilage seemed to appear unaffected by the dual inflammatory treatment seen with lesser GAG than control (G1) MSCs. This may be due to inhibition of the chondrogenic differentiation process (Figure 4.6 showing significantly lower sGAG). ACPs on the other hand formed chondrocytes embedded in a proteoglycan positive matrix reminiscent of a stable phenotype with few areas of hypertrophy and increased levels of empty lacunae (Figure 4.7D). Overall the phenotypic appearance of cartilage formed by ACPs and MSCs correlated with their rate of GAG production i.e., MSCs treated with complete chondrogenic medium showing the most intense staining and decreased GAG levels after exposure to inflammatory stimuli, while ACPs maintained more GAG content even after exposure to these stimuli. However, ACP beads treated with both inflammatory signals (G3) did appear to have acquired a hypertrophic appearance in areas of the pellet shown (Figure 4.7D).

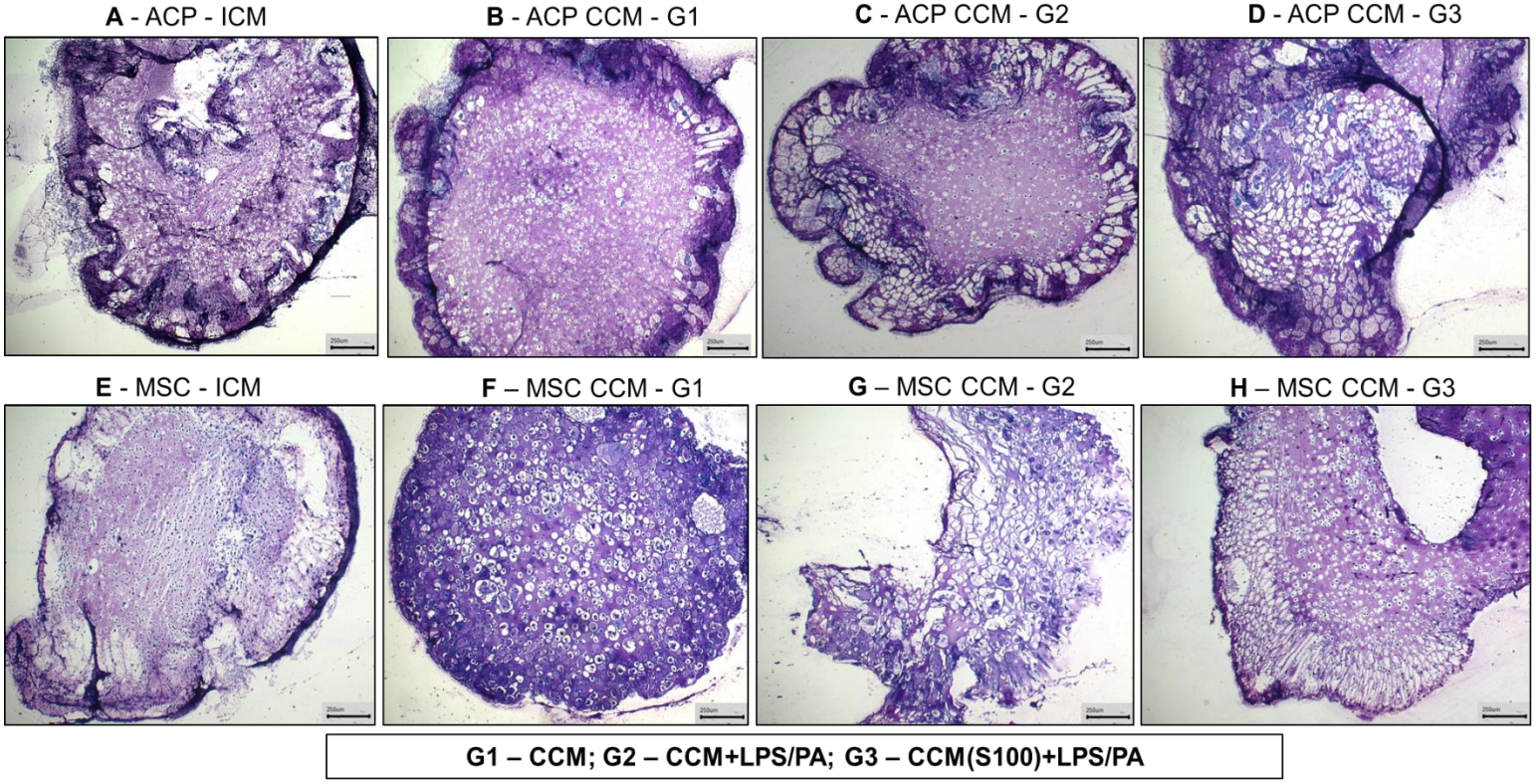

Figure 4.7 Qualitative assessment of the impact of inflammatory insults on matrix proteoglycan deposition. ACPs and MSCs induced towards chondrogenic differentiation with or without TGF-β1 for 28 days (D) were segregated into groups (G)1: unstimulated, G2: stimulated with LPS&PA for the last 24h of culture, G3): simultaneously treated with recombinant S100A8/A9 alarmin complex every 48h until D28 and stimulated with LPS&PA for the last 24h of culture. Pellets fixed and embedded in paraffin were sectioned and stained with Toluidine blue for detection of proteoglycan.

(A, E) ACP and MSC ICM beads formed some cartilage with lower metachromasia apparent between treated groups. (B) G1 ACP CCM differentiated into stable cartilage with uniform proteoglycan deposition and (F) G1 MSC CCM formed terminal cartilage with hypertrophic chondrocytes and high metachromasia. (C, G) G2 ACP beads with decreased areas of cartilage and empty lacunae at the periphery of the bead whereas MSC CCM beads showed irregular proteoglycan distribution, loss of structural integrity and appearance of chondrocyte death. (D, H) G3 ACP treated beads showed areas of hypertrophy with increased levels of empty lacunae whereas treated MSC CCMs showed cell death and depleted matrix at the periphery with remaining chondrocytes showing signs of inhibited differentiation. Scale bar, 250μm.

4.3.6 Acute and chronic inflammatory signals promote hypertrophy in ICM cultured MSCs

Unstimulated (G1)/stimulated (LPS/PA for 24h (G2) or dual stimulation with 24h LPS/PA and S100A8/A9 for 28 days (G3)) (Table 4.2) ACP and MSC beads cultured in ICM for 28 days were evaluated for expression of a panel of pro-inflammatory cytokines (*IL1B, IL33 (*members of *IL1* family*)*, *IL6* and *IL8),* the inflammasome marker (*NLRP3)* and chondrogenic markers associated with the articular (*SOX9, PRG4, ACAN, COL2A1, COL9A1*), fibrocartilaginous (*COL1A1*) and hypertrophic (*COL10A1, MMP13*) phenotypes. Members of the protease/proteoglycanase family (ADAMTS4, ADAM5P) were also included in this analysis. ACPs but not MSCs induced with LPS/PA for 24 hours prior to harvest of the chondrogenic beads (G2) demonstrated significant upregulation of *IL1B*, *NLRP3* and *IL33* (Figure 4.8A) (fold-regulation values are given in Appendix 1; S5). Similarly, ACPs treated with S100A8/A9 continuously throughout the culture period with treatment by LPS/PA for 24 h prior to harvest showed significant upregulation of *IL1B* but not *NLRP3* or *IL33*. *IL6* and *IL8* expression was upregulated by ACPs and MSCs in these treatment groups (G2 and G3) with significantly increased expression seen in S100A8/A9 treated ACPs and MSCs compared to that seen in control and LPS/PA treated beads (G1 and G2) ($p<0.0001$; Figure 4.8A).

Continuous treatment of MSCs with S100A8/A9 led to downregulation of the ECM proteins *PRG4*, *ACAN* and *COL2A1* and significant upregulation of *COL1A1* ($p<0.005$) and the hypertrophic marker *MMP13* ($p<0.0001$) when compared to G1 and G2 (fold-regulation values in Appendix 1; S5). While LPS/PA stimulated MSCs demonstrated upregulation of *ADAM5P*, *COL10A1* and *MMP13* ($p<0.05$), *SOX9* ($p<0.05$) was also significantly upregulated (Figure 4.8B). There was no significant difference observed in expression of *COL9A1* in G2 and G3 MSCs. ACPs reacted in a contrasting manner to MSCs with downregulation of *SOX9*, *ACAN*, *COL2A1, COL9A1*, *COL1A1* in response to S100A8/A9 treatment (G3) and significant upregulation of these markers (*COL1A1:* not significant*)* following insult with LPS/PA without the addition of alarmins (G2).

Additionally, LPS/PA treated ACPs displayed significant upregulation ($p<0.05$) and dual stimulation with S100A8/A9 and LPS/PA resulted in downregulation of *ADAMTS4* and *ADAM5P*. While stimulated ACPs expressed *MMP13* (not significant) the cells maintained an upregulated status of the progenitor marker *PRG4* (Figure 4.8B).

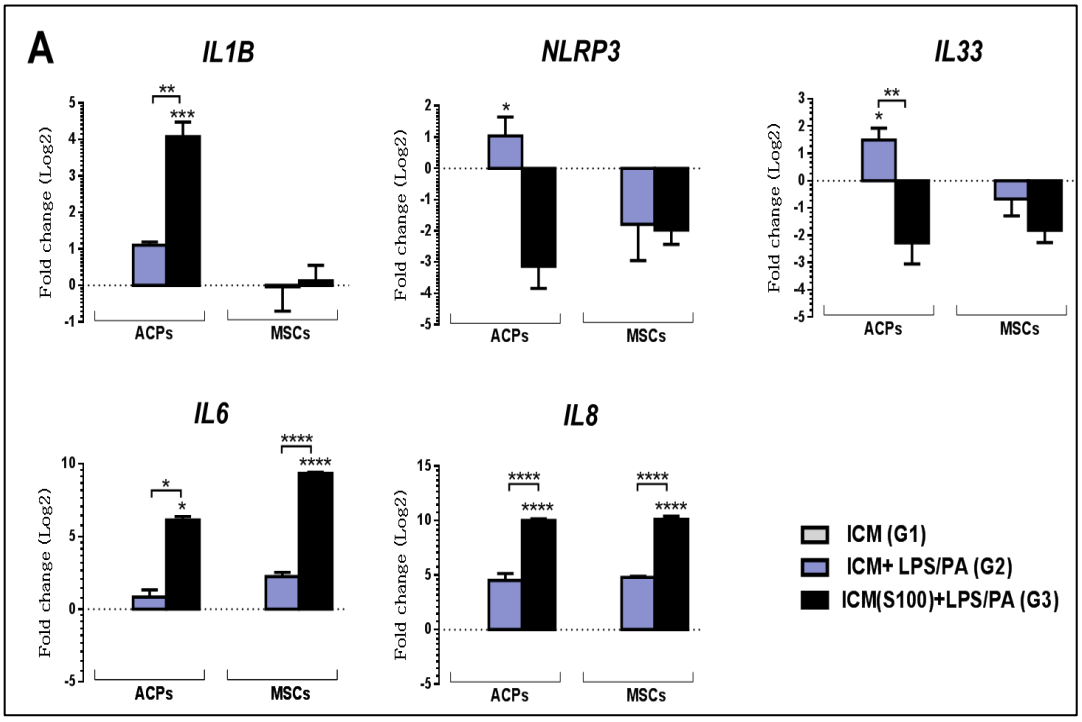

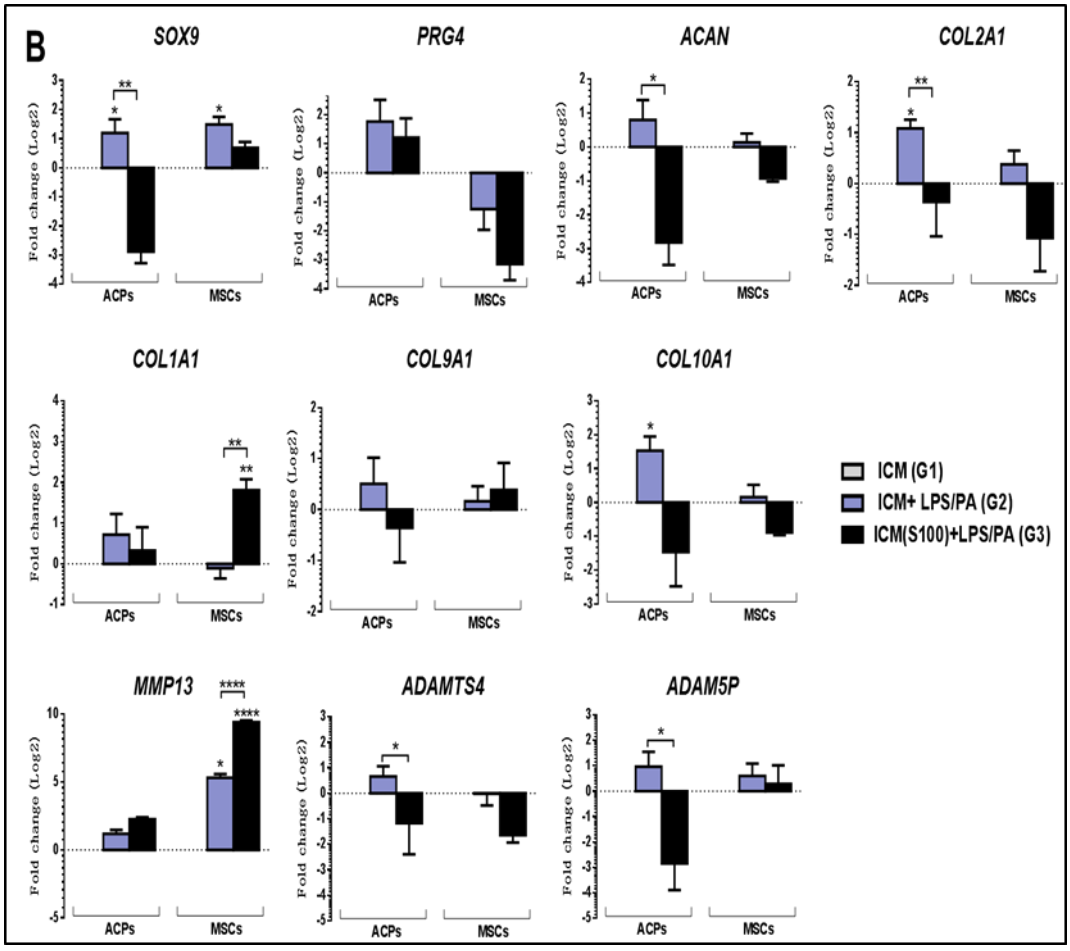

*Figure 4.8 Gene expression analysis of ACPs and MSCs cultured in incomplete chondrogenic medium (ICM). Encapsulated ACP and MSC beads maintained in ICM, divided into groups (G)1: unstimulated, G2: LPS&PA^{+} for the last 24h of culture or G3: G2+ continuous treatment with recombinant S100A8/A9 till day 28. Panel A) Fold-change of pro-inflammatory and inflammasome markers showed ACPs to be more responsive to acute inflammasome insults. Panel B) Expression patterns for chondrogenic markers and metalloproteinases demonstrated MSCs but not ACPs had a hypertrophic phenotype. Values are expressed as Mean±SEM (**n**=2, technical triplicates; normalised to GAPDH) and data is presented as fold change on a logarithmic scale (Log 2). Statistical analysis was performed on 2^(⊥⊥Ct) values & significance determined by two-way ANOVA with Tukey's multiple comparisons test. *P<0.05, **P<0.005, ***P<0.001, ****P<0.0001. Individual asterisks (compared to G1); asterisks on square bars (comparison between G2 &G3).*

4.3.7 A chronic inflammatory environment enables OA-like terminal differentiation and a hypertrophic phenotype in MSCs

Evaluation of the gene expression pattern (fold-regulation values in Appendix 1; S6) in unstimulated (G1)/stimulated (LPS/PA for 24h (G2) or dual stimulation with 24h LPS/PA and S100A8/A9 for 28 days (G3)) (Table 4.2) ACP and MSC beads cultured with TGF-β1 was performed. Analysis was indicative of altered chondrocyte behaviour and induction of a highly inflammatory environment in MSCs (Figure 4.9 A&B). While unstimulated and LPS/PA stimulated MSCs did not express *IL1B*, *NLRP3* or *IL33*, S100A8/A9 treated MSCs displayed significant upregulation of *NLRP3* ($p<0.005$) and *IL1B* ($p<0.005$) which correlate with high caspase-1 activity (Figure 4.9A). In addition, expression of *IL6* and the chemotactic factor *IL8* was highly upregulated in G3 MSC chondrogenic beads compared to G1 and G2 treatments ($p<0.005$ or *IL6* & $p<0.0001$ for *IL8*). While ACPs did demonstrate caspase-1 activity with a decreasing trend from control (G1 pellets) to G3, expression of *IL1B*, *NLRP3* or *IL33* was not seen. However, G2 and G3 ACPs were positive for expression of *IL6* and *IL8* (G3>G2; not significant).

Continuous S100A8/A9 treatment, in conjunction with addition of LPS and PA induced more deleterious effects on the expression of chondrogenic markers in ACPs and MSC (Figure 4.9B). Expression of the master transcription factor *SOX9* was down-regulated in ACPs (not significant) and MSCs ($p<0.0001$) (fold-regulation values in Appendix 1; S6). This led to significant downregulation of *SOX9* targets *ACAN* ($p<0.0005$ in MSCs), *COL2A1* ($p<0.005$ in ACPs and $p<0.0001$ in MSCs) and *COL9A1* ($p<0.0001$- MSCs) when compared to the control group (G1). Downregulated expression of the three collagen genes was observed in LPS/PA treated MSCs and not ACPs.

Changes in expression of *COL1A1* among the three groups was not significant in both cell types. Similarly, alarmin treatment severely impacted chondrogenic differentiation of MSCs but not ACPs with significant upregulation of hypertrophic phenotype markers *COL10A1* ($p<0.0001$) and *MMP13* ($p<0.0001$) compared to control and LPS/PA-treated MSCs. Increased expression of *MMP13* and downregulation of *SOX9* was reflected in upregulation of the proteoglycanase ADAMTS4 ($p<0.05$) but not ADAM5P in the alarmin and LPS/PA treated MSCs (G3). Higher expression of ADAMTS4 correlated

with complete downregulation of the lubricin/proteoglycan marker *PRG4* with significantly lower levels seen in alarmin+LPS/PA treated ACPs. This event was indicative of MSCs behaving like OA-chondrocytes with a hypertrophic phenotype and showing signs of possible de-differentiation and ACPs appearing to be sensitised to chronic alarmin signals while still maintaining their stable articular phenotype.

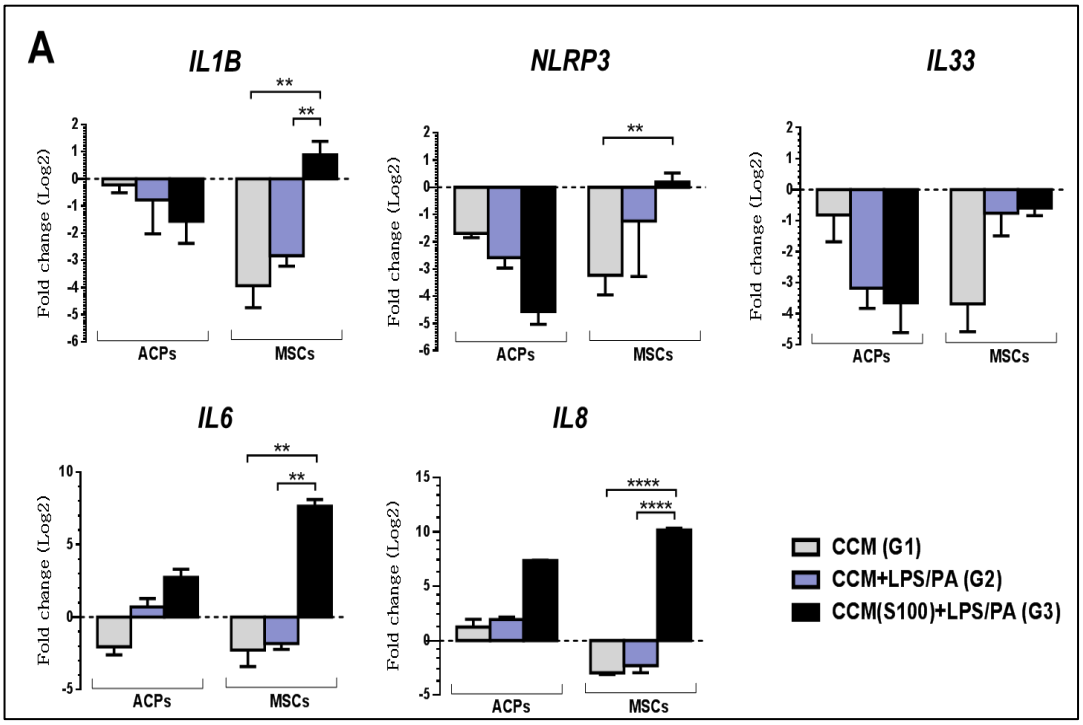

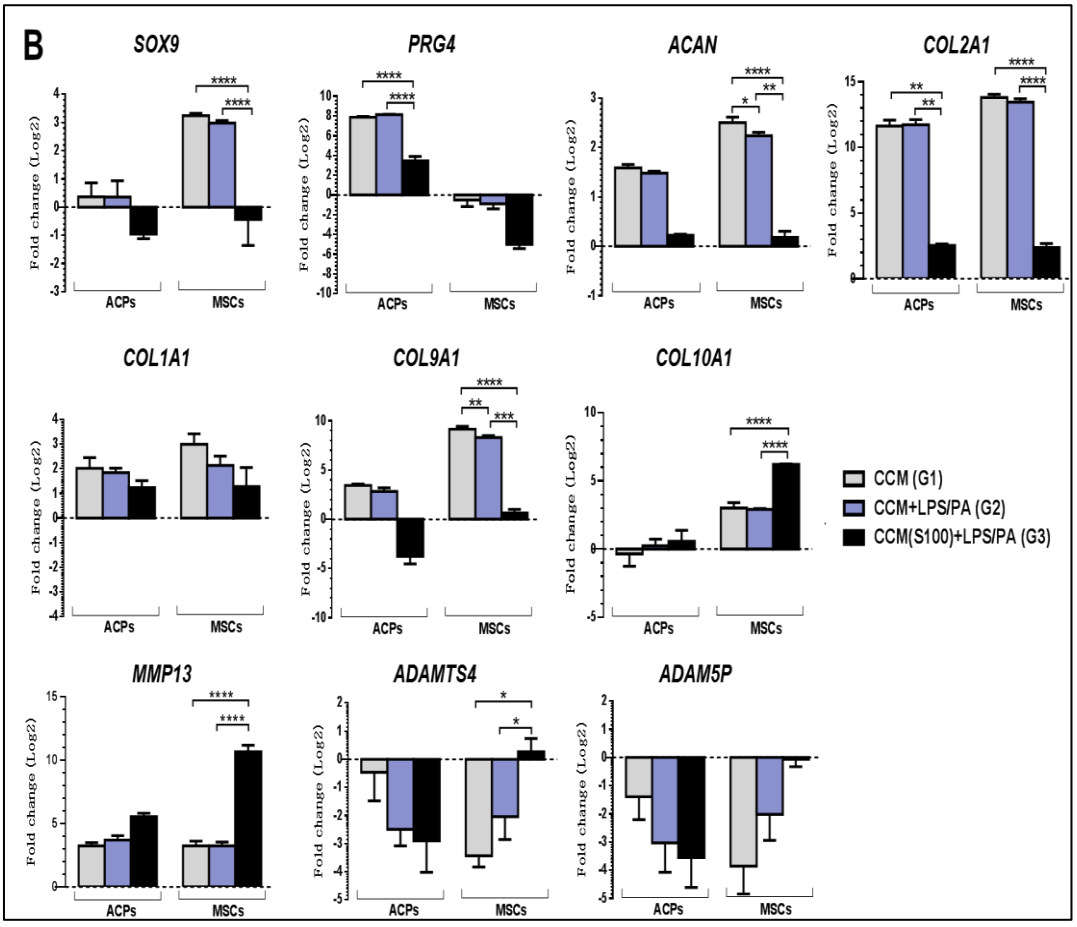

*Figure 4.9 Gene expression analysis of ACPs and MSCs cultured in complete chondrogenic medium (CCM). Encapsulated ACP and MSC beads maintained in CCM were divided into groups (G)1: unstimulated, G2: LPS&PA^{+} for the final 24h in culture or G3: G2+ continuous treatment with recombinant S100A8/A9 till day 28. Panel A) Fold-change of pro-inflammatory and inflammasome markers showed MSCs to be impacted by continuous and not acute inflammatory insults. Panel B) Chondrogenic marker and metalloproteinase expression demonstrated MSCs but not ACPs tended towards a terminal OA-like hypertrophic phenotype. Values expressed as Mean±SEM (**n**=2, technical triplicates; normalised to GAPDH); data is presented as fold change on a logarithmic scale (Log 2). Statistical analysis was performed on 2^(⊥⊥Ct) values & significance determined by two-way ANOVA, Tukey's multiple comparisons test. *P<0.05, **P<0.005, ***P<0.001, ****P<0.0001. Individual asterisks (compared to G1); asterisks on square bars (comparison between G2 &G3).*

4.4 Discussion

The altered function of articular chondrocytes in synovial joints underpins cartilage damage in OA that is further exacerbated by synovial activation. Alarmins such as S100 proteins feature among the numerous inflammatory mediators secreted by activated synoviocytes and found at high levels in the extracellular environment in the OA joint and constantly inducing loops of inflammatory responses and disease progression (van Lent et al., 2012, Sunahori et al., 2006, Zreiqat et al., 2010). Previous studies have identified and established S100A8 and S100A9 alarmins as early amplifiers of inflammation in OA and demonstrated their negative effects in initiating cartilage degradation with maintenance of prolonged expression in the synovium of mice with CIOA and synovial biopsy samples from OA patients (Vogl et al., 2014, van Lent et al., 2012).

Although many *in vitro* studies have demonstrated the pro-inflammatory and catabolic effects of S100A8 and S100A9 homodimers on murine, ovine and human (normal and OA) chondrocytes, the impact of the S100A8/A9 heteromeric complex on cytokines, chemokines, chondrogenic markers or even MMPs at both protein and mRNA levels was insignificant (van Lent et al., 2008a, Zreiqat et al., 2010, Schelbergen et al., 2012, Zreiqat et al., 2007, Van Lent et al., 2008b). This contrasts to the evidence of accumulation of abundant amounts of the heterodimer complex in synovial fluid samples of RA (~50μg/ml) and OA (~5-7μg/ml) patients (Sunahori et al., 2006, Brun et al., 1994). Here the catabolic effects of exposure to the S100A8/A9 heterodimer were assessed in a novel three-dimensional model of stable and terminal articular cartilage generated by differentiation of chondroprogenitors and MSCs, respectively.

One of the most abundant types of FFA found in OA cartilage, palmitate (palmitic acid/PA) has been found to elicit apoptosis and matrix degradation in articular chondrocytes (Alvarez-Garcia et al., 2014). In combination with LPS as a TLR-4 activator, PA was shown to cause activation of the NLRP3 inflammasome and downstream release of IL-1β and members of the IL-1 pathway in human MSCs. In addition, this combination of inflammasome activators also induced apoptosis and inhibited osteogenic differentiation potential of MSCs (Wang et al., 2017, Lu et al., 2012). Here, the pro-

apoptotic and pro-inflammatory effects of inflammasome activators on chondroprogenitors (ACPs) and ACP-derived stable articular cartilage are described. Additionally, the model used demonstrated that a combination of inflammasome activators (LPS/PA) and continuous exposure to the S100A8/A9 heterodimer acted as an inflammatory catalyst orchestrating chondrocyte hypertrophy and cell death in ACPs. On the other hand, the dual inflammatory signal seemed to have inhibited chondrogenic differentiation of MSCs.

Bone-marrow derived MSCs have been described as a promising cell source for tissue engineering strategies due to their multipotent nature as well their paracrine, and chemotactic capacities (Hilfiker et al., 2011, Pittenger et al., 1999, Prockop, 2009). However, when considering their specific use for cartilage repair purposes these cells fail to form a stable articular phenotype. Despite their ability to differentiate into chondrocytes, MSCs invariably form terminal cartilage and display a hypertrophic phenotype during *in vitro* chondrogenesis (Johnstone et al., 1998, Johnstone et al., 2013). ACPs offer the advantage of being developmentally primed for chondrogenesis and generate stable articular chondrocytes with reduced telomerase shortening in subclonal populations with a lower tendency towards hypertrophy (McCarthy et al., 2012, Khan et al., 2009a, Kozhemyakina et al., 2015). Here ACPs and MSCs induced to undergo chondrogenesis for 7, 14, 21 and 28 days in standard pellet culture demonstrated similar effects as previously described. While MSCs demonstrated enhanced GAG production over time, they formed mature cartilage with hypertrophic chondrocytes evident. ACPs on the other hand maintained a steady rate of GAG production and did not seem to undergo hypertrophy. Anderson et al. have shown that while both ACPs and MSCs demonstrated high chondrogenesis in hypoxic conditions, ACP clones expressed significantly lower levels of the hypertrophic genes *COL10A*1 and *MMP13* compared to MSC preparations (Anderson et al., 2016).

As MSC thrive in a 3D environment under physiological conditions and adult chondrocytes cultured *in vitro* pose the risk of de-differentiation if the optimal tissue microenvironment is not controlled, the present study adopted the use of encapsulating ACPs and MSCs in alginate (Debnath et al., 2015, Yamagata et al., 2018). Many studies have shown that culturing bovine and human articular chondrocytes in alginate resulted

in the formation of a compartmentalised matrix with enhanced expression of aggrecan and type II collagen similar to native adult articular cartilage, but also worked as a relevant model to study changes in cartilage phenotype and function during OA (Hauselmann et al., 1994, Hauselmann et al., 1996, Chubinskaya et al., 2001). In the present study chondrogenic differentiation of alginate encapsulated ACPs and MSCs in the presence of TGF-β1 resulted in the formation of stable chondrocytes by ACPs and terminal cartilage with mature chondrocytes by MSCs, with both cell types producing a proteoglycan rich matrix. While sGAG content was maintained by ACPs post stimulation with S100A8/A9 and/or LPS/PA, MSC cultures were negatively impacted. Inflammasome activators and S100A8/A9 alarmins induced significant matrix loss in MSC constructs with reduced sGAG content and chondrocyte apoptosis (lower DNA content and higher caspase-1 activity). In two independent studies van Lent et al. demonstrated that S100A8 and A9 alarmins are typically found in the vicinity of chondrocytes in experimental arthritis and the S100A8 homodimer causes MMP and aggrecanase-mediated pericellular matrix degradation. Furthermore, S100A9-knockout mice, with myeloid cells also lacking the S100A8 protein, displayed reduced cartilage destruction and synovial activation. In studies using wild type mice induced to undergo CIOA it was also shown that both alarmin homodimers contributed to cartilage damage and inflammation in OA (van Lent et al., 2012, Van Lent et al., 2008b, van Lent et al., 2008a).

In the case of long-term exposure, alarmins also seemed to inhibit the chondrogenic process in MSCs. Although cells had the appearance of a rounded hypertrophic phenotype in the construct, they were significantly less differentiated than control MSCs. Basu et al. demonstrated that pre-treatment of MSCs with 0.5μg/ml S100A8/A9 protein prior to their administration into murine full thickness excisional wounds resulted in significant acceleration of wound closure and healing, better than that found with un-treated MSCs. The authors also identified a novel gene expression profile in S100A8/A9 treated MSCs, indicative of a reprogrammed transcriptome towards a protective niche that balances the function of resident and inflammatory cells at the wound healing, improving the overall wound repair mechanisms (Basu et al., 2018). While short-term treatment with alarmins could enhance the immunomodulatory capacities of MSCs, van Lent et al. demonstrated that the expression of S100A8 and S100A9 remained significantly

high, (up to 21 days) post induction of CIOA in mice and contributed towards synovial activation.

Analysis of synovial biopsy samples from patients with early symptomatic OA and end-stage OA also revealed high levels of S100A8 and S100A9 protein expression which correlated with cellularity in the subintima, synovial lining thickness and joint destruction in these patients (van Lent et al., 2012). Therefore prolonged exposure to/long-term prevalence of these alarmins constantly maintains an inflammatory microenvironment in the OA joint, eliciting more cartilage damage.

Previous studies have demonstrated incidence of apoptosis in immature/mature articular cartilage in response to ROS exposure. Cells in the superficial zone of articular cartilage explants were more susceptible to cell death than in the deeper zones. It was also shown that treatment with a pan-caspase inhibitor significantly reduced the rate of matrix loss and tissue deformation (Gilbert et al., 2009, Khan et al., 2008, Candela et al., 2014). Data presented suggest that 1) when articular cartilage is damaged due to chemical/biomechanical stress, chondroprogenitors found in the superficial zone may react to this event by undergoing cell death, leading to articular cartilage degeneration and (2) these cells play an important role in early events in onset of OA. MSCs on the other hand, react to ROS by displaying signs of endoplasmic reticulum (ER) stress, apoptosis (pro-caspase-1 activation) and inflammasome pathway activation (upregulation of IL-1β and NLRP3) (Lu et al., 2012, Wang et al., 2017). The cells are sensitised to inflammatory cues possibly due to their paracrine signalling properties (Bernardo and Fibbe, 2013).

The results obtained from stimulation of monolayer cultures of ACPs and MSCs with a combination of LPS and ATP or PA in order to identify the optimal combination of inflammasome activators further highlighted the capacity of MSCs to resemble osteoarthritic chondrocytes. Cell death via caspase-1 signalling in both cell types was observed, but only MSCs showed upregulation of IL-1β and NLRP3 expression. While both ATP and PA induced pro-apoptotic and pro-inflammatory effects, PA had an enhanced stimulatory activity similar to previously reported work using this FFA (Alvarez-Garcia et al., 2014, Lippiello et al., 1991, Lippiello et al., 1990).

Disruption of ECM homeostasis is a major event during OA progression. D'Lima et al. previously showed that chondrocyte apoptosis is not an independent event but mechanistically linked to matrix degradation. These authors showed that OA chondrocytes have depleted survival mechanisms in addition to their innate avascular nature with cell death further expediting matrix degradation (D'Lima et al., 2006). Significant sGAG loss and high caspase-1 activity was shown in encapsulated MSCs stimulated with the S100A8/A9 complex and LPS/PA and provided a rationale for utilising this combination of stimulators. Alvarez et al, also showed that stimulation of human chondrocytes with palmitate promoted chondrocyte death (via caspase activation) and cartilage destruction (Alvarez-Garcia et al., 2014).

Although stimulated ACPs displayed caspase-1 activity, only ICM-treated ACPs showed upregulation of *IL1B*, *NLRP3* and *IL33* and these genes were downregulated in ACPs treated with CCM to induce differentiation of the cells to a more mature chondrocyte. Past studies documented a higher incidence of acute chondrocyte necrosis and apoptosis in response to blunt trauma, experimental wound generation using biomechanical inputs and ROS/hydrogen peroxide treatment as a chemical stressor in the superficial zone of cartilage populated by chondroprogenitors. Seol et al. demonstrated that these progenitor cells with superior migration abilities were found to migrate to areas adjacent to sites of local chondrocyte death (Duda et al., 2001, Seol et al., 2012, Gilbert et al., 2009, Khan et al., 2008, Dowthwaite et al., 2004).

Chondrogenic progenitor cells have also been thought to contribute to early stages of cartilage repair by restoring levels of the surface zone protein lubricin in injured cartilage within a week of culture. This correlated with high RNA and protein levels of PRG4. This restorative activity of chondrogenic progenitor cells may be associated with their ability to repair superficial defects (Jayasuriya and Chen, 2015, Bao et al., 2011, Teeple et al., 2011, Jay et al., 2010, Wang et al., 2000, Hunziker and Rosenberg, 1996). Concurring with published data, stimulated ICM ACPs initially responded to inflammasome activation via increased casapase-1 activity and expression of *IL1B*, *NLRP3* and *IL33*. However, ACPs that were induced to differentiate to a more mature chondrocyte in response to TGF-β1 treatment responded with reduced although not significant expression of these inflammatory genes. LPS/PA-treated ACPs and MSCs showed slight upregulation of the

pro-inflammatory cytokine marker *IL6* and chemokine *IL8*. Continuous stimulation with the S100A8/A9 complex significantly upregulated these markers in ACPs treated with ICM and MSCs treated with both ICM and CCM.

IL-8 produced by human OA chondrocytes has been described as a mediator of chondrocyte hypertrophy increasing the release of MMP-13 and upregulation of type X collagen (Henrotin et al., 1996, Merz et al., 2003). In line with this, alarmin stimulated MSCs whether treated with ICM or differentiated in response to CCM also demonstrated significant upregulation of *MMP13* and *COL10A1*.

Numerous studies have depicted the catabolic effects of S100A8 and S100A9 homodimers in OA affecting expression of cartilage-specific genes and leading to matrix degradation and joint destruction. Both homodimers have been shown to cause upregulation of IL-6, IL-8, MMPs 1, 3, 9 and 13, and ADAMTS-1, 4, 5 at the mRNA and protein level as well as downregulation of aggrecan and type II collagen (van Lent et al., 2012, Schelbergen et al., 2012, van Lent et al., 2008a, Zreiqat et al., 2010). It is also important to note that these alarmins also contribute to synovitis with activated macrophages in the synovium identified as the source of S100A8/S100A9 in CIOA (van Lent et al., 2012, van den Bosch et al., 2016). In fact, Schelbergen et al. clearly demonstrated that the production/catabolic association of S100A8 and S100A9 to chondrocytes was TLR-4 dependent (Schelbergen et al., 2012). Indeed TLR-4 acts as the major receptor to propagate signalling of the homodimer and is also present in primary chondrocytes (Bobacz et al., 2007). Therefore, the rationale for the use of LPS in the present study was to initiate TLR stimulation, further aiding the downstream DAMP (S100A8/A9):PRR (TLR-4) interaction.

In contrast to previous literature, this is the first study to demonstrate that long term exposure to the S100A8/A9 heterodimer complex causes significant catabolic effects in chondrocytes. Significant downregulation of *PRG4* and *COL2A1* was seen in ACP-derived chondrocytes but the effects of this catabolic signal were more evident in MSC-derived cartilage with significant negative effects on expression of *ACAN*, *COL2A1* and *COL9A1* correlating with downregulation of *S0X9* and upregulation of *ADAMTS4*, *COL10A1* and *MMP13*. SOX9 protein expression is not only critical for chondrogenesis

but also maintaining lineage commitment as it is typically repressed in hypertrophic chondrocytes seen in cartilage growth plates (Lefebvre and Dvir-Ginzberg, 2017, Lefebvre and Smits, 2005). While decreases in *SOX9* expression could also be a consequence of evaluating gene expression at a time point (day 28) beyond TGF-β induced peak promotion of SOX9, previous findings have demonstrated that *SOX9* upregulation causes promotion of *ACAN*, *COMP* and *COL2A1* and regulates or suppresses expression of ADAMTSs (Zhang et al., 2015). Hence downregulation of *SOX9* (also observed in combination of S100A8/A9 and LPS/PA-treated ICM and CCM ACPs) could have contributed to activation of *ADAMTS4, MMP13* and *COL10A1* leading to loss of proteoglycans.

Similar to SOX9, PRG4/lubricin expression has also been linked to lineage commitment since chondroprogenitors have been identified by high *PRG4* expression *in vivo* and more recently in *in vitro* differentiation of ACPs (Zhou et al., 2014, Seol et al., 2012, Anderson et al., 2018). Based on work by Kozhemyakina et al. on identification of the *Prg4*-expressing ACP cell population in mice, Lefebvre proposed that "progenitors choosing the articular surface-lubricating lineage would upregulate *Prg4*, while those engaging in the articular chondrocyte and other cell lineages would turn off *Prg4"* (Kozhemyakina et al., 2015, Lefebvre and Bhattaram, 2015). In the present study MSCs whether treated with TGF-β1 or not, lacked expression of *PRG4*. Subsequent treatment with inflammasome activators/alarmins, demonstrated maximal repression of this gene. This clearly shows that MSCs differentiate into terminal cartilage. Following interaction with inflammatory activators, these cells begin to show signs of hypertrophy typically seen in OA cartilage. Alarmin-treated ACPs on the other hand, showed significant downregulation of *PRG4* in comparison to unstimulated and LPS/PA treated groups. ACPs therefore respond to alarmins with modulation of their chondrogenic commitment status from a progenitor to permanent articular chondrocyte state at the molecular level while maintaining their stable articular phenotype.

Seol et al. proposed that chondrocytes undergoing necrotic/apoptotic cell death upon wounding tend to release chemotactic signals or alarmins like S100 proteins that bind to TLRs and encourage the migration of MSCs and progenitor cells to sites of injury, thereby enabling tissue repair/regeneration (Seol et al., 2012). Therefore, therapies targeting blockade or controlled release of alarmins may reduce hypertrophic events and improve cartilage repair associated with progenitors or MSCs. In conclusion, the data generated in this chapter demonstrated that inflammasome activators act as acute inflammatory insults and elicit pro-apoptotic and altered chondrocyte behaviour while chronic inflammatory input of S100A8/A9 complex in combination with acute insult, creates a pro-inflammatory tissue environment that promotes chondrocyte stress and hypertrophy, mimicking OA-like cartilage degradation.

Chapter 5

Summary and Conclusions

5.1 Retrospective

OA is a chronic degenerative joint disease with pathological events driven by not just cartilage but also the synovium and subchondral bone (Krasnokutsky et al., 2008, Abramson and Attur, 2009). While cartilage damage in OA is mainly a consequence of imbalance in the catabolic and anabolic capacities of chondrocytes, this altered chondrocyte activity is a result of release of high levels of pro-inflammatory cytokines and proteolytic enzymes, thereby creating an inflammatory synovial environment. With continuous crosstalk between chondrocytes and the synovium, activated synoviocytes such as macrophages and T cells release more cartilage-degrading soluble mediators and products of damaged cartilage in turn aggravate synovitis (Haseeb and Haqqi, 2013, Rohner et al., 2012).

Numerous imaging studies have documented synovitis as an important clinical feature of OA that precedes any notable occurrence of cartilage degeneration and is consistently present in both early and late stages of OA (Ayral et al., 2005, Roemer et al., 2011, Krasnokutsky et al., 2011). Also, OA patients (up to 50%) showing synovial activation demonstrated higher severity of cartilage damage (Ayral et al., 2005). Previous studies have established the role of activated SMs in regulating synovial inflammation by influencing the production of IL-1, TNF-α, MMP3, MMP9, MMP13 and aggrecanases, ADAMTS4 and ADAMTS5 in the OA synovium and subsequent osteophyte formation and cartilage destruction during experimental OA (Van Lent et al., 2004, Blom et al., 2004, Bondeson et al., 2006, Bondeson et al., 2010). Apart from MMPs and cytokines, activated macrophages also secrete DAMP signals (or alarmins) like HMGBs and S100 proteins, that interact and stimulate RAGE and TLR signals in OA-affected cartilage and synovium, leading to further amplification of synovial inflammation and cartilage degeneration (Nefla et al., 2016, Loeser et al., 2005, Rosenberg et al., 2017). S100A8 and S100A9 are among the most prominent S100 group of alarmins released by activated SMs, and plasma levels of these homodimers have been shown to correlate with osteophyte progression in patients with early symptomatic OA (Van Lent et al., 2008b, Schelbergen et al., 2016). Also, previous studies have identified these two alarmins mediate cartilage destruction via synovial activation in pre-clinical OA models (van Lent et al., 2012, van den Bosch et al., 2016, Zreiqat et al., 2010). Hence, these findings point towards the involvement of

activated synoviocytes and alarmin-mediated synovial inflammation on cartilage damage and consequent progression of OA.

MSCs have been exhaustively studied for their therapeutic use in cell replacement strategies for OA attenuation/treatment, originally based on their tri-lineage differentiation capacities (particularly chondrocytes, for cartilage repair) (Burke et al., 2016). In addition, reports from previous pre-clinical studies suggest that MSCs exert regenerative effects in treating joint diseases via production of trophic mediators (Murphy et al., 2003, Caplan and Dennis, 2006a). The MSC secretome has been identified as a plethora of secreted proteins that are modulated based on the cells' ability to sense an inflammatory environment and adopt differential phenotypes following active interaction with cellular members of the innate and adaptive immune system. MSCs therefore display both pro- and anti-inflammatory effects via secretion of trophic factors that can further orchestrate either regulation or suppression of activated immune cells (Bernardo and Fibbe, 2013, English et al., 2010, Mancuso et al., 2019). In line with this, MSCs have been shown to modulate synovitis in OA, by switching macrophage polarization from the M1 to the M2 phenotype, while suppressing CD4+ Th1 reactivity and enhancing production of CD4+ Tregs in human OA synovium (Németh et al., 2009, Yang et al., 2009, Van Buul et al., 2012).

Bone-marrow derived MSCs are among the most widely tested MSC source for the treatment of OA cartilage defects (Kong et al., 2017) and Afizah et al. previously showed that marrow-derived MSCs have enhanced chondrogenic capacity when compared to adipose-derived MSCs from same the donors (Afizah et al., 2007). Furthermore, some pre-clinical studies have demonstrated the therapeutic ability of bone-marrow derived MSCs to combat OA, seen with lesser cartilage loss and inhibition of OA progression (Chiang et al., 2016, Caminal et al., 2014, Diekman et al., 2013). However, MSCs tend to form mature fibrocartilage and undergo terminal differentiation leading to a hypertrophic phenotype during *in vitro* chondrogenesis (Johnstone et al., 1998, Johnstone et al., 2013). While studies have demonstrated the therapeutic potential of MSCs in promoting cartilage regeneration in OA joints via activation of endogenous progenitors (Murphy et al., 2003), there is no data to indicate that these cells can successfully differentiate into and maintain a stable articular cartilage phenotype *in vitro* or *in vivo*. Despite their capacity to respond to

an inflammatory environment and secrete trophic mediators (see Chapters 1 and 3), studies have shown that 1) treatment of chondrogenically differentiated hMSCs with catabolic factors like IL-1α and TNF-α and/or conditioned medium from synovial explants led to inhibition of MSC chondrogenesis and 2) that synovial activated macrophages play a vital role in orchestrating this anti-chondrogenic effect (Kruger et al., 2012, Heldens et al., 2012, Fahy et al., 2014, Wehling et al., 2009).

Hence, there is a need for improved MSC-based anti-inflammatory and/or therapeutic strategy to modulate inflammatory events with synchronized and enhanced cartilage repair capacities. As a first step in attempting to achieve this, the work done in this thesis sought to investigate the feasibility of MSCs as immunomodulators and cellular models to study cartilage damage in OA. The main aims of this investigation were to:

1. **Develop a stable and efficient method of vIL10 over-expression of mMSCs using the Tet-On system of adenoviral transduction.**
2. **Assess the immunomodulatory effects of vIL10 over-expressing MSCs on activated macrophages and T cells *in vitro.***
3. **Establish novel *in vitro* models using MSCs and ACPs to investigate the impact of acute and chronic inflammatory effectors in inducing cartilage damage in OA.**

5.2 MSCs efficiently over-express vIL10 in a sustainable and controlled manner

Among the myriad of therapeutic properties MSCs possess, the ability of these cells to migrate and home to injured tissues and express specific trophic factors aiding in anti-inflammation, have favoured the use of engineered MSCs in gene delivery approaches (Jorgensen et al., 2003, Manning et al., 2010). Gene therapy based pre-clinical trials using MSC-mediated delivery of target genes have been successfully demonstrated in models of cancer, myocardial infarction and arthritis (RA and OA) (Liu et al., 2013b, Cao et al., 2011, Li et al., 2014, Li et al., 2007). IL-10 is a potent anti-inflammatory cytokine (Fiorentino et al., 1989) and previous pre-clinical studies showing MSC-mediated delivery of the viral form of IL-10 (vIL10) enabled attenuation of RA (Choi et al., 2008).

The main aim of Chapter 2 was to develop a stable method of efficient adenoviral transduction in mMSCs. In addition, the work done in Chapter 2 sought to investigate the impact of using a pharmacological switch in controlling transgene expression for tunable and inducible anti-inflammatory cytokine delivery by mMSCs. Firstly, additional co-incubation with a chemical agent such as $LaCl_3$ has been shown to enhance transgene expression compared to incubation with an adenoviral construct alone (Palmer et al., 2008) and data reported here also yielded efficient and continuous vIL10 release by mMSCs transduced with ADCMVIL10 using lanthanide-based transduction. Secondly, use of doxycycline as a pharmacological switch to activate the Tet-On system resulted in tightly controlled vIL10 release by ADTET +DOX mMSCs with significantly higher levels of expression compared to ADCMVIL10-MSCs.

Previous studies have demonstrated tetracycline-inducible, controlled vIL10 gene transfer in murine models of experimental arthritis (Apparailly et al., 2002, Perez et al., 2002) and Farrell et al. showed long-term reduction in activated CD4 and CD8 T cell populations in draining lymph nodes of mice with CIOA following administration of vIL10-overexpressing human MSCs (Farrell et al., 2016). This is however the first *in vitro* study to utilise the bi-cistronic Tet-On vector system to generate vIL10 MSCs and to demonstrate enhanced yet sustainable vIL10 expression compared to using a vector system like ADCMVIL10 with uncontrolled transgene expression. Given the fact that cartilage degradation occurs in a joint milieu of pro-inflammatory mediators, the use of

controlled vIL10 MSC therapy for treatment of OA can enhance the immunomodulatory properties of the cells, while protecting them from possible phenotypical alterations such as hypertrophic differentiation in response to inflammatory effectors like MMPs and alarmins *in vivo*. While overexpression of IL-10 by murine MSCs using a retroviral vector previously yielded a release of 22ng/ml which was ten times more than the release observed with Tet-ON MSCs in this chapter, over-dose of IL-10 comes with reversal of immunoregulatory (i.e. immunostimulation as previously reported) effects, which would not be desirable when looking at utilising the Tet-ON system for clinical translation (Choi et al., 2008, Asadullah et al., 2003)The findings of chapter 2 therefore support the use of Tet-On-mediated vIL10 MSCs in investigating the immunomodulatory capacity of these engineered MSCs on activated immune cells *in vitro*.

5.3 vIL10-MSCs effectively modulate inflammation by paracrine and juxtacrine signalling

The therapeutic utility of MSCs for tissue repair/regeneration gained significant interest, since the discovery of the immunomodulatory capability of these cells via secretion of trophic factors (Caplan and Dennis, 2006b, Murphy et al., 2003, English, 2013). Several studies have also proposed that MSCs exert enhanced immunosuppression by 1) sensing the inflammatory stimulus/environment they are exposed to and 2) by adopting differential phenotypes following active interaction with cellular members of the innate immune system and secreting appropriate trophic factors that can further orchestrate either regulation or suppression of activated immune cells (Bernardo and Fibbe, 2013, Prockop and Oh, 2012, Le Blanc and Mougiakakos, 2012, Keating, 2012). Based on generating a controlled system of vIL10 over-expression by mMSCs in Chapter 2, Chapter 3 aimed to investigate the anti-inflammatory efficacy of these engineered MSCs by testing the hypothesis that tetracycline induced vIL10 MSCs modulate inflammatory processes *in vitro* via juxtacrine and paracrine signalling.

Secretome experiments using CMs collected from ADTET +DOX group of MSCs to treat LPS-activated BMs resulted in significant reduction of TNF-α, lower levels of iNOS production and enhanced release of IL-10. This immunosuppressive activity of Tet-On MSCs was significantly higher than untransduced or ADCMVIL10 MSCs. It is important

to note that unlike murine macrophages, endotoxin stimulated human chondrocytes *in vitro* release NO at nanomolar concentrations and OA-affected cartilage express a 150kD isoform of NOS which is completely different in structure and regulatory properties of mouse macrophage derived iNOS (Abramson et al., 2001, Palmer et al., 1993, Blanco et al., 1995). One major difference in the type of soluble effector molecule (one among many) produced by murine and human MSCs, that enable them to sense the inflammatory environment and switch between pro- and anti-inflammatory activities is iNOS (for murine cells) and IDO (for human cells) (Ren et al., 2008, Krampera, 2011). Hence MSC-mediated reduction in NO levels is indicative of an immunomodulatory effect through paracrine signalling and to derive a clinical relevance in terms of biological significance/efficacy future studies in stimulated human macrophages/chondrocytes studying species specific effector molecules would enable further validation.

Similar to secretome assay results, direct co-culture of vIL10 MSCs with activated macrophages resulted in polarisation towards an anti-inflammatory M2 phenotype as illustrated by suppression of the M1 marker, MHC-II and increased CD206 expression with significantly higher levels observed in ADCMVIL10 and ADTET +DOX treated BMs. Despite previous reports demonstrating the presence of both M1 and M2 macrophage phenotypes and increase in M1/M2 ratio in OA synovial fluid, the exact quantity of specific markers leading to disease severity or polarisation status is unknown (De Lange-Brokaar et al., 2012, Blom et al., 2004, Favero et al., 2015, Daghestani et al., 2013, Fahy et al., 2014). Moreover, in a study conducted by Manferdini et al. high level of inter-patient variability was observed in the expression of M1 and M2 markers in the OA synovium (Manferdini et al., 2017). Therefore ADTET +DOX MSC mediated suppression of MHC-II and increased expression of CD206 does indicate a polarisation in macrophage phenotype from M1 to M2, but the actual level of change required to indicate polarisation is difficult to define and requires further exploration. Macrophage polarisation was also replicated at the molecular level, seen with significant downregulation of M1 phenotype chemokine markers *Ccl4*, *Ccl9*, *Cxcl5*, *Pf4* and up-regulation of the anti-inflammatory gene cytokine *Il10* and the M2 marker *Arg1*. In a study conducted by Liu et al. human MSCs over-expressing hsTNFR enabled reduction of joint inflammation in a murine immune competent CIA model, when compared to

untransduced MSCs (Liu et al., 2013b). Further to this using a murine model of acute ischemic stroke, administration of MSC-expressing vIL10 resulted in significant suppression of TNF-α, IL-1β, and IL-6 levels in the serum and brain tissue compared to treatment with the cells alone. This result was indicative of enhanced anti-inflammation and neuroprotection by vIL10 MSCs (Nakajima et al., 2017). A proposed explanation for vIL10 expressing Tet-ON MSCs' ability towards macrophage polarisation and pro-inflammatory cytokine suppression is their possible interaction with EP2 and EP4 receptors on macrophages which could further boost IL-10-mediated immunomodulation (Németh et al., 2009, Hayes et al., 2002). Also, an inflammatory environment created by LPS and IFN-γ may have sensitised MSCs to adopt an anti-inflammatory phenotype and enhance their production of cytokines and chemokines, leading to polarisation of M1 macrophages to an IL-10 secreting regulatory phenotype. While this phenomenon is proposed to occur *in vitro* based on both cellular contact and production of soluble factors, MSCs seem to dampen inflammation by mainly adopting a paracrine route (Bernardo and Fibbe, 2013, Melief et al., 2013b, Melief et al., 2013a). Future experiments correlating the levels of PGE_2 secretion with macrophage polarisation status could validate this proposed mechanism.

Activated CD4+ and CD8+ T cell infiltration is typically seen in synovial aggregates of OA patients and are involved in accelerated osteoclastogenesis and cartilage degradation due to induced expression of TIMP-1 and MIP-1γ for example (Haynes et al., 2002, Hsieh et al., 2013, Shen et al., 2011). In Chapter 3, co-culture of vIL10 MSCs with activated splenocytes demonstrated suppression of $CD4^+$ and not $CD8^+$ lymphocyte proliferation in response to ADCMVIL10 and ADTET +DOX MSCs with maximum inhibition seen with the Tet-ON MSCs. Previous studies have demonstrated suppression of Th1 responses and significant reduction in the amount of activated $CD4^+$ and $CD8^+$ T cells in the popliteal and inguinal lymph nodes of CIA and CIOA mice treated with vIL-10-expressing MSCs (Choi et al., 2008, Farrell et al., 2016). An explanation for this modified efficacy of MSCs towards $CD8^+$ lymphocytes could be the line of murine MSCs used (Schurgers et al., 2010). While $CD8^+$ T cells are found in the synovial membrane and aggregates of OA patients these cytotoxic T cells do not comprise of the major T cell infiltrate and only the helper cells do (Li et al., 2017b, Reidbord and Osial, 1987, Johnell

et al., 1985). Also the only known pathological role of $CD8^+$ T cells is based on induction of TIMP-1 expression and associated OA severity (Hsieh et al., 2013). While data generated in Chapter 3 proved the hypothesis that tetracycline induced vIL10 MSCs can modulate inflammatory processes *in vitro* via juxtacrine and paracrine signalling, it is critical to note that MSCs elicited both forms of signalling, through secretion of trophic factors indicating that paracrine signalling is crucial and possibly superior for MSC-mediated immunomodulation. Future *in vivo* studies investigating the therapeutic feasibility of this inducible system maybe a favourable strategy in the direction of identifying sustainable anti-inflammatory therapies favouring cartilage repair in OA.

5.4 MSC-derived cartilage mimic OA-chondrocyte phenotype in response to inflammatory effectors in OA

Numerous pre-clinical studies have tested and demonstrated the efficacy of using MSCs as vehicles in gene therapeutic strategies for repairing cartilage defects in OA and in attenuating inflammatory responses in RA (Choi et al., 2008, Liu et al., 2013b, Farrell et al., 2016). In one study, Cao at al. showed that administration of MSCs-overexpressing SOX-9 enabled cartilage repair in a rabbit full thickness cartilage defect model (Cao et al., 2011). Glass et al. demonstrated that a doxycycline-inducible vector enabled over-expression of IL-1Ra by MSCs in a controlled manner. These engineered MSCs when encapsulated in 3D woven PCL scaffolds produced cartilage with mechanical properties similar to native articular cartilage(Glass et al., 2014).

While engineering MSCs to express anti-inflammatory cytokines/therapeutic factors may enhance their paracrine properties and even enable or promote chondrogenesis, there is no data to indicate or support successful differentiation of these cells into a stable articular cartilage phenotype when implanted *in vivo*; MSCs form fibrocartilage and have a tendency towards hypertrophic differentiation and mineralisation over-time (Johnstone et al., 1998, Xu et al., 2008, Hellingman et al., 2012). Adding to this point, previous studies have shown that endogenous alarmins like S100s, cytokines and MMPs, found in the activated synovium of OA joint environment, may also be contributing towards inhibition of chondrogenesis of cartilage progenitors and promotion of hypertrophic differentiation of MSCs (Kruger et al., 2012, van Lent et al., 2012, Heldens et al., 2012, Fahy et al., 2014).

Hence, Chapter 4 sought to investigate the impact of acute and chronic inflammatory effectors in inducing cartilage damage in OA. Work performed to achieve this aim focused on establishing novel models of stable and terminal cartilage using ACPs and MSCs encapsulated in alginate and examining the effects of inflammasome activators (LPS and PA) and the S100A8/A9 heterodimer alarmin complex during or post cartilage formation *in vitro*.

While alginate-encapsulated CCM-treated MSCs demonstrated enhanced GAG production compared to standard pellet cultures, both methods of chondrogenic differentiation resulted in formation of terminal cartilage with hypertrophic chondrocytes. The gene expression pattern of CCM-treated MSC beads showed upregulation of hypertrophic markers *COL10A1* and *MMP13* with significantly higher expression seen following LPS/PA alone or dual stimulation with S100A8/A9 alarmins. Again, significant sGAG loss and high caspase-1 activity was seen in encapsulated MSCs stimulated with the S100A8/A9 complex and LPS/PA with these results indicating that MSCs behave like OA chondrocytes to some extent. Chondrocyte apoptosis typically observed during cartilage injury is not an independent event but mechanistically linked to matrix degradation (D'Lima et al., 2006, Alvarez-Garcia et al., 2014). Fernandes et al. compared gene expression patterns of several OA markers between bone-marrow MSC-derived chondrocytes from healthy donors and OA chondrocytes and found *COL10A1* expression in MSC-chondrocytes to be 85-fold higher. Also the proportion of differentiated MSCs expressing the COL10 protein was predominantly higher and less than 1% of OA chondrocytes had synthesized this collagen.(Fernandes et al., 2013).

Previous studies have reported the existence of a small population of MSC-like progenitors (also referred to as chondrogenic progenitor cells in some reports) in mature cartilage with MSC-like differentiation capacities, particularly chondrogenesis (Williams et al., 2010, Dowthwaite et al., 2004, Koelling et al., 2009, Khan et al., 2009b). Interestingly, there is a higher prevalence of these cells in OA cartilage seen as cellular clusters - a hallmark of OA cartilage degeneration (Fickert et al., 2004, Su et al., 2015, Jayasuriya et al., 2018). Jayasuriya et al. conducted a study involving comparison of molecular profiles of immortalised human OA-MSC lines (referred to as 'OA-MSCs') to OA chondrocytes. The comparative analysis revealed higher expression of markers such as *COL10A1* and

RUNX2 in OA-MSCs and subsequent induction of chondrogenesis in these cells resulted in further stimulation of *COL10A1* expression and MMP-13 release when compared to OA chondrocytes. This data implies that these OA-MSCs or MSC-like progenitor cells in the OA cartilage possibly contribute to disease progression in contrast to their previously assumed function of tissue repair in OA cartilage (Jayasuriya et al., 2019, Jayasuriya et al., 2018).

In contrast to the downregulated expression of *COL2A1, ACAN, COL9A1, SOX9* and upregulation of *IL1B, NLRP3, IL6* and *IL8* in S100A8/A9 in LPS/PA treated MSCs, histological analysis showed that chondrogenesis was inhibited. Although cells had the appearance of a rounded hypertrophic phenotype in the construct, they were significantly less differentiated than control MSCs. In a study conducted by Basu et al., S100A8/A9 pre-treated MSCs exhibited improved wound closure and healing compared to non-treated MSCs in murine full thickness wounds. The authors also identified a novel gene expression profile in these alarmin-treated MSCs, indicative of a reprogrammed transcriptome with a protective niche that regulates the function of resident and inflammatory cells, improving overall wound repair mechanisms (Basu et al., 2018). While previous data has established the catabolic role of S100A8 and S100A9 in mediating synovial inflammation and cartilage degradation (van Lent et al., 2012, Schelbergen et al., 2012, Schelbergen et al., 2016, Zreiqat et al., 2010), short-term treatment with alarmins could sensitise MSCs to the OA joint environment and enhance the immunomodulatory capacities of the cells. Alternatively, blocking DAMP interaction with PRRs like TLR, RAGE and HMGBs could inhibit the effects of these alarmins.

5.5 ACPs maintain their progenitor status and retain a stable articular cartilage phenotype.

ACPs are undifferentiated precursor cells of cartilage, developmentally primed to become chondrocytes with minimal tendency towards hypertrophic differentiation, as seen by lower expression of *COL10A1* and *MMP13* in previously published reports, and can generate stable articular chondrocytes(Anderson et al., 2016, Hayes et al., 2001). Unlike MSCs, ACPs maintained a steady rate of GAG production in standard pellet cultures and in alginate constructs irrespective of treatment with inflammatory insults. Although

treatment of ACPs with both inflammatory effectors resulted in caspase-1 activation, only ICM-treated ACPs showed upregulation of *IL1B, NLRP3* and *IL33* and these genes were downregulated in CCM-treated ACPs. This activity of chondrogenic progenitor cells may be associated with their ability to repair superficial defects following initial events of local chondrocyte death and also due to their capacity to produce high levels of *PRG4* (Kozhemyakina et al., 2015, Seol et al., 2012).

In contrast to alarmin-treated ACPs that demonstrated significant downregulation of *PRG4* yet maintained a stable articular cartilage phenotype seen with histological analysis, MSCs, whether treated with TGF-β1 or not, lacked expression of *PRG4*. Subsequent treatments with both inflammatory effectors, resulted in maximal repression of this gene. A possible inference one could draw from this data is that MSCs form only terminal cartilage and do not act as a cartilage progenitor or a progenitor-like cell unless metabolically re-programmed to overexpress *PRG4* (Kozhemyakina et al., 2015, Lefebvre and Bhattaram, 2015). Similar to results obtained in Chapter 4, Ribitsch et al. established a standardized cartilage lesion model comparing differential injury response of foetal and adult ovine cartilage to injury. Among the many cartilage-specific matrix proteins expressed, PRG4 was significantly upregulated in foetal sheep only in response to injury.

Furthermore, analysis of proteins associated with inflammatory responses revealed significant upregulation of alarmins S100A8, S100A9, S100A12 and coiled-coil domain containing 88A (CCDC88A) post-injury in adult but not foetal sheep (Ribitsch et al., 2018). In line with this report, the data generated in Chapter 4 showed that ACPs initially respond to inflammatory insults /inputs as seen by Caspase-1 activity while retaining their capacity towards maintenance of stable cartilage, while MSCs display chondrocyte hypertrophy and exhibit phenotypical and behavioural similarities to OA chondrocytes. Future studies involving simultaneous comparison of chondrocytes derived from early and late OA patients, alongside MSCs and ACPs, utilising this novel inflammation-drive *in vitro* cartilage model should enable further validation of results obtained.

5.6 Conclusions and future directions

This thesis has demonstrated that murine MSCs, transduced and controlled by the Tetracycline system, showed sustainable and tuneable expression of vIL10 that further enabled maximal immunomodulatory potential of these engineered MSCs for the attenuation of inflammatory responses in OA. Furthermore, the establishment of a novel *in vitro* cartilage model driven by critical inflammatory effectors provided preliminary understanding of the feasibility of using MSCs for stable cartilage regeneration and offers scope for improving cartilage regeneration strategies.

One possible future strategy would be to encapsulate Tet-On inducible vIL10 MSCs and investigate the immunomodulatory and cartilage repair capacities of these engineered cells, using the inflammation-driven cartilage model developed in this thesis. The data derived in this thesis also demonstrates the impact of S100A8/A9 in inducing production of pro-inflammatory cytokines and MMPs, typically seen during active synovial inflammation, thereby confirming the role of these alarmins in inflammation-mediated cartilage matrix disruption. However, it would be necessary for future experiments to test the impact of S100A8/A9 in inducing inflammation-driven cartilage damage in the absence of inflammasome activators. This could validate if alarmin release and subsequent catabolic events occur independent of inflammasome activation. Accordingly, this may enable identification of novel biomarkers or therapeutic targets to inhibit or reduce alarmin-mediated early inflammatory events leading to cartilage damage. Furthermore, inclusion of qualitative and quantitative analysis of other hypertrophic markers at timepoints before and after 28 days could enable tracking of minute alterations in differentiation pattern of stem/progenitor cells during cartilage development/damage in OA.

Appendix 1

Supplementary Data

Appendix 1

1. Supplementary Figure 1: Optimisation of macrophage activation

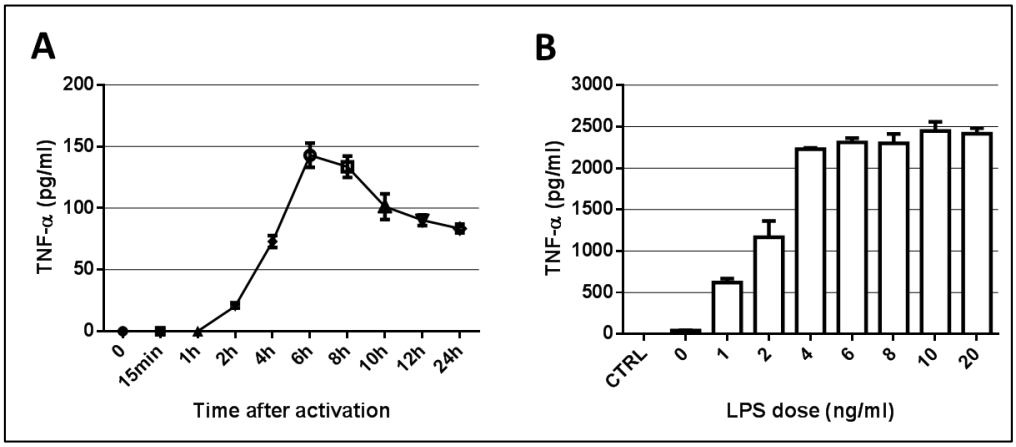

S1: Optimisation of bone-marrow derived murine macrophage (BM) activation. (A) In vitro differentiated BMs were primed with 20ng/ml IFN-γ and 2ng/ml LPS to identify the time point of peak TNF-a release. Secretion of TNF-a was highest at 6h. (B) BMs were activated for 6h with different concentrations ranging from 0 to 20ng/ml of LPS. Highest TNF-a secretion was observed with 10ng LPS beyond which the effect was saturated. Data represented as Mean±SEM (n=1, technical triplicates).

2. **Supplementary Figure 2: Heat map analysis of fold changes in macrophage gene expression**

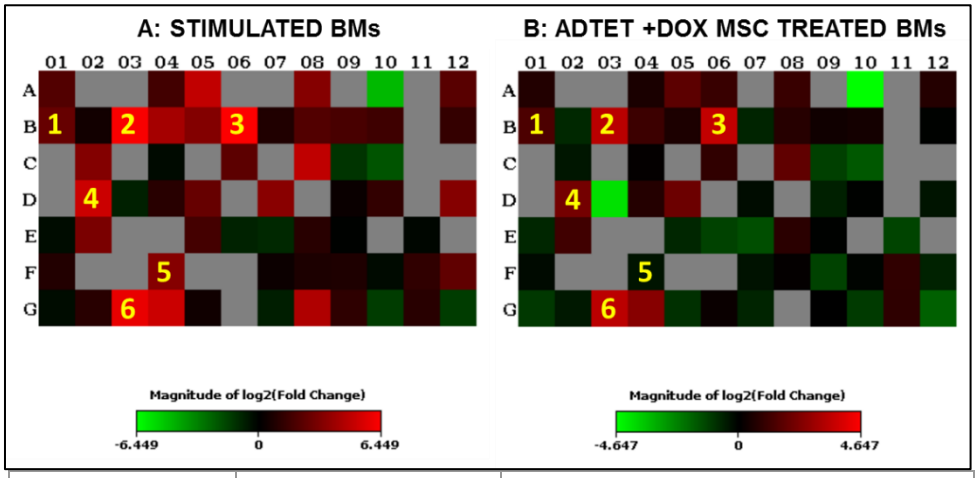

Gene Symbol	Stimulated BMs	ADTET +DOX MSC treated BMs
1: Ccl4	6.01	2.63
2: Ccl6	81.25	10.38
3: Ccl9	87.36	11.94
4: Cxcl5	35.66	4.33
5: Il33	10.32	-1.29
6: Pf4	59.57	10.64

*S2: Heat map analysis of fold changes in macrophage gene expression. BMs were activated with LPS and/or treated with CM from ADTET +DOX MSCs for 24h followed by analysis of changes in gene expression from a panel of 84 mouse inflammatory cytokine and receptor genes. (A) In comparison to stimulated BMs, expression of **1**: Chemokine (C-C motif) ligand 4 (Ccl4), **2**: Ccl6, **3**: Ccl9, **4**: Chemokine (C-X-C motif) ligand 5 (Cxcl5), **5**: Interleukin 33 (Il33) and **6**: Platelet factor 4 (Pf4) were most downregulated in BMs treated with CM from (B) ADTET+DOX MSCs. Visualization of the magnitude of fold changes in expression between the selected groups as over-expressed (red) and under-expressed (green). (C) Fold-regulation (threshold = 2) values of highlighted genes of stimulated BMs vs ADTET +DOX MSC-CM treated BMs. n=1, technical triplicates).*

3. Supplementary Figure 3: Optimisation of BM:MSC co-culture conditions

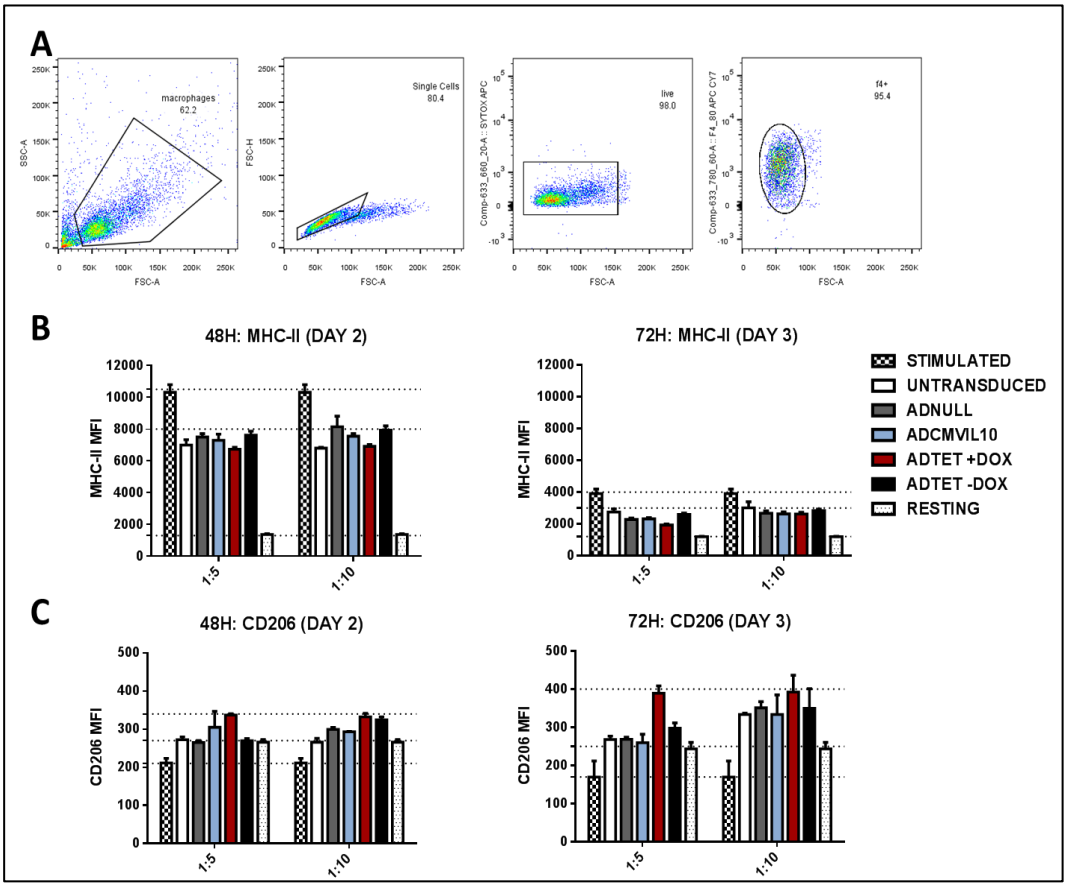

S3: Optimisation of BM:MSC co-culture conditions. BMs at day 6 were stimulated with IFN-γ (overnight) and LPS for 6h. Activated BMs were treated with untransduced or transduced MSCs in direct co-cultures to identify the optimal BMs:MSC ratio and time-point of efficient co-culture in terms of macrophage polarisation from M1 to the M2 phenotype. (A) BMs seeded at ratios 1:5 and 1:10 at day 2 (48h) and 3 (72h) were analysed by flow cytometry by first gating macrophage singlets followed by inclusion of live cells (SYTOX staining) and F4/80^{+} macrophages. (B) Expression of the M1 marker, MHC-II, was consistently reduced (minimal inter-replicate variation) in all groups of MSC treated BMs compared to stimulated BMs at 72h at a ratio of 1:5. (C) Expression of the M2 marker, CD206 in BMs co-cultured with ADTET +DOX MSCs at 72h at a ratio of 1:5 was two times higher in comparison to stimulated BMs. The overall expression pattern of MHC-II and CD206 was more consistent at 72h (1:5 ratio) compared to 48h in all MSC-treated groups. Data represented as Mean±SEM (n=1, technical triplicates).

4. Supplementary Figure 4: Optimisation of MSC:T cell co-culture conditions

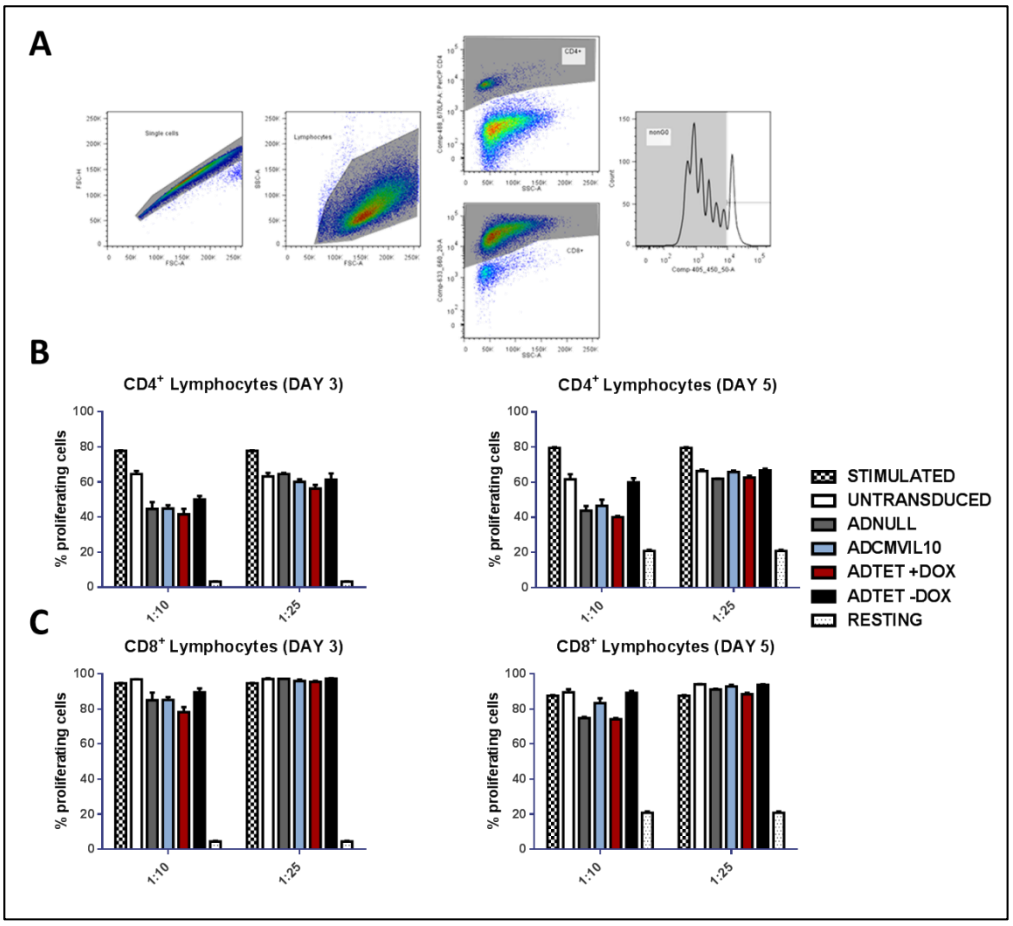

S4: Optimisation of MSC:T cell co-culture conditions. Splenocytes isolated from C57BL/6 murine spleen were labelled with CTV, activated with anti-CD3e and anti-CD28 antibodies and stained for CD4 and CD8. Stimulated cells were co-cultured with MSCs at ratios of 1:10 and 1:25, and analysed by flow cytometry at 3 and 5 days of co-culture to identify the optimal ratio and time-point for observation of immunomodulation of T cell proliferation. (A) Lymphocytes were gated to include single cells followed by live CD4$^+$ and CD8$^+$ T cells after the first generation, quantified by CTV staining. (B) Suppression of CD4$^+$ cell proliferation was higher on day 3 at a ratio of 1:10 compared to 1:25 and day 5. (C) CD8$^+$ lymphocyte proliferation was suppressed at day 3 and 5 at a ratio of 1:10 but not 1:25. Data represented as Mean±SEM (n=1, technical triplicates).

5. Supplementary Figure 5: Mean values* of fold regulation of target genes (ICM data from Figure 4.8A&B)

Target genes	ICM+LPS/PA		ICM(S100)+LPS/PA	
	ACPs	MSCs	ACPs	MSCs
IL1B	2.15	0.97	16.96	1.09
NLRP3	2.05	0.28	0.11	0.25
IL33	2.81	0.63	0.21	0.28
IL6	1.78	4.76	70.94	655.25
IL8	22.83	27.63	1041.43	1113.62
SOX9	2.3	2.81	0.13	1.61
PRG4	3.4	0.42	2.32	0.11
ACAN	1.74	1.09	0.14	0.53
COL2A1	2.12	1.3	0.78	0.47
COL1A1	1.64	0.92	1.25	3.51
COL9A1	1.42	1.11	0.78	1.3
COL10A1	2.89	1.11	0.36	0.54
MMP13	2.28	40.1	4.81	690.1
ADAMTS4	1.57	0.98	0.44	0.32
ADAM5P	1.95	1.51	0.13	1.22

*Values in table derived by $2^{-\Delta\Delta C_T}$ method; ICM values for all genes normalised to *GAPDH* = 1 (baseline); values >/< 1 are considered **up**/**down**-regulated, respectively.

6. Supplementary Figure 6: Mean values* of fold regulation of target genes (CCM data from Figure 4.9A&B)

Target genes	CCM		CCM+LPS/PA		CCM(S100)+LPS/PA	
	ACPs	MSCs	ACPs	MSCs	ACPs	MSCs
IL1B	0.8	0.06	0.58	0.14	0.34	1.84
NLRP3	0.31	0.11	0.16	0.42	0.04	1.14
IL33	0.56	0.07	0.11	0.59	0.07	0.66
IL6	0.24	0.21	1.62	0.28	6.69	199.79
IL8	2.37	0.12	3.84	0.21	162.41	1151.3
SOX9	1.28	9.43	1.27	7.89	0.51	0.73
PRG4	236.8	0.71	281.95	0.53	11.01	0.03
ACAN	38.73	320.62	30.49	173.69	1.66	1.51
COL2A1	3161.68	14377.8	3389.57	11146	5.76	5.15
COL1A1	4.07	7.99	3.58	4.38	2.35	2.42
COL9A1	10.85	569.8	7.10	314.02	0.07	1.55
COL10A1	0.78	8.08	1.17	7.56	1.47	74.26
MMP13	9.47	9.53	13.06	9.46	47.36	1639.87
ADAMTS 4	0.72	0.09	0.17	0.24	0.13	1.19
ADAM5P	0.38	0.06	0.12	0.24	0.08	0.95

*Values in table derived by $2^{-\Delta\Delta C}$T method; ICM values for all genes normalised to *GAPDH* = 1 (baseline); values >/< 1 are considered **up**/**down**-regulated, respectively.

Appendix 2

Appendix 2

Table 1: Mouse MSC medium

Reagent	Volume (500ml)	Final Concentration
MEM-α, GlutaMAX™ (Gibco)	395ml	N/A
Foetal Bovine Serum (FBS; Sigma)	50ml	10%
Equine serum (Sigma)	50ml	10%
Penicillin/Streptomycin 100x solution (P/S; Gibco)	5ml	1%

Table 2: Osteogenic induction medium

Reagent	Volume (100ml)	Final Concentration
DMEM (HG) (Sigma)	77.5ml	N/A
Dexamethasone 1mM (Sigma)	10µl*	100nM
Ascorbic acid 2-P 10mM (Sigma)	0.5ml	50µM
β glycerophosphate 1M (Sigma)	2ml	20mM
L-thyroxine (Sigma)	50µl	50ng/ml
FBS	9ml	9%
Equine serum	9ml	9%
L-glutamine (Sigma)	1ml	2mM
P/S 100x solution	1ml	1%

Table 3: Preparation of standards for calcium assay

Conc. (µg/ml)	Volume 10 mg/dl of std/well
0	0
0.05	0.5µl
0.1	1 µl
0.2	2 µl
0.4	4 µl
0.6	6 µl
0.8	8 µl
1	10µl

Table 4: Adipogenic induction medium

Reagent	Volume (100ml)	Final Concentration
DMEM (HG)	87.6ml	N/A
Dexamethasone 1mM	100µl	1µM
Insulin 1mg/ml (Sigma)	1ml	10µg/ml
Indomethacin 100mM (Sigma)	200µl	200µM
500mM MIX (Sigma)	100µl	500µM
P/S 100X solution	1ml	1%
FBS	10ml	10%

Table 5: Adipogenic maintenance medium

Reagent	Volume (100ml)	Final Concentration
DMEM (HG)	88ml	N/A
Insulin 1mg/ml	1ml	10µg/ml
P/S 100X solution	1ml	1%
FBS	10ml	10%

Table 6: Incomplete chondrogenic medium (ICM)

Reagent	Volume (100ml)	Final Concentration
DMEM (HG)	94ml	N/A
Dexamethasone 1mM	10µl*	100nM
Ascorbic acid 2-P: 5mg/ml	1ml	50µg/ml
L-Proline: 4mg/ml (Sigma)	1ml	40µg/ml
ITS Premix Universal culture supplement (Roche)	1ml	N/A
Sodium pyruvate (Gibco)	1ml	1mM
Antibiotic/Antimycotic 100x solution (Gibco)	1ml	1%

Table 7: Preparation of dilution buffer for GAG quantification

Reagents	Volume for 1L	Concentration
Sodium monobasic (Sigma) – Solution A	13.9g in dH_2O	0.1M
Sodium phosphate dibasic heptahydrate (Sigma) – Solution B	23.84g in dH_2O	0.1M
Sodium phosphate (make 800ml)	342.5ml solution A 157.5ml solution B	50mM
N-acetyl cysteine	0.32g in 1L sodium phosphate	2mM
EDTA (0.5M stock, Sigma)	4ml for 1L	2mM

Table 8: Preparation of DMMB stock solution for GAG quantification

1. 16mg of 1,9-Dimethylmethylene Blue (Sigma) was dissolved in 5ml of 100% Ethanol (Fisher Scientific) overnight on a shaker.
2. To 800ml of deionised water 2.73g Sodium Chloride (Sigma) and 3.04g Glycine (Fisher Scientific) was added along with the dissolved DMMB solution.
3. pH was adjusted to 1.5 using Hydrochloric acid (Sigma).
4. Final volume was made up to 1L and stored away from light.

Table 9: Preparation of C-6-S standard curve for GAG measurement

C-6-S working solution	Dilution buffer	Concentration GAG/well (25µl)
200µl	0µl	2.0µg
170µl	30µl	1.7µg
130µl	70µl	1.3µg
100µl	100µl	1.0µg
70µl	130µl	0.7µg
30µl	170µl	0.3µg
0µl	200µl	0.0µg

Table 10: Preparation of DNA standards for PicoGreen assay

DNA working stock	1xTE	Final concentration DNA/ml (ng)
400µl	0µl	2000
200µl	200µl	1000
100µl	300µl	500
40µl	360µl	200
20µl	380µl	100
10µl	390µl	50
4µl	396µl	20
0µl	400µl	0

Table 11: Surface markers for mMSC & BM characterisation

Receptor	**Clone**	**Fluro-chrome**	**Isotype**	**Supplier**	**Volume /sample**
CD90.2	53-2.1	APC	Rat IgG2a,κ	BD Pharmingen	1µl
Ly-6A/E (Sca-1)	D7	PE	Rat IgG2a, κ	Biolegend	1µl
CD105	MJ7/18	PE	Rat IgG2a, κ	Biolegend	1µl
CD140a	APA5	PE	Rat IgG2a, κ	eBioscience	1µl
CD34	RAM34	Alexa Fluor 647	Rat IgG2a, κ	BD Pharmingen	1µl
CD45	30-F11	APC	Rat IgG2b, κ	BD Pharmingen	1µl
CD11b	M1/70	PE	Rat IgG2b, κ	BD Pharmingen	1µl
F4/80 **(BMs)**	BM8	PE	Rat IgG2a, κ	Biolegend	1µl
CD45.2 **(BMs)**	104	APC	Mouse IgG2a, κ	Biolegend	1µl
CD11b **(BMs)**	M1/70	PE	Rat IgG2b, κ	Biolegend	1µl

Table 12: Isotype controls for mMSC & BM characterisation

Isotype control	Clone	Fluro-chrome	Supplier	Volume /sample
Rat IgG2a,κ	RTK2758	APC	Biolegend	1µl
Rat IgG2a, κ	RTK2758	PE	Biolegend	1µl
Rat IgG2b, κ	RTK4530	APC	Biolegend	1µl
Rat IgG2b, κ	RTK4530	PE	Biolegend	1µl
Rat IgG2a, κ	RTK2758	Alexa Fluor 647	BD Pharmingen	1µl
Mouse IgG2a, κ	MOPC-173	APC	Biolegend	1µl

Table 13: FACS buffer

Reagent	Final Concentration
PBS (Sigma)	N/A
FBS	2%
Sodium azide (NaN_3,Sigma)	0.05%

Table 14: Preparation of 2% DMEM titration medium

Reagent	Volume (100ml)	Final Concentration
DMEM (HG)	97ml	N/A
P/S 100X solution	1ml	1%
FBS	2ml	2%

Table 15: Preparation of 10% DMEM titration medium

Reagent	Volume (100ml)	Final Concentration
DMEM (HG)	89ml	N/A
P/S 100X solution	1ml	1%
FBS	10ml	10%

Table 16: L929 medium

Reagent	Volume (500ml)	Final Concentration
DMEM (HG)	445ml	N/A
P/S 100X solution	5ml	1%
Heat-inactivated (56 °C, 30min) FBS	50ml	10%

Table 17: Macrophage (BM) medium

Reagent	Volume (500ml)	Final Concentration
RPMI-1640 (Sigma)	354.5ml	N/A
L929 CM (M-CSF)	75ml	15%
Heat-inactivated FBS	50ml	10%
P/S 100X solution	5ml	1%
L-Glutamine	5ml	2mM
Non-essential Amino Acids (NEAA; Sigma)	5ml	0.1M
Sodium pyruvate	5ml	1mM
2-β-Mercaptoethanol (Thermo Fisher: Invitrogen)	0.5ml	55μM

Table 18: Working concentrations of mouse cytokine ELISA kits

Cytokine	Capture antibody	Detection antibody	Standard (highest point)
TNF-α	800ng	75ng	2ng/ml
IL-1β/IL-1F2	4μg	500ng	1ng/ml
IL-6	2μg	150ng	1ng/ml
IL-10	4μg	300ng	2ng/ml

Table 19: Greiss reagent

Solution A	**Volume (300ml)**	**Solution B**	**Volume (300ml)**
Sulfanilamide (Sigma)	3g	N-(1-Naphthyl) ethylenediamine dichloride (Sigma)	0.9g
Phosphoric acid (Sigma)	9ml	Phosphoric acid	9ml
Water	291ml	Water	291ml

Table 20: T cell medium

Reagent	**Volume (500ml)**	**Final Concentration**
DMEM (HG)	429.5ml	N/A
Heat-inactivated FBS	50ml	10%
L-Glutamine	5ml	2mM
HEPES 1 M (Sigma-Aldrich)	5ml	10mM
NEAA	5ml	0.1M
P/S 100X solution	5ml	1%
2-β-Mercaptoethanol	0.5ml	50μM

Table 21: Antibodies used in macrophage and T cell co-culture analysis

Receptor	Clone	Fluro-chrome	Isotype control	Supplier	Volume /sample
F4/80	BM8	APC/Cy7	Rat IgG2a, κ	Biolegend	1µl
I-A^b (MHC-II)	AF6-120.1	PE	Rat IgG2b, κ	Biolegend	1µl
CD206	C068C2	BV 421	Rat IgG2a, κ	Biolegend	1µl
CD4	RM4-5	PerCP/Cy5.5	Rat IgG2b, κ	Biolegend	0.05µl
CD8	53-6.7	APC	Rat IgG2a, κ	Biolegend	0.025µl
CD25	PC61	PE	Rat IgG1, λ	Biolegend	1µl

Table 22: Mouse SYBR® Green forward (Fw) and reverse (Rv) primers

Gene Symbol	Primer pair Sequence (5'-3')
Ccl4	Fw: GGTATTCCTGACCAAAAGAG Rv: TCCAAGTCACTCATGTACTC
Ccl6	Fw: CTTTCAAGACACTTCTTCAGAC Rv: CTGCTGATAAAGATGATGCC
Ccl9	Fw: AATGTTTCACATGGGCTTTC Rv: CAATGCATCTCTGAACTCTC
Cxcl5	Fw: TGTTTGCTTAACCGTAACTC Rv: CAGTTAGCTATGACTTCCAC
Pf4 (Cxcl4)	Fw: TAGCCACCCTGAAGAATG Rv: GACATTTAGGCAGCTGATAC
Il33	Fw: TCCCTGAGTACATACAATGAC Rv: CTTTGATGGGACTCATGTTC
Il10	Fw: CAGGACTTTAAGGGTTACTTG Rv: ATTTTCACAGGGGAGAAATC
Arg1	Fw: CTGACCTATGTGTCATTTGG Rv: CATCTGGGAACTTTCCTTTC
Gapdh	Fw: GTGAAGGTCGGTGTGAACG Rv: ATTTGATGTTAGTGGGGTCTCG

Table 23: Human MSC medium

Reagent	Volume (500ml)	Final Concentration
MEM α, GlutaMAX™	445ml	N/A
FBS	50ml	10%
P/S 100X solution	5ml	1%

Table 24: ACP medium

Reagent	Volume (500ml)	Final Concentration
DMEM F12/ Nutrient mixture F12 Ham (1:1 mixture; Sigma)	440ml	N/A
FBS	50ml	10%
Ascorbic acid 2-P:	5ml	0.1mM
Penicillin/Streptomycin 100x solution (P/S; Gibco)	5ml	1%

Table 25: Preparation of Phosphate buffer solution for Toluidine blue stain

Reagent	**Final Concentration**	**Final volume (200ml)**
Buffer solution A- Disodium phosphate (Na_2HPO_4; Sigma)	0.2M	94.7ml
Buffer solution B- Monosodium phosphate (NaH_2PO_4; Sigma)	0.2M	5.3ml
Water	N/A	100ml

Table 26: Human SYBR® Green Forward (Fw) and Reverse (Rv) Primers- Part 1

Gene Symbol	Primer pair Sequence (5'-3')
GAPDH	Fw: ACAGTTGCCATGTAGACC Rv: TTGAGCACAGGGTACTTTA
ACAN	Fw: CACCCCATGCAATTTGAG Rv: AGATCATCACCACACAGTC
COL1A1	Fw: GCTATGATGAGAAATCAACCG Rv: TCATCTCCATTCTTTCCAGG
COL2A1	Fw: GAAGAGTGGAGACTACTGG Rv: CAGATGTGTTTCTTCTCCTTG
COL9A1	Fw: ACCTAAAGGTGACTTGGG Rv: CATTTCTGCCATAGCTGG
COL10A1	Fw: GCTAGTATCCTTGAACTTGG Rv: CCTTTACTCTTTATGGTGTAGG
MMP13	Fw: AGGCTACAACTTGTTTCTTG Rv: AGGTGTAGATAGGAAACATGAG
ADAMTS4	Fw: AGAAGAAGTTTGACAAGTGC Rv: CACATTGTTGTATCCGTACC
ADAM5P	Fw: CTGTGCTTCTTATTACTACTGC Rv: AGCTCTCACTTTCATTTTCC
SOX9	Fw: CTCTGGAGACTTCTGAACG Rv: AGATGTGCGTCTGCTC

Table 26: Human SYBR® Green Forward (Fw) and Reverse (Rv) Primers- Part 2

Gene Symbol	**Primer pair Sequence (5'-3')**
PRG4	Fw: GACTGGCTTATCAAGACAAAG Rv: GGTAACCACATTTGGAAGTC
IL1B	Fw: CTAAACAGATGAAGTGCTCC Rv: GGTCATTCTCCTGGAAGG
IL6	Fw: GCAGAAAAAGGCAAAGAATC Rv: CTACATTTGCCGAAGAGC
IL8	Fw: GTTTTTGAAGAGGGCTGAG Rv: TTTGCTTGAAGTTTCACTGG
IL33	Fw: GCTGGGAAATAAGGTGTTAC Rv: CCAGAAGTCTTTTGTAGGAC
NLRP3	Fw: AGGTGTTGGAATTAGACAAC Rv: AATACATTTCAGACAACCCC

Bibliography

Bibliography

Bibliography

ABHISHEK, A. & DOHERTY, M. 2013. Diagnosis and clinical presentation of osteoarthritis. *Rheum Dis Clin North Am,* 39**,** 45-66.

ABRAMSON, S. B. & ATTUR, M. 2009. Developments in the scientific understanding of osteoarthritis. *Arthritis research & therapy,* 11**,** 227.

ABRAMSON, S. B., ATTUR, M., AMIN, A. R. & CLANCY, R. 2001. Nitric oxide and inflammatory mediators in the perpetuation of osteoarthritis. *Current rheumatology reports,* 3**,** 535-541.

AFFANDI, A. J., SILVA-CARDOSO, S. C., GARCIA, S., LEIJTEN, E. F., VAN KEMPEN, T. S., MARUT, W., VAN ROON, J. A. & RADSTAKE, T. R. 2018. CXCL4 is a novel inducer of human Th17 cells and correlates with IL-17 and IL-22 in psoriatic arthritis. *European journal of immunology,* 48**,** 522-531.

AFIZAH, H., YANG, Z., HUI, J. H., OUYANG, H. W. & LEE, E. H. 2007. A comparison between the chondrogenic potential of human bone marrow stem cells (BMSCs) and adipose-derived stem cells (ADSCs) taken from the same donors. *Tissue Eng,* 13**,** 659-66.

AIGNER, T., MCKENNA, L., ZIEN, A., FAN, Z., GEBHARD, P. M. & ZIMMER, R. 2005. Gene expression profiling of serum-and interleukin-1β-stimulated primary human adult articular chondrocytes–A molecular analysis based on chondrocytes isolated from one donor. *Cytokine,* 31**,** 227-240.

ALAAEDDINE, N., DI BATTISTA, J. A., PELLETIER, J. P., KIANSA, K., CLOUTIER, J. M. & MARTEL-PELLETIER, J. 1999. Inhibition of tumor necrosis factor α–induced prostaglandin E2 production by the antiinflammatory cytokines interleukin-4, interleukin-10, and interleukin-13 in osteoarthritic synovial fibroblasts: Distinct targeting in the signaling pathways. *Arthritis & Rheumatism: Official Journal of the American College of Rheumatology,* 42**,** 710-718.

ALAAEDDINE, N., OLEE, T., HASHIMOTO, S., CREIGHTON-ACHERMANN, L. & LOTZ, M. 2001. Production of the chemokine RANTES by articular chondrocytes and role in cartilage degradation. *Arthritis & Rheumatism: Official Journal of the American College of Rheumatology,* 44**,** 1633-1643.

ALBLOWI, J., TIAN, C., SIQUEIRA, M. F., KAYAL, R. A., MCKENZIE, E., BEHL, Y., GERSTENFELD, L., EINHORN, T. A. & GRAVES, D. T. 2013. Chemokine expression is upregulated in chondrocytes in diabetic fracture healing. *Bone,* 53**,** 294-300.

ALLEN, J. L., COOKE, M. E. & ALLISTON, T. 2012. ECM stiffness primes the TGFβ pathway to promote chondrocyte differentiation. *Molecular biology of the cell,* 23**,** 3731-3742.

ALSALAMEH, S., MOLLENHAUER, J., HAIN, N., STOCK, K. P., KALDEN, J. R. & BURMESTER, G. R. 1990. Cellular immune response toward human articular chondrocytes. T cell reactivities against chondrocyte and fibroblast membranes in

destructive joint diseases. *Arthritis & Rheumatism: Official Journal of the American College of Rheumatology,* 33**,** 1477-1486.

ALTMAN, R., ASCH, E., BLOCH, D., BOLE, G., BORENSTEIN, D., BRANDT, K., CHRISTY, W., COOKE, T. D., GREENWALD, R., HOCHBERG, M. & ET AL. 1986. Development of criteria for the classification and reporting of osteoarthritis. Classification of osteoarthritis of the knee. Diagnostic and Therapeutic Criteria Committee of the American Rheumatism Association. *Arthritis Rheum,* 29**,** 1039-49.

ALVAREZ-GARCIA, O., ROGERS, N. H., SMITH, R. G. & LOTZ, M. K. 2014. Palmitate has proapoptotic and proinflammatory effects on articular cartilage and synergizes with interleukin-1. *Arthritis & Rheumatology,* 66**,** 1779-1788.

AMOS, N., LAUDER, S., EVANS, A., FELDMANN, M. & BONDESON, J. 2006. Adenoviral gene transfer into osteoarthritis synovial cells using the endogenous inhibitor IκBα reveals that most, but not all, inflammatory and destructive mediators are NFκB dependent. *Rheumatology,* 45**,** 1201-1209.

ANDERSON, D. E., MARKWAY, B. D., BOND, D., MCCARTHY, H. E. & JOHNSTONE, B. 2016. Responses to altered oxygen tension are distinct between human stem cells of high and low chondrogenic capacity. *Stem Cell Research & Therapy,* 7**,** 154.

ANDERSON, D. E., MARKWAY, B. D., WEEKES, K. J., MCCARTHY, H. E. & JOHNSTONE, B. 2018. Physioxia promotes the articular chondrocyte-like phenotype in human chondroprogenitor-derived self-organized tissue. *Tissue Engineering Part A,* 24**,** 264-274.

APPARAILLY, F., MILLET, V., NOEL, D., JACQUET, C., SANY, J. & JORGENSEN, C. 2002. Tetracycline-inducible interleukin-10 gene transfer mediated by an adeno-associated virus: application to experimental arthritis. *Hum Gene Ther,* 13**,** 1179-88.

ARDEN, N. & COOPER, C. 2005. *Osteoarthritis handbook*, CRC Press.

ARLAUCKAS, S. P., GARREN, S. B., GARRIS, C. S., KOHLER, R. H., OH, J., PITTET, M. J. & WEISSLEDER, R. 2018. Arg1 expression defines immunosuppressive subsets of tumor-associated macrophages. *Theranostics,* 8**,** 5842.

ARLOV, Ø. & SKJÅK-BRÆK, G. 2017. Sulfated Alginates as Heparin Analogues: A Review of Chemical and Functional Properties. *Molecules (Basel, Switzerland),* 22**,** 778.

ASADULLAH, K., STERRY, W. & VOLK, H. 2003. Interleukin-10 therapy—review of a new approach. *Pharmacological reviews,* 55**,** 241-269.

ASAMI, T., ISHII, M., FUJII, H., NAMKOONG, H., TASAKA, S., MATSUSHITA, K., ISHII, K., YAGI, K., FUJIWARA, H. & FUNATSU, Y. 2013. Modulation of murine macrophage TLR7/8-mediated cytokine expression by mesenchymal stem cell-conditioned medium. *Mediators of inflammation,* 2013.

AUGELLO, A., TASSO, R., NEGRINI, S. M., CANCEDDA, R. & PENNESI, G. 2007. Cell therapy using allogeneic bone marrow mesenchymal stem cells prevents tissue damage in collagen-induced arthritis. *Arthritis & Rheumatism,* 56**,** 1175-1186.

AWAD, H. A., WICKHAM, M. Q., LEDDY, H. A., GIMBLE, J. M. & GUILAK, F. 2004. Chondrogenic differentiation of adipose-derived adult stem cells in agarose, alginate, and gelatin scaffolds. *Biomaterials,* 25**,** 3211-3222.

AYRAL, X., PICKERING, E., WOODWORTH, T., MACKILLOP, N. & DOUGADOS, M. 2005. Synovitis: a potential predictive factor of structural progression of medial tibiofemoral knee osteoarthritis–results of a 1 year longitudinal arthroscopic study in 422 patients. *Osteoarthritis and Cartilage,* 13**,** 361-367.

AYRAL, X., RAVAUD, P., BONVARLET, J. P., SIMONNET, J., LECURIEUX, R., NGUYEN, M., SAUVAGE, E. & DOUGADOS, M. 1999. Arthroscopic evaluation of post-traumatic patellofemoral chondropathy. *J Rheumatol,* 26**,** 1140-7.

BANNURU, R. R., NATOV, N. S., OBADAN, I. E., PRICE, L. L., SCHMID, C. H. & MCALINDON, T. E. 2009. Therapeutic trajectory of hyaluronic acid versus corticosteroids in the treatment of knee osteoarthritis: A systematic review and meta-analysis. *Arthritis Care & Research,* 61**,** 1704-1711.

BAO, J.-P., CHEN, W.-P. & WU, L.-D. 2011. Lubricin: a novel potential biotherapeutic approaches for the treatment of osteoarthritis. *Molecular biology reports,* 38**,** 2879-2885.

BARRY, F. 2019. MSC Therapy for Osteoarthritis: An Unfinished Story. *Journal of Orthopaedic Research®.*

BARRY, F., BOYNTON, R. E., LIU, B. & MURPHY, J. M. 2001. Chondrogenic differentiation of mesenchymal stem cells from bone marrow: differentiation-dependent gene expression of matrix components. *Experimental cell research,* 268**,** 189-200.

BARRY, F. & MURPHY, M. 2013. Mesenchymal stem cells in joint disease and repair. *Nature Reviews Rheumatology,* 9**,** 584.

BARRY, F. P., BOYNTON, R. E., HAYNESWORTH, S., MURPHY, J. M. & ZAIA, J. 1999. The monoclonal antibody SH-2, raised against human mesenchymal stem cells, recognizes an epitope on endoglin (CD105). *Biochemical and Biophysical Research Communications,* 265**,** 134-139.

BARTHOLOMEW, A., PATIL, S., MACKAY, A., NELSON, M., BUYANER, D., HARDY, W., MOSCA, J., STURGEON, C., SIATSKAS, M., MAHMUD, N., FERRER, K., DEANS, R., MOSELEY, A., HOFFMAN, R. & DEVINE, S. M. 2001. Baboon mesenchymal stem cells can be genetically modified to secrete human erythropoietin in vivo. *Hum Gene Ther,* 12**,** 1527-41.

BASU, A., MUNIR, S., MULAW, M. A., SINGH, K., CRISAN, D., SINDRILARU, A., TREIBER, N., WLASCHEK, M., HUBER-LANG, M. & GEBHARD, F. 2018. A novel

S100A8/A9 induced fingerprint of mesenchymal stem cells associated with enhanced wound healing. *Scientific reports,* 8**,** 6205.

BAUGÉ, C., ATTIA, J., LECLERCQ, S., PUJOL, J. P., GALÉRA, P. & BOUMÉDIENE, K. 2008. Interleukin-1β up-regulation of Smad7 via NF-ϰB activation in human chondrocytes. *Arthritis & Rheumatism,* 58**,** 221-226.

BAUGÉ, C., LEGENDRE, F., LECLERCQ, S., ELISSALDE, J., PUJOL, J., GALERA, P. & BOUMEDIENE, K. 2007. Interleukin-1β impairment of transforming growth factor β1 signaling by DOWN-REGULATION of transforming growth factor β receptor type II and up-regulation of Smad7 in human articular chondrocytes. *Arthritis & Rheumatism: Official Journal of the American College of Rheumatology,* 56**,** 3020-3032.

BAUSTIAN, C., HANLEY, S. & CEREDIG, R. 2015. Isolation, selection and culture methods to enhance clonogenicity of mouse bone marrow derived mesenchymal stromal cell precursors. *Stem Cell Res Ther,* 6**,** 151.

BEEKHUIZEN, M., VAN OSCH, G. J., BOT, A. G., HOEKSTRA, M. C., SARIS, D. B., DHERT, W. J. & CREEMERS, L. B. 2013. Inhibition of oncostatin M in osteoarthritic synovial fluid enhances GAG production in osteoarthritic cartilage repair. *Eur Cell Mater,* 26**,** 80-90; discussion 90.

BEHRENDT, P., FELDHEIM, M., PREUSSE-PRANGE, A., WEITKAMP, J., HAAKE, M., EGLIN, D., ROLAUFFS, B., FAY, J., SEEKAMP, A. & GRODZINSKY, A. 2018. Chondrogenic potential of IL-10 in mechanically injured cartilage and cellularized collagen ACI grafts. *Osteoarthritis and cartilage,* 26**,** 264-275.

BEHRENDT, P., PREUSSE-PRANGE, A., KLÜTER, T., HAAKE, M., ROLAUFFS, B., GRODZINSKY, A., LIPPROSS, S. & KURZ, B. 2016. IL-10 reduces apoptosis and extracellular matrix degradation after injurious compression of mature articular cartilage. *Osteoarthritis and cartilage,* 24**,** 1981-1988.

BENITO, M. J., VEALE, D. J., FITZGERALD, O., VAN DEN BERG, W. B. & BRESNIHAN, B. 2005. Synovial tissue inflammation in early and late osteoarthritis. *Ann Rheum Dis,* 64**,** 1263-7.

BERENBAUM, F. 2011. Diabetes-induced osteoarthritis: from a new paradigm to a new phenotype. *Ann Rheum Dis,* 70**,** 1354-6.

BERENBAUM, F. 2013. Osteoarthritis as an inflammatory disease (osteoarthritis is not osteoarthrosis!). *Osteoarthritis Cartilage,* 21**,** 16-21.

BERENBAUM, F., HUMBERT, L., BEREZIAT, G. & THIRION, S. 2003. Concomitant Recruitment of ERK1/2 and p38 MAPK Signalling Pathway Is Required for Activation of Cytoplasmic Phospholipase A2via ATP in Articular Chondrocytes. *Journal of Biological Chemistry,* 278**,** 13680-13687.

BERNARDO, M. E. & FIBBE, W. E. 2013. Mesenchymal stromal cells: sensors and switchers of inflammation. *Cell stem cell,* 13**,** 392-402.

BIANCHI, M. E. 2007. DAMPs, PAMPs and alarmins: all we need to know about danger. *Journal of leukocyte biology,* 81**,** 1-5.

BJÖRK, P., BJÖRK, A., VOGL, T., STENSTRÖM, M., LIBERG, D., OLSSON, A., ROTH, J., IVARS, F. & LEANDERSON, T. 2009. Identification of human S100A9 as a novel target for treatment of autoimmune disease via binding to quinoline-3-carboxamides. *PLoS biology,* 7**,** e1000097.

BLANCO, F. J., GENG, Y. & LOTZ, M. 1995. Differentiation-dependent effects of IL-1 and TGF-beta on human articular chondrocyte proliferation are related to inducible nitric oxide synthase expression. *The Journal of Immunology,* 154**,** 4018-4026.

BLOM, A. B., VAN LENT, P. L., HOLTHUYSEN, A. E., VAN DER KRAAN, P. M., ROTH, J., VAN ROOIJEN, N. & VAN DEN BERG, W. B. 2004. Synovial lining macrophages mediate osteophyte formation during experimental osteoarthritis. *Osteoarthritis and cartilage,* 12**,** 627-635.

BLOM, A. B., VAN LENT, P. L., LIBREGTS, S., HOLTHUYSEN, A. E., VAN DER KRAAN, P. M., VAN ROOIJEN, N. & VAN DEN BERG, W. B. 2007. Crucial role of macrophages in matrix metalloproteinase–mediated cartilage destruction during experimental osteoarthritis: involvement of matrix metalloproteinase 3. *Arthritis & Rheumatism,* 56**,** 147-157.

BOBACZ, K., SUNK, I., HOFSTAETTER, J., AMOYO, L., TOMA, C., AKIRA, S., WEICHHART, T., SAEMANN, M. & SMOLEN, J. 2007. Toll-like receptors and chondrocytes: The lipopolysaccharide-induced decrease in cartilage matrix synthesis is dependent on the presence of toll-like receptor 4 and antagonized by bone morphogenetic protein 7. *Arthritis & Rheumatism,* 56**,** 1880-1893.

BONDESON, J., BLOM, A. B., WAINWRIGHT, S., HUGHES, C., CATERSON, B. & VAN DEN BERG, W. B. 2010. The role of synovial macrophages and macrophage-produced mediators in driving inflammatory and destructive responses in osteoarthritis. *Arthritis & Rheumatism,* 62**,** 647-657.

BONDESON, J., LAUDER, S., WAINWRIGHT, S., AMOS, N., EVANS, A., HUGHES, C., FELDMANN, M. & CATERSON, B. 2007. Adenoviral gene transfer of the endogenous inhibitor IkappaBalpha into human osteoarthritis synovial fibroblasts demonstrates that several matrix metalloproteinases and aggrecanases are nuclear factor-kappaB-dependent. *The Journal of rheumatology,* 34**,** 523-533.

BONDESON, J., WAINWRIGHT, S. D., LAUDER, S., AMOS, N. & HUGHES, C. E. 2006. The role of synovial macrophages and macrophage-produced cytokines in driving aggrecanases, matrix metalloproteinases, and other destructive and inflammatory responses in osteoarthritis. *Arthritis research & therapy,* 8**,** R187.

BONNER JR, W. M., JONSSON JR, H., MALANOS, C. & BRYANT, M. 1975. Changes in the lipids of human articular cartilage with age. *Arthritis & Rheumatism: Official Journal of the American College of Rheumatology,* 18**,** 461-473.

BORZÌ, R. M., MAZZETTI, I., MACOR, S., SILVESTRI, T., BASSI, A., CATTINI, L. & FACCHINI, A. 1999. Flow cytometric analysis of intracellular chemokines in chondrocytes in vivo: constitutive expression and enhancement in osteoarthritis and rheumatoid arthritis. *FEBS letters,* 455**,** 238-242.

BORZI, R. M., MAZZETTI, I., MAGAGNOLI, G., PAOLETTI, S., UGUCCIONI, M., GATTI, R., ORLANDINI, G., CATTINI, L. & FACCHINI, A. 2002. Growth-related oncogene α induction of apoptosis in osteoarthritis chondrocytes. *Arthritis & Rheumatism,* 46**,** 3201-3211.

BOUFFI, C., BONY, C., COURTIES, G., JORGENSEN, C. & NOEL, D. 2010. IL-6-dependent PGE2 secretion by mesenchymal stem cells inhibits local inflammation in experimental arthritis. *PloS one,* 5**,** e14247.

BRESNIHAN, B., FLANAGAN, A. M. & FIRESTEIN, G. S. 2013. Synovium. *Kelley's Textbook of Rheumatology.* Elsevier.

BROEREN, M. G. A., DE VRIES, M., BENNINK, M. B., ARNTZ, O. J., VAN LENT, P. L. E. M., VAN DER KRAAN, P. M., VAN DEN BERG, W. B., VAN DEN HOOGEN, F. H. J., KOENDERS, M. I. & VAN DE LOO, F. A. J. 2016. Suppression of the inflammatory response by disease-inducible interleukin-10 gene therapy in a three-dimensional micromass model of the human synovial membrane. *Arthritis research & therapy,* 18**,** 186-186.

BRUN, J., JONSSON, R. & HAGA, H. 1994. Measurement of plasma calprotectin as an indicator of arthritis and disease activity in patients with inflammatory rheumatic diseases. *The Journal of rheumatology,* 21**,** 733-738.

BUCKWALTER, J. 1990. Articular cartilage; composition, structure, response to injury, and methods of facilating repair. *Articular Cartilage and Knee Joint Function; Basic Science and Arthroscopy***,** 19-56.

BUCKWALTER, J. 1991. Articular cartilage: composition and structure. *Injury and repair of the musculoskeletal soft tissues.*

BUNNELL, B., ESTES, B., GUILAK, F. & GIMBLE, J. 2008. Differentiation of adipose stem cells, Adipose Tissue Protocols. Springer.

BURKE, J., HUNTER, M., KOLHE, R., ISALES, C., HAMRICK, M. & FULZELE, S. 2016. Therapeutic potential of mesenchymal stem cell based therapy for osteoarthritis. *Clinical and translational medicine,* 5**,** 27-27.

BURR, S. P., DAZZI, F. & GARDEN, O. A. 2013. Mesenchymal stromal cells and regulatory T cells: the Yin and Yang of peripheral tolerance? *Immunology and cell biology,* 91**,** 12-18.

CAMINAL, M., FONSECA, C., PERIS, D., MOLL, X., RABANAL, R. M., BARRACHINA, J., CODINA, D., GARCIA, F., CAIRO, J. J., GODIA, F., PLA, A. & VIVES, J. 2014. Use of a chronic model of articular cartilage and meniscal injury for the assessment of long-term effects after autologous mesenchymal stromal cell treatment in sheep. *N Biotechnol,* 31**,** 492-8.

CAMPBELL, L., SAVILLE, C. R., MURRAY, P. J., CRUICKSHANK, S. M. & HARDMAN, M. J. 2013. Local arginase 1 activity is required for cutaneous wound healing. *Journal of Investigative Dermatology,* 133**,** 2461-2470.

CANDELA, M. E., YASUHARA, R., IWAMOTO, M. & ENOMOTO-IWAMOTO, M. 2014. Resident mesenchymal progenitors of articular cartilage. *Matrix Biology,* 39**,** 44-49.

CANTATORE, F., BENAZZO, F., RIBATTI, D., LAPADULA, G., D'AMICO, S., TURSI, A. & PIPITONE, V. 1988. Early alteration of synovial membrane in osteoarthrosis. *Clinical rheumatology,* 7**,** 214-219.

CAO, L., YANG, F., LIU, G., YU, D., LI, H., FAN, Q., GAN, Y., TANG, T. & DAI, K. 2011. The promotion of cartilage defect repair using adenovirus mediated Sox9 gene transfer of rabbit bone marrow mesenchymal stem cells. *Biomaterials,* 32**,** 3910-20.

CAPLAN, A. I. 1991. Mesenchymal stem cells. *J Orthop Res,* 9**,** 641-50.

CAPLAN, A. I. & DENNIS, J. E. 2006a. Mesenchymal stem cells as trophic mediators. *J Cell Biochem,* 98**,** 1076-84.

CAPLAN, A. I. & DENNIS, J. E. 2006b. Mesenchymal stem cells as trophic mediators. *Journal of cellular biochemistry,* 98**,** 1076-1084.

CARMAN, W. J., SOWERS, M., HAWTHORNE, V. M. & WEISSFELD, L. A. 1994. Obesity as a risk factor for osteoarthritis of the hand and wrist: a prospective study. *Am J Epidemiol,* 139**,** 119-29.

CARON, J. P., FERNANDES, J. C., MARTEL-PELLETIER, J., TARDIF, G., MINEAU, F., GENG, C. & PELLETIER, J. P. 1996. Chondroprotective effect of intraarticular injections of interleukin-1 receptor antagonist in experimental osteoarthritis. Suppression of collagenase-1 expression. *Arthritis & Rheumatism: Official Journal of the American College of Rheumatology,* 39**,** 1535-1544.

CHAN, J. K., ROTH, J., OPPENHEIM, J. J., TRACEY, K. J., VOGL, T., FELDMANN, M., HORWOOD, N. & NANCHAHAL, J. 2012. Alarmins: awaiting a clinical response. *The Journal of clinical investigation,* 122**,** 2711-2719.

CHANDRASEKHAR, S., HARVEY, A. K. & HRUBEY, P. S. 1992. Intra-articular administration of interleukin-1 causes prolonged suppression of cartilage proteoglycan synthesis in rats. *Matrix,* 12**,** 1-10.

CHAUFFIER, K., LAIGUILLON, M.-C., BOUGAULT, C., GOSSET, M., PRIAM, S., SALVAT, C., MLADENOVIC, Z., NOURISSAT, G., JACQUES, C. & HOUARD, X.

2012. Induction of the chemokine IL-8/Kc by the articular cartilage: possible influence on osteoarthritis. *Joint Bone Spine,* 79**,** 604-609.

CHEN, H. T., TSOU, H. K., HSU, C. J., TSAI, C. H., KAO, C. H., FONG, Y. C. & TANG, C. H. 2011. Stromal cell-derived factor-1/CXCR4 promotes IL-6 production in human synovial fibroblasts. *Journal of cellular biochemistry,* 112**,** 1219-1227.

CHEN, L.-B., JIANG, X.-B. & YANG, L. 2004. Differentiation of rat marrow mesenchymal stem cells into pancreatic islet beta-cells. *World journal of gastroenterology,* 10**,** 3016-3020.

CHEN, L., LIN, L., WANG, H., WEI, X., FU, X., ZHANG, J. & YU, C. 2008. Suppression of early experimental osteoarthritis by in vivo delivery of the adenoviral vector-mediated NF-κBp65-specific siRNA. *Osteoarthritis and cartilage,* 16**,** 174-184.

CHEN, Y. H., CHUNG, C. C., LIU, Y. C., YEH, S. P., HSU, J. L., HUNG, M. C., SU, H. L. & LI, L. Y. 2016. Enhancer of Zeste Homolog 2 and Histone Deacetylase 9c Regulate Age-Dependent Mesenchymal Stem Cell Differentiation into Osteoblasts and Adipocytes. *Stem Cells,* 34**,** 2183-93.

CHEVALIER, X., EYMARD, F. & RICHETTE, P. 2013. Biologic agents in osteoarthritis: hopes and disappointments. *Nature reviews Rheumatology,* 9**,** 400.

CHIANG, E. R., MA, H. L., WANG, J. P., LIU, C. L., CHEN, T. H. & HUNG, S. C. 2016. Allogeneic Mesenchymal Stem Cells in Combination with Hyaluronic Acid for the Treatment of Osteoarthritis in Rabbits. *PLoS One,* 11**,** e0149835.

CHOI, J. J., YOO, S. A., PARK, S. J., KANG, Y. J., KIM, W. U., OH, I. H. & CHO, C. S. 2008. Mesenchymal stem cells overexpressing interleukin-10 attenuate collagen-induced arthritis in mice. *Clin Exp Immunol,* 153**,** 269-76.

CHUBINSKAYA, S., HUCH, K., SCHULZE, M., OTTEN, L., AYDELOTTE, M. B. & COLE, A. A. 2001. Gene expression by human articular chondrocytes cultured in alginate beads. *Journal of Histochemistry & Cytochemistry,* 49**,** 1211-1219.

CICUTTINI, F. M., BAKER, J. R. & SPECTOR, T. D. 1996. The association of obesity with osteoarthritis of the hand and knee in women: a twin study. *J Rheumatol,* 23**,** 1221-6.

CILLERO-PASTOR, B., MARTIN, M. A., ARENAS, J., LÓPEZ-ARMADA, M. J. & BLANCO, F. J. 2011. Effect of nitric oxide on mitochondrial activity of human synovial cells. *BMC Musculoskeletal Disorders,* 12**,** 42.

CLAVIJO-CORNEJO, D., MARTÍNEZ-FLORES, K., SILVA-LUNA, K., MARTÍNEZ-NAVA, G. A., FERNÁNDEZ-TORRES, J., ZAMUDIO-CUEVAS, Y., GUADALUPE SANTAMARÍA-OLMEDO, M., GRANADOS-MONTIEL, J., PINEDA, C. & LÓPEZ-REYES, A. 2016. The overexpression of NALP3 inflammasome in knee osteoarthritis is associated with synovial membrane prolidase and NADPH oxidase 2. *Oxidative medicine and cellular longevity,* 2016.

COARI, A. I., GIULIO 2000. Usefulness of high resolution US in the evaluation of effusion in osteoarthritic first carpometacarpal joint. *Scandinavian journal of rheumatology,* 29**,** 170-173.

COOKE, T., BENNETT, E. & OHNO, O. 1980. The deposition of immunoglobulins and complement components in osteoarthritic cartilage. *International orthopaedics,* 4**,** 211-217.

COURTIES, A., GUALILLO, O., BERENBAUM, F. & SELLAM, J. 2015. Metabolic stress-induced joint inflammation and osteoarthritis. *Osteoarthritis and cartilage,* 23**,** 1955-1965.

CREMERS, N. A., VAN DEN BOSCH, M. H., VAN DALEN, S., DI CEGLIE, I., ASCONE, G., VAN DE LOO, F., KOENDERS, M., VAN DER KRAAN, P., SLOETJES, A. & VOGL, T. 2017. S100A8/A9 increases the mobilization of pro-inflammatory Ly6C high monocytes to the synovium during experimental osteoarthritis. *Arthritis research & therapy,* 19**,** 217.

CRISAN, M., YAP, S., CASTEILLA, L., CHEN, C.-W., CORSELLI, M., PARK, T. S., ANDRIOLO, G., SUN, B., ZHENG, B. & ZHANG, L. 2008. A perivascular origin for mesenchymal stem cells in multiple human organs. *Cell stem cell,* 3**,** 301-313.

CROP, M. J., BAAN, C. C., KOREVAAR, S. S., IJZERMANS, J. N., PESCATORI, M., STUBBS, A. P., VAN IJCKEN, W. F., DAHLKE, M. H., EGGENHOFER, E., WEIMAR, W. & HOOGDUIJN, M. J. 2010. Inflammatory conditions affect gene expression and function of human adipose tissue-derived mesenchymal stem cells. *Clin Exp Immunol,* 162**,** 474-86.

CUCCHIARINI, M., HENRIONNET, C., MAINARD, D., PINZANO, A. & MADRY, H. 2015. New trends in articular cartilage repair. *Journal of experimental orthopaedics,* 2**,** 8.

CULLEN, S. P., KEARNEY, C. J., CLANCY, D. M. & MARTIN, S. J. 2015. Diverse activators of the NLRP3 inflammasome promote IL-1β secretion by triggering necrosis. *Cell reports,* 11**,** 1535-1548.

CUTLER, A. J., LIMBANI, V., GIRDLESTONE, J. & NAVARRETE, C. V. 2010. Umbilical cord-derived mesenchymal stromal cells modulate monocyte function to suppress T cell proliferation. *The Journal of Immunology,* 185**,** 6617-6623.

D'LIMA, D., HERMIDA, J., HASHIMOTO, S., COLWELL, C. & LOTZ, M. 2006. Caspase inhibitors reduce severity of cartilage lesions in experimental osteoarthritis. *Arthritis & Rheumatism,* 54**,** 1814-1821.

DAGHESTANI, H., MCDANIEL, G., HUEBNER, J., STABLER, T., PIEPER, C., COLEMAN, E. & KRAUS, V. 2013. Soluble macrophage biomarkers are associated with osteoarthritis-related knee inflammation. *Osteoarthritis and Cartilage,* 21**,** S76-S77.

DAI, S., SHAN, Z., NISHIOKA, K. & YUDOH, K. 2005. Implication of interleukin 18 in production of matrix metalloproteinases in articular chondrocytes in arthritis: direct effect on chondrocytes may not be pivotal. *Annals of the rheumatic diseases,* 64**,** 735-742.

DAS, R., JAHR, H., VERHAAR, J., VAN DER LINDEN, J., VAN OSCH, G. & WEINANS, H. 2008. In vitro expansion affects the response of chondrocytes to mechanical stimulation. *Osteoarthritis and cartilage,* 16**,** 385-391.

DE CROMBRUGGHE, B., LEFEBVRE, V., BEHRINGER, R. R., BI, W., MURAKAMI, S. & HUANG, W. 2000. Transcriptional mechanisms of chondrocyte differentiation. *Matrix Biology,* 19**,** 389-394.

DE HOOGE, A. S., VAN DE LOO, F. A., BENNINK, M. B., ARNTZ, O. J., DE HOOGE, P. & VAN DEN BERG, W. B. 2005. Male IL-6 gene knock out mice developed more advanced osteoarthritis upon aging. *Osteoarthritis and cartilage,* 13**,** 66-73.

DE LANGE-BROKAAR, B. J., IOAN-FACSINAY, A., VAN OSCH, G. J., ZUURMOND, A.-M., SCHOONES, J., TOES, R. E., HUIZINGA, T. W. & KLOPPENBURG, M. 2012. Synovial inflammation, immune cells and their cytokines in osteoarthritis: a review. *Osteoarthritis and cartilage,* 20**,** 1484-1499.

DE ROOSTER, H., COX, E. & BREE, H. V. 2000. Prevalence and relevance of antibodies to type-I and-II collagen in synovial fluid of dogs with cranial cruciate ligament damage. *American journal of veterinary research,* 61**,** 1456-1461.

DE VRIES–VAN MELLE, M. L., NARCISI, R., KOPS, N., KOEVOET, W. J., BOS, P. K., MURPHY, J. M., VERHAAR, J. A., VAN DER KRAAN, P. M. & VAN OSCH, G. J. 2013. Chondrogenesis of mesenchymal stem cells in an osteochondral environment is mediated by the subchondral bone. *Tissue Engineering Part A,* 20**,** 23-33.

DE WAAL MALEFYT, R., ABRAMS, J., BENNETT, B., FIGDOR, C. G. & DE VRIES, J. E. 1991a. Interleukin 10 (IL-10) inhibits cytokine synthesis by human monocytes: an autoregulatory role of IL-10 produced by monocytes. *Journal of Experimental Medicine,* 174**,** 1209-1220.

DE WAAL MALEFYT, R., HAANEN, J., SPITS, H., RONCAROLO, M.-G., TE VELDE, A., FIGDOR, C., JOHNSON, K., KASTELEIN, R., YSSEL, H. & DE VRIES, J. 1991b. Interleukin 10 (IL-10) and viral IL-10 strongly reduce antigen-specific human T cell proliferation by diminishing the antigen-presenting capacity of monocytes via downregulation of class II major histocompatibility complex expression. *Journal of Experimental Medicine,* 174**,** 915-924.

DEBNATH, T., SHALINI, U., KONA, L., VIDYA SAGAR, J., KAMARAJU, S. & GADDAM, S. 2015. Development of 3D alginate encapsulation for better chondrogenic differentiation potential than the 2D pellet system. *J Stem Cell Res Ther,* 5**,** 276.

DEN HOLLANDER, W., RAMOS, Y. F., BOMER, N., ELZINGA, S., VAN DER BREGGEN, R., LAKENBERG, N., DE DIJCKER, W. J., SUCHIMAN, H. E., DUIJNISVELD, B. J., HOUWING-DUISTERMAAT, J. J., SLAGBOOM, P. E., BOS,

S. D., NELISSEN, R. G. & MEULENBELT, I. 2015. Transcriptional associations of osteoarthritis-mediated loss of epigenetic control in articular cartilage. *Arthritis Rheumatol,* 67**,** 2108-16.

DENOBLE, A. E., HUFFMAN, K. M., STABLER, T. V., KELLY, S. J., HERSHFIELD, M. S., MCDANIEL, G. E., COLEMAN, R. E. & KRAUS, V. B. 2011. Uric acid is a danger signal of increasing risk for osteoarthritis through inflammasome activation. *Proceedings of the National Academy of Sciences,* 108**,** 2088-2093.

DESANDO, G., CAVALLO, C., SARTONI, F., MARTINI, L., PARRILLI, A., VERONESI, F., FINI, M., GIARDINO, R., FACCHINI, A. & GRIGOLO, B. 2013. Intra-articular delivery of adipose derived stromal cells attenuates osteoarthritis progression in an experimental rabbit model. *Arthritis research & therapy,* 15**,** R22.

DI NICOLA, M., CARLO-STELLA, C., MAGNI, M., MILANESI, M., LONGONI, P. D., MATTEUCCI, P., GRISANTI, S. & GIANNI, A. M. 2002. Human bone marrow stromal cells suppress T-lymphocyte proliferation induced by cellular or nonspecific mitogenic stimuli. *Blood, The Journal of the American Society of Hematology,* 99**,** 3838-3843.

DIDUCH, D. R., JORDAN, L. C., MIERISCH, C. M. & BALIAN, G. 2000. Marrow stromal cells embedded in alginate for repair of osteochondral defects. *Arthroscopy: The Journal of Arthroscopic & Related Surgery,* 16**,** 571-577.

DIEKMAN, B. O., WU, C. L., LOUER, C. R., FURMAN, B. D., HUEBNER, J. L., KRAUS, V. B., OLSON, S. A. & GUILAK, F. 2013. Intra-articular delivery of purified mesenchymal stem cells from C57BL/6 or MRL/MpJ superhealer mice prevents posttraumatic arthritis. *Cell Transplant,* 22**,** 1395-408.

DINARELLO, C. A. 1998. Interleukin-1β, Interleukin-18, and the Interleukin-1β Converting Enzyme a. *Annals of the New York Academy of Sciences,* 856**,** 1-11.

DINGLE, J., SAKLATVALA, J., HEMBRY, R., TYLER, J., FELL, H. & JUBB, R. 1979. A cartilage catabolic factor from synovium. *Biochemical Journal,* 184**,** 177-180.

DINGLE, J. T. 1981. Catabolin--a cartilage catabolic factor from synovium. *Clinical orthopaedics and related research***,** 219-231.

DOMINICI, M., LE BLANC, K., MUELLER, I., SLAPER-CORTENBACH, I., MARINI, F., KRAUSE, D., DEANS, R., KEATING, A., PROCKOP, D. & HORWITZ, E. 2006. Minimal criteria for defining multipotent mesenchymal stromal cells. The International Society for Cellular Therapy position statement. *Cytotherapy,* 8**,** 315-7.

DONATO, R. 2013. R Cannon B, Sorci G, Riuzzi F, Hsu K, J Weber D, et al. Functions of S100 proteins. *Curr Mol Med,* 13**,** 24-57.

DOUGADOS, M. 1996. Synovial fluid cell analysis. *Bailliere's clinical rheumatology,* 10**,** 519-534.

DOWTHWAITE, G. P., BISHOP, J. C., REDMAN, S. N., KHAN, I. M., ROONEY, P., EVANS, D. J., HAUGHTON, L., BAYRAM, Z., BOYER, S. & THOMSON, B. 2004. The surface of articular cartilage contains a progenitor cell population. *Journal of cell science,* 117**,** 889-897.

DRAZAN, K. E., WU, L., BULLINGTON, D. & SHAKED, A. 1996. Viral IL-10 gene therapy inhibits TNF-alpha and IL-1 beta, not IL-6, in the newborn endotoxemic mouse. *J Pediatr Surg,* 31**,** 411-4.

DREIER, R., GRÄSSEL, S., FUCHS, S., SCHAUMBURGER, J. & BRUCKNER, P. 2004. Pro-MMP-9 is a specific macrophage product and is activated by osteoarthritic chondrocytes via MMP-3 or a MT1-MMP/MMP-13 cascade. *Experimental cell research,* 297**,** 303-312.

DUDA, G. N., EILERS, M., LOH, L., HOFFMAN, J. E., KÄÄB, M. & SCHASER, K. 2001. Chondrocyte death precedes structural damage in blunt impact trauma. *Clinical Orthopaedics and Related Research®,* 393**,** 302-309.

DUIJVESTEIN, M., WILDENBERG, M. E., WELLING, M. M., HENNINK, S., MOLENDIJK, I., VAN ZUYLEN, V. L., BOSSE, T., VOS, A. C., DE JONGE-MULLER, E. S., ROELOFS, H., VAN DER WEERD, L., VERSPAGET, H. W., FIBBE, W. E., TE VELDE, A. A., VAN DEN BRINK, G. R. & HOMMES, D. W. 2011. Pretreatment with interferon-gamma enhances the therapeutic activity of mesenchymal stromal cells in animal models of colitis. *Stem Cells,* 29**,** 1549-58.

EEKB, W. Y. & SIQUAN ŽEF, L. 2001. Direct protective effect of interleukin-10 on articular chondrocytes in vitro. *Chinese medical journal,* 114**,** 723-725.

EGGENHOFER, E. & HOOGDUIJN, M. J. 2012. Mesenchymal stem cell-educated macrophages. *Transplantation research,* 1**,** 12.

EHRHARDT, A., XU, H. & KAY, M. A. 2003. Episomal persistence of recombinant adenoviral vector genomes during the cell cycle in vivo. *Journal of virology,* 77**,** 7689-7695.

EL-AZIZ FARAG, A. M., EL-GAZZAR, N., EL HAWA, M. & ATTIA, M. 2017. Study of interleukin 33 in rheumatoid arthritis versus osteoarthritis patients. *Egyptian Rheumatology and Rehabilitation,* 44**,** 159-163.

EMADEDIN, M., FAZELI, R. & FARJAD, R. 2012. Intra-articular injection of autologous mesenchymal stem cells in six patients with knee osteoarthritis. *Archives of Iranian medicine,* 15**,** 422.

ENDRES, M., ANDREAS, K., KALWITZ, G., FREYMANN, U., NEUMANN, K., RINGE, J., SITTINGER, M., HÄUPL, T. & KAPS, C. 2010. Chemokine profile of synovial fluid from normal, osteoarthritis and rheumatoid arthritis patients: CCL25, CXCL10 and XCL1 recruit human subchondral mesenchymal progenitor cells. *Osteoarthritis and cartilage,* 18**,** 1458-1466.

ENGLISH, K. 2013. Mechanisms of mesenchymal stromal cell immunomodulation. *Immunology and cell biology,* 91**,** 19-26.

ENGLISH, K., FRENCH, A. & WOOD, K. J. 2010. Mesenchymal stromal cells: facilitators of successful transplantation? *Cell Stem Cell,* 7**,** 431-42.

ENGLISH, K., RYAN, J., TOBIN, L., MURPHY, M., BARRY, F. & MAHON, B. P. 2009. Cell contact, prostaglandin E2 and transforming growth factor beta 1 play non-redundant roles in human mesenchymal stem cell induction of CD4+ CD25Highforkhead box P3+ regulatory T cells. *Clinical & Experimental Immunology,* 156**,** 149-160.

EVANS, J. G., CHAVEZ-RUEDA, K. A., EDDAOUDI, A., MEYER-BAHLBURG, A., RAWLINGS, D. J., EHRENSTEIN, M. R. & MAURI, C. 2007. Novel suppressive function of transitional 2 B cells in experimental arthritis. *The Journal of Immunology,* 178**,** 7868-7878.

FAHY, N., DE VRIES-VAN MELLE, M., LEHMANN, J., WEI, W., GROTENHUIS, N., FARRELL, E., VAN DER KRAAN, P., MURPHY, J., BASTIAANSEN-JENNISKENS, Y. & VAN OSCH, G. 2014. Human osteoarthritic synovium impacts chondrogenic differentiation of mesenchymal stem cells via macrophage polarisation state. *Osteoarthritis and cartilage,* 22**,** 1167-1175.

FARRELL, E., BOTH, S. K., ODÖRFER, K. I., KOEVOET, W., KOPS, N., O'BRIEN, F. J., DE JONG, R. J. B., VERHAAR, J. A., CUIJPERS, V. & JANSEN, J. 2011. In-vivo generation of bone via endochondral ossification by in-vitro chondrogenic priming of adult human and rat mesenchymal stem cells. *BMC musculoskeletal disorders,* 12**,** 31.

FARRELL, E., FAHY, N., RYAN, A. E., FLATHARTA, C. O., O'FLYNN, L., RITTER, T. & MURPHY, J. M. 2016. vIL-10-overexpressing human MSCs modulate naïve and activated T lymphocytes following induction of collagenase-induced osteoarthritis. *Stem cell research & therapy,* 7**,** 74.

FARRELL, E., VAN DER JAGT, O. P., KOEVOET, W., KOPS, N., VAN MANEN, C. J., HELLINGMAN, C. A., JAHR, H., O'BRIEN, F. J., VERHAAR, J. A. & WEINANS, H. 2008. Chondrogenic priming of human bone marrow stromal cells: a better route to bone repair? *Tissue Engineering Part C: Methods,* 15**,** 285-295.

FASSL, S. K., AUSTERMANN, J., PAPANTONOPOULOU, O., RIEMENSCHNEIDER, M., XUE, J., BERTHELOOT, D., FREISE, N., SPIEKERMANN, C., WITTEN, A. & VIEMANN, D. 2015. Transcriptome assessment reveals a dominant role for TLR4 in the activation of human monocytes by the alarmin MRP8. *The Journal of Immunology,* 194**,** 575-583.

FAVERO, M., RAMONDA, R., GOLDRING, M. B., GOLDRING, S. R. & PUNZI, L. 2015. Early knee osteoarthritis. *RMD open,* 1**,** e000062.

FELSON, D. T., ANDERSON, J. J., NAIMARK, A., WALKER, A. M. & MEENAN, R. F. 1988. Obesity and knee osteoarthritis. The Framingham Study. *Ann Intern Med,* 109**,** 18-24.

FELSON, D. T., LAWRENCE, R. C., DIEPPE, P. A., HIRSCH, R., HELMICK, C. G., JORDAN, J. M., KINGTON, R. S., LANE, N. E., NEVITT, M. C., ZHANG, Y., SOWERS, M., MCALINDON, T., SPECTOR, T. D., POOLE, A. R., YANOVSKI, S. Z., ATESHIAN, G., SHARMA, L., BUCKWALTER, J. A., BRANDT, K. D. & FRIES, J. F. 2000. Osteoarthritis: new insights. Part 1: the disease and its risk factors. *Ann Intern Med,* 133**,** 635-46.

FELSON, D. T., MCLAUGHLIN, S., GOGGINS, J., LAVALLEY, M. P., GALE, M. E., TOTTERMAN, S., LI, W., HILL, C. & GALE, D. 2003. Bone marrow edema and its relation to progression of knee osteoarthritis. *Ann Intern Med,* 139**,** 330-6.

FERNANDES, A. M., HERLOFSEN, S. R., KARLSEN, T. A., KUCHLER, A. M., FLOISAND, Y. & BRINCHMANN, J. E. 2013. Similar properties of chondrocytes from osteoarthritis joints and mesenchymal stem cells from healthy donors for tissue engineering of articular cartilage. *PLoS One,* 8**,** e62994.

FERNANDES, J., TARDIF, G., MARTEL-PELLETIER, J., LASCAU-COMAN, V., DUPUIS, M., MOLDOVAN, F., SHEPPARD, M., KRISHNAN, B. R. & PELLETIER, J.-P. 1999. In vivo transfer of interleukin-1 receptor antagonist gene in osteoarthritic rabbit knee joints: prevention of osteoarthritis progression. *The American journal of pathology,* 154**,** 1159-1169.

FERNANDES, J. C., MARTEL-PELLETIER, J. & PELLETIER, J. P. 2002. The role of cytokines in osteoarthritis pathophysiology. *Biorheology,* 39**,** 237-246.

FICKERT, S., FIEDLER, J. & BRENNER, R. E. 2004. Identification of subpopulations with characteristics of mesenchymal progenitor cells from human osteoarthritic cartilage using triple staining for cell surface markers. *Arthritis Res Ther,* 6**,** R422-32.

FIORENTINO, D. F., BOND, M. W. & MOSMANN, T. R. 1989. Two types of mouse T helper cell. IV. Th2 clones secrete a factor that inhibits cytokine production by Th1 clones. *J Exp Med,* 170**,** 2081-95.

FOELL, D., WITTKOWSKI, H. & ROTH, J. 2007. Mechanisms of disease: a'DAMP'view of inflammatory arthritis. *Nature Reviews Rheumatology,* 3**,** 382.

FRAGONAS, E., VALENTE, M., POZZI-MUCELLI, M., TOFFANIN, R., RIZZO, R., SILVESTRI, F. & VITTUR, F. 2000. Articular cartilage repair in rabbits by using suspensions of allogenic chondrocytes in alginate. *Biomaterials,* 21**,** 795-801.

FRANCHI, L., EIGENBROD, T., MUÑOZ-PLANILLO, R. & NUÑEZ, G. 2009. The inflammasome: a caspase-1-activation platform that regulates immune responses and disease pathogenesis. *Nature immunology,* 10**,** 241.

FRANCHI, L., KANNEGANTI, T.-D., DUBYAK, G. R. & NÚÑEZ, G. 2007. Differential requirement of P2X7 receptor and intracellular K+ for caspase-1 activation induced by intracellular and extracellular bacteria. *Journal of Biological Chemistry,* 282**,** 18810-18818.

FRANÇOIS, M., ROMIEU-MOUREZ, R., LI, M. & GALIPEAU, J. 2012. Human MSC suppression correlates with cytokine induction of indoleamine 2, 3-dioxygenase and bystander M2 macrophage differentiation. *Molecular Therapy,* 20**,** 187-195.

FRIEDENSTEIN, A. J., CHAILAKHJAN, R. K. & LALYKINA, K. S. 1970. The development of fibroblast colonies in monolayer cultures of guinea-pig bone marrow and spleen cells. *Cell Tissue Kinet,* 3**,** 393-403.

FRIEDENSTEIN, A. J., PIATETZKY, S., II & PETRAKOVA, K. V. 1966. Osteogenesis in transplants of bone marrow cells. *J Embryol Exp Morphol,* 16**,** 381-90.

FURMAN, B. D., KIMMERLING, K. A., ZURA, R. D., REILLY, R. M., ZLOWODZKI, M. P., HUEBNER, J. L., KRAUS, V. B., GUILAK, F. & OLSON, S. A. 2015. Brief report: articular ankle fracture results in increased synovitis, synovial macrophage infiltration, and synovial fluid concentrations of inflammatory cytokines and chemokines. *Arthritis & Rheumatology,* 67**,** 1234-1239.

GABAY, C. 2006. Interleukin-6 and chronic inflammation. *Arthritis research & therapy,* 8**,** S3.

GARCIA-CALVO, M., PETERSON, E. P., LEITING, B., RUEL, R., NICHOLSON, D. W. & THORNBERRY, N. A. 1998. Inhibition of human caspases by peptide-based and macromolecular inhibitors. *Journal of Biological Chemistry,* 273**,** 32608-32613.

GERTER, R., KRUEGEL, J. & MIOSGE, N. 2012. New insights into cartilage repair—the role of migratory progenitor cells in osteoarthritis. *Matrix Biology,* 31**,** 206-213.

GHONIEM, A. A., ACIL, Y., WILTFANG, J. & GIERLOFF, M. 2015. Improved adipogenic in vitro differentiation: comparison of different adipogenic cell culture media on human fat and bone stroma cells for fat tissue engineering. *Anat Cell Biol,* 48**,** 85-94.

GILBERT, S. J., SINGHRAO, S. K., KHAN, I. M., GONZALEZ, L. G., THOMSON, B. M., BURDON, D., DUANCE, V. C. & ARCHER, C. W. 2009. Enhanced tissue integration during cartilage repair in vitro can be achieved by inhibiting chondrocyte death at the wound edge. *Tissue Engineering Part A,* 15**,** 1739-1749.

GLASS, K. A., LINK, J. M., BRUNGER, J. M., MOUTOS, F. T., GERSBACH, C. A. & GUILAK, F. 2014. Tissue-engineered cartilage with inducible and tunable immunomodulatory properties. *Biomaterials,* 35**,** 5921-31.

GO, N. F., CASTLE, B. E., BARRETT, R., KASTELEIN, R., DANG, W., MOSMANN, T. R., MOORE, K. W. & HOWARD, M. 1990. Interleukin 10, a novel B cell stimulatory factor: unresponsiveness of X chromosome-linked immunodeficiency B cells. *J Exp Med,* 172**,** 1625-31.

GOLDRING, M., OTERO, M., TSUCHIMOCHI, K., IJIRI, K. & LI, Y. 2008. Defining the roles of inflammatory and anabolic cytokines in cartilage metabolism. *Annals of the rheumatic diseases,* 67**,** iii75-iii82.

GOLDRING, M. B. 2000. The role of the chondrocyte in osteoarthritis. *Arthritis Rheum,* 43**,** 1916-26.

GOLDRING, M. B. 2012. Articular cartilage degradation in osteoarthritis. *HSS journal,* 8**,** 7-9.

GOLDRING, M. B., FUKUO, K., BIRKHEAD, J. R., DUDEK, E. & SANDELL, L. J. 1994. Transcriptional suppression by interleukin-1 and interferon-γ of type II collagen gene expression in human chondrocytes. *Journal of cellular biochemistry,* 54**,** 85-99.

GOLDRING, M. B. & OTERO, M. 2011. Inflammation in osteoarthritis. *Current opinion in rheumatology,* 23**,** 471-478.

GOLDRING, M. B., OTERO, M., PLUMB, D. A., DRAGOMIR, C., FAVERO, M., EL HACHEM, K., HASHIMOTO, K., ROACH, H. I., OLIVOTTO, E., BORZI, R. M. & MARCU, K. B. 2011. Roles of inflammatory and anabolic cytokines in cartilage metabolism: signals and multiple effectors converge upon MMP-13 regulation in osteoarthritis. *Eur Cell Mater,* 21**,** 202-20.

GORDON, G., VILLANUEVA, T., SCHUMACHER, H. & GOHEL, V. 1984. Autopsy study correlating degree of osteoarthritis, synovitis and evidence of articular calcification. *The Journal of rheumatology,* 11**,** 681-686.

GORE, M., TAI, K.-S., SADOSKY, A., LESLIE, D. & STACEY, B. R. 2011. Clinical comorbidities, treatment patterns, and direct medical costs of patients with osteoarthritis in usual care: a retrospective claims database analysis. *Journal of Medical Economics,* 14**,** 497-507.

GOSSEN, M. & BUJARD, H. 1992. Tight control of gene expression in mammalian cells by tetracycline-responsive promoters. *Proc Natl Acad Sci U S A,* 89**,** 5547-51.

GRAHAM, F. L., SMILEY, J., RUSSELL, W. C. & NAIRN, R. 1977. Characteristics of a human cell line transformed by DNA from human adenovirus type 5. *J Gen Virol,* 36**,** 59-74.

GRAYSON, C. W. & DECKER, R. C. 2012. Total joint arthroplasty for persons with osteoarthritis. *PM&R,* 4**,** S97-S103.

GREENHILL, C. J., JONES, G. W., NOWELL, M. A., NEWTON, Z., HARVEY, A. K., MOIDEEN, A. N., COLLINS, F. L., BLOOM, A. C., COLL, R. C. & ROBERTSON, A. A. 2014. Interleukin-10 regulates the inflammasome-driven augmentation of inflammatory arthritis and joint destruction. *Arthritis research & therapy,* 16**,** 419.

GUERNE, P.-A., ZURAW, B. L., VAUGHAN, J. H., CARSON, D. A. & LOTZ, M. 1989. Synovium as a source of interleukin 6 in vitro. Contribution to local and systemic manifestations of arthritis. *The Journal of clinical investigation,* 83**,** 585-592.

GUERNE, P., CARSON, D. & LOTZ, M. 1990. IL-6 production by human articular chondrocytes. Modulation of its synthesis by cytokines, growth factors, and hormones in vitro. *The Journal of Immunology,* 144**,** 499-505.

GURUNG, P., LI, B., MALIREDDI, R. S., LAMKANFI, M., GEIGER, T. L. & KANNEGANTI, T.-D. 2015. Chronic TLR stimulation controls NLRP3 inflammasome activation through IL-10 mediated regulation of NLRP3 expression and caspase-8 activation. *Scientific reports,* 5**,** 14488.

HAJISHENGALLIS, G. & LAMBRIS, J. D. 2011. Microbial manipulation of receptor crosstalk in innate immunity. *Nature Reviews Immunology,* 11**,** 187.

HALPER, J. & KJAER, M. 2014. Basic components of connective tissues and extracellular matrix: elastin, fibrillin, fibulins, fibrinogen, fibronectin, laminin, tenascins and thrombospondins. *Progress in Heritable Soft Connective Tissue Diseases*. Springer.

HAN, X., KITAMOTO, S., WANG, H. & BOISVERT, W. A. 2010. Interleukin-10 overexpression in macrophages suppresses atherosclerosis in hyperlipidemic mice. *Faseb j,* 24**,** 2869-80.

HARRELL, C. R., MARKOVIC, B. S., FELLABAUM, C., ARSENIJEVIC, A. & VOLAREVIC, V. 2019. Mesenchymal stem cell-based therapy of osteoarthritis: Current knowledge and future perspectives. *Biomed Pharmacother,* 109**,** 2318-2326.

HARRINGTON, K., ALVAREZ-VALLINA, L., CRITTENDEN, M., GOUGH, M., CHONG, H., DIAZ, R. M., VASSAUX, G., LEMOINE, N. & VILE, R. 2002. Cells as vehicles for cancer gene therapy: the missing link between targeted vectors and systemic delivery? *Hum Gene Ther,* 13**,** 1263-80.

HASEEB, A. & HAQQI, T. M. 2013. Immunopathogenesis of osteoarthritis. *Clinical immunology,* 146**,** 185-196.

HATSUSHIKA, D., MUNETA, T., HORIE, M., KOGA, H., TSUJI, K. & SEKIYA, I. 2013. Intraarticular injection of synovial stem cells promotes meniscal regeneration in a rabbit massive meniscal defect model. *Journal of Orthopaedic Research,* 31**,** 1354-1359.

HAUSELMANN, H., FERNANDES, R. J., MOK, S. S., SCHMID, T. M., BLOCK, J. A., AYDELOTTE, M. B., KUETTNER, K. E. & THONAR, E. 1994. Phenotypic stability of bovine articular chondrocytes after long-term culture in alginate beads. *Journal of cell science,* 107**,** 17-27.

HAUSELMANN, H. J., MASUDA, K., HUNZIKER, E. B., NEIDHART, M., MOK, S., MICHEL, B. A. & THONAR, E. 1996. Adult human chondrocytes cultured in alginate form a matrix similar to native human articular cartilage. *American Journal of Physiology-Cell Physiology,* 271**,** C742-C752.

HAYES, A., MACPHERSON, S., MORRISON, H., DOWTHWAITE, G. & ARCHER, C. 2001. The development of articular cartilage: evidence for an appositional growth mechanism. *Anatomy and embryology,* 203**,** 469-479.

HAYES, M. M., LANE, B. R., KING, S. R., MARKOVITZ, D. M. & COFFEY, M. J. 2002. Prostaglandin E2 inhibits replication of HIV-1 in macrophages through activation of protein kinase A. *Cellular immunology,* 215**,** 61-71.

HAYNES, M. K., HUME, E. L. & SMITH, J. B. 2002. Phenotypic characterization of inflammatory cells from osteoarthritic synovium and synovial fluids. *Clinical Immunology,* 105**,** 315-325.

HEINEGÅRD, D., LORENZO, P. & SAXNE, T. 2006. CHAPTER 4 - Noncollagenous Proteins; Glycoproteins and Related Proteins A2 - SEIBEL, MARKUS J. *In:* ROBINS, S. P. & BILEZIKIAN, J. P. (eds.) *Dynamics of Bone and Cartilage Metabolism (Second Edition).* Burlington: Academic Press.

HELDENS, G. T., BLANEY DAVIDSON, E. N., VITTERS, E. L., SCHREURS, B. W., PIEK, E., VAN DEN BERG, W. B. & VAN DER KRAAN, P. M. 2012. Catabolic factors and osteoarthritis-conditioned medium inhibit chondrogenesis of human mesenchymal stem cells. *Tissue Eng Part A,* 18**,** 45-54.

HELLINGMAN, C. A., KOEVOET, W. & VAN OSCH, G. J. 2012. Can one generate stable hyaline cartilage from adult mesenchymal stem cells? A developmental approach. *J Tissue Eng Regen Med,* 6**,** e1-e11.

HENROTIN, Y. E., DE GROOTE, D. D., LABASSE, A. H., GASPAR, S. E., ZHENG, S.-X., GEENEN, V. G. & REGINSTER, J.-Y. L. 1996. Effects of exogenous IL-1β, TNFα, IL-6, IL-8 and LIF on cytokine production by human articular chondrocytes. *Osteoarthritis and Cartilage,* 4**,** 163-173.

HILFIKER, A., KASPER, C., HASS, R. & HAVERICH, A. 2011. Mesenchymal stem cells and progenitor cells in connective tissue engineering and regenerative medicine: is there a future for transplantation? *Langenbeck's Archives of Surgery,* 396**,** 489-497.

HILLIQUIN, P., BORDERIE, D., HERNVANN, A., MENKES, C. & EKINDJIAN, O. 1997. Nitric oxide as S-nitrosoproteins in rheumatoid arthritis. *Arthritis & Rheumatism: Official Journal of the American College of Rheumatology,* 40**,** 1512-1517.

HÖLSCHER, C., KÖHLER, G., MÜLLER, U., MOSSMANN, H., SCHAUB, G. A. & BROMBACHER, F. 1998. Defective nitric oxide effector functions lead to extreme susceptibility of Trypanosoma cruzi-infected mice deficient in gamma interferon receptor or inducible nitric oxide synthase. *Infection and immunity,* 66**,** 1208-1215.

HOULIHAN, D. D., MABUCHI, Y., MORIKAWA, S., NIIBE, K., ARAKI, D., SUZUKI, S., OKANO, H. & MATSUZAKI, Y. 2012. Isolation of mouse mesenchymal stem cells on the basis of expression of Sca-1 and PDGFR-alpha. *Nat Protoc,* 7**,** 2103-11.

HSIEH, J.-L., SHIAU, A.-L., LEE, C.-H., YANG, S.-J., LEE, B.-O., JOU, I., WU, C.-L., CHEN, S.-H. & SHEN, P.-C. 2013. CD8+ T cell-induced expression of tissue inhibitor of metalloproteinses-1 exacerbated osteoarthritis. *International journal of molecular sciences,* 14**,** 19951-19970.

HSU, D. H., DE WAAL MALEFYT, R., FIORENTINO, D. F., DANG, M. N., VIEIRA, P., DE VRIES, J., SPITS, H., MOSMANN, T. R. & MOORE, K. W. 1990. Expression of interleukin-10 activity by Epstein-Barr virus protein BCRF1. *Science,* 250**,** 830-2.

HU, Y., LOU, B., WU, X., WU, R., WANG, H., GAO, L., PI, J. & XU, Y. 2018a. Comparative study on in vitro culture of mouse bone marrow mesenchymal stem cells. *Stem cells international,* 2018.

HU, Y., LOU, B., WU, X., WU, R., WANG, H., GAO, L., PI, J. & XU, Y. 2018b. Comparative Study on In Vitro Culture of Mouse Bone Marrow Mesenchymal Stem Cells. *Stem cells international,* 2018**,** 6704583-6704583.

HUNG, S.-C., POCHAMPALLY, R. R., HSU, S.-C., SANCHEZ, C., CHEN, S.-C., SPEES, J. & PROCKOP, D. J. 2007. Short-term exposure of multipotent stromal cells to low oxygen increases their expression of CX3CR1 and CXCR4 and their engraftment in vivo. *PloS one,* 2**,** e416-e416.

HUNG, S. C., LU, C. Y., SHYUE, S. K., LIU, H. C. & HO, L. L. 2004. Lineage differentiation-associated loss of adenoviral susceptibility and Coxsackie-adenovirus receptor expression in human mesenchymal stem cells. *Stem Cells,* 22**,** 1321-9.

HUNZIKER, E. B. & ROSENBERG, L. C. 1996. Repair of partial-thickness defects in articular cartilage: cell recruitment from the synovial membrane. *JBJS,* 78**,** 721-33.

HUSS, R. S., HUDDLESTON, J. I., GOODMAN, S. B., BUTCHER, E. C. & ZABEL, B. A. 2010. Synovial tissue–infiltrating natural killer cells in osteoarthritis and periprosthetic inflammation. *Arthritis & Rheumatism,* 62**,** 3799-3805.

HWANG, N. S., VARGHESE, S. & ELISSEEFF, J. 2007. Cartilage tissue engineering. *Stem cell assays.* Springer.

IANNONE, F., DE BARI, C., DELL ACCIO, F., COVELLI, M., CANTATORE, F. P., PATELLA, V., BIANCO, G. L. & LAPADULA, G. 2001. Interleukin-10 and interleukin-10 receptor in human osteoarthritic and healthy chondrocytes. *Clinical and experimental rheumatology,* 19**,** 139-146.

IBARRA, C., KOSKI, J. A. & WARREN, R. F. 2000. Tissue engineering meniscus: cells and matrix. *The Orthopedic clinics of North America,* 31**,** 411-418.

IIJIMA, H., ISHO, T., KUROKI, H., TAKAHASHI, M. & AOYAMA, T. 2018. Effectiveness of mesenchymal stem cells for treating patients with knee osteoarthritis: a meta-analysis toward the establishment of effective regenerative rehabilitation. *npj Regenerative Medicine,* 3**,** 15.

INOUE, H., TAKAMORI, M., NAGATA, N., NISHIKAWA, T., ODA, H., YAMAMOTO, S. & KOSHIHARA, Y. 2001. An investigation of cell proliferation and soluble mediators induced by interleukin 1β in human synovial fibroblasts: comparative response in osteoarthritis and rheumatoid arthritis. *Inflammation Research,* 50**,** 65-72.

INOUE, H., TAKAMORI, M., SHIMOYAMA, Y., ISHIBASHI, H., YAMAMOTO, S. & KOSHIHARA, Y. 2002. Regulation by PGE2 of the production of interleukin-6, macrophage colony stimulating factor, and vascular endothelial growth factor in human synovial fibroblasts. *British journal of pharmacology,* 136**,** 287-295.

IP, W. E., HOSHI, N., SHOUVAL, D. S., SNAPPER, S. & MEDZHITOV, R. 2017. Anti-inflammatory effect of IL-10 mediated by metabolic reprogramming of macrophages. *Science,* 356**,** 513-519.

ISHII, H., TANAKA, H., KATOH, K., NAKAMURA, H., NAGASHIMA, M. & YOSHINO, S. 2002. Characterization of infiltrating T cells and Th1/Th2-type cytokines in the synovium of patients with osteoarthritis. *Osteoarthritis and cartilage,* 10**,** 277-281.

IWANAGA, T., SHIKICHI, M., KITAMURA, H., YANASE, H. & NOZAWA-INOUE, K. 2000. Morphology and functional roles of synoviocytes in the joint. *Archives of histology and cytology,* 63**,** 17-31.

JASIN, H. 1988. Immune mediated cartilage destruction. *Scandinavian Journal of Rheumatology,* 17**,** 111-116.

JASIN, H. E. 1985. Autoantibody specificities of immune complexes sequestered in articular cartilage of patients with rheumatoid arthritis and osteoarthritis. *Arthritis & Rheumatism: Official Journal of the American College of Rheumatology,* 28**,** 241-248.

JAY, G. D., FLEMING, B. C., WATKINS, B. A., MCHUGH, K. A., ANDERSON, S. C., ZHANG, L. X., TEEPLE, E., WALLER, K. A. & ELSAID, K. A. 2010. Prevention of cartilage degeneration and restoration of chondroprotection by lubricin tribosupplementation in the rat following anterior cruciate ligament transection. *Arthritis & Rheumatism,* 62**,** 2382-2391.

JAYASURIYA, C. T. & CHEN, Q. 2015. Potential benefits and limitations of utilizing chondroprogenitors in cell-based cartilage therapy. *Connective tissue research,* 56**,** 265-271.

JAYASURIYA, C. T., HU, N., LI, J., LEMME, N., TEREK, R., EHRLICH, M. G. & CHEN, Q. 2018. Molecular characterization of mesenchymal stem cells in human osteoarthritis cartilage reveals contribution to the OA phenotype. *Sci Rep,* 8**,** 7044.

JAYASURIYA, C. T., TWOMEY-KOZAK, J., NEWBERRY, J., DESAI, S., FELTMAN, P., FRANCO, J. R., LI, N., TEREK, R., EHRLICH, M. G. & OWENS, B. D. 2019. Human Cartilage-Derived Progenitors Resist Terminal Differentiation and Require CXCR4 Activation to Successfully Bridge Meniscus Tissue Tears. *STEM CELLS,* 37**,** 102-114.

JEONG, B. Y., UDDIN, M. J., PARK, J. H., LEE, J. H., LEE, H. B., MIYATA, T. & HA, H. 2016. Novel plasminogen activator inhibitor-1 inhibitors prevent diabetic kidney injury in a mouse model. *PLoS One,* 11**,** e0157012.

JIANG, D., LIANG, J., FAN, J., YU, S., CHEN, S., LUO, Y., PRESTWICH, G. D., MASCARENHAS, M. M., GARG, H. G. & QUINN, D. A. 2005. Regulation of lung injury and repair by Toll-like receptors and hyaluronan. *Nature medicine,* 11**,** 1173.

JIN, C., FRAYSSINET, P., PELKER, R., CWIRKA, D., HU, B., VIGNERY, A., EISENBARTH, S. C. & FLAVELL, R. A. 2011. NLRP3 inflammasome plays a critical role in the pathogenesis of hydroxyapatite-associated arthropathy. *Proceedings of the National Academy of Sciences,* 108**,** 14867-14872.

JIN, Y., KATO, T., FURU, M., NASU, A., KAJITA, Y., MITSUI, H., UEDA, M., AOYAMA, T., NAKAYAMA, T. & NAKAMURA, T. 2010. Mesenchymal stem cells cultured under hypoxia escape from senescence via down-regulation of p16 and extracellular signal regulated kinase. *Biochemical and biophysical research communications,* 391**,** 1471-1476.

JOHN, T., KOHL, B., MOBASHERI, A., ERTEL, W. & SHAKIBAEI, M. 2007a. Interleukin-18 induces apoptosis in human articular chondrocytes. *Histology and histopathology*.

JOHN, T., MÜLLER, R., OBERHOLZER, A., ZREIQAT, H., KOHL, B., ERTEL, W., HOSTMANN, A., TSCHOEKE, S. & SCHULZE-TANZIL, G. 2007b. Interleukin-10 modulates pro-apoptotic effects of TNF-α in human articular chondrocytes in vitro. *Cytokine,* 40**,** 226-234.

JOHNELL, O., HULTH, A. & HENRICSON, A. 1985. T-lymphocyte subsets and HLA-DR-expressing cells in the osteoarthritic synovialis. *Scandinavian journal of rheumatology,* 14**,** 259-264.

JOHNSTONE, B., ALINI, M., CUCCHIARINI, M., DODGE, G. R., EGLIN, D., GUILAK, F., MADRY, H., MATA, A., MAUCK, R. L., SEMINO, C. E. & STODDART, M. J. 2013. Tissue engineering for articular cartilage repair--the state of the art. *Eur Cell Mater,* 25**,** 248-67.

JOHNSTONE, B., HERING, T. M., CAPLAN, A. I., GOLDBERG, V. M. & YOO, J. U. 1998. In vitro chondrogenesis of bone marrow-derived mesenchymal progenitor cells. *Exp Cell Res,* 238**,** 265-72.

JOOSTEN, L. A., LUBBERTS, E., DUREZ, P., HELSEN, M. M., JACOBS, M. J., GOLDMAN, M. & VAN DEN BERG, W. B. 1997. Role of interleukin-4 and interleukin-10 in murine collagen-induced arthritis. Protective effect of interleukin-4 and interleukin-10 treatment on cartilage destruction. *Arthritis & Rheumatism: Official Journal of the American College of Rheumatology,* 40**,** 249-260.

JOOSTEN, L. A., SMEETS, R. L., KOENDERS, M. I., VAN DEN BERSSELAAR, L. A., HELSEN, M. M., OPPERS-WALGREEN, B., LUBBERTS, E., IWAKURA, Y., VAN DE LOO, F. A. & VAN DEN BERG, W. B. 2004. Interleukin-18 promotes joint inflammation and induces interleukin-1-driven cartilage destruction. *The American journal of pathology,* 165**,** 959-967.

JORGENSEN, C., DJOUAD, F., APPARAILLY, F. & NOEL, D. 2003. Engineering mesenchymal stem cells for immunotherapy. *Gene Ther,* 10**,** 928-31.

KANEKO, S., SATOH, T., CHIBA, J., JU, C., INOUE, K. & KAGAWA, J. 2000. Interleukin–6 and interleukin–8 levels in serum and synovial fluid of patients with osteoarthritis. *Cytokines, cellular & molecular therapy,* 6**,** 71-79.

KAPOOR, M., MARTEL-PELLETIER, J., LAJEUNESSE, D., PELLETIER, J. P. & FAHMI, H. 2011. Role of proinflammatory cytokines in the pathophysiology of osteoarthritis. *Nat Rev Rheumatol,* 7**,** 33-42.

KARAN, A., KARAN, M. A., VURAL, P., ERTEN, N., TAŞÇIOĞLU, C., AKSOY, C., CANBAZ, M. & ONCEL, A. 2003. Synovial fluid nitric oxide levels in patients with knee osteoarthritis. *Clinical rheumatology,* 22**,** 397-399.

KASEMKIJWATTANA, C., HONGENG, S., KESPRAYURA, S., RUNGSINAPORN, V., CHAIPINYO, K. & CHANSIRI, K. 2011. Autologous bone marrow mesenchymal stem cells implantation for cartilage defects: two cases report. *Journal of the Medical Association of Thailand,* 94**,** 395.

KATSIKIS, P. D., CHU, C.-Q., BRENNAN, F. M., MAINI, R. N. & FELDMANN, M. 1994. Immunoregulatory role of interleukin 10 in rheumatoid arthritis. *The Journal of experimental medicine,* 179**,** 1517-1527.

KAVALKOVICH, K. W., BOYNTON, R. E., MURPHY, J. M. & BARRY, F. 2002. Chondrogenic differentiation of human mesenchymal stem cells within an alginate layer culture system. *In Vitro Cellular & Developmental Biology-Animal,* 38**,** 457-466.

KAWAI, T. & AKIRA, S. 2010. The role of pattern-recognition receptors in innate immunity: update on Toll-like receptors. *Nature immunology,* 11**,** 373.

KEATING, A. 2012. Mesenchymal stromal cells: new directions. *Cell stem cell,* 10**,** 709-716.

KERAVALA, A., LECHMAN, E. R., NASH, J., MI, Z. & ROBBINS, P. D. 2006. Human, viral or mutant human IL-10 expressed after local adenovirus-mediated gene transfer are equally effective in ameliorating disease pathology in a rabbit knee model of antigen-induced arthritis. *Arthritis Res Ther,* 8**,** R91.

KHAN, I., GILBERT, S., CATERSON, B., SANDELL, L. & ARCHER, C. 2008. Oxidative stress induces expression of osteoarthritis markers procollagen IIA and 3B3 (−) in adult bovine articular cartilage. *Osteoarthritis and cartilage,* 16**,** 698-707.

KHAN, I. M., BISHOP, J., GILBERT, S. & ARCHER, C. W. 2009a. Clonal chondroprogenitors maintain telomerase activity and Sox9 expression during extended monolayer culture and retain chondrogenic potential. *Osteoarthritis and cartilage,* 17**,** 518-528.

KHAN, I. M., WILLIAMS, R. & ARCHER, C. W. 2009b. One flew over the progenitor's nest: migratory cells find a home in osteoarthritic cartilage. *Cell Stem Cell,* 4**,** 282-4.

KIANI, C., LIWEN, C., WU, Y. J., ALBERT, J. Y. & BURTON, B. Y. 2002. Structure and function of aggrecan. *Cell research,* 12**,** 19.

KIM, H. A., CHO, M. L., CHOI, H. Y., YOON, C. S., JHUN, J. Y., OH, H. J. & KIM, H. Y. 2006. The catabolic pathway mediated by Toll-like receptors in human osteoarthritic chondrocytes. *Arthritis & Rheumatism: Official Journal of the American College of Rheumatology,* 54**,** 2152-2163.

KIM, J. E., LEE, S. M., KIM, S. H., TATMAN, P., GEE, A. O., KIM, D.-H., LEE, K. E., JUNG, Y. & KIM, S. J. 2014. Effect of self-assembled peptide–mesenchymal stem cell complex on the progression of osteoarthritis in a rat model. *International journal of nanomedicine,* 9**,** 141.

KISHIMOTO, T. 2006. Interleukin-6: discovery of a pleiotropic cytokine. *Arthritis Res Ther,* 8 Suppl 2**,** S2.

KOCH, A. E., KUNKEL, S. L., SHAH, M. R., FU, R., MAZARAKIS, D. D., HAINES, G. K., BURDICK, M. D., POPE, R. M. & STRIETER, R. M. 1995. Macrophage Inflammatory Protein-Iβ: A CC Chemokine in Osteoarthritis. *Clinical immunology and immunopathology,* 77**,** 307-314.

KOELLING, S., KRUEGEL, J., IRMER, M., PATH, J. R., SADOWSKI, B., MIRO, X. & MIOSGE, N. 2009. Migratory chondrogenic progenitor cells from repair tissue during the later stages of human osteoarthritis. *Cell stem cell,* 4**,** 324-335.

KONDO, M., YAMAOKA, K., SONOMOTO, K., FUKUYO, S., OSHITA, K., OKADA, Y. & TANAKA, Y. 2013. IL-17 inhibits chondrogenic differentiation of human mesenchymal stem cells. *PLoS One,* 8**,** e79463.

KONG, L., ZHENG, L. Z., QIN, L. & HO, K. K. W. 2017. Role of mesenchymal stem cells in osteoarthritis treatment. *J Orthop Translat,* 9**,** 89-103.

KORN, T., BETTELLI, E., OUKKA, M. & KUCHROO, V. K. 2009. IL-17 and Th17 Cells. *Annual review of immunology,* 27**,** 485-517.

KOVESDI, I., BROUGH, D. E., BRUDER, J. T. & WICKHAM, T. J. 1997. Adenoviral vectors for gene transfer. *Curr Opin Biotechnol,* 8**,** 583-9.

KOZHEMYAKINA, E., ZHANG, M., IONESCU, A., AYTURK, U. M., ONO, N., KOBAYASHI, A., KRONENBERG, H., WARMAN, M. L. & LASSAR, A. B. 2015. Identification of a Prg4-expressing articular cartilage progenitor cell population in mice. *Arthritis & rheumatology,* 67**,** 1261-1273.

KRAMPERA, M. 2011. Mesenchymal stromal cell 'licensing': a multistep process. *Leukemia,* 25**,** 1408-1414.

KRASNOKUTSKY, S., ATTUR, M., PALMER, G., SAMUELS, J. & ABRAMSON, S. B. 2008. Current concepts in the pathogenesis of osteoarthritis. *Osteoarthritis Cartilage,* 16 Suppl 3**,** S1-3.

KRASNOKUTSKY, S., BELITSKAYA-LEVY, I., BENCARDINO, J., SAMUELS, J., ATTUR, M., REGATTE, R., ROSENTHAL, P., GREENBERG, J., SCHWEITZER, M., ABRAMSON, S. B. & RYBAK, L. 2011. Quantitative magnetic resonance imaging evidence of synovial proliferation is associated with radiographic severity of knee osteoarthritis. *Arthritis Rheum,* 63**,** 2983-91.

KRAUS, V. B., MCDANIEL, G., HUEBNER, J. L., STABLER, T. V., PIEPER, C. F., SHIPES, S. W., PETRY, N. A., LOW, P. S., SHEN, J. & MCNEARNEY, T. A. 2016. Direct in vivo evidence of activated macrophages in human osteoarthritis. *Osteoarthritis and cartilage,* 24**,** 1613-1621.

KRUGER, J. P., ENDRES, M., NEUMANN, K., STUHLMULLER, B., MORAWIETZ, L., HAUPL, T. & KAPS, C. 2012. Chondrogenic differentiation of human subchondral progenitor cells is affected by synovial fluid from donors with osteoarthritis or rheumatoid arthritis. *J Orthop Surg Res,* 7**,** 10.

KURODA, T., MARUYAMA, H., SHIMOTORI, M., HIGUCHI, N., KAMEDA, S., TAHARA, H., MIYAZAKI, J.-I. & GEJYO, F. 2006. Effects of viral interleukin 10 introduced by in vivo electroporation on arthrogen-induced arthritis in mice. *The Journal of rheumatology,* 33**,** 455-462.

LADHER, R., CHURCH, V., ALLEN, S., ROBSON, L., ABDELFATTAH, A., BROWN, N., HATTERSLEY, G., ROSEN, V., LUYTEN, F. & DALE, L. 2000. Cloning and expression of the Wnt antagonists Sfrp-2 and Frzb during chick development. *Developmental biology,* 218**,** 183-198.

LATZ, E. 2010. The inflammasomes: mechanisms of activation and function. *Current opinion in immunology,* 22**,** 28-33.

LATZ, E., XIAO, T. S. & STUTZ, A. 2013. Activation and regulation of the inflammasomes. *Nature Reviews Immunology,* 13**,** 397.

LE BLANC, K. & MOUGIAKAKOS, D. 2012. Multipotent mesenchymal stromal cells and the innate immune system. *Nature Reviews Immunology,* 12**,** 383.

LECHMAN, E. R., JAFFURS, D., GHIVIZZANI, S. C., GAMBOTTO, A., KOVESDI, I., MI, Z., EVANS, C. H. & ROBBINS, P. D. 1999. Direct adenoviral gene transfer of viral IL-10 to rabbit knees with experimental arthritis ameliorates disease in both injected and contralateral control knees. *J Immunol,* 163**,** 2202-8.

LEE, S.-H., JANG, A.-S., KIM, Y.-E., CHA, J.-Y., KIM, T.-H., JUNG, S., PARK, S.-K., LEE, Y.-K., WON, J.-H., KIM, Y.-H. & PARK, C.-S. 2010. Modulation of cytokine and nitric oxide by mesenchymal stem cell transfer in lung injury/fibrosis. *Respiratory Research,* 11**,** 16.

LEE, S., SZILAGYI, E., CHEN, L., PREMANAND, K., DIPIETRO, L. A., ENNIS, W. & BARTHOLOMEW, A. M. 2013. Activated mesenchymal stem cells increase wound tensile strength in aged mouse model via macrophages. *journal of surgical research,* 181**,** 20-24.

LEFEBVRE, V. & BHATTARAM, P. 2015. Prg4-expressing cells: articular stem cells or differentiated progeny in the articular chondrocyte lineage? *Arthritis & rheumatology (Hoboken, N.J.),* 67**,** 1151-1154.

LEFEBVRE, V. & DVIR-GINZBERG, M. 2017. SOX9 and the many facets of its regulation in the chondrocyte lineage. *Connect Tissue Res,* 58**,** 2-14.

LEFEBVRE, V. & SMITS, P. 2005. Transcriptional control of chondrocyte fate and differentiation. *Birth Defects Res C Embryo Today,* 75**,** 200-12.

LEIJS, M., VAN BUUL, G., NIEBOER, M., HAECK, J., KOPS, N., BOS, P., VERHAAR, J., BERNSEN, M. & VAN OSCH, G. 2016. Endurable injectable mesenchymal stem cell therapy for osteoarthritis by encapsulation in alginate constructs. *Osteoarthritis and Cartilage,* 24**,** S12-S13.

LI, L., ELLIOTT, J. F. & MOSMANN, T. R. 1994. IL-10 inhibits cytokine production, vascular leakage, and swelling during T helper 1 cell-induced delayed-type hypersensitivity. *J Immunol,* 153**,** 3967-78.

LI, L., LI, F., TIAN, H., YUE, W., LI, S. & CHEN, G. 2014. Human mesenchymal stem cells with adenovirus-mediated TRAIL gene transduction have antitumor effects on esophageal cancer cell line Eca-109. *Acta Biochim Biophys Sin (Shanghai),* 46**,** 471-6.

LI, P. Z., YAN, G. Y., HAN, L., PANG, J., ZHONG, B. S., ZHANG, G. M., WANG, F. & ZHANG, Y. L. 2017a. Overexpression of STRA8, BOULE, and DAZL Genes Promotes Goat Bone Marrow-Derived Mesenchymal Stem Cells In Vitro Transdifferentiation Toward Putative Male Germ Cells. *Reprod Sci,* 24**,** 300-312.

LI, W., MA, N., ONG, L. L., NESSELMANN, C., KLOPSCH, C., LADILOV, Y., FURLANI, D., PIECHACZEK, C., MOEBIUS, J. M., LUTZOW, K., LENDLEIN, A., STAMM, C., LI, R. K. & STEINHOFF, G. 2007. Bcl-2 engineered MSCs inhibited apoptosis and improved heart function. *Stem Cells,* 25**,** 2118-27.

LI, W., REN, G., HUANG, Y., SU, J., HAN, Y., LI, J., CHEN, X., CAO, K., CHEN, Q. & SHOU, P. 2012. Mesenchymal stem cells: a double-edged sword in regulating immune responses. *Cell death and differentiation,* 19**,** 1505.

LI, Y.-S., LUO, W., ZHU, S.-A. & LEI, G.-H. 2017b. T cells in osteoarthritis: alterations and beyond. *Frontiers in immunology,* 8**,** 356.

LIN, Y.-M., HSU, C.-J., LIAO, Y.-Y., CHOU, M.-C. & TANG, C.-H. 2012. The CCL2/CCR2 axis enhances vascular cell adhesion molecule-1 expression in human synovial fibroblasts. *PloS one,* 7**,** e49999.

LIN, Z., FITZGERALD, J. B., XU, J., WILLERS, C., WOOD, D., GRODZINSKY, A. J. & ZHENG, M. H. 2008. Gene expression profiles of human chondrocytes during passaged monolayer cultivation. *Journal of Orthopaedic Research,* 26**,** 1230-1237.

LIPPIELLO, L., FIENHOLD, M. & GRANDJEAN, C. 1990. Metabolic and ultrastructural changes in articular cartilage of rats fed dietary supplements of omega-3 fatty acids. *Arthritis & Rheumatism: Official Journal of the American College of Rheumatology,* 33**,** 1029-1036.

LIPPIELLO, L., WALSH, T. & FIENHOLD, M. 1991. The association of lipid abnormalities with tissue pathology in human osteoarthritic articular cartilage. *Metabolism,* 40**,** 571-576.

LIU-BRYAN, R. & TERKELTAUB, R. 2012. The growing array of innate inflammatory ignition switches in osteoarthritis. *Arthritis and rheumatism,* 64**,** 2055.

LIU-BRYAN, R. & TERKELTAUB, R. 2010. Chondrocyte innate immune myeloid differentiation factor 88–dependent signaling drives procatabolic effects of the endogenous toll-like receptor 2/toll-like receptor 4 ligands low molecular weight hyaluronan and high mobility group box chromosomal protein 1 in mice. *Arthritis & Rheumatism,* 62**,** 2004-2012.

LIU, B., ZHANG, M., ZHAO, J., ZHENG, M. & YANG, H. 2018a. Imbalance of M1/M2 macrophages is linked to severity level of knee osteoarthritis. *Experimental and therapeutic medicine,* 16**,** 5009-5014.

LIU, J.-F., HOU, S.-M., TSAI, C.-H., HUANG, C.-Y., HSU, C.-J. & TANG, C.-H. 2013a. CCN4 induces vascular cell adhesion molecule-1 expression in human synovial fibroblasts and promotes monocyte adhesion. *Biochimica et Biophysica Acta (BBA)-Molecular Cell Research,* 1833**,** 966-975.

LIU, L. N., WANG, G., HENDRICKS, K., LEE, K., BOHNLEIN, E., JUNKER, U. & MOSCA, J. D. 2013b. Comparison of drug and cell-based delivery: Engineered adult mesenchymal stem cells expressing soluble tumor necrosis factor receptor II prevent arthritis in mouse and rat animal models. *Stem cells translational medicine,* 2**,** 362-375.

LIU, Y., LIN, L., ZOU, R., WEN, C., WANG, Z. & LIN, F. 2018b. MSC-derived exosomes promote proliferation and inhibit apoptosis of chondrocytes via lncRNA-KLF3-AS1/miR-206/GIT1 axis in osteoarthritis. *Cell Cycle,* 17**,** 2411-2422.

LOESER, R. F., GOLDRING, S. R., SCANZELLO, C. R. & GOLDRING, M. B. 2012. Osteoarthritis: a disease of the joint as an organ. *Arthritis Rheum,* 64**,** 1697-707.

LOESER, R. F., YAMMANI, R. R., CARLSON, C. S., CHEN, H., COLE, A., IM, H. J., BURSCH, L. S. & YAN, S. D. 2005. Articular chondrocytes express the receptor for advanced glycation end products: potential role in osteoarthritis. *Arthritis & Rheumatism: Official Journal of the American College of Rheumatology,* 52**,** 2376-2385.

LOEUILLE, D., CHARY-VALCKENAERE, I., CHAMPIGNEULLE, J., RAT, A. C., TOUSSAINT, F., PINZANO-WATRIN, A., GOEBEL, J. C., MAINARD, D., BLUM, A. & POUREL, J. 2005. Macroscopic and microscopic features of synovial membrane inflammation in the osteoarthritic knee: correlating magnetic resonance imaging findings with disease severity. *Arthritis & Rheumatism,* 52**,** 3492-3501.

LOTZ, M., TERKELTAUB, R. & VILLIGER, P. 1992. Cartilage and joint inflammation. Regulation of IL-8 expression by human articular chondrocytes. *The Journal of Immunology,* 148**,** 466-473.

LOUGHLIN, J., DOWLING, B., CHAPMAN, K., MARCELLINE, L., MUSTAFA, Z., SOUTHAM, L., FERREIRA, A., CIESIELSKI, C., CARSON, D. A. & CORR, M. 2004. Functional variants within the secreted frizzled-related protein 3 gene are associated with hip osteoarthritis in females. *Proceedings of the National Academy of Sciences,* 101**,** 9757-9762.

LU, J., WANG, Q., HUANG, L., DONG, H., LIN, L., LIN, N., ZHENG, F. & TAN, J. 2012. Palmitate causes endoplasmic reticulum stress and apoptosis in human mesenchymal stem cells: prevention by AMPK activator. *Endocrinology,* 153**,** 5275-5284.

LUCAS, M., ZHANG, X., PRASANNA, V. & MOSSER, D. M. 2005. ERK activation following macrophage FcγR ligation leads to chromatin modifications at the IL-10 locus. *The Journal of Immunology,* 175**,** 469-477.

LUYTEN, F. P., TYLZANOWSKI, P. & LORIES, R. J. 2009. Wnt signaling and osteoarthritis. *Bone,* 44**,** 522-527.

LV, X.-J., ZHOU, G.-D., LIU, Y., LIU, X., CHEN, J.-N., LUO, X.-S. & CAO, Y.-L. 2012. In vitro proliferation and differentiation of adipose-derived stem cells isolated using anti-CD105 magnetic beads. *International journal of molecular medicine,* 30**,** 826-834.

MA, K., TITAN, A. L., STAFFORD, M., HUA ZHENG, C. & LEVENSTON, M. E. 2012. Variations in chondrogenesis of human bone marrow-derived mesenchymal stem cells in fibrin/alginate blended hydrogels. *Acta biomaterialia,* 8**,** 3754-3764.

MA, Y., THORNTON, S., DUWEL, L. E., BOIVIN, G. P., GIANNINI, E. H., LEIDEN, J. M., BLUESTONE, J. A. & HIRSCH, R. 1998. Inhibition of collagen-induced arthritis in mice by viral IL-10 gene transfer. *J Immunol,* 161**,** 1516-24.

MACCARIO, R., PODESTÀ, M., MORETTA, A., COMETA, A., COMOLI, P., MONTAGNA, D., DAUDT, L., IBATICI, A., PIAGGIO, G. & POZZI, S. 2005. Interaction of human mesenchymal stem cells with cells involved in alloantigen-specific immune response favors the differentiation of CD4+ T-cell subsets expressing a regulatory/suppressive phenotype. *Haematologica,* 90**,** 516-525.

MACKANESS, G. 1977. Cellular immunity and the parasite. *Immunity to Blood Parasites of Animals and Man.* Springer.

MACNEIL, I. A., SUDA, T., MOORE, K. W., MOSMANN, T. R. & ZLOTNIK, A. 1990. IL-10, a novel growth cofactor for mature and immature T cells. *J Immunol,* 145**,** 4167-73.

MAGGINI, J., MIRKIN, G., BOGNANNI, I., HOLMBERG, J., PIAZZÓN, I. M., NEPOMNASCHY, I., COSTA, H., CAÑONES, C., RAIDEN, S. & VERMEULEN, M. 2010. Mouse bone marrow-derived mesenchymal stromal cells turn activated macrophages into a regulatory-like profile. *PloS one,* 5**,** e9252.

MALDONADO, M. & NAM, J. 2013. The role of changes in extracellular matrix of cartilage in the presence of inflammation on the pathology of osteoarthritis. *BioMed research international,* 2013.

MAN, S. M. & KANNEGANTI, T. D. 2015. Regulation of inflammasome activation. *Immunological reviews,* 265**,** 6-21.

MANCUSO, P., RAMAN, S., GLYNN, A., BARRY, F. & MURPHY, J. M. 2019. Mesenchymal stem cell therapy for osteoarthritis: the critical role of the cell secretome. *Frontiers in bioengineering and biotechnology,* 7.

MANFERDINI, C., PAOLELLA, F., GABUSI, E., GAMBARI, L., PIACENTINI, A., FILARDO, G., FLEURY-CAPPELLESSO, S., BARBERO, A., MURPHY, M. & LISIGNOLI, G. 2017. Adipose stromal cells mediated switching of the pro-inflammatory profile of M1-like macrophages is facilitated by PGE2: in vitro evaluation. *Osteoarthritis and cartilage,* 25**,** 1161-1171.

MANNING, E., PHAM, S., LI, S., VAZQUEZ-PADRON, R. I., MATHEW, J., RUIZ, P. & SALGAR, S. K. 2010. Interleukin-10 delivery via mesenchymal stem cells: a novel gene therapy approach to prevent lung ischemia-reperfusion injury. *Hum Gene Ther,* 21**,** 713-27.

MANTOVANI, A., BISWAS, S. K., GALDIERO, M. R., SICA, A. & LOCATI, M. 2013. Macrophage plasticity and polarization in tissue repair and remodelling. *The Journal of pathology,* 229**,** 176-185.

MANTOVANI, A., SICA, A., SOZZANI, S., ALLAVENA, P., VECCHI, A. & LOCATI, M. 2004. The chemokine system in diverse forms of macrophage activation and polarization. *Trends in immunology,* 25**,** 677-686.

MAO, L., KITANI, A., STROBER, W. & FUSS, I. J. 2018. The Role of NLRP3 and IL-1β in the Pathogenesis of Inflammatory Bowel Disease. *Frontiers in Immunology,* 9.

MARIATHASAN, S., WEISS, D. S., NEWTON, K., MCBRIDE, J., O'ROURKE, K., ROOSE-GIRMA, M., LEE, W. P., WEINRAUCH, Y., MONACK, D. M. & DIXIT, V. M. 2006. Cryopyrin activates the inflammasome in response to toxins and ATP. *Nature,* 440**,** 228.

MARLOVITS, S., HOMBAUER, M., TRUPPE, M., VECSEI, V. & SCHLEGEL, W. 2004. Changes in the ratio of type-I and type-II collagen expression during monolayer

culture of human chondrocytes. *The Journal of bone and joint surgery. British volume,* 86**,** 286-295.

MARTEL-PELLETIER, J., ALAAEDDINE, N. & PELLETIER, J.-P. 1999. Cytokines and their role in the pathophysiology of osteoarthritis. *Front Biosci,* 4**,** D694-703.

MARTEL-PELLETIER, J., BOILEAU, C., PELLETIER, J.-P. & ROUGHLEY, P. J. 2008. Cartilage in normal and osteoarthritis conditions. *Best practice & research Clinical rheumatology,* 22**,** 351-384.

MARTINON, F., PÉTRILLI, V., MAYOR, A., TARDIVEL, A. & TSCHOPP, J. 2006. Gout-associated uric acid crystals activate the NALP3 inflammasome. *Nature,* 440**,** 237.

MAUMUS, M., ROUSSIGNOL, G., TOUPET, K., PENARIER, G., BENTZ, I., TEIXEIRA, S., OUSTRIC, D., JUNG, M., LEPAGE, O., STEINBERG, R., JORGENSEN, C. & NOEL, D. 2016. Utility of a Mouse Model of Osteoarthritis to Demonstrate Cartilage Protection by IFNγ-Primed Equine Mesenchymal Stem Cells. *Frontiers in Immunology,* 7.

MCALLISTER, M. J., CHEMALY, M., EAKIN, A. J., GIBSON, D. S. & MCGILLIGAN, V. E. 2018. NLRP3 as a potentially novel biomarker for the management of osteoarthritis. *Osteoarthritis and Cartilage,* 26**,** 612-619.

MCCARTHY, H. E., BARA, J. J., BRAKSPEAR, K., SINGHRAO, S. K. & ARCHER, C. W. 2012. The comparison of equine articular cartilage progenitor cells and bone marrow-derived stromal cells as potential cell sources for cartilage repair in the horse. *The Veterinary Journal,* 192**,** 345-351.

MCKINNEY, J., DOAN, T., WANG, L., DEPPEN, J., REECE, D., PUCHA, K., GINN, S., LEVIT, R. & WILLETT, N. 2019. Therapeutic efficacy of intra-articular delivery of encapsulated human mesenchymal stem cells on early stage osteoarthritis. *European cells & materials,* 37**,** 42-59.

MEIRELLES LDA, S. & NARDI, N. B. 2003. Murine marrow-derived mesenchymal stem cell: isolation, in vitro expansion, and characterization. *Br J Haematol,* 123**,** 702-11.

MELIEF, S. M., GEUTSKENS, S. B., FIBBE, W. E. & ROELOFS, H. 2013a. Multipotent stromal cells skew monocytes towards an anti-inflammatory interleukin-10-producing phenotype by production of interleukin-6. *Haematologica,* 98**,** 888-895.

MELIEF, S. M., SCHRAMA, E., BRUGMAN, M. H., TIEMESSEN, M. M., HOOGDUIJN, M. J., FIBBE, W. E. & ROELOFS, H. 2013b. Multipotent stromal cells induce human regulatory T cells through a novel pathway involving skewing of monocytes toward anti-inflammatory macrophages. *Stem Cells,* 31**,** 1980-1991.

MENG, F. & LOWELL, C. A. 1997. Lipopolysaccharide (LPS)-induced macrophage activation and signal transduction in the absence of Src-family kinases Hck, Fgr, and Lyn. *Journal of experimental medicine,* 185**,** 1661-1670.

MENGSHOL, J. A., VINCENTI, M. P., COON, C. I., BARCHOWSKY, A. & BRINCKERHOFF, C. E. 2000. Interleukin-1 induction of collagenase 3 (matrix metalloproteinase 13) gene expression in chondrocytes requires p38, c-Jun N-terminal kinase, and nuclear factor κB: differential regulation of collagenase 1 and collagenase 3. *Arthritis & Rheumatism: Official Journal of the American College of Rheumatology,* 43**,** 801-811.

MERZ, D., LIU, R., JOHNSON, K. & TERKELTAUB, R. 2003. IL-8/CXCL8 and growth-related oncogene α/CXCL1 induce chondrocyte hypertrophic differentiation. *The Journal of Immunology,* 171**,** 4406-4415.

MICHAUD, C. M., MCKENNA, M. T., BEGG, S., TOMIJIMA, N., MAJMUDAR, M., BULZACCHELLI, M. T., EBRAHIM, S., EZZATI, M., SALOMON, J. A. & KREISER, J. G. 2006. The burden of disease and injury in the United States 1996. *Population health metrics,* 4**,** 11.

MIDWOOD, K., SACRE, S., PICCININI, A. M., INGLIS, J., TREBAUL, A., CHAN, E., DREXLER, S., SOFAT, N., KASHIWAGI, M. & OREND, G. 2009. Tenascin-C is an endogenous activator of Toll-like receptor 4 that is essential for maintaining inflammation in arthritic joint disease. *Nature medicine,* 15**,** 774.

MILLIGAN, E. D., LANGER, S. J., SLOANE, E. M., HE, L., WIESELER-FRANK, J., O'CONNOR, K., MARTIN, D., FORSAYETH, J. R., MAIER, S. F., JOHNSON, K., CHAVEZ, R. A., LEINWAND, L. A. & WATKINS, L. R. 2005. Controlling pathological pain by adenovirally driven spinal production of the anti-inflammatory cytokine, interleukin-10. *Eur J Neurosci,* 21**,** 2136-48.

MOBASHERI, A., KALAMEGAM, G., MUSUMECI, G. & BATT, M. E. 2014. Chondrocyte and mesenchymal stem cell-based therapies for cartilage repair in osteoarthritis and related orthopaedic conditions. *Maturitas,* 78**,** 188-198.

MÖLLER, B., PAULUKAT, J., NOLD, M., BEHRENS, M., KUKOC-ZIVOJNOV, N., KALTWASSER, J., PFEILSCHIFTER, J. & MÜHL, H. 2003. Interferon-γ induces expression of interleukin-18 binding protein in fibroblast-like synoviocytes. *Rheumatology,* 42**,** 442-445.

MOORE, K. W., DE WAAL MALEFYT, R., COFFMAN, R. L. & O'GARRA, A. 2001. Interleukin-10 and the interleukin-10 receptor. *Annu Rev Immunol,* 19**,** 683-765.

MOORE, K. W., VIEIRA, P., FIORENTINO, D. F., TROUNSTINE, M. L., KHAN, T. A. & MOSMANN, T. R. 1990. Homology of cytokine synthesis inhibitory factor (IL-10) to the Epstein-Barr virus gene BCRFI. *Science,* 248**,** 1230-4.

MORADI, B., ROSSHIRT, N., TRIPEL, E., KIRSCH, J., BARIE, A., ZEIFANG, F., GOTTERBARM, T. & HAGMANN, S. 2015. Unicompartmental and bicompartmental knee osteoarthritis show different patterns of mononuclear cell infiltration and cytokine release in the affected joints. *Clinical & Experimental Immunology,* 180**,** 143-154.

MORIKAWA, S., MABUCHI, Y., KUBOTA, Y., NAGAI, Y., NIIBE, K., HIRATSU, E., SUZUKI, S., MIYAUCHI-HARA, C., NAGOSHI, N., SUNABORI, T., SHIMMURA, S., MIYAWAKI, A., NAKAGAWA, T., SUDA, T., OKANO, H. & MATSUZAKI, Y. 2009. Prospective identification, isolation, and systemic transplantation of multipotent mesenchymal stem cells in murine bone marrow. *J Exp Med,* 206**,** 2483-96.

MOSKOWITZ, R. & KRESINA, T. 1986. Immunofluorescent analysis of experimental osteoarthritic cartilage and synovium: evidence for selective deposition of immunoglobulin and complement in cartilaginous tissues. *The Journal of rheumatology,* 13**,** 391-396.

MOSSER, D. M. 2003. The many faces of macrophage activation. *Journal of leukocyte biology,* 73**,** 209-212.

MOSSER, D. M. & EDWARDS, J. P. 2008. Exploring the full spectrum of macrophage activation. *Nature reviews immunology,* 8**,** 958.

MOSSER, D. M. & ZHANG, X. 2008. Activation of murine macrophages. *Current protocols in immunology,* 83**,** 14.2. 1-14.2. 8.

MOW, V. C., LAI, W. M., EISENFELD, J. & REDLER, I. 1974. Some surface characteristics of articular cartilage—II. On the stability of articular surface and a possible biomechanical factor in etiology of chondrodegeneration. *Journal of Biomechanics,* 7**,** 457-468.

MOW, V. C., RATCLIFFE, A. & WOO, S. L. 2012. *Biomechanics of diarthrodial joints*, Springer Science & Business Media.

MROSEWSKI, I., JORK, N., GORTE, K., CONRAD, C., WIEGAND, E., KOHL, B., ERTEL, W., JOHN, T., OBERHOLZER, A. & KAPS, C. 2014. Regulation of osteoarthritis-associated key mediators by TNFα and IL-10: effects of IL-10 overexpression in human synovial fibroblasts and a synovial cell line. *Cell and tissue research,* 357**,** 207-223.

MUELLER, M. B. & TUAN, R. S. 2011. Anabolic/catabolic balance in pathogenesis of osteoarthritis: identifying molecular targets. *PM&R,* 3**,** S3-S11.

MUIR, P., HANS, E. C., RACETTE, M., VOLSTAD, N., SAMPLE, S. J., HEATON, C., HOLZMAN, G., SCHAEFER, S. L., BLOOM, D. D., BLEEDORN, J. A., HAO, Z., AMENE, E., SURESH, M. & HEMATTI, P. 2016. Autologous Bone Marrow-Derived Mesenchymal Stem Cells Modulate Molecular Markers of Inflammation in Dogs with Cruciate Ligament Rupture. *PLoS One,* 11**,** e0159095.

MURPHY, J. M., DIXON, K., BECK, S., FABIAN, D., FELDMAN, A. & BARRY, F. 2002. Reduced chondrogenic and adipogenic activity of mesenchymal stem cells from patients with advanced osteoarthritis. *Arthritis & Rheumatism,* 46**,** 704-713.

MURPHY, J. M., FINK, D. J., HUNZIKER, E. B. & BARRY, F. P. 2003. Stem cell therapy in a caprine model of osteoarthritis. *Arthritis & Rheumatism: Official Journal of the American College of Rheumatology,* 48**,** 3464-3474.

MURRAY, P. J., ALLEN, J. E., BISWAS, S. K., FISHER, E. A., GILROY, D. W., GOERDT, S., GORDON, S., HAMILTON, J. A., IVASHKIV, L. B. & LAWRENCE, T. 2014. Macrophage activation and polarization: nomenclature and experimental guidelines. *Immunity,* 41**,** 14-20.

MUSUMECI, G., AIELLO, F. C., SZYCHLINSKA, M. A., DI ROSA, M., CASTROGIOVANNI, P. & MOBASHERI, A. 2015. Osteoarthritis in the XXIst century: risk factors and behaviours that influence disease onset and progression. *Int J Mol Sci,* 16**,** 6093-112.

NABBE, K., BLOM, A., HOLTHUYSEN, A., BOROSS, P., ROTH, J., VERBEEK, S., VAN LENT, P. & VAN DEN BERG, W. 2003. Coordinate expression of activating Fcγ receptors I and III and inhibiting Fcγ receptor type II in the determination of joint inflammation and cartilage destruction during immune complex–mediated arthritis. *Arthritis & Rheumatism,* 48**,** 255-265.

NAKAJIMA, M., NITO, C., SOWA, K., SUDA, S., NISHIYAMA, Y., NAKAMURA-TAKAHASHI, A., NITAHARA-KASAHARA, Y., IMAGAWA, K., HIRATO, T. & UEDA, M. 2017. Mesenchymal stem cells overexpressing interleukin-10 promote neuroprotection in experimental acute ischemic stroke. *Molecular Therapy-Methods & Clinical Development,* 6**,** 102-111.

NAKAMURA, H., TANAKA, M., MASUKO-HONGO, K., YUDOH, K., KATO, T., BEPPU, M. & NISHIOKA, K. 2006. Enhanced production of MMP-1, MMP-3, MMP-13, and RANTES by interaction of chondrocytes with autologous T cells. *Rheumatology international,* 26**,** 984-990.

NAKAMURA, H., YOSHINO, S., KATO, T., TSURUHA, J. & NISHIOKA, K. 1999. T-cell mediated inflammatory pathway in osteoarthritis. *Osteoarthritis and Cartilage,* 7**,** 401-402.

NAM, J., PERERA, P., LIU, J., RATH, B., DESCHNER, J., GASSNER, R., BUTTERFIELD, T. A. & AGARWAL, S. 2011. Sequential alterations in catabolic and anabolic gene expression parallel pathological changes during progression of monoiodoacetate-induced arthritis. *PLoS One,* 6**,** e24320.

NARULA, K. 2000. Interleukin 10—A therapeutic cytokine for chronic inflammatory diseases. *Curr Opin Anti-inflammatory Immunomodulatory Investigational Drugs,* 2**,** 307-313.

NAZEMPOUR, A. & VAN WIE, B. 2016. Chondrocytes, mesenchymal stem cells, and their combination in articular cartilage regenerative medicine. *Annals of biomedical engineering,* 44**,** 1325-1354.

NEFLA, M., HOLZINGER, D., BERENBAUM, F. & JACQUES, C. 2016. The danger from within: alarmins in arthritis. *Nature Reviews Rheumatology,* 12**,** 669.

NELSON, L., MCCARTHY, H. E., FAIRCLOUGH, J., WILLIAMS, R. & ARCHER, C. W. 2014. Evidence of a viable pool of stem cells within human osteoarthritic cartilage. *Cartilage,* 5**,** 203-214.

NÉMETH, K., LEELAHAVANICHKUL, A., YUEN, P. S., MAYER, B., PARMELEE, A., DOI, K., ROBEY, P. G., LEELAHAVANICHKUL, K., KOLLER, B. H. & BROWN, J. M. 2009. Bone marrow stromal cells attenuate sepsis via prostaglandin E 2–dependent reprogramming of host macrophages to increase their interleukin-10 production. *Nature medicine,* 15**,** 42.

NEUHOLD, L. A., KILLAR, L., ZHAO, W., SUNG, M. L., WARNER, L., KULIK, J., TURNER, J., WU, W., BILLINGHURST, C., MEIJERS, T., POOLE, A. R., BABIJ, P. & DEGENNARO, L. J. 2001. Postnatal expression in hyaline cartilage of constitutively active human collagenase-3 (MMP-13) induces osteoarthritis in mice. *J Clin Invest,* 107**,** 35-44.

NIEBAUER, G., WOLF, B., YARMUSH, M. & RICHARDSON, D. 1988. Evaluation of immune complexes and collagen type-specific antibodies in sera and synovial fluids of horses with secondary osteoarthritis. *American journal of veterinary research,* 49**,** 1223-1227.

NISHITANI, K., ITO, H., HIRAMITSU, T., TSUTSUMI, R., TANIDA, S., KITAORI, T., YOSHITOMI, H., KOBAYASHI, M. & NAKAMURA, T. 2010. PGE2 inhibits MMP expression by suppressing MKK4–JNK MAP kinase–c-JUN pathway via EP4 in human articular chondrocytes. *Journal of cellular biochemistry,* 109**,** 425-433.

OKAMURA, Y., WATARI, M., JERUD, E. S., YOUNG, D. W., ISHIZAKA, S. T., ROSE, J., CHOW, J. C. & STRAUSS, J. F. 2001. The extra domain A of fibronectin activates Toll-like receptor 4. *Journal of Biological Chemistry,* 276**,** 10229-10233.

OLEE, T., HASHIMOTO, S., QUACH, J. & LOTZ, M. 1999. IL-18 is produced by articular chondrocytes and induces proinflammatory and catabolic responses. *The Journal of Immunology,* 162**,** 1096-1100.

OLIVEIRA, S. M., AMARAL, I. F., BARBOSA, M. A. & TEIXEIRA, C. C. 2008. Engineering endochondral bone: in vitro studies. *Tissue Engineering Part A,* 15**,** 625-634.

ONUMA, H., MASUKO-HONGO, K., YUAN, G., SAKATA, M., NAKAMURA, H., KATO, T., AOKI, H. & NISHIOKA, K. 2002. Expression of the anaphylatoxin receptor C5aR (CD88) by human articular chondrocytes. *Rheumatology international,* 22**,** 52-55.

OPPENHEIM, J. J. & YANG, D. 2005. Alarmins: chemotactic activators of immune responses. *Current opinion in immunology,* 17**,** 359-365.

OROZCO, L., MUNAR, A., SOLER, R., ALBERCA, M., SOLER, F., HUGUET, M., SENTÍS, J., SÁNCHEZ, A. & GARCÍA-SANCHO, J. 2013. Treatment of knee osteoarthritis with autologous mesenchymal stem cells: a pilot study. *Transplantation,* 95**,** 1535-1541.

OWEN, M. & FRIEDENSTEIN, A. Stromal stem cells: marrow-derived osteogenic precursors. Ciba Found Symp, 1988. Wiley Online Library, 42-60.

PALM, N., ZHU, S. & FLAVELL, R. 2014. Inflammasomes. *Cold Spring Harbor perspectives in biology,* 6**,** a016287-a016287.

PALMER, G., TALABOT-AYER, D., LAMACCHIA, C., TOY, D., SEEMAYER, C. A., VIATTE, S., FINCKH, A., SMITH, D. E. & GABAY, C. 2009. Inhibition of interleukin-33 signaling attenuates the severity of experimental arthritis. *Arthritis & rheumatism: official journal of the American College of Rheumatology,* 60**,** 738-749.

PALMER, G. D., STODDART, M. J., GOUZE, E., GOUZE, J. N., GHIVIZZANI, S. C., PORTER, R. M. & EVANS, C. H. 2008. A simple, lanthanide-based method to enhance the transduction efficiency of adenovirus vectors. *Gene Ther,* 15**,** 357-63.

PALMER, R., HICKERY, M., CHARLES, I., MONCADA, S. & BAYLISS, M. 1993. Induction of nitric oxide synthase in human chondrocytes. *Biochemical and biophysical research communications,* 193**,** 398-405.

PAULI, C., GROGAN, S. P., PATIL, S., OTSUKI, S., HASEGAWA, A., KOZIOL, J., LOTZ, M. K. & D'LIMA, D. D. 2011. Macroscopic and histopathologic analysis of human knee menisci in aging and osteoarthritis. *Osteoarthritis and Cartilage,* 19**,** 1132-1141.

PAWŁOWSKA, J., MIKOSIK, A., SOROCZYNSKA-CYBULA, M., JÓŹWIK, A., ŁUCZKIEWICZ, P., MAZURKIEWICZ, S., LORCZYŃSKI, A., WITKOWSKI, J. & BRYL, E. 2009. Different distribution of CD4 and CD8 T cells in synovial membrane and peripheral blood of rheumatoid arthritis and osteoarthritis patients. *Folia Histochemica et Cytobiologica,* 47**,** 627-632.

PAZÁR, B., EA, H.-K., NARAYAN, S., KOLLY, L., BAGNOUD, N., CHOBAZ, V., ROGER, T., LIOTÉ, F., SO, A. & BUSSO, N. 2011. Basic calcium phosphate crystals induce monocyte/macrophage IL-1β secretion through the NLRP3 inflammasome in vitro. *The Journal of Immunology,* 186**,** 2495-2502.

PEARLE, A. D., SCANZELLO, C. R., GEORGE, S., MANDL, L. A., DICARLO, E. F., PETERSON, M., SCULCO, T. P. & CROW, M. K. 2007. Elevated high-sensitivity C-reactive protein levels are associated with local inflammatory findings in patients with osteoarthritis. *Osteoarthritis Cartilage,* 15**,** 516-23.

PEARLE, A. D., WARREN, R. F. & RODEO, S. A. 2005. Basic science of articular cartilage and osteoarthritis. *Clinics in sports medicine,* 24**,** 1-12.

PEISTER, A., MELLAD, J. A., LARSON, B. L., HALL, B. M., GIBSON, L. F. & PROCKOP, D. J. 2004. Adult stem cells from bone marrow (MSCs) isolated from different strains of inbred mice vary in surface epitopes, rates of proliferation, and differentiation potential. *Blood,* 103**,** 1662-8.

PELLETIER, J. P., CARON, J. P., EVANS, C., ROBBINS, P. D., GEORGESCU, H. I., JOVANOVIC, D., FERNANDES, J. C. & MARTEL-PELLETIER, J. 1997. In vivo suppression of early experimental osteoarthritis by interleukin-1 receptor antagonist using gene therapy. *Arthritis & Rheumatism: Official Journal of the American College of Rheumatology,* 40**,** 1012-1019.

PELLETIER, J. P., MARTEL-PELLETIER, J. & ABRAMSON, S. B. 2001. Osteoarthritis, an inflammatory disease: potential implication for the selection of new therapeutic targets. *Arthritis & Rheumatism: Official Journal of the American College of Rheumatology,* 44**,** 1237-1247.

PELTTARI, K., WINTER, A., STECK, E., GOETZKE, K., HENNIG, T., OCHS, B. G., AIGNER, T. & RICHTER, W. 2006. Premature induction of hypertrophy during in vitro chondrogenesis of human mesenchymal stem cells correlates with calcification and vascular invasion after ectopic transplantation in SCID mice. *Arthritis & Rheumatism: Official Journal of the American College of Rheumatology,* 54**,** 3254-3266.

PERANTEAU, W. H., ZHANG, L., MUVARAK, N., BADILLO, A. T., RADU, A., ZOLTICK, P. W. & LIECHTY, K. W. 2008. IL-10 overexpression decreases inflammatory mediators and promotes regenerative healing in an adult model of scar formation. *J Invest Dermatol,* 128**,** 1852-60.

PEREZ, N., PLENCE, P., MILLET, V., GREUET, D., MINOT, C., NOEL, D., DANOS, O., JORGENSEN, C. & APPARAILLY, F. 2002. Tetracycline transcriptional silencer tightly controls transgene expression after in vivo intramuscular electrotransfer: application to interleukin 10 therapy in experimental arthritis. *Hum Gene Ther,* 13**,** 2161-72.

PÉTRILLI, V., DOSTERT, C., MURUVE, D. A. & TSCHOPP, J. 2007. The inflammasome: a danger sensing complex triggering innate immunity. *Current opinion in immunology,* 19**,** 615-622.

PETTIT, A. R., AHERN, M. J., ZEHNTNER, S., SMITH, M. D. & THOMAS, R. 2001. Comparison of differentiated dendritic cell infiltration of autoimmune and osteoarthritis synovial tissue. *Arthritis & Rheumatism: Official Journal of the American College of Rheumatology,* 44**,** 105-110.

PHINNEY, D. G., KOPEN, G., ISAACSON, R. L. & PROCKOP, D. J. 1999. Plastic adherent stromal cells from the bone marrow of commonly used strains of inbred mice: variations in yield, growth, and differentiation. *Journal of cellular biochemistry,* 72**,** 570-585.

PIGOTT, J. H., ISHIHARA, A., WELLMAN, M. L., RUSSELL, D. S. & BERTONE, A. L. 2013. Investigation of the immune response to autologous, allogeneic, and xenogeneic mesenchymal stem cells after intra-articular injection in horses. *Veterinary immunology and immunopathology,* 156**,** 99-106.

PITTENGER, M. F., MACKAY, A. M., BECK, S. C., JAISWAL, R. K., DOUGLAS, R., MOSCA, J. D., MOORMAN, M. A., SIMONETTI, D. W., CRAIG, S. & MARSHAK,

D. R. 1999. Multilineage potential of adult human mesenchymal stem cells. *Science,* 284**,** 143-7.

PLEUMEEKERS, M. M., NIMESKERN, L., KOEVOET, W. J., KOPS, N., POUBLON, R. M., STOK, K. S. & VAN OSCH, G. J. 2014. The in vitro and in vivo capacity of culture-expanded human cells from several sources encapsulated in alginate to form cartilage. *European cells & materials,* 27**,** 264-280.

POOLE, A., KOBAYASHI, M., YASUDA, T., LAVERTY, S., MWALE, F., KOJIMA, T., SAKAI, T., WAHL, C., EL-MAADAWY, S. & WEBB, G. 2002. Type II collagen degradation and its regulation in articular cartilage in osteoarthritis. *Annals of the rheumatic diseases,* 61**,** ii78-ii81.

PROCKOP, D. J. 2009. Repair of tissues by adult stem/progenitor cells (MSCs): controversies, myths, and changing paradigms. *Molecular Therapy,* 17**,** 939-946.

PROCKOP, D. J. & OH, J. Y. 2012. Mesenchymal stem/stromal cells (MSCs): role as guardians of inflammation. *Molecular therapy,* 20**,** 14-20.

PULSATELLI, L., DOLZANI, P., PIACENTINI, A., SILVESTRI, T., RUGGERI, R., GUALTIERI, G., MELICONI, R. & FACCHINI, A. 1999. Chemokine production by human chondrocytes. *The Journal of rheumatology,* 26**,** 1992-2001.

QIN, L., CHAVIN, K. D., DING, Y., FAVARO, J. P., WOODWARD, J. E., LIN, J., TAHARA, H., ROBBINS, P., SHAKED, A., HO, D. Y. & ET AL. 1995. Multiple vectors effectively achieve gene transfer in a murine cardiac transplantation model. Immunosuppression with TGF-beta 1 or vIL-10. *Transplantation,* 59**,** 809-16.

RADSTAKE, T. R., ROELOFS, M. F., JENNISKENS, Y. M., OPPERS-WALGREEN, B., VAN RIEL, P. L., BARRERA, P., JOOSTEN, L. A. & VAN DEN BERG, W. B. 2004. Expression of Toll-like receptors 2 and 4 in rheumatoid synovial tissue and regulation by proinflammatory cytokines interleukin-12 and interleukin-18 via interferon-γ. *Arthritis & Rheumatism,* 50**,** 3856-3865.

RAMAN, S., FITZGERALD, U. & MURPHY, J. M. 2018. Interplay of Inflammatory Mediators with Epigenetics and Cartilage Modifications in Osteoarthritis. *Frontiers in bioengineering and biotechnology,* 6**,** 22-22.

RATH, M., MÜLLER, I., KROPF, P., CLOSS, E. I. & MUNDER, M. 2014. Metabolism via arginase or nitric oxide synthase: two competing arginine pathways in macrophages. *Frontiers in immunology,* 5**,** 532.

REDISKE, J. J., KOEHNE, C. F., ZHANG, B. & LOTZ, M. 1994. The inducible production of nitric oxide by articular cell types. *Osteoarthritis and Cartilage,* 2**,** 199-206.

REGINATO, A. M., SANZ-RODRIGUEZ, C., DIAZ, A., DHARMAVARAM, R. & JIMENEZ, S. 1993. Transcriptional modulation of cartilage-specific collagen gene

expression by interferon γ and tumour necrosis factor α in cultured human chondrocytes. *Biochemical Journal,* 294**,** 761-769.

REIDBORD, H. & OSIAL, J. T. 1987. Synovial lymphocyte subsets in rheumatoid arthritis and degenerative joint disease. *The Journal of rheumatology,* 14**,** 1089-1094.

REN, G., ZHANG, L., ZHAO, X., XU, G., ZHANG, Y., ROBERTS, A. I., ZHAO, R. C. & SHI, Y. 2008. Mesenchymal stem cell-mediated immunosuppression occurs via concerted action of chemokines and nitric oxide. *Cell stem cell,* 2**,** 141-150.

REPPEL, L., SCHIAVI, J., CHARIF, N., LEGER, L., YU, H., PINZANO, A., HENRIONNET, C., STOLTZ, J.-F., BENSOUSSAN, D. & HUSELSTEIN, C. 2015. Chondrogenic induction of mesenchymal stromal/stem cells from Wharton's jelly embedded in alginate hydrogel and without added growth factor: an alternative stem cell source for cartilage tissue engineering. *Stem cell research & therapy,* 6**,** 260.

REZEND, M. U. D. & CAMPOS, G. C. D. 2013. â˜†. *Revista Brasileira de Ortopedia,* 48**,** 471-474.

RIBITSCH, I., MAYER, R. L., EGERBACHER, M., GABNER, S., KANDULA, M. M., ROSSER, J., HALTMAYER, E., AUER, U., GULTEKIN, S., HUBER, J., BILECK, A., KREIL, D. P., GERNER, C. & JENNER, F. 2018. Fetal articular cartilage regeneration versus adult fibrocartilaginous repair: secretome proteomics unravels molecular mechanisms in an ovine model. *Dis Model Mech,* 11.

RIDZUAN, N., AL ABBAR, A., YIP, W. K., MAQBOOL, M. & RAMASAMY, R. 2016. Characterization and Expression of Senescence Marker in Prolonged Passages of Rat Bone Marrow-Derived Mesenchymal Stem Cells. *Stem Cells International,* 2016**,** 14.

RITTER, S. Y., SUBBAIAH, R., BEBEK, G., CRISH, J., SCANZELLO, C. R., KRASTINS, B., SARRACINO, D., LOPEZ, M. F., CROW, M. K. & AIGNER, T. 2013. Proteomic analysis of synovial fluid from the osteoarthritic knee: comparison with transcriptome analyses of joint tissues. *Arthritis & Rheumatism,* 65**,** 981-992.

ROEMER, F. W., GUERMAZI, A., FELSON, D. T., NIU, J., NEVITT, M. C., CREMA, M. D., LYNCH, J. A., LEWIS, C. E., TORNER, J. & ZHANG, Y. 2011. Presence of MRI-detected joint effusion and synovitis increases the risk of cartilage loss in knees without osteoarthritis at 30-month follow-up: the MOST study. *Ann Rheum Dis,* 70**,** 1804-9.

ROHNER, E., MATZIOLIS, G., PERKA, C., FUCHTMEIER, B., GABER, T., BURMESTER, G. R., BUTTGEREIT, F. & HOFF, P. 2012. Inflammatory synovial fluid microenvironment drives primary human chondrocytes to actively take part in inflammatory joint diseases. *Immunol Res,* 52**,** 169-75.

ROSEN, C. J. & BOUXSEIN, M. L. 2006. Mechanisms of disease: is osteoporosis the obesity of bone? *Nature clinical practice Rheumatology,* 2**,** 35-43.

ROSENBERG, J. H., RAI, V., DILISIO, M. F. & AGRAWAL, D. K. 2017. Damage-associated molecular patterns in the pathogenesis of osteoarthritis: potentially novel therapeutic targets. *Mol Cell Biochem,* 434**,** 171-179.

ROSTOVSKAYA, M. & ANASTASSIADIS, K. 2012. Differential expression of surface markers in mouse bone marrow mesenchymal stromal cell subpopulations with distinct lineage commitment. *PloS one,* 7**,** e51221.

ROUSSET, F., GARCIA, E., DEFRANCE, T., PERONNE, C., VEZZIO, N., HSU, D.-H., KASTELEIN, R., MOORE, K. W. & BANCHEREAU, J. 1992. Interleukin 10 is a potent growth and differentiation factor for activated human B lymphocytes. *Proceedings of the National Academy of Sciences,* 89**,** 1890-1893.

ROWLEY, J. A., MADLAMBAYAN, G. & MOONEY, D. J. 1999. Alginate hydrogels as synthetic extracellular matrix materials. *Biomaterials,* 20**,** 45-53.

RYAN, L. M., KURUP, I. V., DERFUS, B. A. & KUSHNARYOV, V. M. 1992. ATP-induced chondrocalcinosis. *Arthritis & Rheumatism: Official Journal of the American College of Rheumatology,* 35**,** 1520-1525.

RYU, J.-H. & CHUN, J.-S. 2006. Opposing roles of WNT-5A and WNT-11 in interleukin-1β regulation of type II collagen expression in articular chondrocytes. *Journal of Biological Chemistry,* 281**,** 22039-22047.

SADOUK, M. B., PELLETIER, J. P., TARDIF, G., KIANSA, K., CLOUTIER, J. M. & MARTEL-PELLETIER, J. 1995. Human synovial fibroblasts coexpress IL-1 receptor type I and type II mRNA. The increased level of the IL-1 receptor in osteoarthritic cells is related to an increased level of the type I receptor. *Lab Invest,* 73**,** 347-55.

SAHA, N., MOLDOVAN, F., TARDIF, G., PELLETIER, J. P., CLOUTIER, J. M. & MARTEL-PELLETIER, J. 1999. Interleukin-1β–converting enzyme/caspase-1 in human osteoarthritic tissues: localization and role in the maturation of interleukin-1β and interleukin-18. *Arthritis & Rheumatism: Official Journal of the American College of Rheumatology,* 42**,** 1577-1587.

SAKATA, M., MASUKO-HONGO, K., NAKAMURA, H., ONUMA, H., TSURUHA, J., AOKI, H., NISHIOKA, K. & KATO, T. 2003. Osteoarthritic articular chondrocytes stimulate autologous T cell responses in vitro. *Clinical and experimental rheumatology,* 21**,** 704-710.

SAKKAS, L. I., KOUSSIDIS, G., AVGERINOS, E., GAUGHAN, J. & PLATSOUCAS, C. D. 2004. Decreased expression of the CD3ζ chain in T cells infiltrating the synovial membrane of patients with osteoarthritis. *Clin. Diagn. Lab. Immunol.,* 11**,** 195-202.

SAKKAS, L. I. & PLATSOUCAS, C. D. 2007. The role of T cells in the pathogenesis of osteoarthritis. *Arthritis & Rheumatism: Official Journal of the American College of Rheumatology,* 56**,** 409-424.

SAKKAS, L. I., SCANZELLO, C., JOHANSON, N., BURKHOLDER, J., MITRA, A., SALGAME, P., KATSETOS, C. D. & PLATSOUCAS, C. D. 1998. T cells and T-cell cytokine transcripts in the synovial membrane in patients with osteoarthritis. *Clin. Diagn. Lab. Immunol.,* 5**,** 430-437.

SAKLATVALA, J. 1986. Tumour necrosis factor α stimulates resorption and inhibits synthesis of proteoglycan in cartilage. *Nature,* 322**,** 547.

SAKLATVALA, J., PILSWORTH, L. M., SARSFIELD, S. J., GAVRILOVIC, J. & HEATH, J. K. 1984. Pig catabolin is a form of interleukin 1. Cartilage and bone resorb, fibroblasts make prostaglandin and collagenase, and thymocyte proliferation is augmented in response to one protein. *Biochemical journal,* 224**,** 461-466.

SANTANGELO, K., NUOVO, G. & BERTONE, A. 2012. In vivo reduction or blockade of interleukin-1β in primary osteoarthritis influences expression of mediators implicated in pathogenesis. *Osteoarthritis and cartilage,* 20**,** 1610-1618.

SARAIVA, M. & O'GARRA, A. 2010. The regulation of IL-10 production by immune cells. *Nature reviews immunology,* 10**,** 170.

SASSI, N., LAADHAR, L., ALLOUCHE, M., ACHEK, A., KALLEL-SELLAMI, M., MAKNI, S. & SELLAMI, S. 2014a. WNT signaling and chondrocytes: from cell fate determination to osteoarthritis physiopathology. *J Recept Signal Transduct Res,* 34**,** 73-80.

SASSI, N., LAADHAR, L., ALLOUCHE, M., ZANDIEH-DOULABI, B., HAMDOUN, M., KLEIN-NULEND, J., MAKNI, S. & SELLAMI, S. 2014b. Wnt signaling is involved in human articular chondrocyte de-differentiation in vitro. *Biotechnic & Histochemistry,* 89**,** 29-40.

SATO, T., MUROYAMA, Y. & SAITO, T. 2013. Inducible gene expression in postmitotic neurons by an in vivo electroporation-based tetracycline system. *J Neurosci Methods,* 214**,** 170-6.

SAULNIER, N., VIGUIER, E., PERRIER-GROULT, E., CHENU, C., PILLET, E., ROGER, T., MADDENS, S. & BOULOCHER, C. 2015. Intra-articular administration of xenogeneic neonatal mesenchymal stromal cells early after meniscal injury down-regulates metalloproteinase gene expression in synovium and prevents cartilage degradation in a rabbit model of osteoarthritis. *Osteoarthritis and cartilage,* 23**,** 122-133.

SCANZELLO, C., UMOH, E., PESSLER, F., DIAZ-TORNE, C., MILES, T., DICARLO, E., POTTER, H., MANDL, L., MARX, R. & RODEO, S. 2009. Local cytokine profiles in knee osteoarthritis: elevated synovial fluid interleukin-15 differentiates early from end-stage disease. *Osteoarthritis and Cartilage,* 17**,** 1040-1048.

SCANZELLO, C. R. & GOLDRING, S. R. 2012. The role of synovitis in osteoarthritis pathogenesis. *Bone,* 51**,** 249-57.

SCANZELLO, C. R., MCKEON, B., SWAIM, B. H., DICARLO, E., ASOMUGHA, E. U., KANDA, V., NAIR, A., LEE, D. M., RICHMOND, J. C., KATZ, J. N., CROW, M.

K. & GOLDRING, S. R. 2011. Synovial inflammation in patients undergoing arthroscopic meniscectomy: molecular characterization and relationship to symptoms. *Arthritis Rheum,* 63**,** 391-400.

SCANZELLO, C. R., PLAAS, A. & CROW, M. K. 2008. Innate immune system activation in osteoarthritis: is osteoarthritis a chronic wound? *Curr Opin Rheumatol,* 20**,** 565-72.

SCHAEFER, L., BABELOVA, A., KISS, E., HAUSSER, H.-J., BALIOVA, M., KRZYZANKOVA, M., MARSCHE, G., YOUNG, M. F., MIHALIK, D. & GÖTTE, M. 2005. The matrix component biglycan is proinflammatory and signals through Toll-like receptors 4 and 2 in macrophages. *The Journal of clinical investigation,* 115**,** 2223-2233.

SCHELBERGEN, R. F., BLOM, A. B., VAN DEN BOSCH, M. H., SLÖETJES, A., ABDOLLAHI-ROODSAZ, S., SCHREURS, B. W., MORT, J. S., VOGL, T., ROTH, J. & VAN DEN BERG, W. B. 2012. Alarmins S100A8 and S100A9 elicit a catabolic effect in human osteoarthritic chondrocytes that is dependent on Toll-like receptor 4. *Arthritis & Rheumatism,* 64**,** 1477-1487.

SCHELBERGEN, R. F., DE MUNTER, W., VAN DEN BOSCH, M., LAFEBER, F., SLOETJES, A., VOGL, T., ROTH, J., VAN DEN BERG, W., VAN DER KRAAN, P. & BLOM, A. 2016. Alarmins S100A8/S100A9 aggravate osteophyte formation in experimental osteoarthritis and predict osteophyte progression in early human symptomatic osteoarthritis. *Annals of the rheumatic diseases,* 75**,** 218-225.

SCHLAAK, J., PFERS, I., MEYER, K. Z. B. & MÄRKER-HERMANN, E. 1996. Different cytokine profiles in the synovial fluid of patients with osteoarthritis, rheumatoid arthritis and seronegative spondylarthropathies. *Clinical and experimental rheumatology,* 14**,** 155-162.

SCHLIMGEN, R., HOWARD, J., WOOLEY, D., THOMPSON, M., BADEN, L. R., YANG, O. O., CHRISTIANI, D. C., MOSTOSLAVSKY, G., DIAMOND, D. V., DUANE, E. G., BYERS, K., WINTERS, T., GELFAND, J. A., FUJIMOTO, G., HUDSON, T. W. & VYAS, J. M. 2016. Risks Associated With Lentiviral Vector Exposures and Prevention Strategies. *Journal of occupational and environmental medicine,* 58**,** 1159-1166.

SCHMITTGEN, T. D. & LIVAK, K. J. 2008. Analyzing real-time PCR data by the comparative C(T) method. *Nat Protoc,* 3**,** 1101-8.

SCHONIG, K., BUJARD, H. & GOSSEN, M. 2010. The power of reversibility regulating gene activities via tetracycline-controlled transcription. *Methods Enzymol,* 477**,** 429-53.

SCHRODER, K. & TSCHOPP, J. 2010. The inflammasomes. *cell,* 140**,** 821-832.

SCHUH, E., KRAMER, J., ROHWEDEL, J., NOTBOHM, H., MÜLLER, R., GUTSMANN, T. & ROTTER, N. 2010. Effect of matrix elasticity on the maintenance of the chondrogenic phenotype. *Tissue Engineering Part A,* 16**,** 1281-1290.

SCHURGERS, E., KELCHTERMANS, H., MITERA, T., GEBOES, L. & MATTHYS, P. 2010. Discrepancy between the in vitro and in vivo effects of murine mesenchymal stem cells on T-cell proliferation and collagen-induced arthritis. *Arthritis research & therapy,* 12**,** R31.

SCOTTI, C., TONNARELLI, B., PAPADIMITROPOULOS, A., SCHERBERICH, A., SCHAEREN, S., SCHAUERTE, A., LOPEZ-RIOS, J., ZELLER, R., BARBERO, A. & MARTIN, I. 2010. Recapitulation of endochondral bone formation using human adult mesenchymal stem cells as a paradigm for developmental engineering. *Proceedings of the National Academy of Sciences,* 107**,** 7251-7256.

SELLAM, J. & BERENBAUM, F. 2010. The role of synovitis in pathophysiology and clinical symptoms of osteoarthritis. *Nat Rev Rheumatol,* 6**,** 625-35.

SEOL, D., MCCABE, D. J., CHOE, H., ZHENG, H., YU, Y., JANG, K., WALTER, M. W., LEHMAN, A. D., DING, L. & BUCKWALTER, J. A. 2012. Chondrogenic progenitor cells respond to cartilage injury. *Arthritis & Rheumatism,* 64**,** 3626-3637.

SHAO, B.-Z., XU, Z.-Q., HAN, B.-Z., SU, D.-F. & LIU, C. 2015. NLRP3 inflammasome and its inhibitors: a review. *Frontiers in pharmacology,* 6**,** 262.

SHEN, P.-C., WU, C.-L., JOU, I.-M., LEE, C.-H., JUAN, H.-Y., LEE, P.-J., CHEN, S.-H. & HSIEH, J.-L. 2011. T helper cells promote disease progression of osteoarthritis by inducing macrophage inflammatory protein-1γ. *Osteoarthritis and cartilage,* 19**,** 728-736.

SHI, J., ZHAO, W., YING, H., ZHANG, Y., DU, J., CHEN, S., LI, J. & SHEN, B. 2018. Estradiol inhibits NLRP 3 inflammasome in fibroblast-like synoviocytes activated by lipopolysaccharide and adenosine triphosphate. *International journal of rheumatic diseases,* 21**,** 2002-2010.

SHI, K., HAYASHIDA, K., KANEKO, M., HASHIMOTO, J., TOMITA, T., LIPSKY, P. E., YOSHIKAWA, H. & OCHI, T. 2001. Lymphoid chemokine B cell-attracting chemokine-1 (CXCL13) is expressed in germinal center of ectopic lymphoid follicles within the synovium of chronic arthritis patients. *The Journal of Immunology,* 166**,** 650-655.

SHLOPOV, B. V., GUMANOVSKAYA, M. L. & HASTY, K. A. 2000. Autocrine regulation of collagenase 3 (matrix metalloproteinase 13) during osteoarthritis. *Arthritis & Rheumatism: Official Journal of the American College of Rheumatology,* 43**,** 195-205.

SITCHERAN, R., COGSWELL, P. C. & BALDWIN, A. S. 2003. NF-κB mediates inhibition of mesenchymal cell differentiation through a posttranscriptional gene silencing mechanism. *Genes & development,* 17**,** 2368-2373.

SMITH, M. D., O'DONNELL, J., HIGHTON, J., PALMER, D. G., ROZENBILDS, M. & ROBERTS-THOMSON, P. J. 1992. Immunohistochemical analysis of synovial membranes from inflammatory and non-inflammatory arthritides: scarcity of CD5 positive B cells and IL2 receptor bearing T cells. *Pathology,* 24**,** 19-26.

SOHN, D. H., SOKOLOVE, J., SHARPE, O., ERHART, J. C., CHANDRA, P. E., LAHEY, L. J., LINDSTROM, T. M., HWANG, I., BOYER, K. A., ANDRIACCHI, T. P. & ROBINSON, W. H. 2012. Plasma proteins present in osteoarthritic synovial fluid can stimulate cytokine production via Toll-like receptor 4. *Arthritis Res Ther,* 14**,** R7.

SOKOLOVE, J. & LEPUS, C. M. 2013. Role of inflammation in the pathogenesis of osteoarthritis: latest findings and interpretations. *Therapeutic advances in musculoskeletal disease,* 5**,** 77-94.

SOPHIA FOX, A. J., BEDI, A. & RODEO, S. A. 2009. The basic science of articular cartilage: structure, composition, and function. *Sports Health,* 1**,** 461-8.

STANNUS, O., JONES, G., CICUTTINI, F., PARAMESWARAN, V., QUINN, S., BURGESS, J. & DING, C. 2010. Circulating levels of IL-6 and TNF-α are associated with knee radiographic osteoarthritis and knee cartilage loss in older adults. *Osteoarthritis and cartilage,* 18**,** 1441-1447.

STUCKY, E. C., ERNDT-MARINO, J., SCHLOSS, R. S., YARMUSH, M. L. & SHREIBER, D. I. 2017. Prostaglandin E2 Produced by Alginate-Encapsulated Mesenchymal Stromal Cells Modulates the Astrocyte Inflammatory Response. *Nano LIFE,* 7.

STUCKY, E. C., SCHLOSS, R. S., YARMUSH, M. L. & SHREIBER, D. I. 2015. Alginate micro-encapsulation of mesenchymal stromal cells enhances modulation of the neuro-inflammatory response. *Cytotherapy,* 17**,** 1353-64.

SU, S.-L., TSAI, C.-D., LEE, C.-H., SALTER, D. & LEE, H.-S. 2005. Expression and regulation of Toll-like receptor 2 by IL-1β and fibronectin fragments in human articular chondrocytes. *Osteoarthritis and cartilage,* 13**,** 879-886.

SU, X., ZUO, W., WU, Z., CHEN, J., WU, N., MA, P., XIA, Z., JIANG, C., YE, Z., LIU, S., LIU, J., ZHOU, G., WAN, C. & QIU, G. 2015. CD146 as a new marker for an increased chondroprogenitor cell sub-population in the later stages of osteoarthritis. *J Orthop Res,* 33**,** 84-91.

SUN, X. H., LIU, Y., HAN, Y. & WANG, J. 2016. Expression and Significance of High-Mobility Group Protein B1 (HMGB1) and the Receptor for Advanced Glycation End-Product (RAGE) in Knee Osteoarthritis. *Med Sci Monit,* 22**,** 2105-12.

SUN, Y., MA, J., LI, D., LI, P., ZHOU, X., LI, Y., HE, Z., QIN, L., LIANG, L. & LUO, X. 2019. Interleukin-10 inhibits interleukin-1β production and inflammasome activation of microglia in epileptic seizures. *Journal of Neuroinflammation,* 16**,** 66.

SUNAHORI, K., YAMAMURA, M., YAMANA, J., TAKASUGI, K., KAWASHIMA, M., YAMAMOTO, H., CHAZIN, W. J., NAKATANI, Y., YUI, S. & MAKINO, H. 2006. The S100A8/A9 heterodimer amplifies proinflammatory cytokine production by macrophages via activation of nuclear factor kappa B and p38 mitogen-activated protein kinase in rheumatoid arthritis. *Arthritis research & therapy,* 8**,** R69.

SUURMOND, J., DORJEE, A. L., BOON, M. R., KNOL, E. F., HUIZINGA, T. W., TOES, R. E. & SCHUERWEGH, A. J. 2015. Mast cells are the main interleukin 17-positive cells in anticitrullinated protein antibody-positive and-negative rheumatoid arthritis and osteoarthritis synovium (Retraction of vol 12, R150, 2011). *ARTHRITIS RESEARCH & THERAPY,* 17.

TAKAGI, T. & JASIN, H. E. 1992. Interactions between anticollagen antibodies and chondrocytes. *Arthritis & Rheumatism: Official Journal of the American College of Rheumatology,* 35**,** 224-230.

TALABOT-AYER, D., MCKEE, T., GINDRE, P., BAS, S., BAETEN, D. L., GABAY, C. & PALMER, G. 2012. Distinct serum and synovial fluid interleukin (IL)-33 levels in rheumatoid arthritis, psoriatic arthritis and osteoarthritis. *Joint Bone Spine,* 79**,** 32-37.

TEEPLE, E., ELSAID, K. A., JAY, G. D., ZHANG, L., BADGER, G. J., AKELMAN, M., BLISS, T. F. & FLEMING, B. C. 2011. Effects of Supplemental Intra-articular Lubricin and Hyaluronic Acid on the Progression of Posttraumatic Arthritis in the Anterior Cruciate Ligament–Deficient Rat Knee. *The American journal of sports medicine,* 39**,** 164-172.

TER HUURNE, M., SCHELBERGEN, R., BLATTES, R., BLOM, A., DE MUNTER, W., GREVERS, L. C., JEANSON, J., NOËL, D., CASTEILLA, L. & JORGENSEN, C. 2012. Antiinflammatory and chondroprotective effects of intraarticular injection of adipose-derived stem cells in experimental osteoarthritis. *Arthritis & Rheumatism,* 64**,** 3604-3613.

TERMEER, C., BENEDIX, F., SLEEMAN, J., FIEBER, C., VOITH, U., AHRENS, T., MIYAKE, K., FREUDENBERG, M., GALANOS, C. & SIMON, J. C. 2002. Oligosaccharides of Hyaluronan activate dendritic cells via toll-like receptor 4. *Journal of Experimental Medicine,* 195**,** 99-111.

TETLOW, L. C. & WOOLLEY, D. E. 2006. Histamine and PGE(2) stimulate the production of interleukins -6 and -8 by human articular chondrocytes in vitro. 6. Human and clinical aspects of histamine. *Inflamm Res,* 55 Suppl 1**,** S73-4.

TILG, H., ULMER, H., KASER, A. & WEISS, G. 2002. Role of IL-10 for induction of anemia during inflammation. *The Journal of Immunology,* 169**,** 2204-2209.

TOMCHUCK, S. L., ZWEZDARYK, K. J., COFFELT, S. B., WATERMAN, R. S., DANKA, E. S. & SCANDURRO, A. B. 2008. Toll-like receptors on human mesenchymal stem cells drive their migration and immunomodulating responses. *Stem cells,* 26**,** 99-107.

TROYER, D. L. & WEISS, M. L. 2008. Concise review: Wharton's Jelly-derived cells are a primitive stromal cell population. *Stem cells,* 26**,** 591-599.

UDAGAWA, N., HORWOOD, N. J., ELLIOTT, J., MACKAY, A., OWENS, J., OKAMURA, H., KURIMOTO, M., CHAMBERS, T. J., MARTIN, T. J. & GILLESPIE, M. T. 1997. Interleukin-18 (interferon-γ–inducing factor) is produced by osteoblasts and

acts via granulocyte/macrophage colony-stimulating factor and not via interferon-γ to inhibit osteoclast formation. *Journal of Experimental Medicine,* 185**,** 1005-1012.

UTOMO, L., VAN OSCH, G. J., BAYON, Y., VERHAAR, J. & BASTIAANSEN-JENNISKENS, Y. 2016. Guiding synovial inflammation by macrophage phenotype modulation: an in vitro study towards a therapy for osteoarthritis. *Osteoarthritis and cartilage,* 24**,** 1629-1638.

VAN BUUL, G., VILLAFUERTES, E., BOS, P., WAARSING, J., KOPS, N., NARCISI, R., WEINANS, H., VERHAAR, J., BERNSEN, M. & VAN OSCH, G. 2012. Mesenchymal stem cells secrete factors that inhibit inflammatory processes in short-term osteoarthritic synovium and cartilage explant culture. *Osteoarthritis and Cartilage,* 20**,** 1186-1196.

VAN DE LOO, F. A., ARNTZ, O. J. & VAN DEN BERG, W. B. 1997. Effect of interleukin 1 and leukaemia inhibitory factor on chondrocyte metabolism in articular cartilage from normal and interleukin-6-deficient mice: role of nitric oxide and IL-6 in the suppression of proteoglycan synthesis. *Cytokine,* 9**,** 453-62.

VAN DEN BOSCH, M. H., BLOM, A. B., SCHELBERGEN, R. F., KOENDERS, M. I., VAN DE LOO, F. A., VAN DEN BERG, W. B., VOGL, T., ROTH, J., VAN DER KRAAN, P. M. & VAN LENT, P. L. 2016. Alarmin S100A9 induces proinflammatory and catabolic effects predominantly in the M1 macrophages of human osteoarthritic synovium. *The Journal of rheumatology,* 43**,** 1874-1884.

VAN DER KRAAN, P. & VAN DEN BERG, W. 2012a. Chondrocyte hypertrophy and osteoarthritis: role in initiation and progression of cartilage degeneration? *Osteoarthritis and cartilage,* 20**,** 223-232.

VAN DER KRAAN, P. M. & VAN DEN BERG, W. B. 2007. Osteophytes: relevance and biology. *Osteoarthritis and Cartilage,* 15**,** 237-244.

VAN DER KRAAN, P. M. & VAN DEN BERG, W. B. 2012b. Chondrocyte hypertrophy and osteoarthritis: role in initiation and progression of cartilage degeneration? *Osteoarthritis Cartilage,* 20**,** 223-32.

VAN LENT, P., BLOM, A., HOLTHUYSEN, A., JACOBS, C., VAN DE PUTTE, L. & VAN DEN BERG, W. 1997. Monocytes/macrophages rather than PMN are involved in early cartilage degradation in cationic immune complex arthritis in mice. *Journal of leukocyte biology,* 61**,** 267-278.

VAN LENT, P., BLOM, A., VAN DER KRAAN, P., HOLTHUYSEN, A., VITTERS, E., VAN ROOIJEN, N., SMEETS, R., NABBE, K. & VAN DEN BERG, W. 2004. Crucial role of synovial lining macrophages in the promotion of transforming growth factor β–mediated osteophyte formation. *Arthritis & Rheumatism: Official Journal of the American College of Rheumatology,* 50**,** 103-111.

VAN LENT, P., GREVERS, L., BLOM, A., ARNTZ, O., VAN DE LOO, F., VAN DER KRAAN, P., ABDOLLAHI-ROODSAZ, S., SRIKRISHNA, G., FREEZE, H. &

SLOETJES, A. 2008a. Stimulation of chondrocyte-mediated cartilage destruction by S100A8 in experimental murine arthritis. *Arthritis & Rheumatism: Official Journal of the American College of Rheumatology,* 58**,** 3776-3787.

VAN LENT, P., GREVERS, L., BLOM, A., SLOETJES, A., MORT, J., VOGL, T., NACKEN, W., VAN DEN BERG, W. & ROTH, J. 2008b. Myeloid-related proteins S100A8/S100A9 regulate joint inflammation and cartilage destruction during antigen-induced arthritis. *Annals of the rheumatic diseases,* 67**,** 1750-1758.

VAN LENT, P., HOLTHUYSEN, A., VAN ROOIJEN, N., VAN DE PUTTE, L. & VAN DEN BERG, W. 1998. Local removal of phagocytic synovial lining cells by clodronate-liposomes decreases cartilage destruction during collagen type II arthritis. *Annals of the rheumatic diseases,* 57**,** 408-413.

VAN LENT, P., NABBE, K. C., BOROSS, P., BLOM, A. B., ROTH, J., HOLTHUYSEN, A., SLOETJES, A., VERBEEK, S. & VAN DEN BERG, W. 2003. The inhibitory receptor FcγRII reduces joint inflammation and destruction in experimental immune complex-mediated arthritides not only by inhibition of FcγRI/III but also by efficient clearance and endocytosis of immune complexes. *The American journal of pathology,* 163**,** 1839-1848.

VAN LENT, P. L., BLOM, A. B., SCHELBERGEN, R. F., SLOETJES, A., LAFEBER, F. P., LEMS, W. F., CATS, H., VOGL, T., ROTH, J. & VAN DEN BERG, W. B. 2012. Active involvement of alarmins S100A8 and S100A9 in the regulation of synovial activation and joint destruction during mouse and human osteoarthritis. *Arthritis Rheum,* 64**,** 1466-76.

VAN LENT, P. L. & VAN DEN BERG, W. B. 2013. Mesenchymal stem cell therapy in osteoarthritis: advanced tissue repair or intervention with smouldering synovial activation? : BioMed Central.

VAN SUSANTE, J. L., BUMA, P., VAN OSCH, G. J., VERSLEYEN, D., VAN DER KRAAN, P. M., VAN DER BERG, W. B. & HOMMINGA, G. N. 1995. Culture of chondrocytes in alginate and collagen carrier gels. *Acta orthopaedica Scandinavica,* 66**,** 549-556.

VERMEIJ, E. A., BROEREN, M. G., BENNINK, M. B., ARNTZ, O. J., GJERTSSON, I., VAN LENT, P. L., VAN DEN BERG, W. B., KOENDERS, M. I. & VAN DE LOO, F. A. 2015. Disease-regulated local IL-10 gene therapy diminishes synovitis and cartilage proteoglycan depletion in experimental arthritis. *Ann Rheum Dis,* 74**,** 2084-91.

VIEIRA, P., DE WAAL-MALEFYT, R., DANG, M. N., JOHNSON, K. E., KASTELEIN, R., FIORENTINO, D. F., DEVRIES, J. E., RONCAROLO, M. G., MOSMANN, T. R. & MOORE, K. W. 1991. Isolation and expression of human cytokine synthesis inhibitory factor cDNA clones: homology to Epstein-Barr virus open reading frame BCRFI. *Proc Natl Acad Sci U S A,* 88**,** 1172-6.

VISTE, A., PIPERNO, M., DESMARCHELIER, R., GROSCLAUDE, S., MOYEN, B. & FESSY, M.-H. 2012. Autologous chondrocyte implantation for traumatic full-thickness cartilage defects of the knee in 14 patients: 6-year functional outcomes. *Orthopaedics & Traumatology: Surgery & Research,* 98**,** 737-743.

VOGL, T., EISENBLÄTTER, M., VÖLLER, T., ZENKER, S., HERMANN, S., VAN LENT, P., FAUST, A., GEYER, C., PETERSEN, B. & ROEBROCK, K. 2014. Alarmin S100A8/S100A9 as a biomarker for molecular imaging of local inflammatory activity. *Nature communications,* 5**,** 4593.

VOGL, T., STRATIS, A., WIXLER, V., VÖLLER, T., THURAINAYAGAM, S., JORCH, S. K., ZENKER, S., DREILING, A., CHAKRABORTY, D. & FRÖHLING, M. 2018. Autoinhibitory regulation of S100A8/S100A9 alarmin activity locally restricts sterile inflammation. *The Journal of clinical investigation,* 128**,** 1852-1866.

VUOLTEENAHO, K., MOILANEN, T., KNOWLES, R. & MOILANEN, E. 2007. The role of nitric oxide in osteoarthritis. *Scandinavian journal of rheumatology,* 36**,** 247-258.

WALDMANN, T. & TAGAYA, Y. 1999. The multifaceted regulation of interleukin-15 expression and the role of this cytokine in NK cell differentiation and host response to intracellular pathogens. *Annual review of immunology,* 17**,** 19-49.

WANG, L., CHEN, K., WAN, X., WANG, F., GUO, Z. & MO, Z. 2017. NLRP3 inflammasome activation in mesenchymal stem cells inhibits osteogenic differentiation and enhances adipogenic differentiation. *Biochemical and biophysical research communications,* 484**,** 871-877.

WANG, Q., BREINAN, H. A., HSU, H. P. & SPECTOR, M. 2000. Healing of defects in canine articular cartilage: Distribution of nonvascular α-smooth muscle actin-containing cells. *Wound Repair and Regeneration,* 8**,** 145-158.

WANG, Q., ROZELLE, A. L., LEPUS, C. M., SCANZELLO, C. R., SONG, J. J., LARSEN, D. M., CRISH, J. F., BEBEK, G., RITTER, S. Y. & LINDSTROM, T. M. 2011. Identification of a central role for complement in osteoarthritis. *Nature medicine,* 17**,** 1674.

WANG, Y., HUANG, X., TANG, Y., LIN, H. & ZHOU, N. 2016. Effects of panax notoginseng saponins on the osteogenic differentiation of rabbit bone mesenchymal stem cells through TGF-β1 signaling pathway. *BMC complementary and alternative medicine,* 16**,** 319-319.

WATERMAN, R. S., TOMCHUCK, S. L., HENKLE, S. L. & BETANCOURT, A. M. 2010. A new mesenchymal stem cell (MSC) paradigm: polarization into a pro-inflammatory MSC1 or an Immunosuppressive MSC2 phenotype. *PloS one,* 5**,** e10088.

WEHLING, N., PALMER, G. D., PILAPIL, C., LIU, F., WELLS, J. W., MULLER, P. E., EVANS, C. H. & PORTER, R. M. 2009. Interleukin-1beta and tumor necrosis factor alpha inhibit chondrogenesis by human mesenchymal stem cells through NF-kappaB-dependent pathways. *Arthritis Rheum,* 60**,** 801-12.

WEI, T., KULKARNI, N. H., ZENG, Q. Q., HELVERING, L. M., LIN, X., LAWRENCE, F., HALE, L., CHAMBERS, M. G., LIN, C., HARVEY, A., MA, Y. L., CAIN, R. L., OSKINS, J., CAROZZA, M. A., EDMONDSON, D. D., HU, T., MILES, R. R., RYAN, T. P., ONYIA, J. E. & MITCHELL, P. G. 2010. Analysis of early changes in the articular cartilage transcriptisome in the rat meniscal tear model of osteoarthritis: pathway comparisons with the rat anterior cruciate transection model and with human osteoarthritic cartilage. *Osteoarthritis Cartilage,* 18**,** 992-1000.

WEINANS, H., SIEBELT, M., AGRICOLA, R., BOTTER, S., PISCAER, T. & WAARSING, J. 2012. Pathophysiology of peri-articular bone changes in osteoarthritis. *Bone,* 51**,** 190-196.

WEINBERG, S. E., SENA, L. A. & CHANDEL, N. S. 2015. Mitochondria in the regulation of innate and adaptive immunity. *Immunity,* 42**,** 406-417.

WEISS, M. L. & TROYER, D. L. 2006. Stem cells in the umbilical cord. *Stem cell reviews,* 2**,** 155-162.

WEN, H., GRIS, D., LEI, Y., JHA, S., ZHANG, L., HUANG, M. T.-H., BRICKEY, W. J. & TING, J. P. 2011. Fatty acid–induced NLRP3-ASC inflammasome activation interferes with insulin signaling. *Nature immunology,* 12**,** 408.

WILLIAMS, R., KHAN, I. M., RICHARDSON, K., NELSON, L., MCCARTHY, H. E., ANALBELSI, T., SINGHRAO, S. K., DOWTHWAITE, G. P., JONES, R. E. & BAIRD, D. M. 2010. Identification and clonal characterisation of a progenitor cell sub-population in normal human articular cartilage. *PloS one,* 5**,** e13246.

WILLIAMS, R. J., 3RD & HARNLY, H. W. 2007. Microfracture: indications, technique, and results. *Instr Course Lect,* 56**,** 419-28.

WITTENAUER, R., SMITH, L., ADEN, K., WITTENAUER, R., SMITH, L. & ADEN, K. 2013. Priority medicines for Europe and the world "A public health approach to innovation" Update on 2004 background paper background paper 6.12 osteoarthritis. *Geneva, Switzerland: World Health Organization*.

WOJDASIEWICZ, P., PONIATOWSKI, L. A. & SZUKIEWICZ, D. 2014. The role of inflammatory and anti-inflammatory cytokines in the pathogenesis of osteoarthritis. *Mediators Inflamm,* 2014**,** 561459.

WOOLEY, P. H., GRIMM, M. J. & RADIN, E. L. 2005. The structure and function of joints. *Arthritis and Allied Conditions. A Textbook of Rheumatology, Lippincott Williams & Wilkins, Philadelphia***,** 149-173.

XIAOQIANG, E., CAO, Y., MENG, H., QI, Y., DU, G., XU, J. & BI, Z. 2012. Dendritic cells of synovium in experimental model of osteoarthritis of rabbits. *Cellular Physiology and Biochemistry,* 30**,** 23-32.

XISHAN, Z., HAOJUN, Y., BAOXIN, H., XINNA, Z., NI, J., HONGMEI, Z., XIAOLI, W. & JUN, R. 2014. Mouse Flk-1+Sca-1- mesenchymal stem cells: functional plasticity in vitro and immunoregulation in vivo. *Transplantation,* 97**,** 509-17.

XU, J., WANG, W., LUDEMAN, M., CHENG, K., HAYAMI, T., LOTZ, J. C. & KAPILA, S. 2008. Chondrogenic differentiation of human mesenchymal stem cells in three-dimensional alginate gels. *Tissue Engineering Part A,* 14**,** 667-680.

XUE, R., LI, J. Y. S., YEH, Y., YANG, L. & CHIEN, S. 2013. Effects of matrix elasticity and cell density on human mesenchymal stem cells differentiation. *Journal of Orthopaedic Research,* 31**,** 1360-1365.

YAMAGATA, K., NAKAYAMADA, S. & TANAKA, Y. 2018. Use of mesenchymal stem cells seeded on the scaffold in articular cartilage repair. *Inflammation and regeneration,* 38**,** 4.

YAMAMOTO, M., SATO, S., HEMMI, H., HOSHINO, K., KAISHO, T., SANJO, H., TAKEUCHI, O., SUGIYAMA, M., OKABE, M. & TAKEDA, K. 2003. Role of adaptor TRIF in the MyD88-independent toll-like receptor signaling pathway. *Science,* 301**,** 640-643.

YANG, F., ZHOU, S., WANG, C., HUANG, Y., LI, H., WANG, Y., ZHU, Z., TANG, J. & YAN, M. 2017. Epigenetic modifications of interleukin-6 in synovial fibroblasts from osteoarthritis patients. *Sci Rep,* 7**,** 43592.

YANG, K., SARIS, D., GEUZE, R., VAN RIJEN, M., VAN DER HELM, Y., VERBOUT, A., CREEMERS, L. & DHERT, W. 2006. Altered in vitro chondrogenic properties of chondrocytes harvested from unaffected cartilage in osteoarthritic joints. *Osteoarthritis and cartilage,* 14**,** 561-570.

YANG, S.-H., PARK, M.-J., YOON, I.-H., KIM, S.-Y., HONG, S.-H., SHIN, J.-Y., NAM, H.-Y., KIM, Y.-H., KIM, B. & PARK, C.-G. 2009. Soluble mediators from mesenchymal stem cells suppress T cell proliferation by inducing IL-10. *Experimental & molecular medicine,* 41**,** 315.

YANG, Y., TOPOL, L., LEE, H. & WU, J. 2003. Wnt5a and Wnt5b exhibit distinct activities in coordinating chondrocyte proliferation and differentiation. *Development,* 130**,** 1003-1015.

YEO, L., ADLARD, N., BIEHL, M., JUAREZ, M., SMALLIE, T., SNOW, M., BUCKLEY, C., RAZA, K., FILER, A. & SCHEEL-TOELLNER, D. 2016. Expression of chemokines CXCL4 and CXCL7 by synovial macrophages defines an early stage of rheumatoid arthritis. *Annals of the rheumatic diseases,* 75**,** 763-771.

YOO, J. U., BARTHEL, T. S., NISHIMURA, K., SOLCHAGA, L., CAPLAN, A. I., GOLDBERG, V. M. & JOHNSTONE, B. 1998. The chondrogenic potential of human bone-marrow-derived mesenchymal progenitor cells. *JBJS,* 80**,** 1745-57.

YUASA, T., OTANI, T., KOIKE, T., IWAMOTO, M. & ENOMOTO-IWAMOTO, M. 2008. Wnt/β-catenin signaling stimulates matrix catabolic genes and activity in articular chondrocytes: its possible role in joint degeneration. *Laboratory Investigation,* 88**,** 264.

ZAIM, M., KARAMAN, S., CETIN, G. & ISIK, S. 2012. Donor age and long-term culture affect differentiation and proliferation of human bone marrow mesenchymal stem cells. *Ann Hematol,* 91**,** 1175-86.

ZASLAV, K., MCADAMS, T., SCOPP, J., THEOSADAKIS, J., MAHAJAN, V. & GOBBI, A. 2012. New frontiers for cartilage repair and protection. *Cartilage,* 3**,** 77S-86S.

ZDANOV, A., SCHALK-HIHI, C., MENON, S., MOORE, K. W. & WLODAWER, A. 1997. Crystal structure of Epstein-Barr virus protein BCRF1, a homolog of cellular interleukin-10. *Journal of molecular biology,* 268**,** 460-467.

ZHA, Q.-B., WEI, H.-X., LI, C.-G., LIANG, Y.-D., XU, L.-H., BAI, W.-J., PAN, H., HE, X.-H. & OUYANG, D.-Y. 2016. ATP-Induced Inflammasome Activation and Pyroptosis Is Regulated by AMP-Activated Protein Kinase in Macrophages. *Frontiers in immunology,* 7**,** 597-597.

ZHANG, Q., JI, Q., WANG, X., KANG, L., FU, Y., YIN, Y., LI, Z., LIU, Y., XU, X. & WANG, Y. 2015. SOX9 is a regulator of ADAMTSs-induced cartilage degeneration at the early stage of human osteoarthritis. *Osteoarthritis Cartilage,* 23**,** 2259-2268.

ZHANG, W., OUYANG, H., DASS, C. R. & XU, J. 2016. Current research on pharmacologic and regenerative therapies for osteoarthritis. *Bone research,* 4**,** 15040.

ZHANG, X., MAO, Z. & YU, C. 2004. Suppression of early experimental osteoarthritis by gene transfer of interleukin-1 receptor antagonist and interleukin-10. *Journal of orthopaedic research,* 22**,** 742-750.

ZHAO, L. R., XING, R. L., WANG, P. M., ZHANG, N. S., YIN, S. J., LI, X. C. & ZHANG, L. 2018. NLRP1 and NLRP3 inflammasomes mediate LPS/ATP‐induced pyroptosis in knee osteoarthritis. *Molecular medicine reports,* 17**,** 5463-5469.

ZHONG, Z., WEN, Z. & DARNELL, J. E. 1994. Stat3: a STAT family member activated by tyrosine phosphorylation in response to epidermal growth factor and interleukin-6. *Science,* 264**,** 95-98.

ZHOU, C., ZHENG, H., SEOL, D., YU, Y. & MARTIN, J. A. 2014. Gene expression profiles reveal that chondrogenic progenitor cells and synovial cells are closely related. *Journal of Orthopaedic Research,* 32**,** 981-988.

ZREIQAT, H., BELLUOCCIO, D., SMITH, M. M., WILSON, R., ROWLEY, L. A., JONES, K., RAMASWAMY, Y., VOGL, T., ROTH, J. & BATEMAN, J. F. 2010. S100A8 and S100A9 in experimental osteoarthritis. *Arthritis research & therapy,* 12**,** R16.

ZREIQAT, H., HOWLETT, C., GRONTHOS, S., HUME, D. & GECZY, C. 2007. S100A8/S100A9 and their association with cartilage and bone. *Journal of molecular histology,* 38**,** 381-391.